# Dynamic Modelling and Optimal Control

# of Sugar Crystallisation in a

# Multi-compartment Continuous Vacuum Pan

DAVID JOHN LOVE   B.Sc. Eng. (Chem.)

# Abstract

The objective of this work was to determine the operating conditions which would maximise the crystallisation performance of continuous vacuum pans used in the sugar industry. The specific application investigated in detail is crystallisation of high grade product sugar (A-sugar) in a South African raw cane sugar factory.

The optimisation studies are based on a detailed dynamic mathematical model of a continuous pan. Whilst this model is based on the published work of others, the selection of variables and the formulation of the equations have been structured to produce a modular model of an individual compartment with the minimum number of independent variables. The independent variables have also been selected to meet the requirements of both a state-space control formulation and those necessary for the dynamic programming technique of optimisation. The modular compartment models are linked together to model a multi-compartment pan and the steady state model is derived as a special case of the dynamic model.

For the model to simulate the conditions in South African sugar factories adequately requires appropriate descriptions of sucrose solubility and growth kinetics. Given the limited applicability of published data, experiments were undertaken to determine these parameters. Sucrose solubility in impure solutions was determined in laboratory tests designed to approach equilibrium by dissolution at conditions approximating those during pan boiling. The dependence of crystal growth rate on the concentration of impurity present in the mother liquor was investigated in both laboratory scale and pilot scale batch pan boiling experiments. The primary dependence of crystal growth rate on the super-saturation driving force was determined by fitting the steady state model to results of tests on an industrial scale continuous pan.

The dynamic programming technique was used in conjunction with the mathematical model to determine the operating conditions which maximise steady state crystallisation performance. Using the crystallisation parameters determined for South African conditions, this approach has shown that the conventional wisdom of running with high crystal contents in all compartments of continuous pans boiling A-massecuite is not optimum. Pans should operate at lower crystal contents in earlier compartments, only increasing to higher crystal contents towards the final compartment. The specific values depend on seed conditions, pan design and the solubility and growth kinetics.

To reap the benefits of being able to determine the optimum steady state operating condition for a continuous pan, it is necessary to be able to achieve effective steady state operation under industrial conditions. This requires both a steady loading on the pan and effective control of the crystallisation conditions within the pan. To stabilise loading, a strategy has been developed which uses buffer tanks in an optimal way to damp out flow fluctuations. This strategy accommodates multiple buffer tanks in series without the amplification of disturbances that occurs with some of the simpler published techniques.

The dynamic behaviour of absolute pressure control and compartment feed control were investigated in an industrial scale pan. This work has demonstrated the importance of high quality absolute pressure control and developed techniques for effective automatic tuning of pan feed controls.

As part of this research, computer control systems were developed as tools to provide the appropriate monitoring and control of the experiments undertaken.

To Margaret and Michelle

# Declaration

This thesis is based on research which was conducted either whilst I was employed by the Tongaat-Hulett Sugar Company (THS) or making use of their production and research facilities. I was given assistance by employees of THS in carrying out various aspects of the experimental parts of the research, as formally referred to in the acknowledgements. Otherwise, unless specifically indicated to the contrary in the text, this thesis is my own original and unaided work. It has not been submitted in part, or in whole to any other University.

_____                    _____

Mike Mulholland                                          David Love

(Supervisor)

# Preface

This thesis is based on research which was conducted either whilst I was employed by the Tongaat-Hulett Sugar Company (THS) or making use of their production and research facilities. The research was conducted, and is best understood, within the context of Tongaat Hulett's efforts to perfect continuous pan boiling technology as described in section 1.3 of the thesis. The successful efforts of the THS team which developed and commercialised a unique design of continuous pan were recognised locally by the award of both the 1993 Chemical Engineering Innovation Award of the South African Institution of Chemical Engineers and the 1994 Annual Award of the Associated Scientific and Technical Societies of South Africa.

As a member of this team, which comprised THS staff from design, Research and Development, production and the technical support departments of the company, it is hopefully instructive to describe my personal contributions as part of the team and to identify the research that I undertook personally.

A crucial aspect of the Tongaat Hulett design of continuous pan is the emphasis on achieving appropriate flow characteristics for the massecuite in the pan. This is an important aspect in the successful conversion of batch processes to continuous processes and which had been the rationale behind the application of tracer testing to a number of processes in the local sugar industry (Rouillard and Smith, 1981). The residence time distributions obtained from tracer tests can be analysed both qualitatively and quantitatively to provide insights into the flow patterns within the process unit being tested. My own involvement in measurement and optimisation of flow patterns began when I was employed in the Research and Development Department of Huletts Sugar (subsequently to become THS after a merger). My initial work was directed at improving the performance of continuous clarifiers (Love, 1980) which was supported by research to develop appropriate analytical techniques (Morel du Boil, 1980). I also developed techniques for conducting and analysing tracer tests on diffusers (a counter-current leaching process for extracting sucrose from shredded cane) using a two dimensional dispersion model (Love and Rein, 1980). This background subsequently led to my involvement as a member of the team which conducted and analysed tracer tests on continuous pans (Rein, Cox and Love, 1985)

When THS made the decision to proceed with the construction of the new Felixton mill, I was

working as a process design engineer in the company's central technical department ( Technical Management Department) which undertook the design of the new mill in-house (Renton, 1985). As a member of the process design team, I undertook the detailed design of some of the ancillaries for the six new continuous pans installed in the new factory (viz, entrainment separators, direct contact barometric condensers, feed distribution systems, steam spargers (jiggers) condensate drains and massecuite transfer ports between compartments.)

After the construction of the Felixton factory, I joined the production management team at the new factory and worked there for three years from 1984 to 1987, with one of my areas of responsibility being the optimisation of the performance of the new continuous A pans. Much of my efforts to understand and improve operations , being of a production rather than research nature, were not published but provided me with a more comprehensive understanding of real production problems which in turn provided direction and background to my subsequent research.

My work on the control and instrumentation problems on the continuous pans during this period, in close collaboration with an electrical engineering colleague, resulted in an investigation into the use of boiling point elevation as a control signal, a modified method of controlling pan throughput and the development of a method of tuning feed control loops ( Love and Chilvers, 1986).

Despite the significant effort expended by both production and technical support staff, the continuous A pans at the new Felixton mill performed below design during their first years of operation. The original design had been for an A massecuite exhaustion of 66 (Reid and Rein, 1983) but the season average A massecuite exhaustions for the first four years of operation were significantly below this, viz.:

> 1984/85 season : 56,64
>
> 1985/86 season : 59,75
>
> 1986/87 season : 59,95
>
> and    1987/88 season : 60,20.

Being a new technology, there was little past experience at the time to assist in understanding the shortfall in performance, and only one other local continuous A pan installation for comparison (at the Maidstone mill). As part of my efforts to improve the A pan performance, I performed some production comparisons between the Felixton and Maidstone continuous A pans and co-ordinated three weeks of close attention to A pan operations when I and two other experienced

sugar technologists provided 24 hour supervision and testing in three eight hour shifts. I also was part of the team that conducted detailed tests on the pans. The tracer tests were used to measure residence time distributions (Rein, Cox and Love, 1985) whilst simultaneously collecting data for analysis by a steady state computer model (Hoekstra, 1985).

None of this testing managed to produce a significant increase in performance, but it did indicate that there was a lack of knowledge as to the relationship between crystallisation performance and crystallisation loading. The definition of performance and loading are not well specified but it is reasonable to expect that the performance of a process unit will reduce as the loading is increased. There was also evidence of a wide variation in the reported growth rates of sucrose crystals. Specifically, Hoekstra (1985) found that the crystal growth rates estimated from an analysis of the tests on the Felixton A-pans was only one tenth of that predicted from published correlations for the Australian cane sugar industry. As is described in Chapter 2, the data published in the paper by Rein, Cox and Love (1985) can be analysed (Appendix G) to show that the crystal growth rates (on a number basis) achieved in the test continuous A-Pan at Amatikulu were more than double those achieved on either the production continuous A-Pans at either Felixton or Maidstone.

It was within this context of the many unanswered questions about both the fundamentals and practice of operating continuous A pans that I resigned from my production position at Felixton and registered for full time research at the University of Natal to undertake a study into the dynamic behaviour and optimum control of a continuous pan. The scope of this research work is detailed in section 1.5 of this thesis. The ultimate objective was to provide clear recommendations on how a continuous pan should be operated in a production environment to achieve maximum performance. THS undertook to provide me with access to their factories, information and research facilities to support this project

After a period of three years of full time research, I was offered a position back at THS in their central technical department, where I continued the research part time. During this period I investigated techniques for reconciliation of mass balances and developed a simplified technique which could be applied using the numerical analysis capabilities of spreadsheets. The technique was initially applied to work on continuous centrifugals (Hubbard and Love, 1998) and is used in this research for analysing the results on full scale continuous pans. Whilst initially I was able to make some progress with the research, and the responsibilities of my position at Tongaat Hulett Sugar kept me involved in the operation, development and commercialisation of continuous pan

technology, it became increasingly difficult to devote sufficient time to completing the research.

I resigned from THS in 1997 to allow more time to complete the research whilst working part-time as an independent consultant. THS continued to provide me with access to their research facilities, specifically laboratory and pilot pans for the measurement of crystal growth kinetics.

# Acknowledgements

With this research having been conducted over an extended period of time, there are many people to thank, for their assistance, guidance and support.

It has been a privilege to have been a member of the team that developed the Tongaat-Hulett Continuous Pan, the focus of this research. The success of the pan, both technically and commercially is largely due to both the leadership and technical input of Dr Peter Rein. My thanks for his support for this research over many years.

This research would not have been possible without the support of the management and staff of Tongaat Hulett Sugar, covering production, technical services and research and development. The presence of many experienced and capable, engineers and sugar technologists provided an ideal environment for conducting research which has a close link to industrial scale operation.

The idea for this research germinated when I worked in production at the new Felixton mill in the mid 1980's. It was here that I was introduced to the practicalities of pan boiling in a production environment by experienced sugar technologists. I was also fortunate in being able to work closely with Richard Chilvers who shared and encouraged my enthusiasm for applying science rather than "standard practice" for solving production problems. Our collaboration resulted in the development of the "two step" technique for tuning pan feed controls and encouraged me to continue to look for more fundamental answers to production problems.

After I had left Felixton mill, the staff there continued to support my experiments to quantify sugar crystallisation and its control in a "real world" situation. Special thanks must go to Rob Archibald, Guy Montocchio and Rob Whitelaw for allowing me to meddle with their pan boiling processes and to Bill Elsworth, Andrew Gillespie, Dave Lees and Warren Reed for many modifications to the instrumentation and control systems.

The Tongaat Hulett Technical Management Department (TMD) provided excellent technical backup and support for my research. I was able to use, modify and construct new equipment at their expense (the sucrose solubility apparatus, the laboratory pan and the new pilot pan). The laboratory staff of TMD analysed many samples, using both conventional sugar industry analytical techniques and the image analysis program that I developed for determining crystal

# TABLE OF CONTENTS

# CHAPTER 1

## 1. Introduction

### 1.1 Readers Unfamiliar with Sugar Technology

This introductory chapter assumes a knowledge of the sugar manufacturing process and its terminology. For readers with an interest in the control, modelling and optimisation aspects of this thesis, but who are unfamiliar with the specifics of sugar manufacture, the necessary background is provided in subsequent chapters (in particular Chapter 3).

### 1.2 Pan Boiling for Sucrose Crystallisation

At the heart of the sugar manufacturing process is the operation of sucrose crystallisation. Despite the age of the industry, much of the technology of industrial sucrose crystallisation has remained an art rather than a science as other aspects of sugar technology have progressed. The skill of experienced operators (pan boilers) has been crucial to the operation of a sugar factory. This has been particularly so for raw sugar factories where the impurities in the raw material (either sugar cane or sugar beet) have an enormous influence on the crystallisation process.

In addition to a lack of scientific knowledge relevant to industrial sucrose crystallisation , two characteristics of the process have severely limited the range of techniques which can be applied to improve the process.

* Firstly, the low change in solubility of sucrose with temperature has relegated cooling crystallisation to a secondary process. Evaporative crystallisation (under vacuum) is the major crystallisation process.
* Secondly, the high viscosities of the impure sucrose solutions from which the crystals must be grown precludes the use of size classification by settling to selectively remove crystals from the process once they have grown to the required size, a mechanism often used in continuous crystallisers for other products (Rein, 1992).

Consequently, as other unit operations within the sugar factory were converted from batch to continuous operation, crystallisation continued to be carried out in batch evaporative crystallisers

under vacuum (vacuum pans).

In recent years there has been a slow but steady move towards continuous pan boiling. The first patent for a continuous vacuum pan was awarded in 1932, but it is only in the last approximately 25 years that continuous pan boiling has become a practical proposition (Rouillard,1988). The first continuous pan in the South African sugar industry was installed at the Maidstone factory in 1976.

## 1.3     Tongaat Hulett Sugar Company and Continuous Pan Boiling Technology

As described in the preface, this thesis is based on research which was conducted either as an employee of the Tongaat-Hulett Sugar Company (THS) or making use of their production and research facilities. The research has thus been conducted, and is best understood, within the context of Tongaat Hulett's efforts to perfect continuous pan boiling technology.

Tongaat-Hulett have been involved in continuous pan boiling from the time of the installation of the first production unit in South Africa, through to the development and marketing of their own design of continuous pan. Tongaat Hulett as a sugar production company, rather than an equipment manufacturing company, were able to combine detailed engineering design, considerable operating experience and research and development effort to produce a practically successful design which has achieved considerable commercial success. Tongaat Hulett sell pan designs directly to the Southern African Sugar industry but have used an established sugar equipment company in the United Kingdom ( Fletcher Smith) as agents to market their design to the rest of the world sugar industry. By the end of 1999 a total of 116 pans of the THS design were installed world wide (Cox, personal communication, 1999), making THS a world leader in continuous pan technology. For comparison, the other major design of natural circulation continuous pan (Fives Cail Babcock) at approximately the same time had manufactured 150 pans to their original design and 30 pans of a new design (Journet, 1999).

The significant engineering and scientific effort in achieving this success has been recognised locally by the award of both the 1993 Chemical Engineering Innovation Award of the South African Institution of Chemical Engineers and the 1994 Annual Award of the Associated

Scientific and Technical Societies of South Africa.

Tongaat Hulett's experience with continuous vacuum pans began when the first commercial unit in the South African Sugar Industry was installed at their Maidstone factory 1976. This pan, designed by Fives Cail Babcock (FCB) was installed to process C massecuite and although it demonstrated the potential of continuous processing, it required modification before acceptable performance could be achieved and, even then, was unable to meet its guaranteed capacity (Graham and Radford, 1977). Further efforts to characterise and optimise the performance (Mathesius, Graham and Pillay, 1978, Julienne and Munsammy, 1981) provided more operating data which confirmed the low heat transfer rates and demonstrated that the pans had poor massecuite flow characteristics.

THS began tests to see whether the benefits of continuous pan boiling could be achieved at minimal cost by converting batch pans into continuous pans (Rein, 1986). This began with the conversion of a batch pan at the Mount Edgecombe mill into a continuous C-pan which demonstrated improved heat transfer rates compared with the FCB pan (attributed to the vertical tube calandria) and improved flow characteristics (attributed to careful design of the massecuite flow path). The efforts in developing an alternative design of continuous pan were given extra impetus when THS took the decision to build a new sugar mill at Felixton ( Renton, 1985).As the largest sugar mill in South Africa at the time, it was to require six large continuous pans when constructed.

A particularly important question that needed to be answered for the design of the new Felixton mill was whether a continuous pan could be designed for producing A-massecuite. Whilst by that time, continuous pan boiling was proven on B and C massecuite, no factories were operating continuous pans on A-massecuite (Kruger, 1983, Rein, 1986). A brief test boiling of A massecuite in the FCB pan at Maidstone in 1977 had showed that the process was feasible but that encrustation of heating surfaces could be a significant problem (Kruger, 1983).

To test continuous boiling of A-massecuite more fully, a batch pan at the Amatikulu mill was converted into a six compartment continuous pan (Kruger, 1983, Rein, 1986). These tests proved that good quality crystal could be achieved with continuous A-pans, a particular concern since this is the final product of the factory. Whilst good evaporation rates were achieved, the pan did

not have suitable circulation and this resulted in rapid and unacceptable build-up of encrustation on the heating surfaces.

At this stage of the investigation, a new continuous pan was required to expand the capacity of the pan floor at the Maidstone factory. This provided THS with an opportunity to design and build a new continuous pan which would be the prototype for the pans required for the new Felixton factory. Although originally planned as a B-massecuite pan, provision was made to operate the pan on A, B or C-massecuite. Comprehensive testing on A-massecuite proved that this process was entirely feasible and led to the decision to install continuous A-pans at the new Felixton factory (Kruger, 1983). Testing of the Maidstone pan on all three grades of massecuite confirmed that the design had met the requirements of good circulation and had high heat transfer rates. With slight modifications, the design formed the basis for the six continuous pans installed in the new Felixton factory where continuous pans were used on all three grades of massecuite for the first time in South Africa (Rein, 1983).

Tongaat Hulett continued to advance the technology of continuous pan boiling in a number of areas, publishing many of the findings. A steady state computer model of a continuous pan was developed to analyse the results of performance tests (Hoekstra, 1985) and used to predict behaviour under different operating conditions (Hoekstra, 1986). Tracer tests were used to measure residence time distributions and estimate the flow characteristics of continuous pans (Rein, Cox and Love, 1985). The measurement of conventional electrical conductivity proved to be a less than satisfactory signal for the control of continuous A-pans and led Tongaat Hulett to develop a radio frequency conductivity measurement for this purpose (Radford and Cox, 1986). These RF conductivity probes proved to have a significant market demand and considerable further development was invested in this technology (Radford, Tayfield and Cox, 1988). The dynamic behaviour of feed control loops was investigated and a technique developed for setting the tuning parameters of the automatic controller (Love and Chilvers,1986).

With proven and competitive continuous pan boiling technology, the developments that Tongaat Hulett have made since the innovative new design of the mid eighties have been incremental but significant operating experience and performance data has been gathered (Rein, 1990, Rein, 1992, Rein and Msimanga, 1999). Whilst most applications have been in raw sugar processing, the pan has also proved successful on refinery recovery boilings (Schorn and Meadows, 1998).

## 1.4    Scope of this Thesis

The scope of the research for this thesis was defined to provide a better understanding of the dynamics and operation of continuous pans with the objective of specifying an operating policy which would maximise pan performance. Based on the experience of THS in the development of continuous pan boiling technology and a review of the literature, the approach taken in this research was to use a mathematical model as the basis for understanding pan behaviour. Where possible, the parameters of the mathematical model were to be determined by fitting the model to the results of plant scale tests to give a model which is capable of providing realistic predictions of industrial performance. Where it is not practical to vary parameters on an industrial scale, the model parameters were to be investigated by testing product streams from the local industry on a laboratory or pilot scale. This was deemed to be preferable to accepting published correlations with limited or unknown applicability (eg values determined for the Australian cane sugar industry).

The scope of the research is illustrated diagrammatically in Figure 1.1. Here it is possible to see the interdependence of the different aspects of the research and how they contribute to the overall objective of defining an optimal operating policy for a continuous pan.

The mathematical model is built up in a modular form, starting with a dynamic model of a single compartment. Single compartment models can then be linked together to produce a dynamic model of a multi-compartment pan. The steady state model is obtained as a special case of the dynamic model where the time derivatives are set to zero. The structure of the model is selected to provide a model that is appropriate for both control and optimisation studies. The growth rate dependency on supersaturation was determined by fitting the steady state model to full scale pan tests. The correlation to define saturation in impure solutions was investigated by measurements made using a specially designed laboratory apparatus. The dependence of crystal growth rate on level of impurity in the mother liquor was investigated both in laboratory/pilot scale batch pan boiling tests and by interpreting available industrial pan boiling data for different grades of massecuite.

The dynamic behaviour of the pan was investigated, both by simulation using the dynamic models of the pan, and by measurements on a full scale pan.

KEY

| Full Scale Continuous Pan Tests | Laboratory/Pilot Scale Batch Pan Tests | Laboratory Equilibrium Apparatus |

Development of a PC Based Control System

Measurement of Dynamics of Feed Control Loops

Measurement of Dynamics of Absolute Pressure Control

Measurement of Sucrose Crystal Growth Rates (Practically Achieveable)

Measurement of Sucrose Crystal Growth Rates (Effect of S.A. Impurities)

Measurement of Sucrose Solubility in Impure Solutions (S.A. Conditions)

Development and Evaluation of Feed Control Loop Tuning Techniques

Equation for Impurity Effect on Growth Rate

Practical Growth Rate Equation

Equation for Sucrose Solubility in Impure Solutions

Policy for Optimal Operation of a Multi-Compartment Continuous Pan

Dynamic Model of a Single Compartment of a Continuous Pan

Simulation of Dynamic Behaviour of Single Compartment

Dynamic Model of a Multi-Compartment Continuous Pan

Simulation of Dynamic Behaviour of Multi-Compartment Continuous Pan

Development of a Strategy to Stabilise Throughput by the Optimum use of Buffer Tanks

Steady State Model of a Multi-Compartment Continuous Pan

Simulation of Steady State Behaviour of Multi-Compartment Continuous Pan

Determination of Optimum Operating Profile for a Continuous Pan by Dynamic Programming

**Figure 1.1** : Diagrammatic representation of the scope of this research

The dimensions of the optimisation problem preclude the use of conventional optimisation techniques and necessitate the use of dynamic programming which uses Bellman's "principle of optimality" to overcome the "curse of dimensionality" (Bellman, 1957).

The long time constants for crystallisation in a continuous pan ( of the order of 5 to 10 hours) combined with the importance of steady state operating conditions for a continuous process results in a requirement for a steady production load if the optimal operating conditions are to be maintained. This requirement leads to a need to stabilise the production rate of a continuous pan through the optimal use of buffer tanks within the process.

The final objective of the different aspects of the research is to specify an operating policy for a continuous pan to enable it to achieve maximum capacity and performance , covering :

1       A specification of the optimal steady state operating conditions.

2       Recommendations on how to maintain this optimal state by;

    —       stabilisation of throughput by the effective use of buffer tanks.

    —       accurate absolute pressure control to avoid unwanted dynamic behaviour.

    —       correct operation and tuning of feed control loops to maintain stable conditions in compartments..

## 1.5       Structure of this Thesis

Following on from this introductory chapter, Chapter 2 provides a summary of published information on the fundamentals of sucrose crystal growth. This covers  information on the solubility and crystallisation kinetics of sucrose in both pure and impure solutions. It also gives some background on the measurements that are traditionally used in the sugar industry to characterise concentrations of sucrose and impurities in solutions and to quantify the size and spread in size of sucrose crystals.

Chapter 3 provides the background to the terminology and processes of the sugar industry that are applicable to the process of pan boiling (vacuum evaporative crystallisation). Beginning with a summary of terminology, the chapter then goes on to describe how sucrose separation is accomplished in a multistage process of crystallisation and separation steps with appropriate recycle streams, known as a boiling scheme. The dominant boiling scheme of the South African

Sugar Industry is described. Background is also provided on the technology of both batch and continuous pan boiling . Alternative measurements used to monitor and control the pan boiling process, and the control strategies that are employed in continuous pans are described.

With the background to this investigation into continuous pan boiling having been given in Chapters 1 to 3, Chapter 4 begins to describe the research personally undertaken to investigate continuous pan boiling. The chapter describes the mathematical model which provides the basis for understanding and optimising continuous pan performance. Starting with a review of published work on the modelling of pans, a state space model is formulated, using the approach developed originally by P G Wright (Wright and White, 1974). The innovation in this present work is the selection of variables and structuring of the model to provide a modular model suitable for both control and optimisation studies (specifically the dynamic programming study described in Chapter 8).

Chapter 5 describes work personally undertaken to determine a relationship to describe the solubility of sucrose in the impure solutions encountered in the South African sugar industry. The chapter describes the experimental apparatus, the experimental techniques and the collection and analysis of results. The result is an equation which characterises the solubility of sucrose under conditions of temperature and levels of impurities appropriate to A-massecuite pan boiling.

Chapter 6 describes the research personally conducted to determine the effect of impurities commonly found in local raw cane juices on the kinetics of sucrose crystallisation. This covers initial testing and method development on a laboratory scale batch pan followed by the design of a pilot scale batch pan specifically intended for collecting kinetic data applicable to full scale boiling. The well known difficulties of simulating pan boiling on a small scale (Clark, 1999) resulted in most of the work concentrating on method development with unfortunately very little reliable data being generated on the purity dependence of growth rate.

Since it is the crystal growth rate achievable in full scale pans that is important for optimising production, Chapter 7 describes detailed testing of a full scale production pan and the analysis of the results (by fitting the model developed in Chapter 4) to determine growth rate kinetics. Production constraints prevent significant purity variations in full scale testing and thus the

purity dependence of crystal growth rate is not determined by fitting the model to the data but rather taken as that derived from other sources (ie as described in Chapter 2 ,section 2.6 and in Chapter 6)

Chapter 8 describes the development of an optimisation technique based on dynamic programming and the mathematical model developed in Chapter 4 (incorporating the appropriate solubility and growth rate correlations developed in Chapters 5, 6 and 7 ). The optimisation technique is used to determine the optimum steady state conditions at which the pan must operate (ie the crystal content and supersaturation profile) to achieve maximum crystallisation performance.

Chapter 9 describes measurement and analysis of the dynamic behaviour of individual pan compartments to provide recommendations on how they can be most effectively maintained at the optimum steady state.

In Chapter 10, to provide further insights into the dynamic behaviour of the pan, the dynamic model developed in Chapter 4 is used to simulate the dynamic response of the pan. These quantitative simulation results are used to provide a better qualitative understanding of the dynamic behaviour of the pan. This is achieved by identifying and explaining the contributions of the three simultaneous mechanisms of concentration/dilution, "wash-out" and crystallisation to the overall dynamic response.

The long time constants traditionally encountered in continuous pan boiling (of the order of 5 to 10 hours) mean that for any change in throughput, steady state will not be achieved for at least this period of time, negating much of the benefit of knowing what the optimum steady state operating conditions should be . To stabilise pan throughput the factory buffer tanks must be used in an optimal way. Chapter 11 reviews the literature on strategies for the optimum use of buffer tanks and highlights the limitations of available theories for dealing with a sequence of buffer tanks in series. The development of a novel buffer strategy is described which uses Linear Quadratic Gaussian Control theory to handle multiple tanks in series. The performance and advantages of this novel strategy are demonstrated in the results of computer simulations and compared with simulations of one of the more advanced published strategies.

Chapter 12 describes the development of a computer control system to support this research, and provide a platform for control studies. The system uses a specific real time operating system (MultiDos Plus) and a structured programming language (Pascal) and shows how these two elements can be combined to achieve a flexible computer control system. The system is capable of being easily tailored to the requirements of different installations without the constraints which many commercial control systems have in terms of implementing advanced control strategies and numerical techniques.

Chapter 13 provides the final conclusions, summarising the recommendations for both what the optimal steady state conditions for a continuous pan should be and how the pan should be best maintained at these optimal conditions in a production environment. Specific recommendations are provided for the product streams that were tested in the research.

To improve the readability of the thesis, supplementary material is relegated to a number of appendices.

# CHAPTER 2

## 2.    Mechanisms and Rates of Sucrose Crystal Growth

### 2.1 General

The growth rate of sucrose crystals is a major rate limiting step in the sugar production process, particularly in raw cane sugar factories where impurities can significantly reduce the crystallisation rate. In particular, the crystallisation rate is the major factor in determining the installed capacity of the vacuum pans (evaporative crystallisers) and cooling crystallisers. (Heat transfer requirements can become the limiting factor at the high crystallisation rates achieved in white sugar pans of refineries but this is not normally the case in raw sugar factories). Since pans and crystallisers constitute a major capital investment, the process of sucrose crystallisation from aqueous solutions has been the subject of many investigations. These investigations range from studies of the fundamentals of pure sucrose solubility to more empirical studies of growth rates in the impure solutions of raw sugar factory syrups and much of the work has been summarised in review articles over the years (eg Honig, 1958, Smythe, 1971, van Hook, 1977, van Hook, 1981, Murandi et al., 1988, and van Hook et al.,1997).

Underlying the studies of crystallisation is the concept of solubility since this is fundamental to defining the driving force for crystallisation (viz. the extent to which the concentration greater than that at saturation). There is an extensive body of literature on sucrose solubility in both pure and impure solutions which is reviewed in this chapter. The area of interest for this thesis is sucrose solubility in relatively high purity cane sugar solutions (approximately 65 to 90 purity) at pan boiling temperatures (65 to 70°C), but unfortunately this is an area which has not received much attention in the literature. Fortunately there is well corroborated data on the solubility of pure sucrose solutions (section 2.2 ) and this is used as the basis for understanding and interpreting the solubility data that are available for impure solutions (section 2.3).

Whilst there is a coherence in the literature on sucrose solubility, a review of the literature on rates of crystallisation is apt to leave one with a feeling akin to that of Samuel Taylor Coleridge who complained that zoology as he studied it was so weighed down and crushed by a profusion of particular information, "without evincing the least promise of systematising itself by any inward combination of its parts," that it was in danger of falling apart. (Medawar, 1984). This is sadly similar to the comment of Smythe (1971) when discussing the state of sucrose

crystallisation research more than thirty years ago that "there is still, however, no generally applicable theory which allows a quantitative evaluation of factors which influence the important practical process of crystallisation from solution".

For the particular requirements of this thesis it is necessary to be able to predict quantitatively how fast sucrose crystals will grow as a function of operating conditions in industrial scale equipment - specifically vacuum pans. This has been the guiding principle in reviewing the published data on sucrose crystallisation and means that most of the quantitative data on crystallisation rates reported for laboratory measurements only has use in understanding mechanisms. The mechanisms of crystallisation are best understood for the simpler case of pure sucrose solutions (section 2.4). The effects of impurities on sucrose crystallisation are complex and particularly difficult to quantify effectively (section 2.5).

There is fortunately some published data on industrial and pilot scale crystallisation which have been analysed to provide some data on rates of crystallisation which are applicable to industrial scale pan boiling (section 2.5)

## 2.2    Solubility of Sucrose in Pure Aqueous Solutions

At a fundamental level of analysis, sucrose molecules can be considered to be held in aqueous solution by the attraction between the sucrose hydroxyl groups (eight per molecule) and the water molecules. In dilute solutions each sucrose molecule is surrounded by up to eleven water molecules which satisfy its attraction sites completely (Allen et al., 1974). Removal of water molecules from a solution will eventually result in a situation where there are insufficient water molecules to satisfy all the attraction sites of the sucrose present, and attraction between sucrose molecules will begin. Below a certain concentration, a sucrose crystal added to the solution will dissolve, indicating that the attraction of the solution is greater than the attraction of the crystal face. The concentration at which this dissolution no longer occurs, (and no growth of the crystals yet takes place) is defined as a saturated solution. The ratio of water molecules to sucrose molecules at saturation is dependent on temperature, and has been determined to be (Culp, 1981) :

$$N = 10.65 - 0.0674 \cdot T \qquad (2.1)$$

where :

$N$      is the water/sucrose molecular ratio

$T$      is the solution temperature (°C)

At concentrations above saturation, existing crystals will grow, but in the absence of crystals, no crystallisation will take place unless the concentration is high enough to overcome the high surface energy of "micro-packets" of sucrose molecules, causing them to grow rapidly to become a viable crystal nucleus (Wright, 1983). This formation of new crystals is known as "nucleation", "fine grain" or "false grain". The solubility of sucrose is more usually presented empirically in the form of the diagram shown in Figure 2.1.
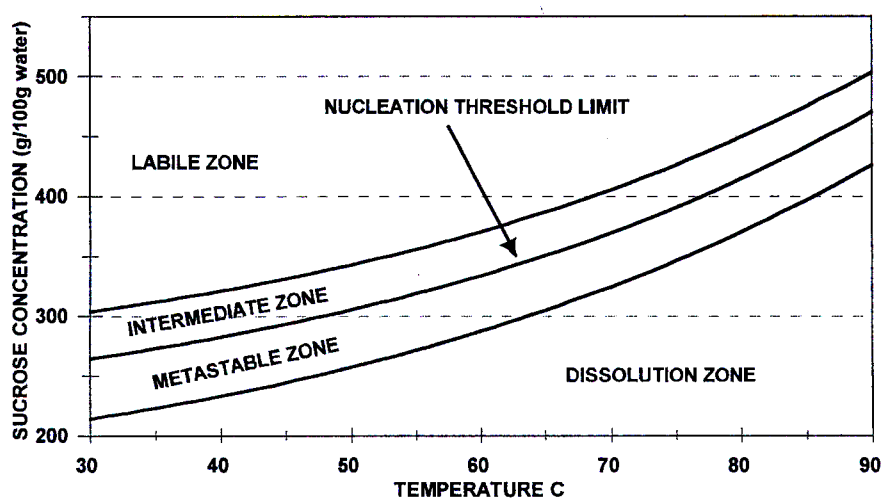


**Figure 2.1** Solubility diagram for aqueous solutions of pure sucrose

This concentration/temperature diagram is divided into four distinct zones, viz:

- The dissolution zone, where the mother liquor is below saturation and crystals dissolve.

- The metastable zone, where the mother liquor is above saturation and existing crystals grow but no new nucleation occurs.

- The intermediate zone, where the mother liquor is at a high enough level of saturation for new crystals to appear, but only in the presence of existing crystals, (i.e. a secondary process).

- The labile zone, where the mother liquor concentration is high enough to produce spontaneous and homogenous nucleation of crystals from the solution.

Of major importance is the exact specification of the saturation line which forms the boundary line between the dissolution and metastable zones. The original data of Herzfeld (1892) were found to be in error which encouraged further work to produce a definitive set of tables for sucrose solubility (discussion on the paper by van Hook and van Hook (1959)).

McGinnis (1978) has summarised the solubility data which have the tentative approval of ICUMSA (Schneider, 1979), based on the work of Charles (1960) and Vavrinecz (1962) but misquotes the correlations developed by these researchers. The correct correlations are :
Derived by Charles:

$$C_{s,p} = 64.397 + 0.07251 \times T + 0.0020569 \times T^2 - 9.035 \times 10^{-6} \times T^3 \qquad (2.2)$$

Derived by Vavrinecz:

$$\begin{aligned} C_{s,p} = {} & 64.447 + 0.08222 \times T \\ & + 0.0016169 \times T^2 - 1.558 \times 10^{-6} \times T^3 - 4.63 \times 10^{-8} \times T^4 \end{aligned} \qquad (2.3)$$

where ;

$\quad C_{s,p}$      is the concentration of a pure saturated sucrose solution expressed as a mass percent of the solution

$\quad T$      is the solution temperature (°C)

These correlations appear to have achieved general acceptance, with the cubic equation having been used by Broadfoot (1980) and the quartic equation having been used by Heffels (1986) and Bubnik and Kadlec (1992).

An alternative measure of the concentration of a sucrose solution is the sucrose to water ratio. For a saturated sucrose solution, this can be determined from the mass percent value as follows :

$$SW_{s,p} = \frac{C_{s,p}}{(100 - C_{s,p})} \qquad (2.4)$$

where ;

$\quad SW_{s,p}$      is the sucrose to water ratio of a pure saturated solution

## 2.3      Solubility of Sucrose in Impure Aqueous Solutions

The solubility of sucrose in impure solutions is different from that in pure solutions as a result of the physicochemical effects of the impurities. The magnitude and nature of the effects will depend on both the quantity and type of impurities present. Considering the range and variability of impurities that will be present under industrial conditions, it is not surprising that no definitive correlations for sucrose solubility in impure solutions are available. More work appears to have been done on solubility in impure beet sugar solutions than that in impure cane sugar solutions. Because of the similarities between beet and cane, some of the work on beet sugar is applicable to the cane sugar solutions.

The accepted method for expressing sucrose solubilities in impure solutions is to relate the solubility to that of a pure sucrose solution by using the concept of the "Solubility Coefficient" . The solubility coefficient, $SC$, is defined as ;

$$SC = \frac{SW_{s,i}}{SW_{s,p}}$$

(2.5)

where;

$SW_{s,i}$     is the sucrose to water ratio of the impure saturated solution

$SW_{s,p}$     is the sucrose to water ratio of a pure saturated solution at the same temperature

Vavrinecz (1978/79) provides a useful summary at the end of his review paper in which he classifies impurities into four groups viz.

1       Nonsucrose material which has no effect on either water or sucrose. Compounds which approach this ideal behaviour are carbohydrates without water of crystallisation which are very soluble in water.

2       Nonsucrose material which ties up water. Consequently less sucrose is found in solution, corresponding to the solubility power of the remaining water. Examples are water-of-crystallisation-free or strongly hydrated nonsucroses (fructose) and electrolytes which do not complex with sucrose (sulphates).

3       Nonsucrose material which binds with sucrose only. Compounds which approach this ideal behaviour are the alkali salts of week acids (eg alkali carbonates).

4       Nonsucrose material which binds with both sucrose and water. Most nonsucroses in beet

factory solutions are reported to belong in this class. In lower concentrations of these

impurities (ie in high purity solutions) a reduction in sucrose solubility is observed

(sometimes referred to as "salting out"). At higher concentrations of these impurities, on

the other hand, an increase in sucrose solubility occurs.

Wiklund (1946) was apparently the first to consolidate these effects into a simple rule. Based on

experimental evidence he suggested that the solubility coefficient was independent of temperature

and, for any particular impurities, only dependent on the impurity to water ratio of the solution.

Kelly (1954), in studying the effects of glucose and fructose on sucrose solubilities, showed a

linear relationship of the form :

$$SC = 1 - h \cdot IW$$

(2.6)

where :

   $IW$       is the impurity to water ratio of the impure solution

   $h$        is a positive constant which is a measure of the particular nonsucrose's ability

              to bind with water

He found that the value of $h$ for fructose was very low (viz. 0.02) indicating that fructose

approximated to the compounds of group 1 described above, whilst the value for glucose was

significantly higher (viz. 0.08) indicating that glucose would belong to group 2.

Wagnerowski et al. (1961) proposed that, above some minimum value of impurity/water ratio,

the solubility coefficient was linearly dependent on the impurity/water ratio ie ;

$$SC = m \cdot IW + b$$

(2.7)

where ;

   $m,b$      are constants, dependent on the nature of the impurities but independent of

              temperature or concentration of the solution

When $b = 1$ and $m$ is positive, this describes the behaviour of compounds which belong to group

3. Since most nonsucrose compounds also bind some water, a value of $b$ slightly less than 1 is

able to describe this effect.

The equation of Wagnerowski et al. does not apply for low impurity/water ratios where the

solubility coefficient must be equal to unity at zero impurity/water ratio and will normally first

reduce in value for an increasing impurity/water ratio before changing direction and becoming an

asymptote to the linear dependence of equation 2.7. Vavrinecz (1978/79) describes how

Wagnerowski's equation can be extended to accommodate this initial nonlinearity as follows ;

$$SC = m \cdot IW + b + (1 - b) \cdot e^{-c \cdot IW} \qquad (2.8)$$

where ;

   $m,b,c$    are constants, dependent on the nature of the impurities but independent of

            temperature or concentration of the solution

This equation describes compounds which belong to group 4 (with the water binding properties of the nonsucrose compounds asymptotic to a limiting value).The ability of this equation, to describe a range of different dependencies of solubility coefficient on impurity/water ratio is illustrated in Figure 2.2.
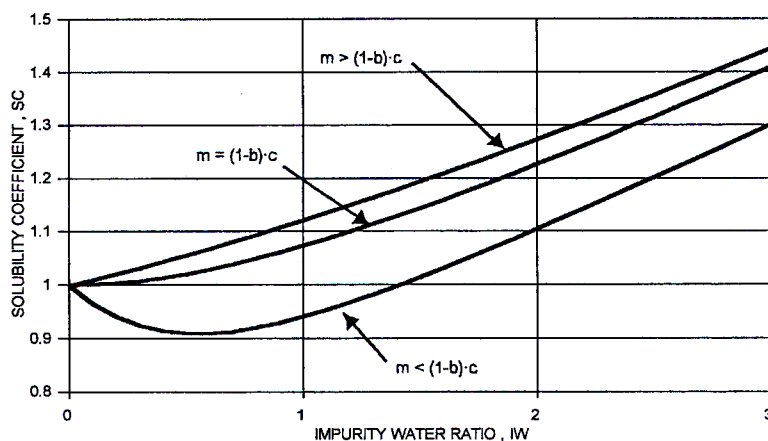


**Figure 2.2** Form of the Solubility Coefficient Function

Vavrincez (1978/79) has shown that the experimental results of numerous research workers in the beet sugar industry can be represented by this temperature independent function, including the early work of Schukow(1900), Nees and Hungerford (1936) and Grut (1936/37). He published tables of the three constants $m$, $b$ and $c$ for a range of actual factory molasses solutions. He quotes the range of values for the three constants for industrial sucrose solutions

as;     $m = 0.1$ to $0.4$

        $b = 0.5$ to $0.9$

        $c = 1$ to $3$

For those instances where the solubility coefficient can be shown to be temperature dependent, Vavrinecz recommends making the constants temperature dependent eg. ;

$$b = b_0 + b' \cdot T \tag{2.9}$$

The wide use of the "Polish Test" ( described by McGinnis, 1978) in the beet sugar industry is based on the assumption that the solubility coefficient is independent of temperature. In this test saturation is achieved by dissolution of crystals into molasses at a high temperature (normally 80°C as reported by Vaccari et al. (1993)). The solubility coefficient determined at this temperature is assumed to be unchanged at normal processing temperatures of between 40 and 70°C. Despite this assumption Vaccari et al. (1993) have shown significant variations in solubility coefficient with temperature for beet molasses, particularly at impurity to water ratios above 1. Bubnik and Kadlec (1992) analysed published data on the solubility of beet molasses and commented on the wide variability of solubility coefficient and also found evidence of significant temperature dependence.

The work on solubility coefficients within the cane sugar industry appears to be much more limited than that for the beet sugar industry. The work is often of an empirical rather than a fundamental nature where impurities are grouped together ( eg inorganic salts simply measured as "ash".) These empirical studies have usually had a specific aim in mind, which has influenced both the experimental method and the range of conditions studied. The four main reasons for determining the solubility of sucrose in impure solutions are ;

1.      To enable the supersaturation to be estimated for conditions during pan boiling (eg Broadfoot and Steindl, 1980, Quin and Wright, 1992) .

2.      To enable the supersaturation to be estimated for conditions during cooling crystallisation (eg Lionnet & Rein, 1980, Rein, 1980, Rouillard, 1980, Maudarbocus & White, 1978, Maudarbocus & White, 1983, Rouillard, 1978).

3.      To provide a measure of the maximum extent to which sucrose can be removed from the final molasses (eg Bruijn et al., 1972, Bruijn et al., 1980, Bruijn, 1977, Morera & Mischuk, 1978, Moritsugu, 1974).

4.      To determine the temperature to which final massecuites can be reheated before centrifugation without crystal dissolution. (eg Jesic, 1977).

The main techniques which have been used to estimate solubility are ;

1.      Saturation temperature measurement (eg Harman, 1933, Rush and Meredyth, 1959, Wright, 1978, Wright, 1980, Quin and Wright, 1992).

2.      Achievement of equilibrium conditions by crystallisation (eg Bruijn, 1977).

3.      Achievement of equilibrium conditions by dissolution (eg Broadfoot & Steindl, 1980).

4.      Modelling of growth conditions (eg Wright and White, 1974, Lionnet and Rein, 1980).

A summary of relevant correlations for solubility coefficients which have been developed by these methods for the cane sugar industry is given in Table 2.1. Temperature in °C is represented by $T$, and the reducing sugar to ash mass ratio by $RSA$.

| Code | Equation | |
|------|----------|---|
| A | $SC = 1 - 0.088 \cdot IW$ | (2.10) |
| B | $SC = 0.73 + 0.09 \cdot IW - 0.15 \cdot RSA$ | (2.11) |
| C | $SC = 1 - 5.75 / T \cdot IW^{(1+0.28 \cdot IW)}$ | (2.12) |
| D | $SC = 0.742 + 0.182 \cdot IW - 0.346 \cdot RSA$ | (2.13) |
| E | $SC = 1 - 0.0341 \cdot IW - 0.0295 \cdot RSA$ | (2.14) |
| F | $SC = 2.09 + 0.099 \cdot IW - 0.272 \cdot RSA - 0.00374 \cdot (T + 273)$ | (2.15) |
| G | $SC = 1 - 0.027 \cdot IW$ | (2.16) |
| H | $SC = 1 - 0.11 \cdot IW$ | (2.17) |
| I | $SC = 0.975 - 0.286 \cdot RSA + 0.04 \cdot RSA \cdot IW$ | (2.18) |
| J | $SC = 1 + IW \cdot (- 0.0425 + 0.0336 \cdot IW - 0374 \cdot RSA - 0.0017 \cdot T)$ | (2.19) |
| K | $SC = 1 + IW \cdot (0.0052 + 0.025 \cdot IW - 0.713 \cdot RSA)$ | (2.20) |
| L | $SC = 1 + (- 0.1371 + 0.005 \cdot IW - 0.0417 \cdot RSA \cdot 0.00209 \cdot T)$ | (2.21) |

**Table 2.1** Equations for Solubility Coefficient of Impure Sucrose Solutions

The origins of these equations and their ranges of applicability are given in Table 2.2. The question marks indicates a lack of information in the original source.

| Code | Reference | Temperature Range | IW Range | RSA Range |
|------|-----------|-------------------|----------|-----------|
| A | Wright & White (1974) | 60 to 70°C | ? | 1.3 |
|  | Developed by fitting pan model to data collected on pan boiling ||||
| B | Maudarbocus & White (1978) | ? | 2 to 5 | 0.6 to 1.7 |
|  | Based on unpublished data of Wright - measurement technique not described ||||
| C | Broadfoot & Steindl (1980) | 50 to 65°C | 0.5 to 3.5 | 0.68 to 1.71 |
|  | Equilibrium approached by dissolution of crystals in stirred vessel ||||
| D | Lionnet & Rein (1980) | 30 to 45°C | 3.3 to 7.3 | 0.6 to 1.6 |
|  | Developed by fitting a cooling crystalliser model to pilot plant data ||||
| E | Rouillard (1980) | 30 to 60°C | 0 to 2 | 0.64 to 1.36 |
|  | Equilibrium approached by dissolution of crystals in stirred vessel ||||
| F | Rouillard (1980) | 30 to 60°C | 2 to 5 | 0.64 to 1.36 |
|  | Equilibrium approached by dissolution of crystals in stirred vessel ||||
| G | Broadfoot (1980) | ? | ? | ? |
|  | Molasses from factory tests of continuous pan, saturated in laboratory batch pan ||||
| H | Maudarbocus & White (1983) | ? | ? | ? |
|  | Based on solubility data published by Smythe (1967) ||||
| I | Broadfoot (1984) | 45 to 50°C | 3 to 5 | ? |
|  | Reported as applying to unpublished data on Queensland molasses ||||
| J | Hoekstra (1989) | 40 to 50°C | 3.2 to 4.5 | 0.56 to 1.13 |
|  | Re-evaluation of the raw data from SMRI tests as described by Rouillard (1980) ||||
| K | Hoekstra (1989) | 45 to 50°C | 4.2 to 6 | 1.04 to 1.48 |
|  | Re-evaluation of the raw data from the tests of Lionnet & Rein (1980) ||||
| L | Hoekstra (1989) | 50 to 85°C | 0.8 to 3.6 | 0.96 to 2.43 |
|  | Re-evaluation of graphical data presented in Meade & Chen (1977) ||||

**Table 2.2** Origins and Ranges of Applicability of Solubility Coefficient Equations

To provide a comparative summary of the predictions of these correlations, Figure 2.3 gives a plot of the predictions of all of the above equations. For those equations which require it, the

temperature is set at 70 °C and the reducing sugar ash ratio is set at 1.0.
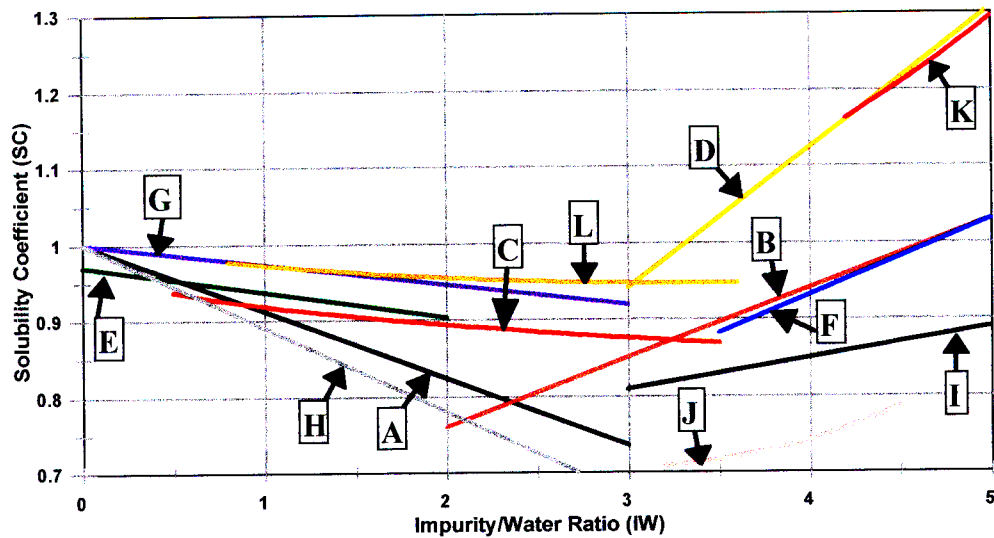


**Figure 2.3** : Correlations for sucrose solubility in impure cane syrups/molasses

From this graph, a number of issues are evident :

—       there is a wide variation between the predictions of the different equations.

—       there are two distinct types of dependence of SC on IW : decreasing SC with increasing
         IW at low IW and increasing SC with increasing IW at high IW.

—       the transition between the two regions may be anywhere between IW = 2 and IW = 3.6.

By definition SC should be equal to 1 at an IW value of 0. Most of the equations for low IW
values (A, C, G and L) do have this correct asymptote but most of those for higher IW values
(B, D, F and I) do not. The form of the equation proposed by Hoekstra (1989) (used for
correlations I, J and K) does have the correct asymptote but has only been used over a  limited
range of IW values. Equation 2.8 would probably apply to data across the full range of IW
values but unfortunately it does not appear to have been applied to cane sugar solubility data.

In the comparisons presented above, no direct mention has been made of the extensive body of
data for the South African Sugar industry on "target purity" (Bruijn, 1964, Bruijn et al., 1972,
Matthesius and Mellet, 1976, Bruijn et al., 1980, Rein and Smith, 1981). Because of the form
that these data are presented in, they cannot usually be interpreted in terms of a relationship
between SC and IW. The data do however provide valuable insights into sucrose solubility at low

purities and low temperatures.

The definition of a target purity involves the determination of the lowest practical purity to which molasses can be reduced by crystallisation over a long time (48 hours) and at a low temperature (40°C) and is known as a "boiling down test" . Lionnet and Rein (1980) published data on their boiling down tests which showed lower purities than the target purity equation of Matthesius and Mellet (1976), indicating that they had more closely approached equilibrium. Although the results of these boiling down tests are not presented in the way that they can be analysed in terms of an SC versus IW relationship, Lionnet and Rein (1980) did however show that the results of their boiling down tests were closely matched by the prediction of their equation (D) for an IW value of 5. In a subsequent paper, Rein and Smith (1981) analysed the data presented by Lionnet and Rein (1980) and some subsequent boiling down test results. They demonstrated that the target purity equation of the South African Sugar Milling Research Institute (SMRI) predicted equilibrium purity results two percentage units of purity too high when using the same analytical techniques for analysing the molasses samples. They also proposed a new target purity equation which was applicable to molasses analysed by the more modern methods of analysis using gas liquid chromatography - highlighting the important differences that result from using different analytical methods. Smith (1995) updated the target purity equation to accommodate conditions of low reducing sugar ash levels. This equation has been confirmed by Sahadeo (1998)

Crystallisation or dissolution of sucrose is driven by the degree to which the sucrose concentration is different from that at saturation. A number of different methods of quantifying this degree of "supersaturation" have been used in crystallisation research with their relative merits being at one time an issue of contention (see discussion on the paper by Golovin and Gerasimenko (1959)). The standard method of defining supersaturation subsequently defined by ICUMSA (Schneider 1979), and used in this thesis is :

$$SS = \frac{SW}{SW_s}$$

(2.22)

where :

$ss$     is the degree of supersaturation

$SW$     is the mass ratio of sucrose to water in the solution

$SW_s$    is the mass ratio of sucrose to water of a saturated solution at the same

temperature and the same mass ratio of non-sucrose (impurity) to water

## 2.4    Sucrose Crystal Growth from Pure Aqueous Solutions

Despite the limitations of the literature on sucrose crystallisation mentioned in section 2.1, it is

possible to glean from the literature a qualitative picture of the crystallisation process applicable

to industrial pan boiling. It is clear that crystallisation is, at least, a two step process as shown in

the diagram in Figure 2.4
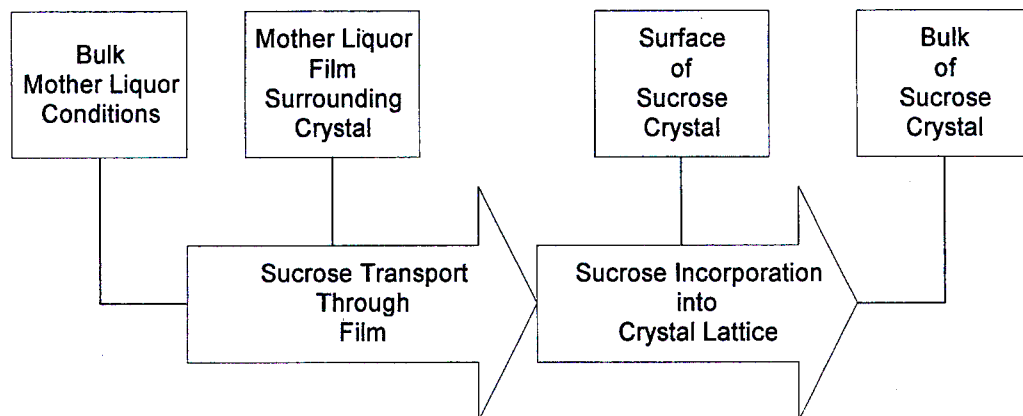


**Figure 2.4** : Basic mechanisms of Sucrose Crystallisation

The sucrose molecules must first be transported to the crystal surface. Once they are present at

the surface, they must be incorporated into the crystal lattice. It is useful to consider each of

these mechanisms individually before considering the overall effect of both mechanisms operating

in concert.

The first stage of sucrose transport is a typical chemical engineering mass transfer process of the

type associated with a convective boundary layer. It is convenient (and conventional) to define

the driving force in terms of supersaturation difference rather than concentration difference. The

mass transfer process (sometimes referred to as volume diffusion) is a first order process,

meaning that it has a linear dependence on the supersaturation driving force.

$$G = k_d \cdot os \qquad (2.23)$$

Where the over-saturation, *os*, is the extent to which the supersaturation is greater than one ie :

$$os = ss - 1 \tag{2.24}$$

The mass transfer coefficient, $k_d$ will be dependent on the hydrodynamic conditions. The mass transfer coefficient can be correlated by the used of the simplified Frössling equation (Maurandi et al., 1988, Maurandi, 1989) which uses the dimensionless Sherwood ($Sh$), Schmidt ($Sc$) and Reynolds ($Re$) numbers :

$$Sh = \Phi \cdot Re^{1/2} \cdot Sc^{1/3} \tag{2.25}$$

Where :

$$Sh = \frac{k_d \cdot l}{D} \tag{2.26}$$

$$Sc = \frac{\eta}{\rho \cdot D} \tag{2.27}$$

$$Re = \frac{u \cdot \rho \cdot l}{\eta} \tag{2.28}$$

Unfortunately most researchers do not appear to have analysed their data in this way nor do they supply sufficient experimental details for this to be done retrospectively. In consequence most laboratory data on crystal growth are only applicable to the specific experimental technique under which the data were gathered and cannot be compared sensibly with results gathered using different techniques. The applicability to industrial scale pan boiling is even more remote.

The mass transfer coefficient, $k_d$ ,is reported to have an Arrhenius type of temperature dependence. Smythe (1971) reports an activation energy of between 29 to 38 kJ/mole whilst Maurandi et al. (1988) report a value of between 10 and 20 kJ/mole on the basis of both their own and other researchers' work.

The incorporation step is significantly more complex and can be considered as being comprised of three steps viz

−       adsorption onto the surface of the crystal.

−       diffusion on the surface of the crystal towards active crystal sites.

−       incorporation into the crystal lattice at the crystal site..

Critical to this analysis is the existence of "active sites" on the crystal surface . Mullin (1992) describes a range of theories which have been employed to describe how the process is initiated (eg two dimensional nucleation) and propagated (eg incorporation at kinks). Burton, Cabrera and Frank (1951) developed a theory (BCF) based on growth spirals which are initiated by a screw dislocation in the crystal lattice. For sustained growth, the screw dislocations obviate the need for repeated two dimensional nucleation. These growth spirals are well documented for sucrose crystals (eg Albon and Dunning, 1959) and the BCF theory has been successfully applied to the analysis of measurements of the growth of single faces of single crystals (Nikolic and Valcic, 1991) The growth rate dependence on supersaturation predicted by the BCF theory is given by :

$$G = k_i \cdot \frac{os^2}{os_1} \cdot \tanh\left(\frac{os_1}{os}\right) \qquad\qquad (2.29)$$

This form of equation has the interesting characteristic of predicting second order kinetics at low levels of over-saturation (ie growth proportional to over-saturation squared) and first order kinetics (growth directly proportional to over-saturation) at higher levels of over-saturation, a characteristic which is often observed in practice. In a detailed application of the BCF theory as undertaken by Nikolic and Valcic (1991) the parameters $k_i$ and $os_1$ can be related to fundamental properties of the crystal such as edge free energies and numbers of dislocations on the crystal surface. The theory does predict that for large numbers of dislocations, the value of $os_1$ becomes small and the growth kinetics show very little second order dependence. For most practical applications, the parameters $k_i$ and $os_1$ would simply be selected to model the shape of the growth curve measured experimentally.

If the growth equation were applied to large numbers of less perfect larger crystals as will normally be encountered in industrial practice, $os_1$ will be small and the process will appear first order.

The surface incorporation coefficient, $k_i$, is also reported to have an Arrhenius type of temperature dependence. Maurandi et al. (1988) report that a range of published data is consistent in reporting an activation energy of between 70 and 78 kJ/mole.

The actual rate at which crystals will grow will clearly be dependent on the combined effect of these two mechanisms. Consequently one or other of the mechanisms may be rate controlling or they may both have a significant effect on the resulting growth rate. It appears to be generally accepted (eg Maurandi et al., 1988, Pautrat et al., 1996, van Hook, 1977) that for pure sucrose, surface incorporation is the rate controlling step at lower temperatures - ie below 50 to 60 °C. (Note that van Hook contradicts this in his review of 1981, but this is almost certainly an error in the writing rather than a disagreement with the consensus view.) Above the 50 to 60 °C range, it is the transport mechanism that is limiting whilst within the 50 to 60 °C range both mechanisms are expected to play a significant part.

Given the ranges of influence of the two mechanisms and their different activation energies, the overall apparent activation energy for the crystal growth process can be expected to vary between the two values as a function of temperature. Maurandi et al. (1988) have produced a graph based on published data which shows how the activation energy varies with temperature up to 80 °C (Figure 2.5).
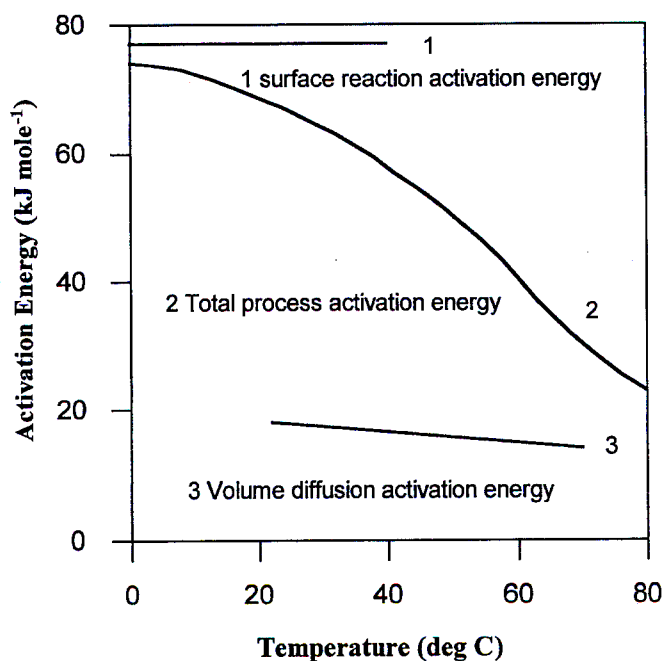


**Figure 2.5** Apparent Activation Energy for Sucrose Crystal Growth

The simplification that mass transfer is not limiting at low temperatures, (ie below 45 °C, Pautrat et al., 1996) must however be treated with caution since Smythe (1959) demonstrated clearly that even at 40 °C, the rate of crystallisation of stagnant crystals can be doubled by introducing agitation.

An alternative explanation of the mechanism of sucrose crystal growth, originally proposed by Silin is described by Smythe (1971). This is also a two stage process and has an intermediate concentration (or supersaturation) which separates the driving force into two sections. The transport mechanism is assumed to be first order whilst the incorporation mechanism is assumed to be second order. The equations for the two mechanisms can be combined to give an explicit equation describing the resulting growth rate in terms of the overall driving force (ie without any knowledge of the intermediate concentration.). This growth equation is similar to the BCF analysis in that it also predicts second order behaviour at low supersaturations and tends to first order behaviour at high supersaturations.

Unfortunately most of the published data on growth rates relate very narrowly to the procedures used in measurement and are not analysed in a way that contributes to a generalised quantitative description of crystallisation that can be universally applied. A major factor confounding any attempt to co-ordinate different studies is that growth rates of individual crystals differ widely. This has been well known for many years (eg McGinnis, 1971) and has been attributed to variations in numbers of defects or crystal dislocations. Laboratory investigations of crystal growth appear to have concentrated on removing this inherent (and important) variability from their experiments by careful selection and/or preparation of crystals (eg Smythe, 1959, Nicol and Parker, 1971) before beginning any growth measurements!

Recent studies (White et al., 1998) report that the variability in growth rate is a property of a crystal which remains with the crystal as it grows and that a variation in inherent growth rate of a factor of 10 between crystals can be expected. If a batch of crystals with the same growth history are examined, the fast growing crystals will be larger than the slow growing crystals. Whilst the previous statement may seem obvious when stated in this context, measurements of growth rates of large and small crystals can lead to the erroneous conclusion that large crystals grow faster than small crystals when the correct interpretation is that fast growing crystals are larger than slow growing crystals (given their common history). It is probable that this fact has

added to variations in the reported dependence of growth on crystal size.

The traditional McCabe's Law predicts that increase in length of a crystal with time is independent of the crystal length (ie size independent growth rate). Van Hook (1980) reported a weak dependence of growth on size, whereas Pautrat et al. (1996) report growth rates that increase by a factor of four when the size increases by a factor of three. Guimaraes et al. (1995) report size dependent growth rates in a fluidised bed crystalliser, but these might well be as a result of different hydrodynamic conditions of the experiments with different sizes. White and Wright (1971) showed that growth rates of multiple crystals could be modelled without assuming any size dependence but rather assuming a distribution in growth rates.

A further factor that may influence growth rate measurements has been reported by Grabka and Wawro (1998). They measured growth rates that varied by a factor of approximately two, depending on the time/temperature history of the mother liquor from which the crystals were grown for identical conditions during the growth period. They attribute this to an optimum size of packets of sucrose molecules developing in the liquor prior to crystallisation.

## 2.5    Sucrose Crystal Growth from Impure Aqueous Solutions

The complexities of sucrose crystal growth from pure solutions are greatly increased when considering the growth in impure solutions. The same basic two step growth process can be assumed to apply but, for the particular area of interest of pan boiling, the mechanisms by which the impurities can effect the growth rate are many and interacting. These are summarised most effectively in a diagram as shown in Figure 2.6

The major ways in which impurities affect growth rates are through :

–       altering the sucrose solubility (as described in section 2.3 ).

–       altering the mass transfer by an increase in liquor viscosity (either directly at a micro level or indirectly through macro effects on agitation and shear).

–       affecting the lattice incorporation mechanism (eg by adsorption onto the crystal surface or into the crystal lattice).
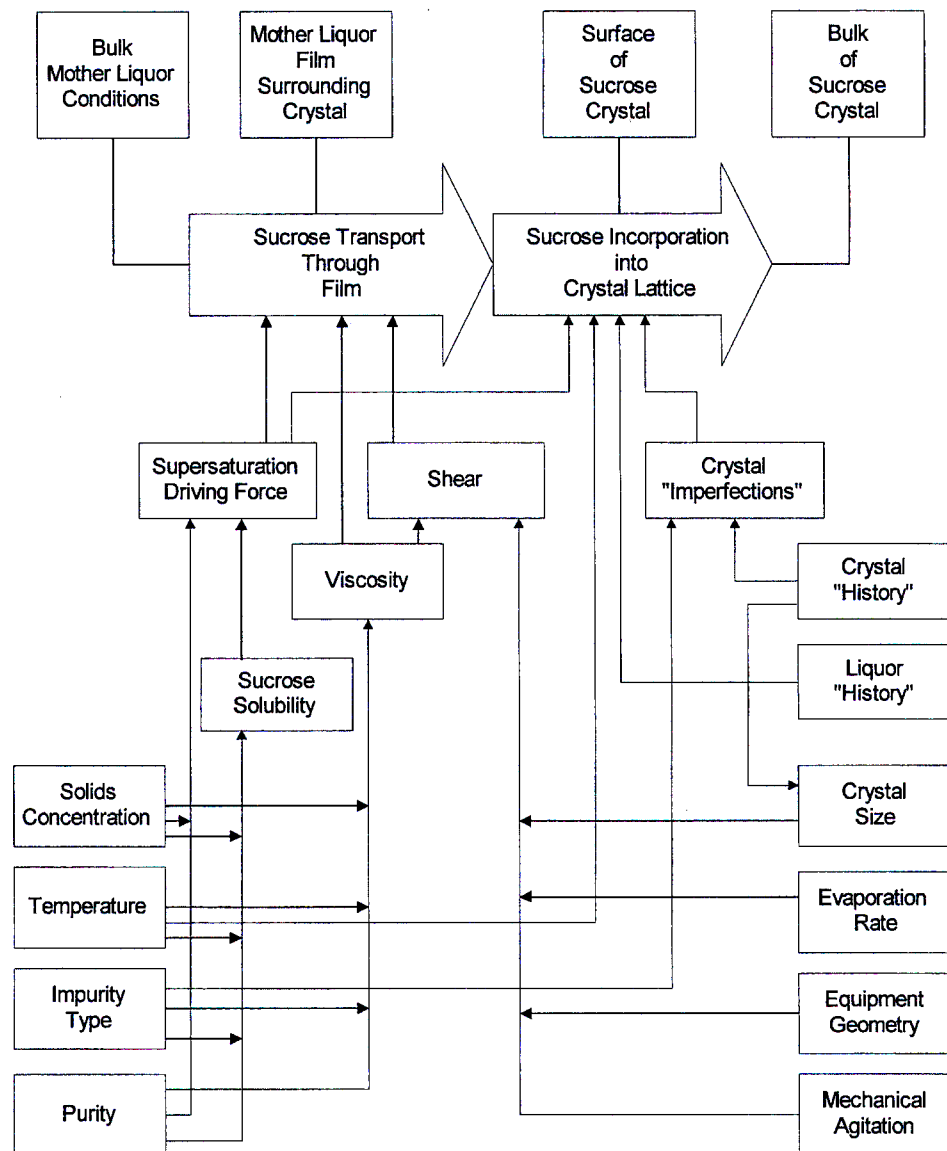
**Figure 2.6** : Factors affecting the mechanisms of crystal growth in impure solutions

Smythe (1971) has demonstrated in laboratory growth rate experiments how fructose and glucose slow down growth rates by retarding the transport mechanism whilst raffinose slows down growth rates by retarding the crystal incorporation mechanism.

The impurities that alter the crystal incorporation mechanism are often associated with changes in crystal shape. There is an extensive body of literature on sucrose crystal morphology (eg Kelly,1982) and the effects that impurities have on the shape (often called habit) of sucrose crystals. The changes in crystal shape result from the fact that the growth rates of particular

crystal faces are retarded by the impurities. It is thus inevitable that deformed crystal shapes go hand in hand with slower growth rates. Raffinose is reported to be the major contributor to crystal deformation in the beet sugar industry whilst oligosaccharides and dextran (a polysaccharide) have been suspected to be the major contributing impurities in cane sugar (Bubnik et al., 1992). Morel du Boil (1985, 1991, 1995, 1996) has investigated crystal habit modification in the local, South African, cane sugar industry where dextran levels are normally low. She has determined that the compounds which cause crystallisation problems in the local industry are primarily oligosaccharides. Morel du Boil (1985) also measured the effect of oligosaccharides on crystal growth rates (at 60°C, gentle agitation and supersaturation of 1.04) and plotted the data with a line proposing a linear decrease in growth rate with increasing impurity to water ratio. The data show a decrease in growth rate to one fifth of the rate for pure sucrose solutions as the impurity to water ratio increased from 0 to 0.6.

Broadfoot and Steindl (1980) measured the effect of the impurities in molasses samples from Queensland in Australia on crystal growth rates. Their measurements were done using a laboratory technique similar to that developed by Smythe (1959) with individual crystals held stationary in the flow path of a variable speed impeller. The measurements were performed at 50°C and at a supersaturation of approximately 1.23. The results show that stirring does have an effect on growth rates, and increasingly so at higher impurity to water ratios. This indicates the importance of the mass transfer mechanism under these conditions. Their results show an exponential dependence of growth rate on impurity water ratio of the same magnitude as found by Wright and White (1974) ie

$$Growth \propto \exp(-1.75 \cdot IW) \tag{2.30}$$

In comparison to the results of du Boil quoted above, this dependence predicts only a three fold decrease in growth rate as the impurity water rate increases from 0 to 0.6. Alternatively, fitting an exponential curve of this type to the data presented by Morel du Boil gives a coefficient of - 2.33.

The purity dependence of growth rate ( which is discussed further below in terms of the parameter $K_3$ of the growth equation of Wright and White ) measured by different researchers can be summarised as shown in Table 2.3.

| Source | $K_3$ |
|---|---|
| Wright and White (1974) | 1.75 |
| Broadfoot and Steindl (1980) | 1.75 |
| Li-Wu and Corripio (1985) | 2.45 |
| Morel du Boil (1985) | 2.33 |

**Table 2.3** The Dependence of Crystal Growth Rate on Impurity Concentration

Wright and White (1974) published a comprehensive equation for predicting crystal growth rates in vacuum pans. There are unfortunately a number of errors and contradictions in this often cited paper and these errors have been corrected here by reference to original sources and subsequent publications and also by ensuring consistent use of SI units.

$$G = K_1 \cdot (SS - (1 + K_0)) \cdot \exp(K_2 - K_3 \cdot IW) \qquad (2.31)$$

The parameters can be interpreted as follows :

$K_0$ is a constant to take account of the non-linearity of growth rate at low over-saturation

   (this growth equation only applies for values of SS > 1 + 1.5 $\cdot K_0$ where linearity prevails )

$K_1$ is the major proportionality constant relating growth rate to the degree of over-saturation

$K_2$ is used to describe the extent to which growth rate varies with temperature

$K_3$ describes the dependence of growth rate on the level of impurities present

The parameter $K_2$ defines an Arrhenius type of temperature dependence, defining it as :

$$K_2 = -\frac{Ea}{R} \cdot \left( \frac{1}{273.16 + T} - \frac{1}{333.16} \right) \qquad (2.32)$$

where   $Ea$ is the activation energy in kJ/mol.

        $R$ is the universal gas constant (8.314 $\cdot 10^{-3}$ kJ/ mol $^\circ$K ).

and    $T$ is the temperature $^\circ$C (clearly adjusting for growth rates around a norm of 60 $^\circ$C).

Wright and White (1974) also expressed the activation energy as a function of both temperature and level of impurities as follows :

$$Ea = 46.06 - 0.84 \cdot (T - 60) + 33.5 \cdot IW \qquad (2.33)$$

The equation is reported to have a temperature range of between 45 and 75 $^\circ$C and an impurity

to water range from 0 to 4. The dependence of activation energy on impurity to water ratio is apparently based on a single data point at $IW = 0.5$ and $T = 60°C$. The applicability of this dependence is thus dubious, confirmed by the fact that the equation predicts an activation energy of 180 kJ/mol at $IW = 4$ and $T = 60°C$. This is more than double the value reported for the crystal incorporation mechanism (as described in section 2.4). It is thus advisable to avoid this use of the dependence of activation energy on impurity to water ratio, as has been done by Broadfoot (1980), who uses the equation :

$$Ea = 62.8 - 0.84 \cdot (T - 60) \tag{2.34}$$

Wright and White (1974) determined the following values for the parameters of the growth equation by fitting a mathematical model of a batch pan to data from an experimental pan in a raw sugar factory:        $K_0 = 0.005$

$K_1 = 7420$        (microns/hr)

and        $K_3 = 1.75$.

Given the basis on which these parameters were determined, the growth equation has a much greater promise of applicability to industrial scale measurements than attempting to use measurements gathered from laboratory scale tests.

This growth equation of Wright and White has been used by a number of researchers over the years (eg Broadfoot,1980, Li-Wu and Corripio, 1985, Hoekstra, 1985 & 1986, Rodriguez et al., 1989, White et al., 1998, Vigh and Hurtado, 1999) but there is significant evidence that although the form of the equation is correct, the equation predicts growth rates that are substantially higher than have been achieved elsewhere.

Li-Wu and Corripio (1985) fitted the growth equation to data from a pilot pan and determined new values for the parameters $K_0$, $K_1$ and $K_3$. Their values of :

$K_0 = 0.005$

$K_1 = 6000$        (microns/hr)

$K_3 = 2.45$

predict growth rates 3.5 times lower than those of Wright and White at the impurity water ratios encountered towards the end of an A-massecuite boiling (ie $IW = 1.5$ ).

Hoekstra (1985) found that the Wright and White equation predicted growth rates that were ten

times greater than those measured in continuous pans in South Africa!

White et al. (1998) measured crystal growth rates in pure sucrose solutions in an agitated laboratory crystalliser at 50°C and also found values about one tenth of those predicted by the equation of Wright and White (1974).

Equation 2.30 does not directly predict the crystal growth rates that are achievable in industrial practice as these are also dependent on the degree of supersaturation that can be achieved without the appearance of secondary nucleation or false grain. The maximum supersaturation which can be tolerated in impure solutions without forming false grain (the false grain boundary) has been the subject of a number of investigations (Wright,1983).

Penklis and Wright (1963) developed the following correlation for purities in the range 55 to 80 :

$$SSn = 1.129 - 0.284 \cdot \left( \frac{100 - Pty}{100} \right) + \left( 2.333 - 0.0709 \cdot (T - 60) \right) \cdot \left( \frac{100 - Pty}{100} \right)^2 \quad (2.35)$$

where

| | |
|---|---|
| *SSn* | is the superatursaturation above which nucleation will occur (in the presence of existing crystals). |
| *T* | is the temperature at which growth is taking place, in °C. |
| *Pty* | is the purity of the mother liquor from which the crystallisation is taking place. |

Broadfoot and Wright (1972) developed the following correlation for purities in the range 70 to 100 (the full details of the test work being subsequently reported by Broadfoot (1980)) :

$$SSn = 2.864 - 3.516 \cdot \frac{Pty}{100} + 1.81 \cdot \left( \frac{Pty}{100} \right)^2 - 0.00177 \cdot CC \quad (2.36)$$

where   *CC* is the massecuite crystal content

For the investigations of this thesis, the correlation of Broadfoot and Wright (1972) has been assumed to apply over the purity range 100 to 70 with the correlation of Penklis and Wright (1963) assumed to apply over the range 70 to 55. At a temperature of 65°C and a 35% crystal content, this provides an estimate of the supersaturation boundary without a major discontinuity.

Given the variability in operating conditions which is normal in industrial operation, it is also assumed that a practical limit to supersaturation is given by taking 75% of the degree of over-saturation predicted by these equations. This implies somewhat better control than is implicit in the use of a "realistic 'safe' operating level" of 60% suggested by Broadfoot (1980). Using the assumption of 75% predicts operating levels of supersaturation similar to those quoted by Wright (1983) for cane sugar boilings viz.:

| | | |
|---|---|---|
| for high purity boilings during feeding | : | 1.05 to 1.10 |
| for high purity boilings during "boilback" and "heavy-up" | : | 1.15 to 1.20 |
| for low purity recovery boilings during early stages | : | 1.15 to 1.25 |
| for low purity recovery boilings at the end of the strike | : | 1.30 |

The predictions of the Wright and White growth equation (2.31), using levels of supersaturation limited by a "practically achievable" approach to the superaturation boundary are compared to industrial data in the next section.

## 2.6    Sucrose Crystal Growth Rates Applicable to Industrial Scale Pan Boiling

The growth equation of Wright & White (1974) has been shown in the previous section to have a form which is sufficiently detailed to be able to model the rate of crystallisation in industrial scale pan boiling. It has also been shown that if the numerical values of the parameters reported by Wright and White are used, the equation predicts growth rates that are significantly higher than those quoted by other researchers. Some of the discrepancies may be due to the propagation of errors in the printing of the original paper and others may be due to the inappropriate form of the dependence of activation energy on impurity to water ratio.

The Wright and White equation has been incorporated into a spreadsheet calculation to predict the crystal growth rates in pan operation, using the following assumptions and modifications

—      the activation energy is a function of temperature only (according to equation 2.33)

—      the printing errors in the original paper are corrected

—      pans operate at 75% of the levels of over-saturation at the nucleation boundary

—      the nucleation boundary is defined by equations 2.34 and 2.35 as described previously

Growth rates calculated in this way for purities from 100 to 50 can be compared with other

published data on growth rates that are reported to be achieved in industrial pans.

Wright (1983) reports the following values for average crystallisation rates for industrial batch pan boiling for the cane sugar industry :

| | |
|---|---|
| for high purity refinery strikes | 300 microns/hr |
| for high purity raw sugar strikes | 150 microns/hr |
| for low purity exhaustion strikes | 20 microns/hr |

To compare these values to the predictions of the Wright and White equation , it is necessary to assume an appropriate range of purities over which they apply. Wright (1983) provides a table of values for a material balance over a practical three boiling scheme as used in the Australian sugar industry. To convert this information into relevant purity ranges, the following assumptions have been used :

— The footing for the A-massecuite boiling is prepared from a magma of the same purity as the A-massecuite purity.

— The magma is washed up and the crystal content reduced to 15% before the growth phase starts (based on the results of Broadfoot, Miller and Bartholomew, 1996)

— The extent of crystallisation that takes place in the C pans is limited to achieving only 75% of the maximum crystal content as opposed to the 90% of the maximum crystal content achieved by the combination of pans and cooling crystallisers (Wright 1983)

The purity ranges estimated in this way are :

| | |
|---|---|
| for high purity refinery strikes | 99 |
| for high purity raw sugar strikes | 84 to 73 |
| for low purity exhaustion strikes | 64 to 46 |

Figure 2.7 below gives a graphical comparison of the Wright and White equation with these estimates of average industrial data.
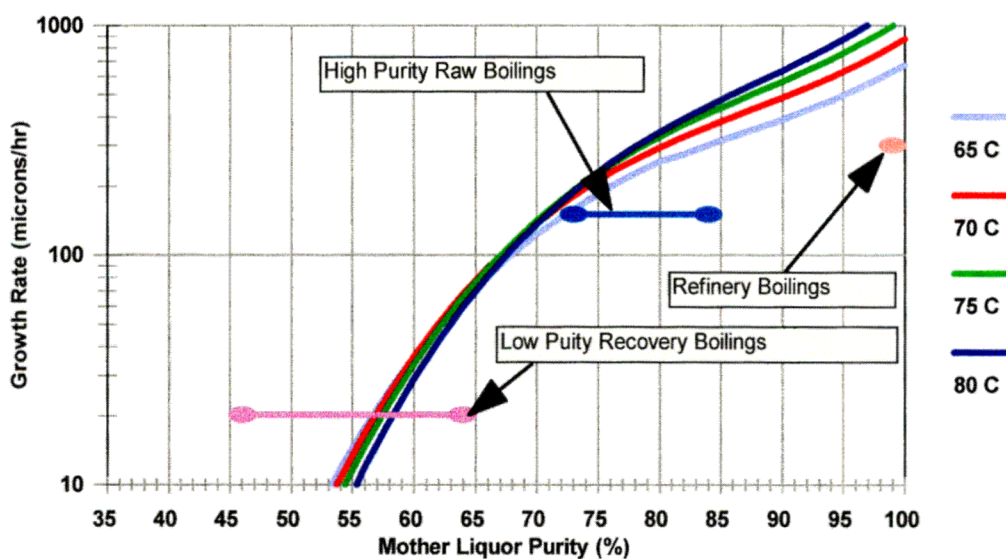
**Figure 2.7** Comparison of Growth Equation of Wright and White with average industrial data

It is clear that the equation of Wright and White predicts a strong dependence of growth rate on mother liquor purity. Over the purity range of a high purity raw sugar boiling the growth rate is predicted to vary by a factor of about 2 or more depending on temperature. For low purity recovery boilings, the purity dependence is even greater but the correlations do not apply over the full range so a comparative figure over the boiling range cannot be quoted. The strong dependence (ie steep slope of the curve) makes comparisons between the growth equation and the average values for different boilings difficult. The average growth rate is not a simple average of maximum and minimum growth rates. The average growth rates will fall between the maximum and minimum growth rates, but will depend on what portion of the growing cycle is spent at each growing condition. Since pan boiling is a fed batch process, this is not a simple dependence and is a function of the boiling strategy. There is, at least, a general agreement between the growth equation and the quoted values for raw sugar boilings in that the growth line passes between the purities that define the maximum and minimum growth rates for the case of low purity recovery boilings and close to the low purity end of the range for high purity raw boilings.

The predicted growth rate for refined sugar boilings (approximately 99 purity) is significantly higher than that reported as average industrial performance. This would be expected since, as discussed in the previous section, the crystallisation rate in refined sugar pans is often

constrained for a significant portion of the cycle by evaporation rate limitations.

In an attempt to consolidate knowledge on practically achievable sucrose crystal growth rates, data from the published literature which relates to pilot and industrial scale pan boiling has been re-evaluated to express results in terms of linear growth rates. Appendix G details the sources of this information and the techniques necessary to interpret them. The data are summarised in Figure 2.8 below.
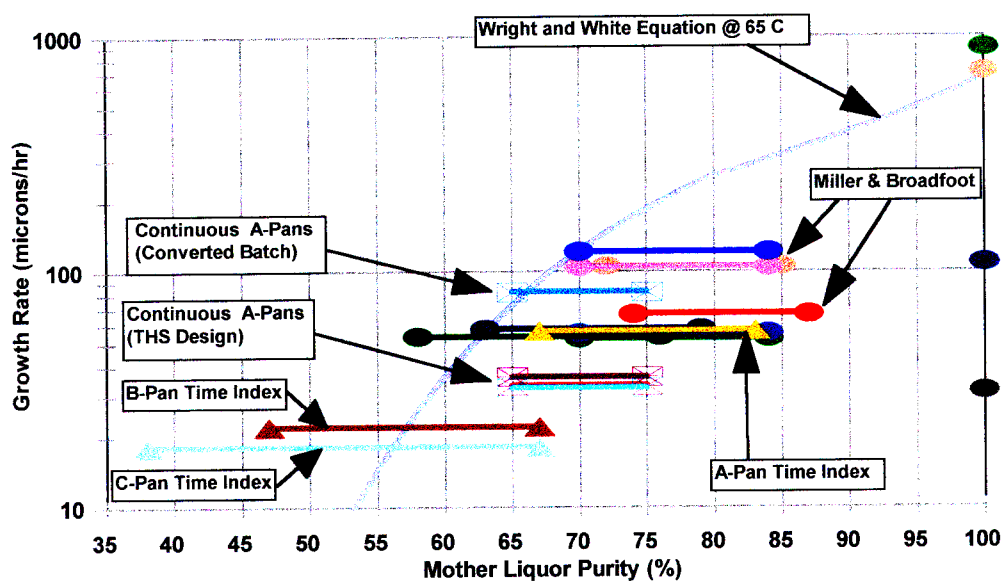


**Figure 2.8** Crystal growth rates on pilot and industrial scale pan boiling

The primary area of interest for this research is in high purity raw sugar boilings (ie A-massecuite boilings covering the range of approximately 90 to 65 purity). To help define the variation in growth rate with purity, data on refined sugar boilings and B and C-massecuite boilings in a raw sugar factory are also included.

Displaying the data on a single graph, as done in Figure 2.8, presents some difficulties with clarity but it does facilitate comparisons between the data. The four basic sources of data are displayed according to the following conventions :

—        solid triangles and lines

          interpretation of batch pan production data according to the concept of pan time index proposed by Archibald and Smith (1975).

- solid circles and lines

     Crystal growth rate measurements of Miller and Broadfoot (1997) on high grade batch

     pans in the Australian industry, corrected to a standard boiling temperature of 65°C.

- crossed squares and lines

     Crystal growth rate measurements in continuous A-pans, estimated from the crystal

     residence time measurements of Rein, Cox and Love (1985).

- solid circles

     Pilot (laboratory) and full scale refined sugar boilings as measured by Lionnet (1999).


The following conclusions are evident from the presentation of the data in this way :


- It is again difficult to make quantitative comparisons between the growth equation and

     the average values for the different grades of massecuite because of the steepness of the

     growth curve and the wide range of purities across a single boiling.

- For the high grade (A-massecuite) boilings, the growth equation clearly overestimates the

     growth rates that are achieved in practice.

- The growth equation gives reasonable approximation to the initial growth rates in refined

     sugar pans although it should be noted that industrial scale pans normally operate closer

     to 80 °C. The much lower values measured in the latter stages of refined boilings are in

     line with evaporation limited growth.

- The Australian data on growth rates in high grade batch pans show growth rates ranging

     between at least as fast as those estimated from pan time indexes for local batch pans,

     and up to twice as fast.

- Other than the continuous A-Pan at Amatikulu, the growth rates reported for the

     Tongaat-Hulett continuous A-Pans show values of only about 65% of those estimated for

     South African batch A-pans. This may be, in part, due to the fact that they only operate

     at the lower purity portion of the full range of purities encountered in A-massecuite

     boiling.

- The Amatikulu continuous A-pan showed growth rates about 45 % higher than those

     estimated for South African batch A-pans and more than double those for the Tongaat -

     Hulett continuous pan.


Unfortunately, the anomalous behaviour of the Amatikulu continuous A-Pan, which was a

conversion of a standard batch pan, cannot be checked experimentally as the pan was converted back into a batch pan shortly after the test work was completed on it.

The extent to which average growth rates are a function of the inherent growth properties of the particular impurities present in local sugar cane and to what extent they are a consequence of, and can be influenced by, selecting operating conditions during the process of pan boiling is the major focus of the research reported in this thesis.

# CHAPTER 3

## 3. Pan Boiling

### 3.1 Terminology

The sugar industry uses many terms with specific meanings which are well known and understood within the industry but can be a hindrance to understanding for people who are unfamiliar with them. It is possible to replace the "sugar industry jargon" with more generalised engineering and scientific terminology but this would make explanations and discussions significantly more ponderous. For example, a "batch pan" would become a "discontinuous vacuum evaporating crystalliser". To assist readers who are not familiar with sugar industry terminology a brief list of terms and their explanation is provided below.

Analyses and performance figures :

*absolute pressure*

> used to imply the pressure at which the contents of a pan are boiling, measured in absolute units (as distinct from the pressure of the heating steam, which may also be expressed in absolute units)

*boiling point elevation*

> The rise in boiling point of a solution (due to the dissolved solids) above the boiling point of water at the prevailing pressure.

*brix*

> The estimated dissolved solids content of a sample (expressed as a mass percent), usually determined by measuring the refractive index of a solution - sometimes referred to as refractometer brix. In some contexts the term will refer to the dissolved solids themselves (eg ....the total mass of brix in the vessel...).

*crystal content*

> The mass fraction of crystalline sucrose in a massecuite sample, usually expressed as a mass percent of crystal on mass of massecuite.

*crystal deposition rate*

> A term coined to quantify the crystallisation performed in a continuous pan, expressing the quantity of sucrose crystallised per hour per cubic metre of massecuite held in the pan.

*dry solids*

    The solids content of a sample determined normally by vacuum oven drying.

*exhaustion*

    Applied to a massecuite stream, it describes the percentage of the sucrose in the stream which is present in crystalline form. Applied to a process, it describes the percentage of the sucrose fed to the process which is recovered in crystalline form.

*Nutsch*

    As a verb this describes the process of pressure filtering a sample of massecuite. As an adjective, it describes the molasses separated from the massecuite and the analyses of this molasses and as such describes the properties of the mother-liquor of the crystallisation process

*pol*

    The estimated sucrose content of a sample (expressed as a mass percent), determined by measuring the rotation of polarised light when it is passed through a sample of the solution. The pol of a concentrated solution or solid is calculated from the measurement on a diluted solution.

*purity*

    The sucrose content of a sample expressed as a percentage of the soluble solids present. This may be either an apparent purity (calculated as pol as a percent of brix) or true purity (calculated as sucrose as a percent of dry solids)

*sucrose*

    The true sucrose content of a sample, the analytical method now accepted as most accurate being by high pressure gas/liquid chromatography.

## Products and Procedures

*A, B and C*

    Letters used to characterise the traditional three crystallisation steps (and the products and processes associated with them) of a three boiling system in a raw sugar factory (see section 4.2)

*false grain*

    Secondary nucleation of sucrose which can occur during the crystallisation process - an unwanted situation which adversely affects subsequent separation steps and degrades the quality of the crystal sucrose product .

*incondensible gasses*

> Constituents of a vapour stream which do not condense at around atmospheric temperatures. These will usually be the constituent gasses of air, but may include the products of unwanted chemical degradation such as carbon dioxide

*liquor*

> A term similar to syrup or molasses, but usually used for higher purity solutions

*magma*

> A mixture of sucrose crystals and mother liquor created by adding water or molasses to crystals

*massecuite*

> The mixture of sucrose crystals and their mother liquor during the crystallisation process

*molasses*

> A concentrated, impure solution of sucrose created by separating the mother-liquor from the sucrose crystals which have been crystallised from it.

*raw sugar*

> The product sugar from a cane sugar factory made by the first crystallisation from concentrated cane juice (syrup) from the extraction process

*refined sugar*

> A synonym for white sugar.

*remelt*

> A syrup created by dissolving crystals from a subsequent crystallisation for return back to the primary crystallisation process

*seed*

> Small crystals, or a slurry containing small crystals which are to be grown to larger sizes in the production process. As a verb this describes the process of initiating the crystallisation process by the addition of seed.

*strike*

> as a verb this refers to the process of emptying the massecuite from a batch pan at the end of the batch cycle. As a noun it refers to the complete cycle (as in .. the number of strikes boiled each day...)

*syrup*

> A concentrated, impure solution of sucrose normally created by concentrating

the juice obtained from the extraction process.

*vapour*

> Steam (at pressures either above or below atmospheric pressure) which has been produced by the boiling of some factory product. Steam used for the sugar boiling process is normally "vapour" which is produced by the multiple effect evaporation plant

*VHP sugar*

> A high quality raw sugar with low levels of impurity (contains approximately 99.4% sucrose), the initials standing for "Very High Pol".

*white sugar*

> High purity sucrose crystals (approximately 99.9 %) normally produced in the cane sugar industry by crystallisation from a liquor created by dissolving raw sugar (to produce a melt).

Equipment

*calandria*

> The indirect heating medium for a pan. Usually consisting of a steam chest and tubes so arranged as to allow steam/vapour to condense on the outside of the tubes whilst the massecuite circulates through the tubes where it boils as a result of the heat transferred.

*centrifuge or centrifugal*

> Usually of the perforated basket type and used to separate sucrose crystals from molasses

*crystalliser*

> A vessel used to achieve crystallisation by cooling and usually requiring mechanical agitation to promote heat transfer and prevent crystal settling

*pan  (or vacuum pan)*

> A vessel used to perform evaporative crystallisation under vacuum. It may be either a batch or a continuous process vessel hence batch pan or continuous pan

*remelter*

> Device for dissolving impure sucrose crystals to create a remelt stream to be recycled for reprocessing.

## 3.2    Boiling Schemes

In a raw sugar factory, sucrose and other soluble solids are extracted from the cane stalks by a combination of shredding, leaching and pressing to produce a juice with a solids concentration of approximately 12% . This juice from the extraction plant is first clarified and then concentrated in a multiple effect evaporator. The product of these processes is called syrup and contains the soluble impurities and the dissolved sucrose. To recover the sucrose from this impure solution, cane sugar factories use crystallisation both as a means to produce a solid (water free) sucrose product and as a purification process. Crystallisation from the syrup produces a brown sugar which can either be sold directly to consumers or can become the feed stream to a separate refining process where it is dissolved and purified by recrystallisation and other means to produce a high quality white sugar. The brown sugar is called variously A-sugar, VHP sugar, high pol sugar or raw sugar depending on its quality or the context in which it is being described. For cane sugar factories there is as yet no proven cost effective technology for producing high quality white sugar directly from the impure syrup. Most of the sugar produced in South African raw sugar factories is intended for refining and is produced as high quality VHP sugar. In addition to needing to produce this sugar with minimal impurities, a raw sugar factory must recover the maximum quantity of sucrose possible in crystalline form, by producing an impurities stream (final molasses) containing a minimum of sucrose. The processes or unit operations used to accomplish these two requirements are :

—    evaporative crystallisation under vacuum (pan boiling) to produce a massecuite (slurry of sugar crystals suspended in the mother liquor from which they have been crystallised )

—    Cooling crystallisation where further crystal growth is achieved by reducing the temperature of the massecuite over time whilst stirring.

—    centrifugation to separate the crystals from their mother liquor.

The particular way in which these unit operations are combined to achieve the two objectives of maximising sugar quality and sugar recovery is known as a "boiling scheme". The factors that need to be considered in selecting a boiling scheme are :

—    syrup quality (ie concentration and type of impurities)

—    capital cost of equipment for each unit operation

—    relative values of sucrose sold as sugar and sold in molasses

—    the product specification for the sugar.

Wright (1983) and Chen and Chou (1993) provide useful descriptions of the more common boiling schemes that are used in the cane sugar industry. The South African sugar industry has effectively standardised on a three boiling partial remelt scheme because of the requirements of centralised marketing of high quality export sugar. This scheme (not modified as subsequently suggested by van Hengel, 1983) is shown in the form of a simplified process flow diagram of Figure 3.1.
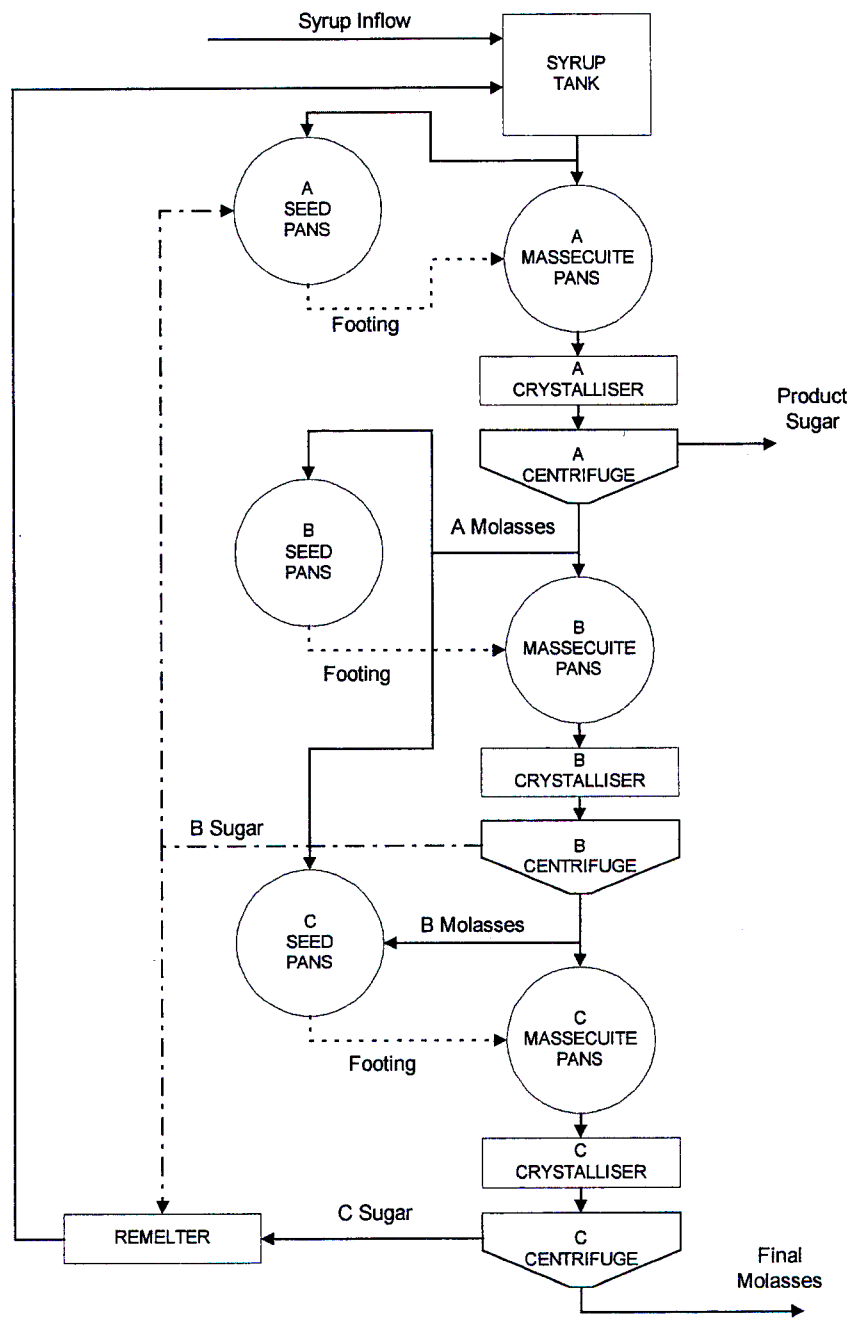


**Figure 3.1** Standard South African Three Boiling Partial Remelt Scheme

Archibald and Smith (1975) reported on the ability of this boiling system to accommodate variations in the quantities of sucrose and impurities which need to be processed. van Hengel (1983) provides some background to the original formulation of the boiling scheme and how it has altered slightly over the years. He also proposed a slight modification to the boiling scheme which was subsequently implemented in a factory (de Robillard and van Hengel, 1984).

A measure termed "exhaustion" is used to quantify the performance of each stage of boiling (ie the combined performance of pans, crystallisers and centrifugals). The exhaustion of a stage is the percentage of sucrose in the massecuite stream which appears in the sugar stream. With this boiling scheme there is a strong incentive to maximise the exhaustion of the A massecuite because any sucrose not removed in a first pass through the "A station" must be recycled either as remelt or magma if it is to recovered as product sugar. Increases in sugar recycle of this kind increase energy consumption, require more capital and result in increased losses due to chemical degradation.

With this boiling scheme, the B and C sugars are of similar purity to the incoming syrup. As a consequence, the purity of the A seed boiling is approximately the same as that for the A massecuite boiling which uses the A seed as a footing. This is in contrast to the situation with the C boilings where the C seed is boiled at a higher purity (using A molasses) to ensure a good quality and uniform crop of crystals. The purity of the C massecuite then drops throughout the C massecuite boiling where B molasses is used as the feed material.

The consequence of approximately constant purity throughout the A massecuite boiling is used to advantage in simplifying the optimisation problem addressed in Chapter 8.

## 3.3    Batch Pans

Batch pans are the process equipment which has traditionally been used in the sugar industry for growing sugar crystals by evaporative crystallisation under vacuum. The design and operation of these units is well described in standard sugar technology texts (eg Chen and Chou, 1993, Hugot, 1986 ) and review articles (Wright, 1974, Wright 1983). Only a brief background is provided in this chapter.

Batch pans have been used in the sugar industry for over a hundred years, and have evolved over time with the improvements being based on a mixture of experience, common sense and science. Unfortunately the complexities of three phase flow (crystal, mother liquor and vapour bubbles) have been difficult to model and attempts at applying engineering calculations to improve the basic design of pans has had limited success. These problems are described in some detail in Chapter 6 in relation to the design of an experimental batch pan.

A diagram of a typical modern batch pan as currently designed by Tongaat-Hulett Sugar is given in Figure 3.2 below.
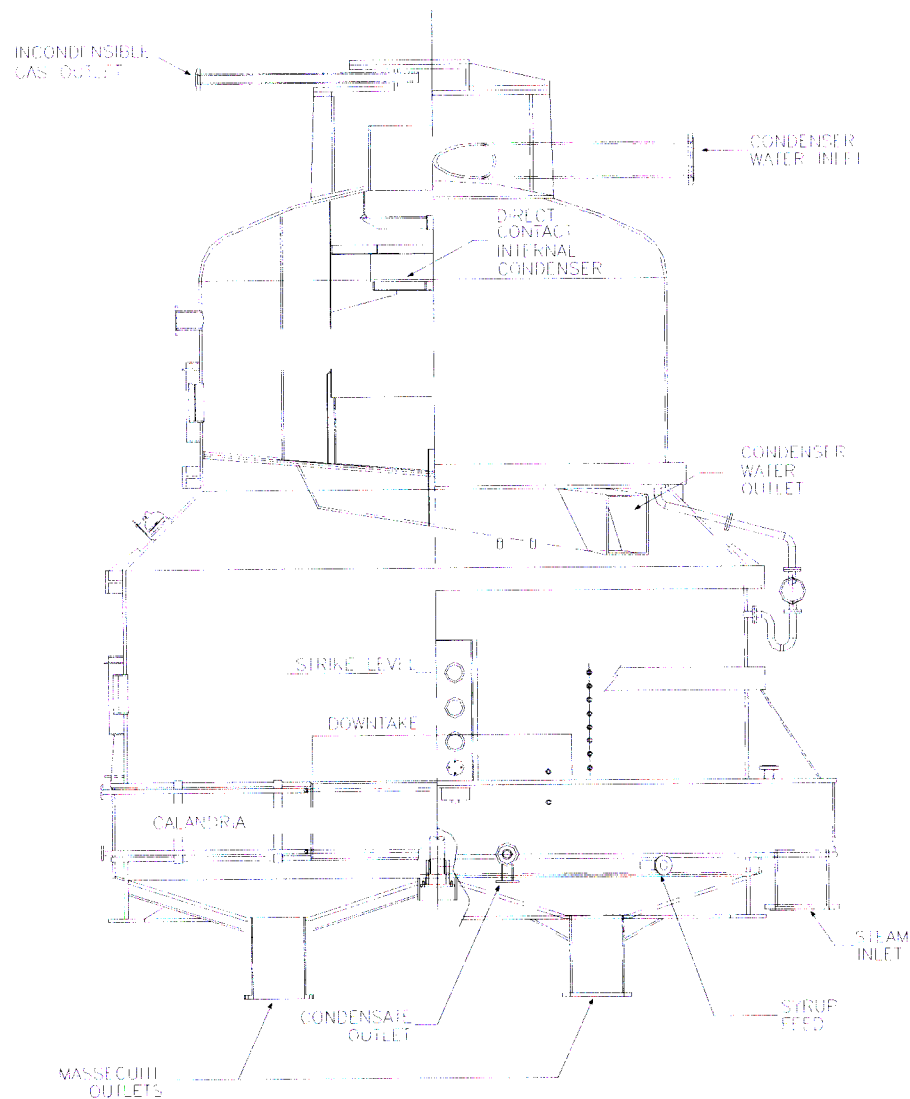
**Figure 3.2** Batch Pan of Tongaat Hulett Design

The main features of the pan are

—       a vessel, primarily a vertical cylinder, which is capable of operating under full vacuum ( operating conditions can be as low as 8kPa absolute )

—       a heating calandria formed by vertical tubes between two horizontal tube plates. The tubes are 100mm internal diameter. The steam condenses on the outside of the tubes whilst the massecuite is inside the tubes where it boils.

—       a central "down-take" which allows the massecuite which is pumped up the tubes by the boiling action to be circulated back to the bottom of the tubes.

—       feed pipes which allow molasses and water to be distributed into the boiling massecuite below the level of the tubes.

—       a bottom of the vessel which is shaped both to promote circulation of the massecuite in the pan (avoiding dead areas) and to allow full drainage of the viscous massecuite via drain valves.

—       an entrainment separator (eg a set of baffles) to remove any droplets of liquid from the vapour before it leaves the vessel.

The vapour outlet is connected to a condenser ( the pan shown in Figure 3.2 has the condenser constructed within the body of the pan) which is conventionally of the direct contact type. To allow the pan to be boiled under vacuum, a vacuum pump is necessary to remove any gas which is not condensed in the condenser (mostly air which leaks into the pan). Some batch pans, particularly those used for producing refined sugar, are fitted with stirrers in the downtake to promote circulation. Most pans used in raw sugar factories rely on the natural circulation caused by the massecuite boiling up the tubes (the thermosyphon effect). Pans without stirrers often make use of jigger steam. This is the addition of steam directly into the massecuite through a distributor below the calandria. The bubbles so produced rise up through the calandria tubes and promote circulation.

When no stirrer is present, the circulation is primarily dependant on the evaporation rate. Thus, to achieve a variation in the effective evaporation rate, water may be fed to the pan to cancel the concentrating effect of all or some of the evaporation.

The procedure for growing crystals in a batch pan varies slightly depending on the specifics of the particular massecuite being produced. Details of the various options are well described by

Tayfield et al. (1980), in terms of the requirements of automating the pan boiling procedure. The sequence required for a slurry seeded B-massecuite gives a reasonably comprehensive summary of the steps of the pan boiling procedure :

- fill the pan with A-molasses to a level just above the calandria.
- concentrate the molasses to a level appropriate for seeding (ensuring that the liquid level does not drop below the top of the calandria).
- stabilise the concentration at this value.
- seed the molasses with an appropriate quantity of slurry (finely milled white sugar suspended in alcohol).
- hold the pan on water for a period at this concentration to allow seed development.
- reduce the concentration slightly (thinning) to prevent any further secondary nucleation.
- allow grain to grow (bringing the grain together) without significant addition of new mother liquor - achieved by feeding with water or a combination of water and molasses.
- once a reasonable level of crystal content has been achieved, proceed with crystallisation with full feeding of molasses.
- once the pan is full, concentrate to the point where the crystal content impedes circulation.
- discharge the pan contents.

To achieve the maximum crystallisation performance from a batch pan, there are a number of principles which must be adhered to. These are discussed in Chapter 8 in relation to the determination of optimal operating conditions for pan boiling.

## 3.4     Continuous Pans

Many of the processes in the sugar industry were originally conducted in batch mode (eg clarification, evaporation, cooling crystallisation, centrifugation). Over the years these have been converted to continuous processes. As discussed briefly in Chapter 1, pan boiling was one of the last unit operations to be converted to continuous operation and the early development has been reviewed in the literature survey by Rouillard (1988).

The development of the continuous pan has taken a significantly different route to the development of continuous crystallisers that are used in other industries (Mullin, 1992,

Mersmann, 1995) for two major reasons. Firstly, the requirements for a narrow size distribution of product sucrose crystals precludes the use of mixed suspension mixed product removal (MSMPR) crystallisers. Secondly, the high viscosities of sugar liquors and the small differences in density between sucrose crystals and the mother liquor prevent the use of crystallisers which rely on gravity separation and recycle of small crystals.

The route followed in the design of continuous pans has been to accept that the unit will operate with an input of seed massecuite (normally prepared in a batch pan). The continuous pan is then designed with a flow path that provides an approximately equal residence time for all the seed crystals. This average residence time must be long enough for the crystals to achieve the necessary growth. The pan must obviously be provided with the necessary heating surface and feed system to allow feed (syrup or molasses) to be added and concentrated as crystallisation takes place, as happens in batch pans. The time dependent growth of a batch pan is thus converted to a position dependent growth along the flow path of the continuous pan.

Two broad approaches to providing a flow path with narrow spread in residence times have been used in different designs of continuous pans. One involves the use of a long narrow flow path whilst the other uses the conventional chemical reactor technique of a number of continuously stirred tank reactors (CSTRs) in series. A brief summary of commercial designs which fall into these two categories is given below. Many publications have tracked the development and commercialisation of these pans and so, where possible, only more recent references are provided here.:

Long Flow Path Designs

   Langreney Pan (Langreney, 1977)

      Originally designed as a rectangular vessel with a long narrow flow path, the design was subsequently modified to achieve the same effect in a vessel built in the shape of a ring (doughnut). The heating is via a calandria with vertical tubes, as in a conventional batch pan.

   Racecourse Pan (McDougall and Wallace, 1982)

      Constructed as two 13m long vessels each divided in half lengthwise . The massecuite flow path is created by connecting the two halves of each vessel in series and then connecting the two vessels in series, resulting in a total flow path length of 52m. The calandria is constructed by welding square steel tubes

together (with spacers so as to provide a steam flow path).

## CSTR based designs

### Seaford Pan (Goddard, 1991)

This is a multi-compartment stirred pan. It has heating plates and a low installed heating surface to make it applicable to early stages of crystallisation where crystal contents and evaporation requirements are low.

### BMA - VKT Pan (Bosse, 1996)

A design based on connecting four or five conventional stirred batch pans in series. The pans are mounted one above the other in a "tower" to save floor space and to provide the head necessary to drive the massecuite from the one compartment to the next without the necessity for inter-stage pumping.

### Fives-Cail Babcock (FCB) Pan (Journet, 1999)

A multi compartment pan, originally designed with vertical heating plates. Subsequent designs had horizontal tube heating and most recently, mechanical stirring is now offered for each compartment.

### The KNK Pan (Gebler and Bubnik, 1997)

Developed on low purity beet massecuites in the Czech Republic, this design with six compartments and heating by horizontal U tubes is similar to the FCB design.

### Sugar Research Institute - Australia (SRI) Pan (Broadfoot, 1999)

A multi-compartment pan with varying compartment sizes. Heating is by a calandria with vertical tubes. The bottom of the calandria is sloped (and thus uses a range of tube lengths) in order to promote good circulation.

### Tongaat-Hulett Sugar - Fletcher Smith (THS-FS) Pan (Rein and Msimanga, 1999)

The development of this pan has been discussed in some detail in Chapter 1. The multi-compartment pan with vertical tubular calandria has proved successful in terms of both cost and performance.

The THS-FS pan is the design which has been the focus of the research reported in this thesis. Typical drawings in figures 3.3 and 3.4 show the construction of the pan in elevation and plan respectively. The pan is shown in elevation with an integral entrainment elimination device and direct contact condenser as is usually the case in the Southern African Industry. The pan is

shown with ten compartments, but this may vary with different designs. The calandria has a single steam inlet and operates at a common pressure for all compartments.
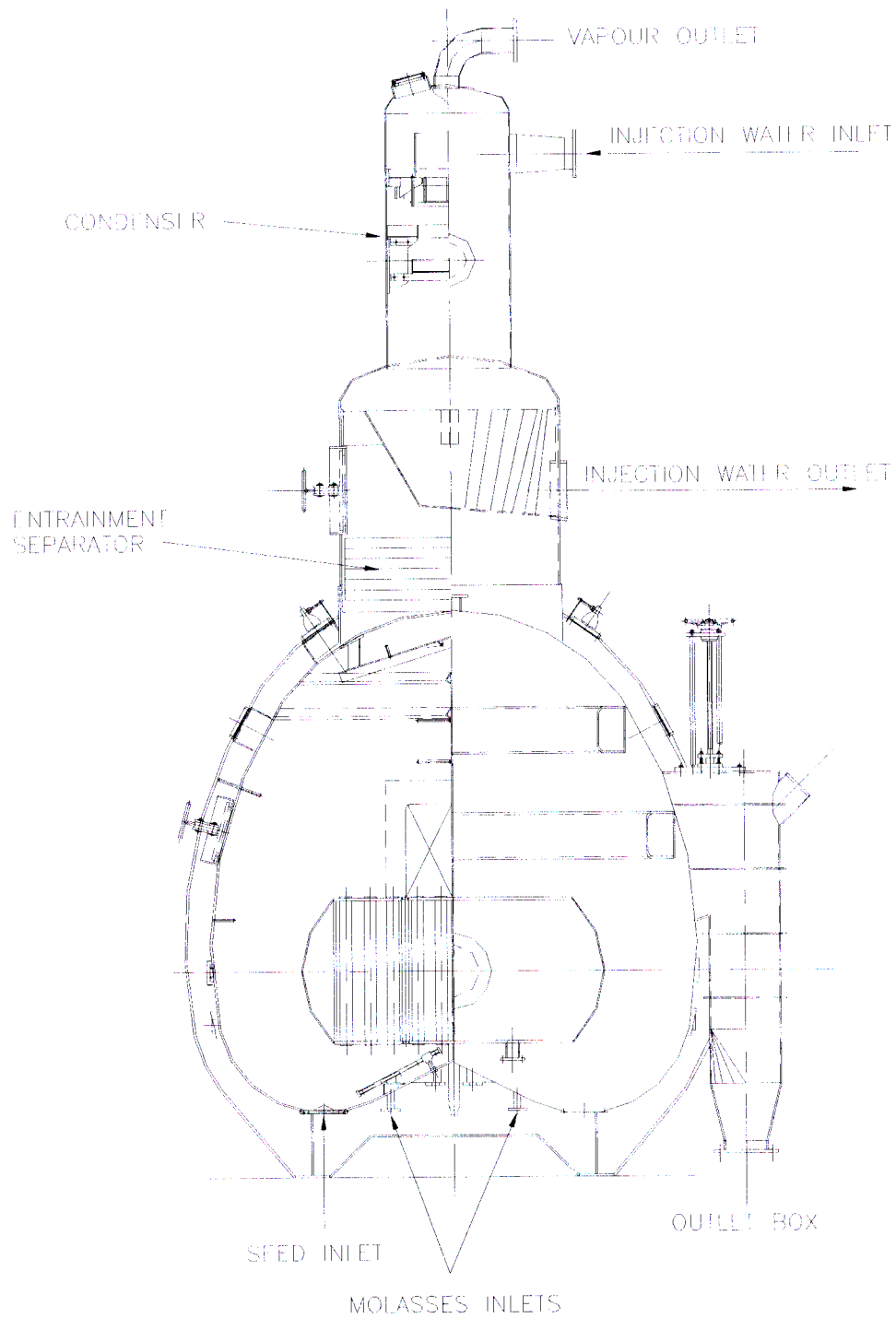


**Figure 3.3** End Elevation view of THS-FS Continuous Pan
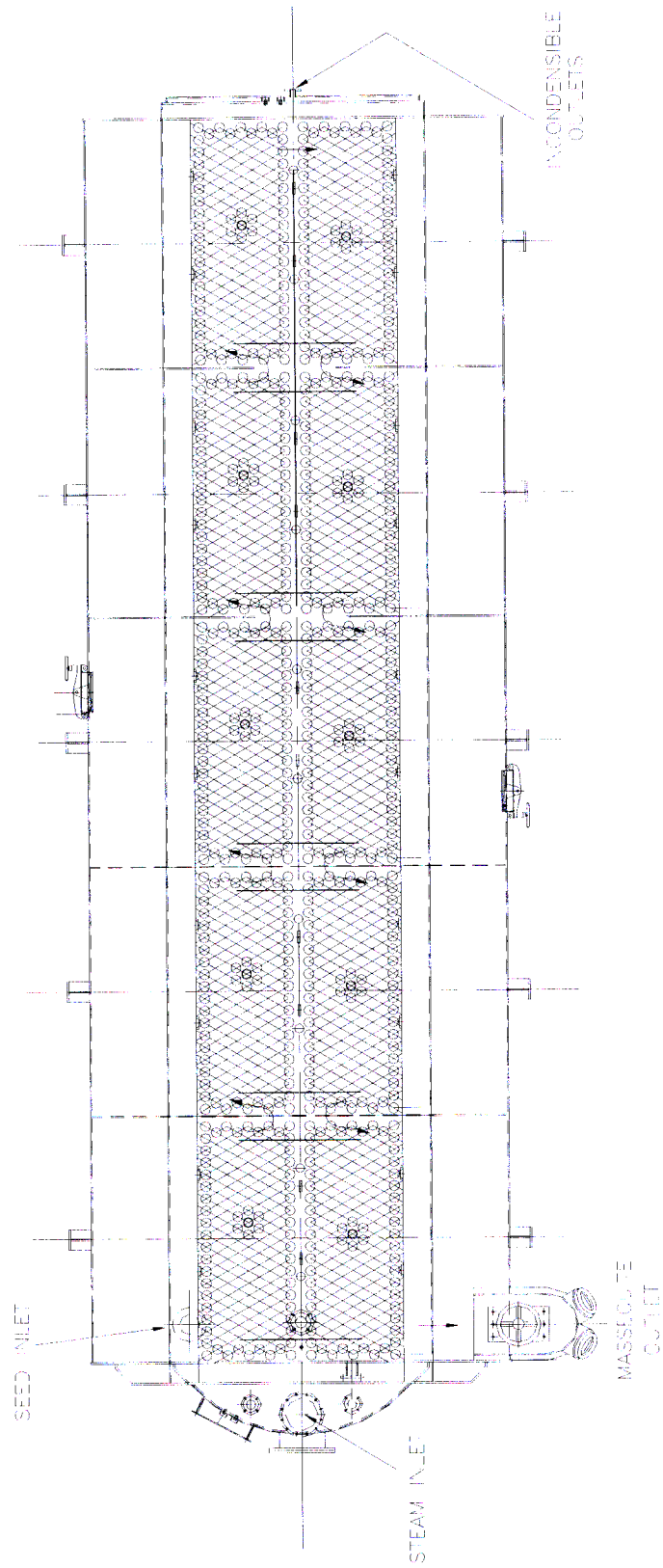
**Figure 3.4** Plan view of THS-FS Continuous Pan

Some pans have been designed with a calandria that is divided into two sections , each with its own steam inlet, which can be operated at different pressures.

## 3.5     Laboratory Measurements for Pan Boiling

Effective pan boiling requires the normal range of analytical laboratory measurements for monitoring performance. These techniques are well described in the manuals of laboratory procedures for the sugar industry (Anon, 1985, Anon 1991, Schneider, 1979).

As is evident from the discussions of the mechanisms of sucrose crystallisation in Chapter 2, the major measurements of interest are the levels of sucrose (both as crystal and in solution), water and impurity present in a sample. Crystal size is also important but measurement of this requires a different type of technique and is discussed in detail in Appendix A.

Unfortunately the analytical procedures which have been adopted for use for monitoring and controlling factory performance have been selected for their benefits of simplicity, speed and repeatability. For accurate analysis, more complex procedures are available, but are normally only performed for special investigations or on weekly composite samples. These analyses are not normally available at factory laboratories, but are conducted at better equipped and staffed central laboratories.

The techniques of interest in this work are those used to measure total dissolved solids content of a solution (or by difference its water content) and its sucrose content.

The approximate measurement used to estimate soluble solids content is "brix" which is based on the measurement of the refractive index of the sample. The approximate measurement used to estimate the dissolved sucrose content is "pol" which is based on a measurement of the rotation of polarised light by the sample. Both of these tests are accurate for pure sucrose solutions but are increasingly in error as the level of impurities increases. The magnitude of the errors are dependent on the nature of impurities which are themselves dependent on seasonal, climatic and geographic variations and can be expected to vary slowly at a given sugar factory. This allows a weekly determined correction factor to be applied to the average pol and brix data to correct the mass balances.

The accurate measurement for dissolved solids (often referred to as dry solids) is by vacuum oven drying or by a Karl-Fisher titration to determine the moisture content. The accurate measurement for sucrose content is by high pressure gas liquid chromatography (HPGLC).

When a purity (sucrose as a percent of soluble solids) is calculated from pol and brix readings it is referred to as apparent purity, and when it is calculated from sucrose and dry solids analyses, it is referred to as true purity.

There are advantages and disadvantages to be weighed when deciding on which analytical techniques to use for experimental work, particularly for high grade raw sugar boilings where the levels of impurity are comparatively low. During the early development of high grade continuous pans by THS (Rein et al., 1985) , numerous samples of syrup  massecuite and molasses were analysed by both the approximate and accurate analytical  procedures ( pol, brix , sucrose and dry solids). This (unpublished) data showed that :

–       within the range of variability,  pol and sucrose values were equal (ie no offset)

–       the dry solids results were slightly greater that the brix results (contrary to accepted behaviour)

The anomaly in the dry solids results was subsequently attributed to problems with the vacuum oven drying procedure.

Given this lack of benefits of the extra analytical load demonstrated in this earlier work on high grade continuous pans, this present work has concentrated on using conventional pol and brix analyses. This has an advantage that the measurements are directly comparable with factory performance figures. However, given the variability in the effect of the level and type of impurities on pol and brix readings, it was decided to investigate methods of correcting pol and brix readings to give unbiased estimates of  sucrose and dry solids. This would be particularly advantageous for applying to mass balances. The significance of the differences between the approximate and accurate analyses was also highlighted when analysing the results of the tests to measure the solubility of sucrose in impure solutions (chapter 5).

The issue of developing correlations to estimate one type of measurement from another has been addressed by a number of authors. Archibald and Smith (1975) developed correlations to

estimate refractometric brix from an earlier analytical technique of spindle brix. Batterham Frew and Wright (1974) proposed the following correlation for estimating dry solids concentration from the brix output of an on-line refractometer :

$$DS = brix - 8.68 \cdot \left( 1 - \frac{Pty}{100} \right) \tag{3.1}$$

Matthesius and Mellet (1976) proposed a correlation to estimate true purity from refractometer gravity purity. Saska and Oubrahim (1989) subsequently used this relationship to estimate dry solids content from refractometric brix according to the relationship :

$$DS = \left( \frac{0.0093}{Suc} + \frac{1.013}{brix} \right)^{-1} \tag{3.2}$$

Maurandi et al. (1988) proposed a simple proportionality constant to relate water content by the Karl Fisher procedure to that estimated by refractometric brix.

Hoekstra suggested the correlation given by equation 3.3 for correcting brix readings to provide an estimate of dry solids content. This has been used by Hubbard and Love (1998) for performing mass balances over a high grade centrifuge.

$$DS = brix \cdot (1 - 0.00066 \cdot (brix - pol)) \tag{3.3}$$

This equation was developed by analysing the results of a number of other researchers who had been measuring the properties of C-massecuite and C-sugar in studies of C-centrifugal performance. Hoekstra also included some data on average C-molasses analyses for the entire South African sugar industry. The format of the equation is correct in that it predicts that dry solids is equal to brix for pure sucrose solutions (ie those for which pol = brix). However the ability of the equation to accurately correct measurements in the range of A-massecuite boiling was not checked when it was formulated. The errors between the prediction of equation 3.3 and the original raw data (covering the low purity range) are shown in figure 3.5. The errors are calculated as the predicted dry solids from equation 3.3 (termed $DSp$ ) less the measured dry solids concentration ( termed $DS$). All these dry solids concentrations are expressed as mass percent of total mass.
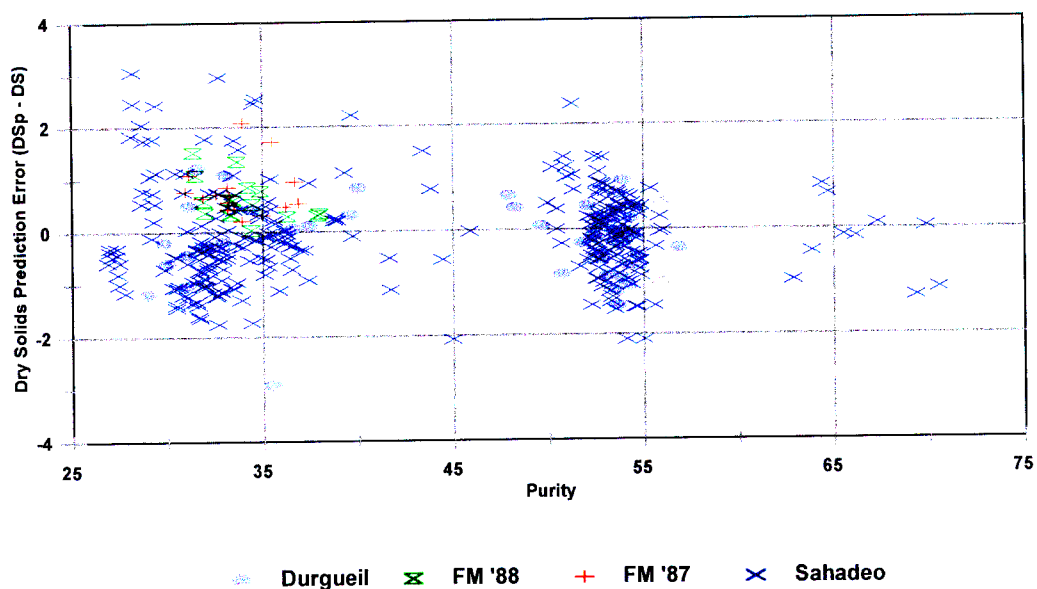
Figure 3.5 Errors of equation 3.3 for predicting dry solids from brix and pol readings

Subsequently some data became available which could check the validity of equation 3.3 at higher purities. A sugar industry sponsored study was undertaken at the Felixton factory in 1990 to quantify the relative extent to which losses occurred from cane crushing to concentration to syrup and from syrup to raw sugar and final molasses. The weekly average syrup samples were analysed for dry solids as well as brix and pol. The prediction error of equation 3.3 applied to these data is shown in Figure 3.6, where the scale of the y-axis which shows the magnitude of the error has been kept the same as in Figure 3.5. It is clear that the equation makes appropriate corrections in this high purity range and is thus suitable for use in correcting data measured on A-massecuite.
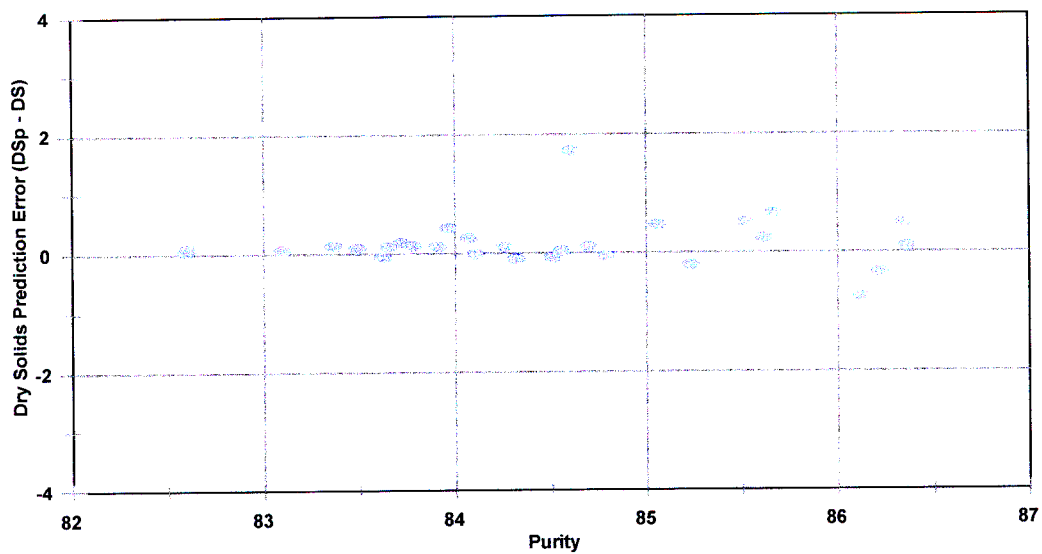
**Figure 3.6** Errors in prediction of dry solids in syrup using equation 3.3

Hoekstra also proposed a correlation for correcting pol readings to obtain an estimate of the true sucrose content. This proposal was not based on any analysis of data but relied on the following assumptions :

- the difference between pol and sucrose remains in a constant ratio to the amount of non-sucrose (ie the difference between dry solids and sucrose)

- the nature of this relationship can be determined for the final molasses from a factory (available throughout the local industry on a weekly basis) and then applied to any other process stream in the factory

- although the impurities are known to change through the factory, the high purity products, whose impurities are most different from final molasses, will have the smallest corrections and thus the importance of this effect is greatly reduced.

Mathematically this can be expressed in terms of a constant , $K$, as follows:

$$K = \frac{pol - Suc}{DS - Suc}$$

(3.4)

This relationship can be manipulated to give another constant, $R$, which is given by :

$$R = \frac{Suc - pol}{DS - pol}$$

$$= \frac{-K}{1 - K}$$

(3.5)

This constant can be included in the following identity :

$$Suc = pol + (DS - pol) \cdot \frac{(Suc - pol)}{(DS - pol)}$$

$$= pol + (DS - pol) \cdot R$$

(3.6)

Using dry solids ($DS$) estimated from equation 3.3, and the value of $R$ which can be calculated from the weekly data published for final molasses, it is possible to estimate the true sucrose value from pol data using equation 3.6.

The data from the industry sponsored survey mentioned above has been used to check the ability of this technique to estimate the sucrose content of a high purity streams (syrup and mixed juice). This is shown in Figure 3.7 below.
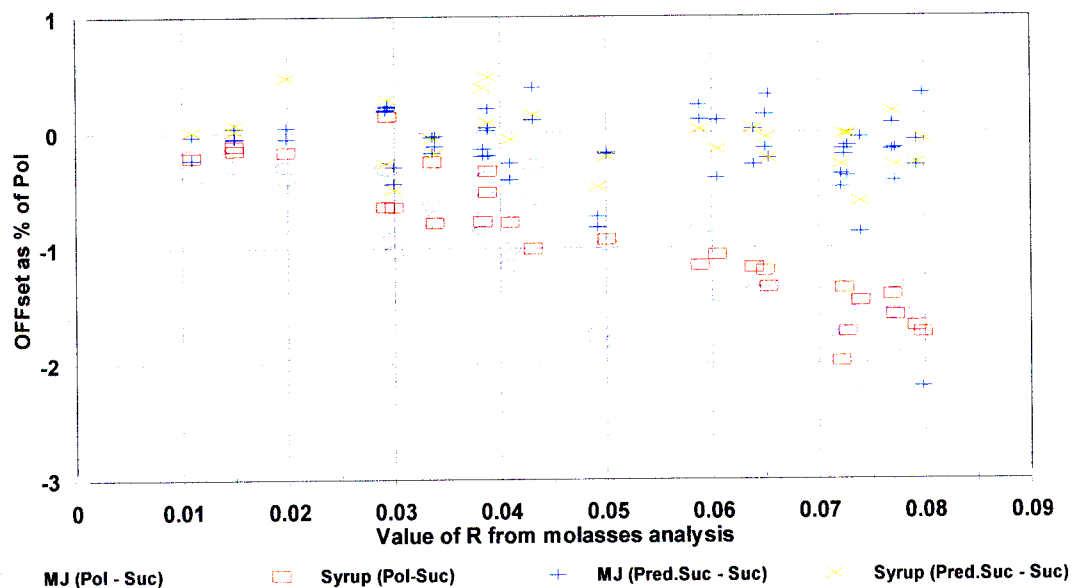


**Figure 3.7** Correction of pol to sucrose using equations 3.3 and 3.6

For comparison, the graph also shows the offset between pol and sucrose measurements as a function of the parameter $R$. These results demonstrate the ability of equations 3.3 and 3.6 to estimate the sucrose concentration from pol and brix measurements despite the off-set between pol and sucrose measurements varying from as low as about 0.1 units to as much as 2 units.

## 3.6    On-Line Measurements for Pan Boiling

Even the simpler analyses of pol and brix described above are time consuming and unsuitable for controlling the progress of pan boiling. Although experienced operators (pan boilers) are able to make some estimates of boiling conditions from the look and feel of the massecuite, on-line measurements are necessary for automatic control and also provide valuable indications for manual operation.

Conventional measurements of temperature, pressure and flow provide no particular problems when applied to pan boiling. Level measurement is slightly more difficult but when other methods have proved unsuitable (eg differential pressure sensors, capacitance level probes) a simple set of discrete conductivity level detectors has been used to estimate level.

In a classic optimisation study, Frew (1973) showed that to maximise crystallisation performance, it is necessary to be able to measure and control both super-saturation and crystal content. These can be considered as monitoring the driving force for crystallisation and the degree of progress of crystallisation. On-line crystal size measurement would be informative but is not essential as an on-line control signal. Although some applications of on-line crystal size measurement have been reported (Dijkstra et al, 1996, Hogg et al, 1986) it appears to still be an exotic measurement that has not yet demonstrated reliability as an industrial measurement.

The measurement of crystal content and super-saturation are unfortunately difficult and/or expensive to measure on-line. Consequently a number of measurement techniques have been developed which approximate one or the other of the desired measurements or respond to a combination of both. A summary of the major types of measurement in use is given below.

*Electrical conductivity* (Wright ,1984)

> conventional electrical conductivity is affected by both crystal content and mother liquor

concentration. The combined effect makes conductivity an effective means of controlling pan boiling. Conductivity measurements are reliant on the presence of ionic impurities and are most effective when these levels are relatively large and invariant. It is for this reason that conductivity is most effective as a control signal on low purity boilings.

*Viscosity or consistency* (Hashimoto et al., 1985)

measurement devices are available which measure the consistency or effective viscosity of the combination of crystal and mother liquor. The response is similar to that of electrical conductivity measurements

*Boiling point elevation*   (Sockhill and Wright, 1960, Foster et al., 1960, Batterham and Norgate, 1977, Batterham, Frew and Wright, 1973, Grimsey and Brown, 1994, Peacock and Starzak, 1995)

The measurement of BPE provides an indication of the concentration of the mother-liquor, almost independent of the level of crystal content. In batch pans, measurement is complicated by superheating effects which vary as boiling progresses. The superheating effects are significantly reduced in continuous pans but the absence of sensitivity to crystal content means that BPE must be used with caution if it is the only measurement available.

*Nuclear density meters* (Donovan, 1988)

Nuclear density meters can provide accurate measurements of massecuite density, which is closely correlated with crystal content. The output is relatively insensitive to mother liquor concentration.

*On-line refractometers* (Rozsa, 1996)

On-line refractometers can provide accurate measurements of mother liquor concentration independent of crystal content . They rely on internal reflection of light from the surface of a prism in contact with the mother liquor and thus do not provide the averaging effects present in other measurement techniques. Effective circulation of massecuite past the face of the prism is thus essential to the usefulness of this type of measurement.

*Microwave Absorption* (Reuter et al., 1998)

Microwave adsorption measurements are sensitive to the concentration of water in the massecuite and as such are primarily a measurement of crystal content.

*Radio Frequency Conductivity*   ( Reichard and Vidler, 1975, Moller, 1984, Radford and Cox, 1986, Radford et al., 1988, Reichard et al., 1992, Ehrenberg and Kessler, 1997)

A number of devices are available which measure the electrical properties of a massecuite at frequencies in the VHF range. This results in measurements which are affected by both the conventional conductivity and by dielectric constant. The advantages over conventional conductivity are ,

- an ability to operate in the absence of ionic impurities

- an ability to tolerate some encrustation of the electrodes without affecting the readings

- the option of producing separate outputs representing the resistive and capacitive chacteristics of the massecuite, which show different sensitivities to crystal content and mother liquor concentration.

*Software sensors* (Kapur et al, 1991, Acharya, 1984, de Azevedo, et al. 1993)

A number of researchers have investigated the options of combining the results of a number of measurements, using mathematical correlations and algorithms to estimate the parameters required for a more scientific control of pan boiling (ie crystal content and mother liquor super-saturation in their correct engineering units).

In the absence of any cost effective and accurate measurements of crystal content and mother liquor super-saturation, most users appear to make their own compromises in terms of instrumentation that they select and the control strategy that they employ. In many instances it is possible to use a single measurement because the dynamics of the equipment and the crystallisation process create a relationship between super-saturation and crystal content which allows the single measurement to be adequate for control.

In this research, which concentrates on high purity boilings encountered in cane sugar factories, the Tongaat-Hulett Radio Frequency probe and the boiling point elevation measurements have been used to monitor and control the crystallisation process.

## 3.7 Control Systems for Continuous Pans

The details of batch pan controls are more complex than those needed for continuous pans because of the combination of a batch cycle combined with regulatory control. Whilst some of the specifics are useful, the details are not directly applicable to continuous pans.

The control system originally recommended by Tongaat-Hulett Sugar for their continuous pans was reported on by Rein (1986). As a result of operational experience at the Felixton factory, this original scheme was extended to include an evaporation rate control which operates by adjusting a remote set-point to the calandria pressure controller. A seed flow control was also included to maintain a constant seed to massecuite ratio as pan throughput was varied. This improved control system was reported on by Rein (1992), and is shown in Figure 3.8 below.
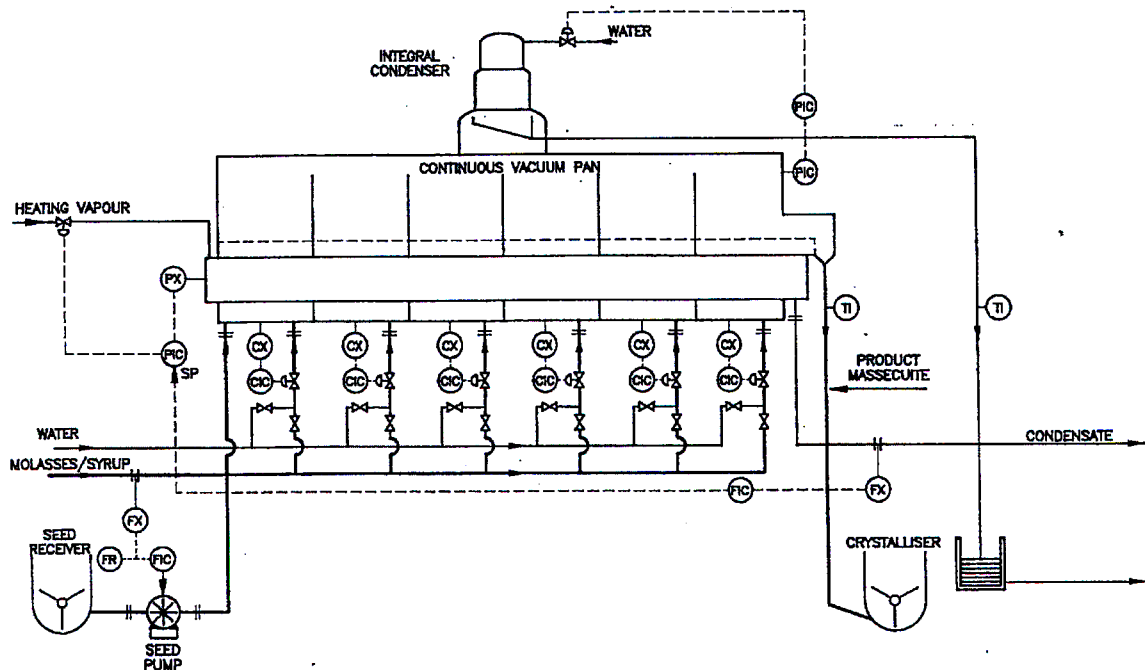


**Figure 3.8** Control Scheme for a continuous pan

For clarity, the diagram shows only 6 compartments although the number is normally either ten or twelve. The controls can be summarised as follows :

—    The absolute pressure in the pan body is controlled by adjusting the flow of condenser
     cooling water

—    The pressure in the calandria is controlled by throttling steam flow into the calandria

—    The condensate flow is measured by a magnetic flow meter. The flow is controlled by
     adjusting the set-point of the calandria pressure controller

—    Sensors (Conventional conductivity, RF Probes or Boiling Point Elevation
     measurements) are provided in each compartment. An individual controller for each
     compartment adjusts feed flow to maintain the contents at the desired set-point. The
     selection of either water or molasses feed for each compartment is made manually by the
     operator.

—    The syrup/molasses flow to the pan will be primarily a consequence of the evaporation
     rate and the number of compartments selected to feed syrup/molasses. The resulting flow
     is measured with a magnetic flow meter. To maintain a constant seed to massecuite ratio,
     the seed pump speed is adjusted to keep it in a constant ratio to the syrup flow.

Slightly different control strategies have been reported by other manufacturers and users of
continuous pans. An SRI pan (Davies et al., 1989) was fitted with automatic actuation of both
water and syrup/molasses valves. The control strategy sets the syrup/molasses valve to provide
the required rate of feed whilst the water valve is regulated by a conductivity controller. The pan
was fitted with two calandrias and the steam flow to each could be measured by differential
pressure cells and controlled by butterfly valves.

The VKT pan because of its completely self contained compartments has independent control of
absolute pressure and calandria pressure for each compartment (Austmeyer, 1990). The design
also requires massecuite level control in each compartment because of the need to regulate the
massecuite flow between compartments. Brunner et al. (1992) report on feed control to each
compartment based on the measurement from a nuclear density gauge and operating by sending a
remote set point to a feed flow controller which uses a magnetic flow meter as sensor. It is not
clear why this level of complexity is required.

# CHAPTER 4

## 4. Dynamic Model of a Multi-Compartment Continuous Pan

### 4.1 General

Mathematical models are useful tools for investigating the behaviour of processing equipment. Clearly a mathematical model is always only an approximation to reality but if it is a sufficiently accurate approximation it can be a valuable tool. Increased complexity and longer computing times (since most useful models will require a numerical solution) are the cost of achieving a closer congruity between the model and actual operating conditions. It is thus important in formulating a mathematical model to select the variables and the equations describing their inter-relationship carefully so as to achieve the best compromise between the complexity and accuracy of the model. This balance is also dependent on how the model is to be used. The applicability of the model can often be improved if its parameters are determined by fitting the model to experimental data, under the same conditions that it is intended to simulate or predict.

The approach adopted in this work has been to develop a mathematical model of a multi-compartment continuous pan which had the flexibility to be used for the following investigations:

— Dynamic behaviour of a single compartment of a continuous pan.

— Dynamic behaviour of a multi-compartment continuous pan.

— Steady state behaviour of a multi compartment pan, to be used in either a parameter fitting (performance evaluation) mode or a predictive (simulation) mode.

— Determination of optimum steady state operating conditions for a multi-compartment continuous pan.

With this intention of a uniform approach to modelling for a range of applications, the requirements for the basic model are:

— A modular model. By formulating a general model of a single compartment, a multi-compartment pan model can be constructed by cascading the required number of compartment models. The product massecuite output of one compartment becomes the seed massecuite input to the next compartment.

— A dynamic model. By beginning with the formulation of a dynamic model, the steady state model can be derived as a special case by setting all time derivatives

to zero.

– A model that approaches linearity. Whilst the equations describing the behaviour of even a single compartment are inherently non-linear, the choice of independent variables will have an influence on the extent of this non-linearity. A simplified linear model is a useful tool for dynamic analysis, particularly for the design and analysis of linear control systems.

– Applicability for dynamic programming. The choice of independent variables is important for the application of the "dynamic programming" optimisation technique. This is discussed in detail in Chapter 8.

Given this wide range of requirements, the formulation of the final model was inevitably an iterative process. This thesis does not attempt to document the process but rather summarises the eventual formulation that met the requirements.

## 4.2 Batch Pan Models

Since batch vacuum pans have been in operation for over a hundred years and continuous pans are a relatively recent innovation it is natural that the first efforts at modelling the evaporative crystallisation process would be applied to batch boilings. Evans, Trearchis and Jones (1970) published a model to be used as part of a control system. Whilst the scope of the model extended to both heat transfer and mass transfer, the format of the empirical growth rate expression was not justified with any data or references. Wright and White (1968) presented a well structured and researched model of a batch pan which became the basis of much of the subsequent Australian research in this field. Wright and White (1974) extended their own work to simulate how the crystal size distribution would vary through the boiling process. Frew (1973) used the model as the basis of an optimisation investigation. Li-Wu and Corripio (1985a) in Louisiana used the Wright and White model to evaluate the performance of a pan and as the basis for developing a Dynamic Matrix Control strategy (Li-Wu and Corripio, 1985b).

Particular features of the model of Wright and White (1974) are

– No attempt is made to model the complexities of heat and momentum transfer

– It accommodates dispersion in growth rates using a specific parameter, p (White and Wright, 1971)

- It assumes a symmetrical size distribution which is modelled by two moments (Frew, 1973)
- It has been used as the basis of a multi-compartment continuous pan model, originally outlined by Wright and White (1974) and subsequently used by Broadfoot (1980)
- The format of the growth equation (discussed in Chapter 2) has sufficient parameters to accommodate the major factors affecting growth rate

Other researchers such as Bonnenfant (1985) and Ditl et al. (1990) have also developed models but without any evidence of specific improvements or advantages over the original work of Wright and White. Depeyre et al. (1989) developed a batch pan model as the basis of a control system. The model is more complex than that of Wright and White in that it does not treat the pan as a CSTR (continuously stirred tank reactor) but rather considers it as several compartments selected to simulate parts of the pan. The benefits of this added complexity are not quantified but the complexity of the model was such that it could not be used on-line but required that standard profiles (termed abacuses in the paper) be developed off-line using the model. These profiles were then used as the basis of an on-line control strategy.

A research group from Universidad Central de las Villas published a set of papers ( Torres et al., 1990, Herrera F, 1990 and Rodriguez and Torres, 1990) describing the development of an empirical model of a vacuum pan, based on difference equations, which could be used as the basis for developing a control strategy. The mathematical description does not attempt to model any of the fundamentals of mass balance and crystal growth and thus has very limited utility for providing insight into the performance of operating pans.

The model of Ditl et al. (1990) is a more complex batch pan model than that of Wright and White. This model expands on earlier models (which only simulated the crystal growth phase of the batch cycle) and encompasses all four phases of the cycle viz. filling and concentrating, seeding, crystal growth and ,finally, tightening and discharge. The model also simulates the heat transfer and mixing characteristics of the pan.

Whilst in terms of the development of appropriate mathematical models of pans the scope of the

model of Ditl et al. (1990) may appear impressive, its utility is doubtful for a number of reasons :

—    It has insufficient modelling of the dispersion in crystal growth rates and its effect on the crystal size distribution.

—    It includes a model of secondary nucleation during growth - an occurrence to be avoided in good pan boiling practice.

—    It includes the relationships of other researchers (eg for Nusselt number and viscosity ) which may be of limited accuracy and applicability.

—    It appears to be an "over-parameterised" model which may improve the ability of the model to fit experimental data, but at the expense of a reduced confidence in the significance of the fitted parameters.

## 4.3 Formulation of a Continuous Pan Model

Wright and White (1974) described briefly how their batch pan model could be extended to describe the behaviour of a multi-compartment continuous pan. Broadfoot (1980), used this formulation as the basis for a thesis on continuous pans and outlines the derivation of the equations. The mass balances are conventional component balances whilst the population balances are formulated according to the procedures of Randolph and Larson. The dispersion in growth rates is modelled with a dispersion parameter, $p$, as described by White and Wright (1971). This dispersion parameter concept has been used in analysing the results of tests on industrial scale continuous pans in South Africa by Rein, Cox and Love (1985).

Heat transfer is not included in the Wright and White (1974) model. This is a sensible approach since any attempt to try to model the heat transfer coefficient as a function of massecuite conditions, is easily rendered invalid by fouling of the heating surfaces. In any event, the required rate of heat transfer can be independently set at design time by the selection of the quantity and configuration of heating surface which is installed or it can be set during operation by adjusting the calandria steam pressure.

Hoekstra (1985) formulated a computer program for modelling the steady state behaviour of continuous pans based on the approach of Wright and White. This program was used within Tongaat-Hulett sugar for both the design and evaluation of continuous pans (Hoekstra, 1986).

Hoekstra's model did not try to include the complexities of spreads in residence time distribution or heat transfer and circulation which were addressed in separate studies (Rein, Cox and Love, 1985 and Rouillard, 1985).

The modelling in this thesis is based on the approach originally outlined by Wright and White (1974), in the belief that it represents an appropriate compromise between complexity and simplicity. The formulation is described in detail in Appendix B, using the descriptions of particle size distributions documented in Appendix A. The fundamental component of the model is a single compartment which is assumed to behave as a continuously stirred tank reactor (CSTR). The complete pan model is then constructed by linking as many compartments in series as are necessary to simulate the actual construction of the pan. An innovation in the formulation used in this present research has been to solve the equations symbolically to provide a set of equations which approximates the standard state space format of :

$$\dot{x} = A \cdot x + B \cdot u \qquad \text{(4.1)}$$

$$y = C \cdot x \qquad \text{(4.2)}$$

where :

      $x$      is a vector of plant states

      $u$      is a vector of plant inputs

      $y$      is a vector of plant outputs

      $A$, $B$, and $C$ are matrices with constant coefficients

and,    the dot above a variable defines the time derivative (here, of the vector of plant states).

Since the equations which describe pan behaviour are non-linear, the coefficients of the matrices $A$, $B$, and $C$ will not all be constant but will in some instances be dependent on the vectors $x$ and $u$. This non-linearity can be addressed by evaluating the coefficients of the matrices for values of $x$ and $u$ which define normal operating conditions.

An important part of the modelling process is the selection of the particular variables (from the wide range of possible variables which can be used to describe pan behaviour) which are used to define the states, inputs and outputs of the model. State variables can be distinguished from input variables in that they must appear as derivatives in the equations and can be thought of as defining the characteristics of the system which have "memory" or the ability to accumulate.

There are however a number of alternative sets of state variables which could be chosen, as could different sets of input variables, each providing a full description of a pan compartment. The selection of appropriate state, input and output variables is not self evident and required a combination of some intuition and iteration to arrive at the final selection which addressed :

—      the need to describe the process by the minimum number of independent variables.

—      the need for the differential equations to approximate linearity. ( eg using flows rather than concentrations as variables is more likely to result in equations which approach linearity since concentrations, being ratios, introduce an inherent non-linearity).

—      the ability for the model to operate as a module of a complete pan model. The outputs of one module should be easily configurable as inputs to the next module, allowing a full pan to be created by a simple cascading of individual modules.

—      the appropriateness of the model to be used as the basis of a dynamic programming optimisation (as discussed in Chapter 8).

The variables finally selected, which match these criteria, are shown in Figure 4.1 below :

| Total mass flow | (kg/s) | $u8$ |

**Evaporation**

**Individual Pan Compartment**

| Mass of dissolved sucrose | (kg) | $x1$ |
| Mass of water | (kg) | $x2$ |
| 1st moment of crytal size | (m) | $x3$ |
| 2nd moment of crystal size | (m2) | $x4$ |

**Seed Massecuite Input**

| Total mass flow | (kg/s) | $u1$ |
| Mass flow of water | (kg/s) | $u2$ |
| Mass flow of dissolved sucrose | (kg/s) | $u3$ |
| 1st moment of crystal size | (m) | $u4$ |
| 2nd moment of crystal size | (m2) | $u5$ |

**Product Massecuite Output**

| Total mass flow | (kg/s) | $y1$ |
| Mass flow of water | (kg/s) | $y2$ |
| Mass flow of dissolved sucrose | (kg/s) | $y3$ |
| 1st moment of crystal size | (m) | $y4$ |
| 2nd moment of crystal size | (m2) | $y5$ |

**Syrup/Water Feed**

| Total mass flow | (kg/s) | $u6$ |
| Mass flow of dissolved sucrose | (kg/s) | $u7$ |

**Figure 4.1** Definition of variables for single compartment model

It is clear that in cascading compartment models of this format, the outputs $y1$ to $y5$ from one compartment become the inputs $u1$ to $u5$ of the next compartment.

In pursuing a model which is an accurate representation of industrial practice, issues that have been specifically addressed in this research work are :

— Rather than assuming that the crystal size distribution is symmetric, the distribution is assumed to follow a gamma distribution. Previous work (Frew, 1973 and Broadfoot, 1980) used the assumption of a symmetric distribution to express the third moment of the size distribution in terms of the first two moments, as described in equation A.34. Unfortunately this simplifying assumption is not appropriate for modelling South African A-massecuite where the crystal size distribution has been found to be asymmetrical (eg Rein and Archibald, 1989, Hoekstra, 1985, Hoekstra, 1986). The gamma distribution was selected from a range of possible asymmetrical distributions because of both its particularly appropriate properties (see section A-4) and its ability to fit experimental data . The assumption of a gamma distribution results in a different expression for calculating the third moment from the first two moments (equation A.40).

— The correlations for sucrose solubility in impure solutions presented in the literature have been critically reviewed (Chapter 2) and investigated experimentally for molasses samples from the local industry (Chapter 5).

— Published parameters for the Wright and White growth equation have also been reviewed (Chapter 2) and compared with growth data derived from other appropriate published sources (Appendix G). Crystal growth rates that are attainable in South African A-massecuite boilings have also been investigated in specially conducted test work on experimental scale batch pans (Chapter 6) and full scale continuous pans (Chapter 7).

The detailed formulation of the model equations for a single compartment is described in Appendix B. The major assumptions used in the formulation are :

— The compartment behaves as a fully mixed tank or CSTR (continuously stirred tank reactor) where the properties of the massecuite leaving the compartment are equal to the uniform properties of the massecuite in the compartment.

— The mass of massecuite in the compartment remains constant.

— The purity of the massecuite entering the compartment is constant and equal to the purity of the feed to the compartment. This implies constant massecuite purity throughout the

continuous pan and allows a considerable simplification of the equations. It also simplifies the determination of an optimum operating profile described in Chapter 8. Whilst this assumption is appropriate for the intended study of A-massecuite boiling within the traditional South African boiling scheme (see Chapter 3) it does prevent the model from being applied to other grades of massecuite and boiling schemes where this assumption does not apply.

—     No agglomeration, breakage or nucleation of crystals takes place.

—     Sucrose solubility is defined by a simple form of the relationship between solubility coefficient and impurity to water ratio (viz. equation 2.6). This is appropriate for the low values of impurity to water ratio encountered in A-massecuite boiling but would not be appropriate for lower purity boilings.

—     The growth rate of crystals is described by equation 2.31, based on the work of Wright and White (1974).

—     There is a dispersion in growth rates which can be described by a single parameter, $p$ (see section B-12)


Using these assumptions it is possible to formulate the set of differential equations which describe the behaviour of a single compartment by using the fundamental balance relationship :


$$\text{Flow in} \;-\; \text{Flow out} \;=\; \text{Accumulation} \;-\; \text{Reaction (Generation)}$$


This relationship is applied separately to each of the following "components" :

     Number of crystals.

     Size distribution of crystals (subsequently converted into moment balances).

     Total mass of massecuite.

     Mass of water.

     Mass of dissolved sucrose.


By suitable algebraic manipulation, it is possible to convert these equations into the standard state space format described by equations 4.1 and 4.2. The details of both the formulation and manipulation of the equations are described in detail in Appendix B. The final equations which result can be more clearly described by using the following set of intermediate functions :

$$g0(x, u) = \frac{\dfrac{x1}{x2}}{K_4 \cdot \left(1 - K_5 \cdot \dfrac{(CT_n - x2)}{x2} \cdot \left(1 - \dfrac{pur}{100}\right)\right)} \tag{4.3}$$

$$g1(x, u) = \frac{(u1 - u2) \cdot \dfrac{pur}{100} - u3}{\rho_x \cdot \alpha_v \cdot \left(2 \cdot \dfrac{u5^2}{u4} - u5 \cdot u4\right)} \tag{4.4}$$

$$g2(x, u) = \frac{(CT_n - x2) \cdot \dfrac{pur}{100} - x1}{\rho_x \cdot \alpha_v \cdot \left(2 \cdot \dfrac{x4^2}{x3} - x4 \cdot x3\right)} \tag{4.5}$$

$$g3(x, u) = K_1 \cdot \left(g0(x, u) - (1 + K_0)\right) \cdot \exp\left(K_2 - K_3 \cdot \frac{(CT_n - x2)}{x2} \cdot \left(1 - \frac{pur}{100}\right)\right) \tag{4.6}$$

These intermediate functions have the following physical significance :

$g0(x, u)$ is the prevailing supersaturation in the compartment

$g1(x, u)$ is the number flow rate of crystals into the compartment

$g2(x, u)$ is the number of crystals in the compartment

$g3(x, u)$ is the linear growth rate of the crystals in the compartment

The four state equations which describe the behaviour of the compartment , using these intermediate functions are :

$$\frac{dx1}{dt} = f1(x, u)$$

$$= u3 + u7 - (u1 + u6 - u8) \cdot \frac{x1}{CT_n} - 3 \cdot \rho_s \cdot \alpha_v \cdot g2(x, u) \cdot g3(x, u) \cdot (x4 + p \cdot x3) \tag{4.7}$$

$$\frac{dx2}{dt} = f2(x, u)$$

$$= u2 + \left( u6 - u7 \cdot \frac{100}{pur} \right) - u8 - (u1 + u6 - u8) \cdot \frac{x2}{CT_n} \tag{4.8}$$

$$\frac{dx3}{dt} = f3(x, u)$$

$$= \frac{g1(x, u)}{g2(x, u)} \cdot (u4 - x3) + g3(x, u) \tag{4.9}$$

$$\frac{dx4}{dt} = f4(x, u)$$

$$= \frac{g1(x, u)}{g2(x, u)} \cdot (u5 - x4) + 2 \cdot g3(x, u) \cdot x3 + p \cdot g3(x, u) \tag{4.10}$$

The output variables $y1$ to $y5$ define the product massecuite leaving the compartment and correspond to the input variables $u1$ to $u5$ which define the seed massecuite entering the compartment. The calculations for these variables are relatively simple, being based an overall total mass balance and close relationships to the corresponding state variables, and are given by:

$$y1 = u1 + u6 - u8 \tag{4.11}$$

$$y2 = (u1 + u6 - u8) \cdot \frac{x2}{CT_n} \tag{4.12}$$

$$y3 = (u1 + u6 - u8) \cdot \frac{x1}{CT_n} \tag{4.13}$$

$$y4 = x3 \tag{4.14}$$

$$y5 = x4 \tag{4.15}$$

The variables used in these equations but not defined in Figure 4.1 are :

| | |
|---|---|
| $\rho_x$ | Density of crystal sucrose |
| $\alpha_v$ | Volume shape factor of crystals |
| $p$ | Size dispersion parameter |
| $K_0$ | Offset defining level of supersaturation above which linear growth exists |
| $K_1$ | Proportional dependence of growth on oversaturation |
| $K_2$ | Factor adjusting growth rate for variation of temperature from a "normal" value |
| $K_3$ | Factor defining exponential dependance of growth rate on impurity/water ratio |
| $K_4$ | SW ratio of pure sucrose solution at saturation and at compartment temperature |
| $K_5$ | Constant relating solubility coefficient to IW ratio. |
| $CT_n$ | Total mass in the pan compartment |
| $pur$ | Common purity of the massecuite and the pan feed syrup |

These equations are too complex to solve analytically to determine the time response of the compartment to any given inputs. The conventional method of (numerically) solving this type of problem is to use the Runge-Kutta technique as has been done in Chapter 10.

## 4.4 Steady State Model as a Special Case

A steady state model of a continuous pan compartment can be simply generated by setting the time derivative of the vector of plant states to zero.

The consequence of this is that to find the state ( the vector $x$ ) of an individual compartment, given the input vector $u$ , it is necessary to solve the set of simultaneous equations which are defined by :

$$0 = f1(x, u) \tag{4.16}$$

$$0 = f2(x, u) \tag{4.17}$$

$$0 = f3(x, u) \tag{4.18}$$

$$0 = f4(x, u) \tag{4.19}$$

It is clear from equation 4.8 that equation 4.12 can be solved independently of the other three equations to yield the steady state value for $x2$. The steady state values of $x1$, $x3$ and $x4$ need to be determined by solving equations 4.11, 4.13 and 4.14 simultaneously.

The standard method for solving such a set of simultaneous non linear equations is to use the Newton-Raphson technique which is well described in texts on numerical analysis (Press et al., 1989, Burden, Faires and Reynolds, 1981, Carnahan, Luther and Wilkes, 1969). The Newton-Raphson method is an iterative technique which takes an initial estimate of the solution and improves it in steps. For the general case of a set of n non-linear equations defined by:

$$f_1(x_1, x_2 \ldots x_n) = 0$$
$$f_2(x_1, x_2 \ldots x_n) = 0$$
$$\vdots \qquad \vdots$$
$$f_n(x_1, x_2 \ldots x_n) = 0 \tag{4.20}$$

*or*

$$F(x) = 0$$

The Newton-Raphson technique updates the estimates of the solution using the following relationship :

$$x^{(k+1)} = x^{(k)} - J\left(x^{(k)}\right)^{-1} \cdot F\left(x^{(k)}\right) \tag{4.21}$$

where the Jacobian matrix $J(x)$ is a matrix of partial derivatives defined as :

$$J(x) = \begin{pmatrix} \dfrac{\partial f_1(x)}{\partial x_1} & \dfrac{\partial f_1(x)}{\partial x_2} & \cdots & \dfrac{\partial f_1(x)}{\partial x_n} \\ \dfrac{\partial f_2(x)}{\partial x_1} & \dfrac{\partial f_2(x)}{\partial x_2} & \cdots & \dfrac{\partial f_2(x)}{\partial x_n} \\ \vdots & \vdots & & \vdots \\ \dfrac{\partial f_n(x)}{\partial x_1} & \dfrac{\partial f_n(x)}{\partial x_2} & & \dfrac{\partial f_n(x)}{\partial x_n} \end{pmatrix} \tag{4.22}$$

In applying the Newton-Raphson technique to the solution of equations 4.11, 4.13 and 4.14 in this research, the approach (and numerical routines written in Pascal) of Press et al. (1989) has been used. As implied by equation 4.21, for each iterative step it is necessary to solve a set of linear simultaneous equations. Rather than do this by calculation of the inverse of the Jacobian matrix as indicated in equation 4.21, Press et al. recommend the solving by the use of the techniques of lower/upper decomposition and back substitution.

Rather than attempt to calculate the elements of the Jacobian from symbolic evaluations of the partial derivatives, it was found that simple finite difference approximations gave acceptable performance. Although techniques are available for reducing the computational effort of repeatedly recalculating the Jacobian matrix (eg Broyden, 1965) these were not found to be necessary as convergence was achieved in four or five iterations. Two factors which probably contributed to the good performance of the standard Newton-Raphson technique in this application were :

—    Good initial estimates of the steady state. For the first compartment of the pan it was necessary to use some engineering judgement, but for subsequent compartments, the steady state of the previous compartment provides a good first estimate.

—    Applied to equations which are only slightly non-linear, the Newton-Raphson technique will converge more rapidly than when applied to those which show a high degree on non-

linearity. The efforts in the selection of appropriate variables to approximate linearity during the formulation of the compartment equations will thus have contributed to a more rapid solution of the equations.


Computer routines, written in the Pascal language, were developed to use the techniques described here to determine the steady state operating conditions of a continuous pan. These were then incorporated in computer programs which specific objectives which are described in more detail in Appendix E.

The MODPAN program is designed to estimate growth kinetics by fitting the steady state model to results of tests on an industrial scale continuous pan (Chapter 7)

The OPTPAN program is designed to calculate the optimum steady state operating conditions by the use of dynamic programming (Chapter 8).

The SIMPAN program is designed to simulate an operating continuous pan with either manual of automatically controlled pan feed to the pan compartments.

# CHAPTER 5

## 5. Measurements of Sucrose Solubility in Impure Solutions

### 5.1 Selection of Method

The background to sucrose solubility in impure aqueous solutions of sucrose has been discussed in detail in chapter 2 . It is clear from that review of theory and published data that there is a dearth of solubility data for high purity products at high temperatures (ie the conditions defined by A-pan boiling in particular) for the South African sugar industry.

The reason for the investigation into sucrose solubility reported here is to provide information which can be used for evaluating growth rate measurements in pans. Specifically, the solubility of sucrose in the impure mother liquor must be known for the super-saturation driving force to be estimated.

When analysing results from tests on pans by fitting a mathematical model to the data, it is possible to include an expression for solubility coefficient, SC, as a function of some of the operating parameters (eg impurity/water ratio ,IW, and reducing sugar/ash ratio, RSA). The parameters in the expression for the solubility coefficient can then be fitted at the same time as the parameters for the growth rate equation. This approach has been used to evaluate data on batch pans (Wright and White, 1974) and on cooling crystallisation at low purities (Lionnet and Rein 1980) . Unfortunately, this is unlikely to provide estimates of any value (or statistical significance) in the instance of evaluating results of continuous A-pan performance since there is usually little variation in the mother liquor conditions (either temperature brix or purity) over the pan. There is also an inherent difficulty in discriminating between the effects of the magnitude of the super-saturation driving force and the mass transfer coefficient on the growth rates of crystals.

Given this background, the study of sucrose solubility presented in this chapter was undertaken to provide a better basis for evaluating and simulating the performance of high purity pan boiling.

The objectives were :

1       To develop a procedure for measuring sucrose solubilities in impure solutions at conditions of temperature and purity that are relevant to high purity pan boiling.

2       To develop a relationship for SC vs IW for local raw factory streams which can be used in preference to assuming the applicability of published data for another cane sugar industry.

3       To compare the SC - IW relationship for South African molasses with that determined for other industries to indicate the extent of the error that has been inherent in assuming published data from other industries

4       To check on the applicability (or otherwise) of the assumption that the solubility coefficient, SC, remains constant with temperature.

The beet sugar industry has undertaken comprehensive investigations into solubility in impure solutions (Vavrinecz 1978/79). The "Polish Test" often referred to in beet literature (eg Bohn et al., 1991) is a standard procedure for determining sucrose solubility in impure solutions. This test is described in some detail by McGinnis (1978). There appear to be a number of variations in the detail of the test originally proposed by Wagnerowski et al. (1962) but the basic principle is to approach saturation by dissolution of added crystals which are stirred in an under-saturated solution. This is done at temperatures significantly higher than the temperature of interest and relies on the Wiklund assumption of constant solubility coefficient with temperature to estimate the solubility at the temperature of interest. McGinnis (1978) quotes a wide range of times reported as being necessary to reach equilibrium, from as little as 45 minutes to as long as 24 hours (for tests at 80°C). The 45 minute period appears to be sufficient for equilibrium to be reached, as this test has been validated against a test with a 3 hour mixing time.

There are two major problems with applying this type of technique to cane sugar syrups and molasses. Firstly there is no guarantee that the solubility coefficient is constant with temperature. Jessic (1977) found no effect of temperature on solubility coefficient for some samples from the Hawaiian cane sugar industry whilst Broadfoot and Steindl (1980) did find a temperature dependence for samples from the Australian cane sugar industry. Secondly the significant levels of monosaccharides as impurities in cane molasses are particularly prone to thermal degradation at high temperatures (particularly if stirring times are prolonged to cope with the higher viscosities and slower dissolution rates of cane molasses). The degradation would change the composition of the molasses and thus render the solubility data incorrect.

The techniques for estimating solubility by measuring the temperature at which small crystals just begin to dissolve ( Harman, 1933, Rush and Meredyth, 1959, Wright, 1978, Wright, 1980 and Quin and Wright, 1992) can provide rapid answers about solubility. Unfortunately they also depend on the assumption of constant solubility coefficient with temperature if they are to be used to provide an estimate of solubility in units of concentration. Their application to cane molasses samples is thus limited.

Approaching equilibrium by crystallisation (eg Bruijn, 1977) is the method conventionally used for determining sucrose solubility in low purity syrups at low temperatures because of the impracticality of obtaining under-saturated solutions under these conditions. Wright (1983) warns against the accuracy of data obtained by this method.

The preferred alternative of approaching equilibrium by dissolution has two major advantages over the crystallisation method (provided under-saturated syrups can be obtained). Firstly, the rate of dissolution is significantly faster than crystallisation for the same degree of under or over-saturation. This ratio of dissolution rate to crystallisation rate for the same magnitude of driving force was investigated by Nicol & Parker (1971). By evaluating published data, they determined the following ratios :

—        4.7  - based on data of Kukharenko

—        10   - based on data of Charles

—        3.5  - based on data of Mantovani

Nicol & Parker (1971) determined ratios between 3 and 10 in their own experiments whilst Wright (1983) quotes a ratio of 5.

The second advantage of approaching saturation by dissolution is the absence of a "non-linearity" at low values of under-saturation. In contrast, for small values of over-saturation, the crystallisation rate dependence on degree of over-saturation decreases significantly, as shown in Figure 5.1 below (taken from Wright and White,1974). This will significantly increase the time required to reach equilibrium conditions by crystallisation. A similar "non-linearity" does not apply to the dissolution process.

Broadfoot and Steindl (1980) performed tests to determine equilibrium solubility, where they approached equilibrium by dissolution of crystals. They determined the initial, slightly under-

saturated, conditions using a photometric method (Wright, 1978) and allowed approximately 20 hours for equilibrium to be reached.
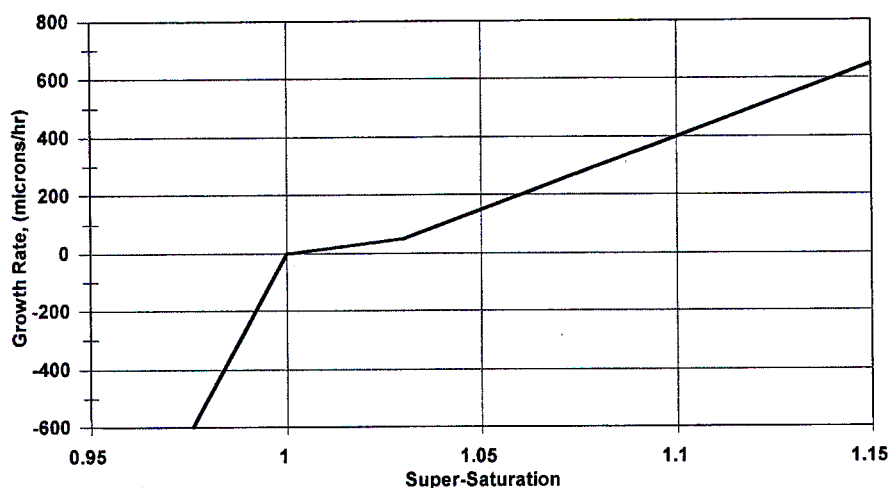


**Figure 5.1** Effect of super-saturation on rates of growth and dissolution

Charles (1960) gives an illuminating comparison of the differences between approaching equilibrium by dissolution and by crystallisation for a pure sugar solution at 15.25 °C. Equilibrium appears to be approached after only one hour by dissolution whilst approximately 75 hours is required to achieve equilibrium by crystallisation. There is some evidence that the saturation value is never reached by crystallisation, stabilising at some small value above saturation but Charles states that this cannot be confirmed because of the limitations of accuracy of the test procedure.

Given this background the approach selected for this work was to approach equilibrium in a stirred vessel by dissolution of crystals. This is obviously limited to situations where it is possible to obtain or create solutions which are under-saturated at the temperature of interest.

As discussed in Chapter 3 (section 3.5) pol and brix analyses were used in the experimental work for this thesis as measures of sucrose and solids concentration. The preliminary calculations of solubility data were thus calculated using these analyses. The consequences of using these approximate analyses were investigated by using the relationships derived in Chapter 3 (equations 3.3 and 3.6) to estimate true sucrose and dry solids content from pol and brix and re-calculating the sucrose solubility data. This effect of the type of analysis on calculated levels of

sucrose solubility, which is discussed at the end of this chapter, must be kept in mind when comparing the results of different researchers.

## 5.2    Experimental Apparatus

The experimental technique was developed using a modification of an apparatus originally designed for determining target purity differences.(Bruijn et al., 1977). The original apparatus used a jacketed vessel firstly as the steam heated body of a miniature pan, then as stirred water jacketed crystalliser and finally as a Nutsch apparatus to separate a sample of the mother liquor. In the test work reported here it was the stirred water jacketed vessel and Nutsch capabilities which were used. A diagram of the jacketed vessel is shown in Figure 5.2.
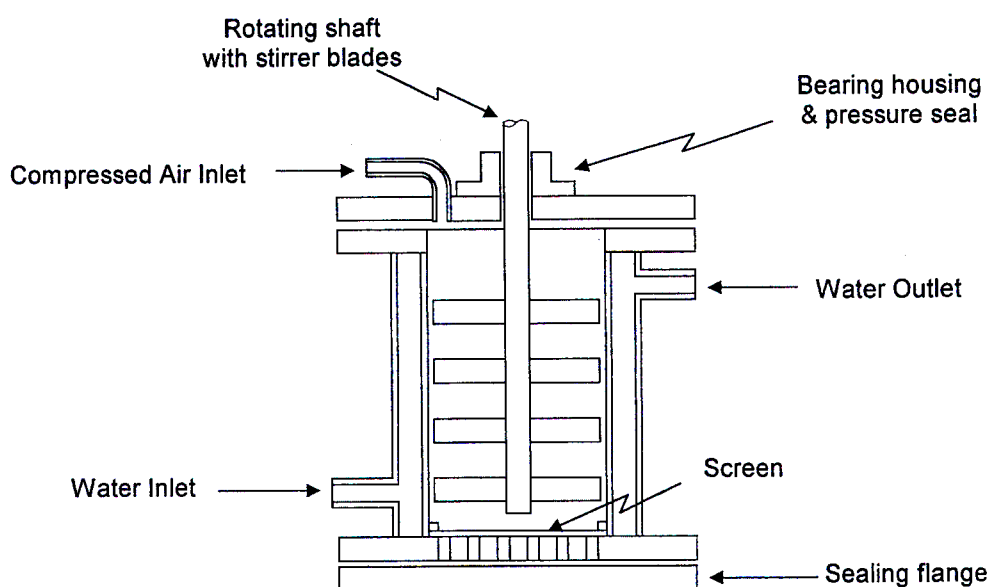


**Figure 5.2** Water jacketed vessel for sucrose solubility measurements.

One of the requirements of the original apparatus was the ability to handle highly viscous massecuites as a consequence of the low purities and low temperatures. Under these conditions slow stirring speeds are necessary to minimise heat generation from the input of mechanical power. Settling of crystal is insignificant under these conditions and stirring is applied to promote heat and mass transfer.

Initial tests using this apparatus for determining solubilities at higher purities of interest for this research showed poor repeatability and also could not reproduce the well accepted values for

pure sucrose. Visual observation of the stirring in a glass beaker of similar size to the normal jacketed vessel showed significant settling of crystals leaving a crystal free liquor at the top of the beaker - clearly an unacceptable condition for attaining equilibrium between crystals and mother liquor. Tests with modifications to the stirrer blades proved unsuccessful in preventing the settling of crystals. An increase in stirrer speed from 11 rpm to 62 rpm was however successful in ensuring good mixing with the worst case of a pure sucrose mother liquor at saturation conditions. The speed change was achieved by converting from the original chain drive to a rubber belt drive with suitably sized pulleys, the lower viscosities permitting this change without any slippage in the drive belts being evident. The ability to operate with the very limited torque capabilities of the simple rubber belt drives compared with the original chain drive was an indication that despite the increased speed, the input of heat to the molasses sample by the conversion of mechanical work was unlikely to be a concern.

The stirring mechanism was capable of accepting 6 jacketed vessels simultaneously. The jacketed vessels could then be connected to a supply of water from a computer controlled water bath, configured as shown in Figure 5.3.
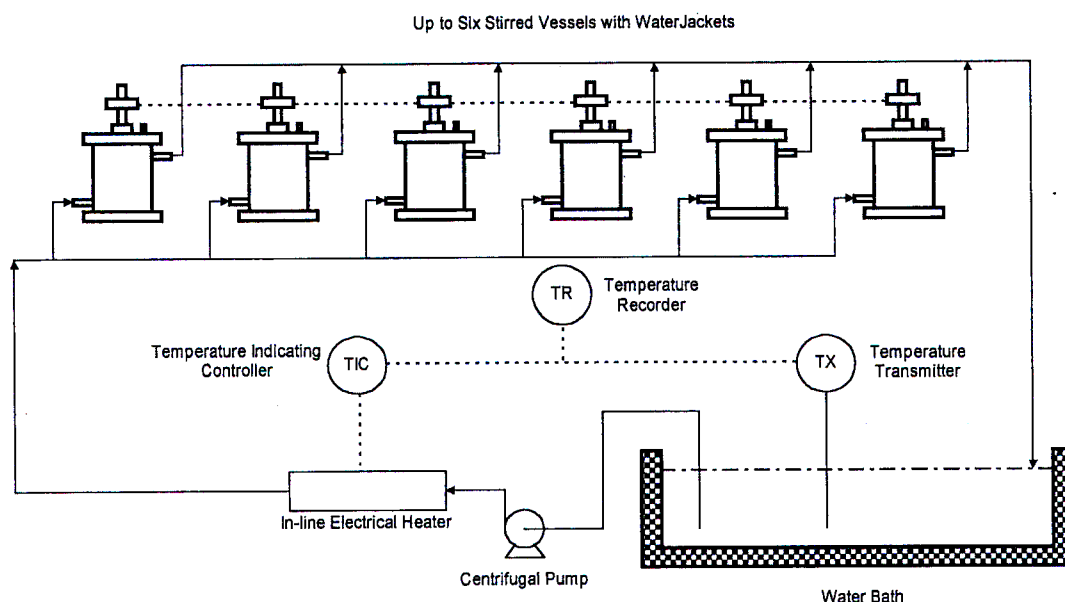


**Figure 5.3** Temperature control of jacketed equilibrium vessels with recirculating water

A version of the computer control system described in Chapter 12 was used for the temperature control. This enabled much more precise and accurate control of the circulating water

temperature than was possible with a standard water bath thermostat. Full PID control was implemented with time-proportional on/off switching of the electrical heater using a solid-state relay. The provision of a dedicated centrifugal pump for circulating the water (rather than using the rudimentary pump of a conventional water bath thermostat) ensured that high rates of water circulation could be achieved. The drop in water temperature as it circulated through the jacketed vessels was less than 0,1°C at steady state - ensuring accurate control of the temperature of the magma (the combination of crystals mixed with a mother liquor) as it reached equilibrium. The generation of heat from the stirring of the molasses in the pots was not of concern, since heat had to be added to the circulating water to maintain constant temperature.

## 5.3    Experimental Technique

In the broadest terms, the procedure devised for determining the solubility of sucrose in impure solutions is as follows:

—        prepare a solution approximately at saturation at the temperature of interest

—        mix in a sample of white sugar crystals heated to the same temperature

—        heat briefly to remove any crystals which may have nucleated during this process

—        cool to below the temperature of interest to promote crystallisation and remove sucrose from the mother liquor and render it under-saturated at the temperature of interest

—        heat to the temperature of interest

—        hold at this temperature overnight whilst agitating, allowing the mother liquor to approach saturation conditions by dissolution.

—        separate the mother liquor and analyse for the concentration sucrose and impurities

This procedure is similar to that described by Broadfoot and Steindl (1980).

The experimental technique is described below for determining solubility coefficients of impure solutions at 70 °C. The intention is to gather data on SC at a range of I/Ws The highest I/W will be defined by the starting material - the highest values of impurity water ratio which can be tested being limited to that achievable with a low purity C molasses.

Samples of molasses are created at a range of impurity water ratios (IW), from the highest IW possible with the available molasses sample, down to values close to zero (ie pure sucrose). These samples are then brought into equilibrium with added sucrose crystals ,by dissolution, at

the temperature of interest (here 70 °C).

The procedure for each sample added to a single jacketed vessel is as follows :

1    Analyse the sample of molasses under consideration to determine brix and purity

2    Calculate the quantities of molasses, sucrose and water which must be mixed together to give 520 g of solution of the required impurity to water ratio and at a concentration which approximates saturation at 70 °C. The calculation is automated on spreadsheet. It assumes the solubility coefficient relationship of Wright and White (1974) to give an approximation of the concentration at saturation. The sucrose is added in the form of starch free icing sugar to promote rapid dissolution.

3    Heat the mixture rapidly in a microwave oven in order to dissolve the sucrose.

4    Place the mixture in a preset water-bath set at 70°C

5    Connect the jacketed mixing vessel to the circulating water supply which is controlled to 70 °C. Allow the water to circulate and heat the vessel to this temperature.

6    Weigh out 200 g of large sugar crystals (white sugar sieved to provide the sieve fraction between 550 and 850 μm for this purpose) and heat in an oven to over 70°C. Large crystals are selected to ensure that no crystals dissolve to the size that they could pass through the Nutsch screen at the end of the test.

7    Add crystals to the solution being held in the water bath. Mix thoroughly and transfer into the heated jacketed vessel.

8    Attach the jacketed vessel to the top flange and stirrer mechanism. Begin stirring.

9    Raise the circulating water temperature to 80°C to dissolve out any fine grain that might have nucleated during this mixing and addition phase. (Approximately 30 minutes)

10   Switch off heating and allow to cool to 50°C (approximately 120 minutes).

11   Hold at 50 °C for approximately 30 to 60 minutes. This process will allow crystallisation to take place, removing sucrose from the mother liquor and creating a solution that is undersaturated at the temperature under investigation ( 70 °C).

12   Increase the circulating water temperature to 70 °C over a period of approximately 120 minutes and set to control at this value.

13   Leave sample stirring overnight (>16hours) to reach equilibrium.

14   Separate a sample of mother liquor (Nutsch molasses) by removing bottom flange and applying compressed air to the top connection. Discard the first approximately 50 g as

this may contain molasses from the drainage holes that was not in equilibrium with the crystals .

15    Check a sample of crystals from the jacketed vessel under a microscope to ensure that they show the characteristic rounded shape (like a used bar of soap) of crystals that have undergone dissolution - confirming that equilibrium has been approached by dissolution.

16    Check a sample of Nutsch molasses under the microscope to ensure that there is no evidence of small grain which will inflate the purity of the molasses when analysed.

17    Check the chart recording to ensure that the temperature remained under control for the duration of the test. (Any temperature excursions would inevitably give spurious results)

18    Analyse the molasses sample for brix and pol using standard methods of analysis for high purity factory products.

19    Calculate purity, sucrose/water ratio, solubility coefficient and impurity/water ratio using the approximation that pol is equivalent to sucrose concentration, and brix is equivalent to dry solids concentration.

For tests to determine the solubility at 80 °C the initial solutions are created for and at this temperature, raised to 90 °C to dissolve spurious nucleation, cooled to 60 °C to produce an under-saturated mother liquor and then finally held at 80 °C for equilibration to take place.

For tests to determine the solubility at 60 °C the initial solutions are created for and at this temperature, raised to 70 °C to dissolve spurious nucleation, cooled to 40 °C to produce an under-saturated mother liquor and then finally held at 60 °C for equilibration to take place.

This design of experiment, where molasses samples are held at relatively high temperatures for over 16 hours, does risk the possibility of chemical destruction of sucrose and monosaccharides. The Maillard reaction (Newell, 1979) is well known to take place under these conditions although its effect is most severe at lower purities and higher brixes (as encountered in C-massecuite). The Maillard reaction is accompanied by the evolution of carbon dioxide and a consequent swelling of the molasses/massecuite sample. The Maillard reaction is also known to cause a reddening in the colour of massecuite when it occurs during factory processing.

The occurrence of Maillard reaction during the test procedure could be expected to impede the equilibration process due to the presence of small bubbles. The reaction products would also

change the nature of the impurities and such parameters as the reducing sugar to ash ratio of the sample. For the specific aspects of sucrose to water ratio and impurity to water ratio, the occurrence of thermal degredation is not of direct concern since the sample analysis is only undertaken at the end of the test and will thus take into account the changes that have occurred.

In the experiments conducted, there was no obvious evidence of the Maillard reaction, either sample swelling and flowing out of the compressed air inlet (see Figure 5.2) or of any obvious colour change to the molasses samples. Future tests should investigate thermal degradation with detailed analysis of the changes in sugars (sucrose, fructose and glucose) over the test period, particularly given the variability of the results measured in these tests (as evident in Figure 5.6)

The question of whether sufficient time is allowed for the crystals and mother liquor to reach equilibrium can be investigated by a computer simulation of the procedure. A simple simulation was developed as a spreadsheet program based on the following (conservative) assumptions for the case of determining solubility at 70°C

- the growth rate of crystals in A pans is approximately 50 $\mu$m/hr at a supersaturation of 1,1 (based on data presented in Chapter 2)

- For dissolution rates five times as fast as crystallisation rates (Wright, 1983) the specific dissolution rate is thus 2500 $\mu$m/hr/unit of SS

- The mother liquor and added crystal come to equilibrium when cooled to 50 °C (saturation estimated by the equation of Wright and White, 1974)

- The crystals have a characteristic dimension, Dc, of 800 $\mu$m

- The mass of a single crystal is given by $m = \alpha_v \cdot \rho_x \cdot Dc^3$

  where ,          $\alpha_v = 0,34$          and          $\rho_x = 1587 \text{ kg/m}^3$

  ( following the approach of Lionnet, 1998)

To simulate the dissolution process, the initial conditions are first estimated as follows :

- Calculate the number of crystals added

- calculate the mother liquor conditions and the increase in sucrose crystal mass as a result of achieving a mother liquor which is saturated at 50°C

- calculate the increased size of the crystals (assuming that the number of crystals remains constant).

The simulation then tracks the dissolution process in small time increments (one minute),

calculating at each instant :

—　　　the new crystal size based on the dissolution rate estimated for the degree of saturation at the previous time interval, the crystal size at the previous time interval and the length of the time interval

—　　　the mass of crystal sucrose, assuming the number of crystals remains constant

—　　　the composition of the mother liquor as a result of the decrease in the mass of crystal sucrose

—　　　the degree of super-saturation in the mother liquor as a result of the prevailing temperature and composition.

The simulation is then repeated for each time interval, allowing the changes in crystal size and mother liquor to be estimated over the duration of the test. A graph of the results of the simulation is shown in figure 5.4 below.
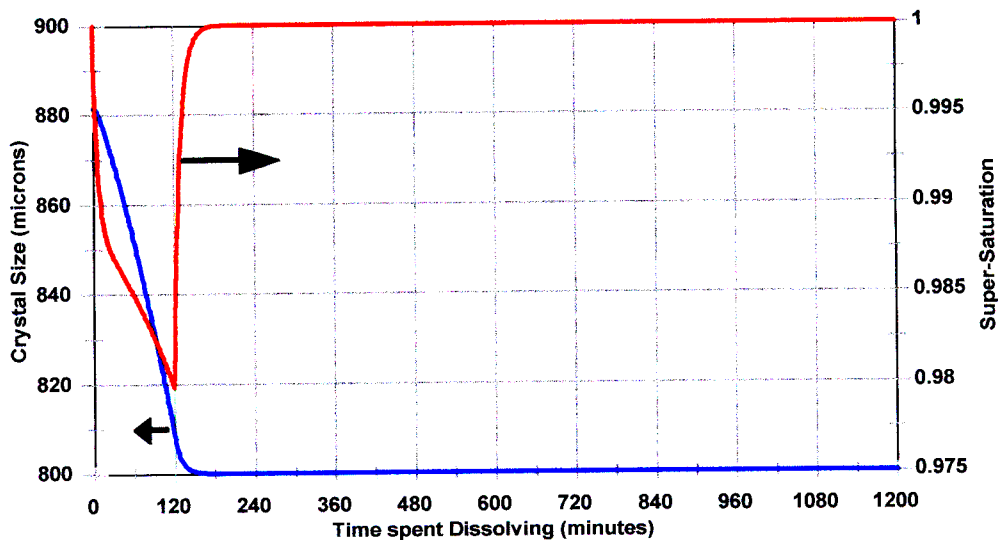


**Figure 5.4** Simulation of equilibrium test procedure

It is clear that equilibrium is achieved approximately one hour after the temperature reached 70°C (during the first two hours the temperature is increased linearly from 50°C to 70°C). The allowance of 16 hours to reach equilibrium is thus most generous and will allow for significantly lower dissolution rates than those assumed.

## 5.4 Results

The particular interest of this work is in sucrose solubility as applied to the boiling of A-massecuites in raw sugar factories. The boiling temperatures are usually in the range of 65 to 70°C being a compromise between high temperatures for faster crystallisation and lower temperatures to prevent thermal degradation. The primary temperature of interest for this work was selected as 70°C. Tests were performed using three different molasses samples as the base material and the results are summarised in Table 5.1 below :

| A molasses RS/Ash = 0.97 | | B molasses RS/Ash = 1.38 | | C molasses RS/Ash = 0.81 | |
|---|---|---|---|---|---|
| Purity | Brix | Purity | Brix | Purity | Brix |
| 69.58 | 82.35 | 60.99 | 83.45 | 49.26 | 87.5 |
| 71.52 | 81.8 | 61.33 | 83.4 | 51.03 | 87.1 |
| 72.49 | 81.6 | 61.62 | 83.25 | 55.55 | 85.6 |
| 74.05 | 81.3 | 63.05 | 82.95 | 61.35 | 83.95 |
| 76.13 | 81.05 | 65.58 | 82.5 | 68.33 | 82.25 |
| 77.45 | 80.7 | 66.18 | 82.5 | 75.88 | 80.65 |
| 79.94 | 80.25 | 68.35 | 82 | 79.97 | 79.9 |
| 81.04 | 79.9 | 69.36 | 81.75 | 84.54 | 78.9 |
| 84.66 | 79.2 | 72.35 | 81.2 | 94.06 | 77.45 |
| 87.61 | 78.7 | 73.44 | 81.15 | | |
| 91.08 | 77.95 | 76.36 | 80.6 | | |
| 94.9 | 77.4 | 77.15 | 80.3 | | |
| | | 81.21 | 79.55 | | |
| | | 85.03 | 78.85 | | |
| | | 89.46 | 78.25 | | |
| | | 94.25 | 77.4 | | |
| | | 99.54 | 76.7 | | |
| | | 99.67 | 76.75 | | |
| | | 99.67 | 76.6 | | |
| | | 99.67 | 76.75 | | |

**Table 5.1** Equilibrium Tests at 70°C - three different sources of molasses

Using these data (and the assumption that brix approximates dry solids and pol approximates sucrose) it is possible to calculate impurity to water ratios (IW) and sucrose to water ratios (SW) using the following equations.

$$IW = \frac{DS - Pty \cdot DS \div 100}{100 - DS} \qquad (5.1)$$

Where DS is the dry solids concentration (in %) and Pty is the purity (in %).

$$SW = \frac{Pty \cdot DS \div 100}{100 - DS} \qquad (5.2)$$

Using the correlation of Charles (equation 2.2) to calculate the sucrose to water ratio for a pure sucrose solution at 70 °C as 3.247, it is then possible to calculate the solubility coefficient SC for each test. The results are summarised in Table 5.2 below.

| A molasses | | | B molasses | | | C molasses | | |
|---|---|---|---|---|---|---|---|---|
| SW | IW | SC | SW | IW | SC | SW | IW | SC |
| 3.246 | 1.419 | 0.999 | 3.075 | 1.967 | 0.947 | 3.448 | 3.552 | 1.061 |
| 3.214 | 1.280 | 0.989 | 3.081 | 1.943 | 0.948 | 3.446 | 3.306 | 1.061 |
| 3.215 | 1.220 | 0.990 | 3.063 | 1.908 | 0.943 | 3.302 | 2.642 | 1.016 |
| 3.219 | 1.128 | 0.991 | 3.067 | 1.798 | 0.944 | 3.209 | 2.022 | 0.988 |
| 3.256 | 1.021 | 1.002 | 3.092 | 1.623 | 0.952 | 3.166 | 1.468 | 0.975 |
| 3.238 | 0.943 | 0.997 | 3.120 | 1.594 | 0.960 | 3.163 | 1.005 | 0.974 |
| 3.248 | 0.815 | 1.000 | 3.114 | 1.442 | 0.958 | 3.179 | 0.796 | 0.979 |
| 3.221 | 0.754 | 0.992 | 3.107 | 1.373 | 0.956 | 3.161 | 0.578 | 0.973 |
| 3.224 | 0.584 | 0.992 | 3.125 | 1.194 | 0.962 | 3.231 | 0.204 | 0.994 |
| 3.237 | 0.458 | 0.996 | 3.162 | 1.143 | 0.973 | | | |
| 3.220 | 0.315 | 0.991 | 3.172 | 0.982 | 0.977 | | | |
| 3.250 | 0.175 | 1.000 | 3.145 | 0.931 | 0.968 | | | |
| | | | 3.159 | 0.731 | 0.972 | | | |
| | | | 3.170 | 0.558 | 0.976 | | | |
| | | | 3.219 | 0.379 | 0.991 | | | |
| | | | 3.228 | 0.197 | 0.994 | | | |
| | | | 3.277 | 0.015 | 1.009 | | | |
| | | | 3.290 | 0.011 | 1.013 | | | |
| | | | 3.263 | 0.011 | 1.004 | | | |
| | | | 3.290 | 0.011 | 1.013 | | | |

**Table 5.2** Interpretation of Equilibrium Test Results 70°C, in terms of SW, IW and SC

These data are plotted in Figure 5.5 below, along with lines showing the relationships proposed by Wright and White (1974) and Rouillard (1980).
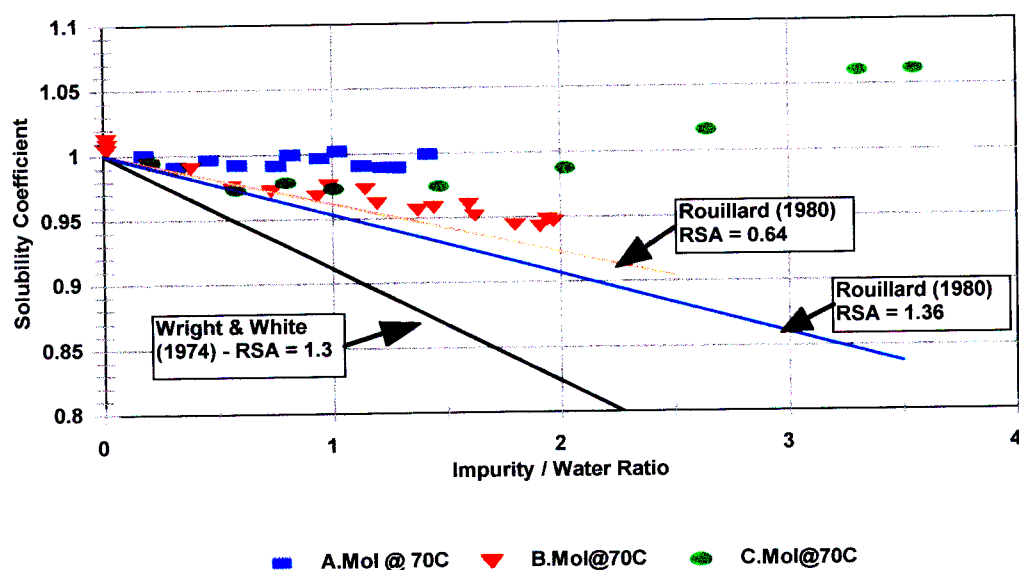
**Figure 5.5** Solubility Coefficient data calculated from pol and brix measurements for three different sources of molasses at 70°C.

The following points are evident from this experimental data :

—       The A-molasses data show a solubility coefficient of approximately unity across the full range tested (up to an IW ratio of 1.4).

—       The B-molasses data show an approximately linear decrease in SC with increasing IW for values of IW to about 2.0.

—       The C-molasses data show a decrease in SC with increasing IW, but only to about 1.5.

—       There is a difference in slope of the lines for the different samples of molasses but no relationship with RSA ratio is evident.

—       The slope of lines for all samples is less than that predicted by either the equations of Wright and White (1974) or Rouillard (1980).

—       At higher IW ratios (C-molasses samples) the SC increases to values greater than 1 (as reported for South African molasses by Rouillard (1980) and Lionnet and Rein (1980)).

Straight lines can be fitted to the data for each of these samples of massecuite. The line is assumed to pass through the point SC = 1 at IW = 0, being the definition of a pure sucrose solution. For the C molasses sample, only the data up to an IW ratio of 1.5 are included in the fit since the linear decrease clearly does not apply to values beyond this limit. The results of the least squares fits are presented in Table 5.3 below :

| | A Molasses | B molasses | C molasses |
|---|---|---|---|
| Number of points | 12 | 20 | 5 |
| Slope of Line | - 0.0052 | -0.0288 | -0.0234 |
| Std. Error of Slope | 0.0015 | 0.0012 | 0.0041 |
| r squared | 0.5132 | 0.9692 | 0.8918 |
| t-statistic | 3.405 | 24.46 | 5.74 |
| t-statistic for 95% | 2.201 | 2.093 | 2.776 |

**Table 5.3** Results of fitting straight lines to equilibrium results.

The slope of the correlation line is close to zero in all three cases (particularly for the A molasses based data). However, the fact that the calculated t-statistic is greater than the standard value for a 95% confidence level indicates that the correlation between solubility coefficient and impurity to water ratio is however still statistically significant in all three cases..

| C molasses @ 60 °C | | C molasses @ 80 °C | |
|---|---|---|---|
| Purity | Brix | Purity | Brix |
| 43.78 | 86.8 | 50.81 | 89.15 |
| 44.38 | 86.75 | 51.21 | 88.95 |
| 46.4 | 86.2 | 51.32 | 88.75 |
| 46.43 | 86.15 | 57.11 | 87.2 |
| 46.47 | 86.4 | 63.52 | 85.8 |
| 49.62 | 85.15 | 67.61 | 85.05 |
| 53.98 | 83.55 | 70.61 | 84.2 |
| 54.06 | 83.15 | 76.11 | 83.3 |
| 55.4 | 83.85 | 78.45 | 82.55 |
| 62.11 | 81.55 | 84.51 | 81.65 |
| 64.78 | 81.2 | 88.22 | 81.05 |
| 67.08 | 80.05 | 93.46 | 80.25 |
| 71.53 | 79.55 | | |
| 75.58 | 78.2 | | |
| 80.45 | 77.75 | | |
| 85.08 | 76.4 | | |
| 86.6 | 77.25 | | |
| 89.53 | 75.9 | | |
| 89.83 | 76.2 | | |
| 93.97 | 75.85 | | |
| 94.19 | 75.7 | | |
| 94.32 | 75.7 | | |

**Table 5.4** Results of Equilibrium Tests at varying Temperatures - single source of molasses

The results in Table 5.4 above are from tests conducted to investigate the effect of temperature on the relationship between solubility coefficient SC and impurity to water ratio. The tests, which measured solubility at both 60 °C and 80 °C, were on a range of samples which were based on the C molasses.

These data can also be processed to provide results in terms of impurity/water ratio and solubility coefficient :

| C molasses @ 60 °C | | | C molasses @ 80 °C | | |
|---|---|---|---|---|---|
| SW | IW | SC | SW | IW | SC |
| 2.879 | 3.697 | 1.000 | 4.175 | 4.042 | 1.127 |
| 2.906 | 3.642 | 1.010 | 4.122 | 3.927 | 1.113 |
| 2.898 | 3.348 | 1.007 | 4.049 | 3.840 | 1.093 |
| 2.888 | 3.332 | 1.004 | 3.891 | 2.922 | 1.050 |
| 2.952 | 3.401 | 1.026 | 3.838 | 2.204 | 1.036 |
| 2.845 | 2.889 | 0.989 | 3.846 | 1.843 | 1.038 |
| 2.742 | 2.337 | 0.953 | 3.763 | 1.566 | 1.016 |
| 2.668 | 2.267 | 0.927 | 3.796 | 1.192 | 1.025 |
| 2.876 | 2.316 | 1.000 | 3.711 | 1.019 | 1.002 |
| 2.745 | 1.675 | 0.954 | 3.760 | 0.689 | 1.015 |
| 2.798 | 1.521 | 0.972 | 3.773 | 0.504 | 1.018 |
| 2.692 | 1.321 | 0.935 | 3.798 | 0.266 | 1.025 |
| 2.782 | 1.107 | 0.967 | | | |
| 2.711 | 0.876 | 0.942 | | | |
| 2.811 | 0.683 | 0.977 | | | |
| 2.754 | 0.483 | 0.957 | | | |
| 2.941 | 0.455 | 1.022 | | | |
| 2.820 | 0.330 | 0.980 | | | |
| 2.876 | 0.326 | 0.999 | | | |
| 2.951 | 0.189 | 1.026 | | | |
| 2.934 | 0.181 | 1.020 | | | |
| 2.938 | 0.177 | 1.021 | | | |

**Table 5.5** Analysis of Equilibrium Test Results at Varying Temperatures

These data are plotted in the graph below along with the data previously presented for the tests on C molasses at 70 °C .The data unfortunately show significantly more scatter than was evident for the results of the tests using the A and B molasses samples. Despite this scatter, there is some evidence of higher values of SC for higher temperatures at the same impurity water ratio.
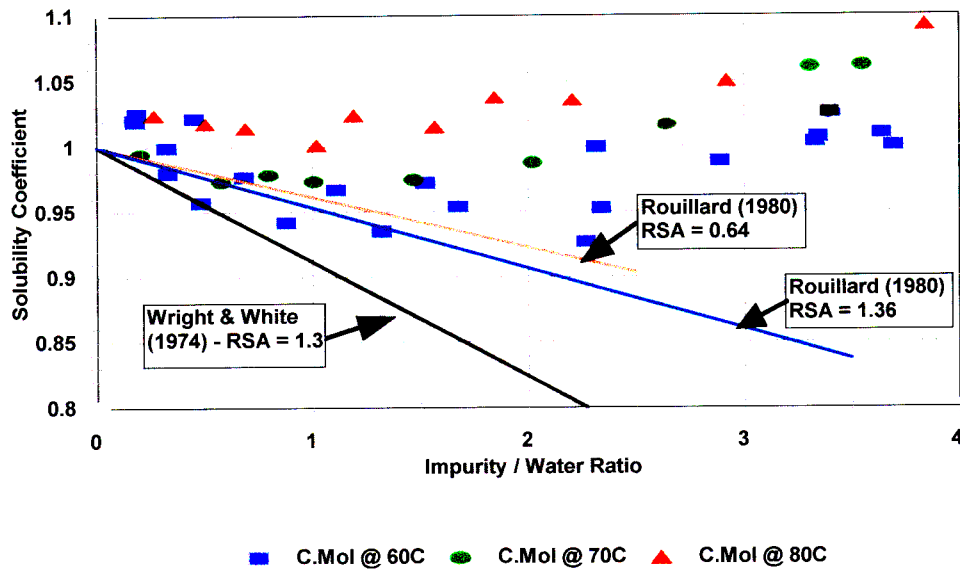
**Figure 5.6** Solubility Coefficient data calculated from pol and brix measurements

The data for 80 °C must be treated with caution however because of the increased likelihood of thermal degradation of both sucrose and reducing sugars at these elevated temperatures.

In summary, if pol and brix measurements are assumed to approximate sucrose and dry solids measurements, it is possible to recommend the following :

–       Given the evidence of some effect of temperature on the relationship between SC and IW, the data collected at 70 °C are the most appropriate to pan boiling.

–       The data for A-molasses appear to be an anomaly in that they do not show the decrease in SC with increasing IW, for low values of IW shown in the other tests (excluding the high temperature C-molasses results which may have been adversely affected by thermal degredation) and in the data of Rouillard (1980).

–       Despite the variability of the IW - SC relationship between samples, these results (and the limited data of Rouillard, 1980) indicate that the relationship of Wright and White (1974) as used by Hoekstra (1985) is inappropriate for South African molasses samples if based on pol and brix data..

–       Until a more comprehensive body of solubility data is available, the relationship determined for the B molasses samples should be used for investigations relating to A-massecuite boiling.

# CHAPTER 6

## 6. Measurements of Growth in Experimental Scale Pans

### 6.1 General

The mathematical models of the crystallisation process used in this thesis use equations which predict the growth rate of sucrose crystals as a function the operating conditions during pan boiling. Unfortunately, as discussed in Chapter 2, there is a limited quantity of good quality crystal growth rate data which is directly applicable to pan boiling. This lack of data appears to be more a consequence of the experimental difficulties rather than as a result of a lack of interest in this area.

The scope of this thesis was not primarily directed at addressing the lack of information on crystal growth rates but attempts have been made to update the parameters of the growth equations with values determined for the specific conditions being studied (viz. A-massecuite crystallisation in South African raw sugar factories). Chapter 7 describes how the parameter describing the overall dependency of growth rate on oversaturation, $K_1$, and the parameter describing the dispersion in growth rates, $p$ , were obtained by fitting the steady state continuous pan model to measurements from a full scale pan operating in normal production. Unfortunately this approach is not appropriate for determining the parameter which describes the dependency of growth rate on purity, $K_3$, owing to the limited variation in mother liquor purity in the full scale tests. This prompted the attempt to determine this parameter from measurements made using experimental scale batch pan tests. Testing on an experimental scale pan allows variation in the operating conditions significant enough to properly identify the relationships between operating conditions and growth rate, without the constraints of production which would normally preclude such experiments.

Before discussing the difficulties specific to using experimental scale pan boiling to obtain crystal growth rate data applicable to full scale pan boiling, it is instructive to consider the difficulties inherent in determining a quantitative description of crystal growth rate. Growth rate, being a description of dynamic behaviour, is inevitably more complex to measure than quantities that relate to steady state behaviour (such as concentrations at saturation). An added complexity arises in trying to relate growth rate to operating condition since, within a closed (batch) system, many of these will vary along with the growth process. There are, however, numerous laboratory

methods for measuring crystal growth rates as summarised by Garside, Mersmann and Nyvlt (1990), Only a limited number of these techniques are applicable to impure sucrose solutions because of their high viscosity and the small density difference between crystals and their mother liquor. Despite these limitations, a number of specialised laboratory techniques have been devised to measure sucrose crystal growth whilst avoiding the complexities of pan boiling (eg Smythe, 1959, Broadfoot and Steindl, 1980, Nicol and Parker, 1971, Guimaraes et al., 1995, Vaccari et al., 1996, Pautrat et al., 1996).

A common approach of many of these techniques is to use small closed systems (from a few litres down to tens of millilitres) into which accurately measured (using laboratory balances) quantities of mother liquor and crystals are added. The concentrations of mother liquor are sometimes set by combining accurately weighed amounts of sucrose and water. In general, the test methods appear to have been designed to address four main issues viz

- *Fixing the conditions under which crystallisation takes place*

  By mixing together crystal and mother liquor it is possible to create almost any desired growing condition in terms of both crystal size and mother liquor properties. This is particularly useful in removing correlations between the independent variables being investigated for their effect on crystallisation. By using small quantities of crystal relative to the quantity of mother liquor, the change in mother liquor properties as crystallisation progresses can be minimised, allowing changes in crystal size or mass to be measured at approximately constant operating conditions.

- *Obtaining accurate measurements*

  Operating on a small laboratory scale facilitates accurate measurements. Temperatures can be measured with accurate laboratory thermometers. Masses can be measured on precision laboratory balances. The samples that are used for analysis will be large relative to the test, reducing the likelihood of poorly representative sampling. Small numbers of crystals being tested means that the actual changes in mass or size of individual crystals can be measured, rather than relying on estimates of the change in average crystal size with time made by analysing the changes in the size distribution of particles in samples taken a known time interval apart.

- *Control of conditions*

  By using closed systems there is little other to control than stirring rate and operating temperature. Without external disturbances, accurate control of the temperature to within

0.1 °C appears to be possible with a good quality laboratory water bath.

–      *Achieving repeatability by use of a standardised technique*

Because there is much about the crystallisation process that is not fully understood, careful attention to detail is used to control the poorly understood or difficult to measure aspects of crystallisation so as to achieve repeatability of the measurements. Examples of this are  hand selecting starting crystals with similar levels of imperfections, and conditioning the liquor prior to mixing it with the crystals.

Whilst these laboratory techniques may be precise, and give useful insights into the magnitude of specific effects on crystal growth rates (such as shear at the crystal surface), their applicability to industrial pan boiling is questionable.

The ideal situation is obviously to determine the parameters of the equations which describe crystal growth rate from measurements on the pan boiling process itself. To provide accurate data in this way requires addressing the four issues addressed above for the laboratory scale tests. This was the motivation behind the laboratory and pilot scale test work described in this chapter. The same four main issues addressed by other crystallisation measurement techniques (as described above) need to be addressed in measuring crystal growth rates during pan boiling. The approach in dealing with the increased complexity of these issues was as follows:

–      *Fixing the conditions under which crystallisation takes place*

By operating an experimental scale pan, there is much greater flexibility in altering pan boiling conditions without the constraints of production requirements. Without the materials handling problems of an industrial scale pan there are greater opportunities for creating massecuites by mixing crystals and molasses/syrup.

–      *Obtaining accurate measurements*

Both the size of the equipment and the requirements of control systems described below, mean that accurate laboratory measurements (eg temperatures measured using accurate mercury in glass thermometers) need to be replaced by less accurate, industrial plant type measurements (eg temperature measured by a PT100 sensor connected to a  4 - 20 mA temperature transmitter). The options for very high accuracy electronic instrumentation was generally outside the budget of this research and thus the approach was to calibrate the sensor-transmitter-indicator combinations against accurate laboratory measurements.

–    *Control of conditions*

By moving away from measuring crystallisation in a closed system, the control requirements become significantly more complex. In a batch pan its is necessary to control operating pressure, evaporation rate and feed into the pan. Given the complexities of dynamic behaviour, poor control will undoubtably lead to errors in interpreting the data to estimate the crystallisation rate and the conditions which are driving it. Good quality control is possible, but requires close attention to the equipment details and appropriate tuning of the control loops. The difficulties that other researchers may have had in achieving stable control are not always evident, but the trends presented by Wright and White (1974) show considerable fluctuations in supersaturation during the batch boilings they used for estimating growth kinetics. The trends presented by de Azevedo et al (1993) show very poor pressure control and it would be doubtful if any meaningful crystallisation rate data could be obtained from tests conducted under such unstable conditions.

–    *Achieving repeatability by use of a standardised technique*

Pan boiling is often considered as more of an art than a science. This is particularly so in regard to the seeding of the pan, with many options possible in terms of combinations of quantity and quality of the seed crystals and the temperature and concentration at which it is added. Significant effort is necessary to develop appropriate and repeatable seeding techniques for particular products.

The usefulness of data obtained from experimental scale pan boiling is not only dependent on achieving good repeatability. It is also necessary to have confidence that the results adequately reflect the behaviour that will be achieved in full scale equipment. As a first requirement in providing this confidence, the experimental scale pan needs to achieve similar average crystal growth rates and crystal size distributions to those achieved on full scale.

As is shown in Chapter 8, the dependency of crystallisation rate on the purity of the mother liquor from which the crystals are being crystallised is a major factor in determining the optimum operating conditions for a continuous pan. Given this importance, a considerable portion of the time and effort expended in this research was invested in experimental scale pan boiling directed at quantifying this relationship. Unfortunately the investment in this aspect of the research provided very little return in terms of quantitative measures of growth kinetics. On a more

positive note, the achievements in equipment and method development will hopefully provide the necessary platform for successful future research into growth kinetics.

## 6.2    Laboratory and Pilot Scale Pan Boiling

Whilst small scale pan boiling offers significant advantages over full scale tests for obtaining better quality data on sucrose crystallisation, there are significant problems which need to be addressed. Clark (1999) expressed concern over the use of laboratory scale crystallisation for the evaluation of emerging purification technologies. His concerns relate to the ability to simulate full scale operations adequately on a laboratory scale. He specifically mentions poor circulation and difficulties in control of supersaturation as particular problems of experimental scale pans. Garside et al. (1990) recommend a minimum volume for an experimental evaporating crystalliser of 20 litres, stating that in smaller vessels, the bubbles influence the fluid dynamics too much. Wright and White (1974) commented on the fact that much work on crystallisation was "restricted to idealised laboratory experimentation , which is often quite unrelated to the performance of the industrial crystallisation process". To avoid this limitation in their work, they obtained the parameters for their batch pan model by fitting the model to results from a pan in a factory that was available for "off production" experimental boilings.

Laboratory scale pans have been used within the South African sugar industry for a number of years. Bruijn (1964) described the construction of two laboratory pans at the Sugar Milling Research Institute (SMRI). These pans had strike volumes of 4.2 and 13 litres respectively and were designed to produce sugar for filterability tests from different starting materials. No particular attempt appeared to have been made to simulate full scale pan performance directly and the sugar from the experimental pans proved to have much better filterability than that achieved from equivalent raw material in full scale pans. The larger pan was subsequently fitted with a viscosity measurement and used for "boiling-down" tests designed to determine the lowest purity to which massecuite can be exhausted by crystallisation. The pan proved to be too large for efficient testing of this type and a new design of experimental pan with a strike volume of only 500 to 600ml, known as the boiling down apparatus, was developed (Bruijn, 1977). This system proved to be very useful in obtaining the necessary practical equilibrium data (target purity) with a duplicate apparatus being used by Tongaat-Hulett for extending the investigation (Rein and Smith, 1981). Whilst these pans provided the data which are used to evaluate factory

performance in terms of approach to maximum possible recovery of sugar from final molasses, the pans were not operated to try and simulate the operating procedures of full scale pans.

The 13 litre SMRI pan was upgraded by fitting it with extra instrumentation and computer control (Wienese et al., 1987) and initially used for the study of impurity transfer in A-boilings (Lionnet, 1987). The pan was subsequently used to study impurity transfer in white pan boilings (Lionnet, 1998). These investigations were aimed at understanding the effect of different levels and types of impurity on the products of a standardised pan boiling procedure rather than attempting to simulate full scale performance. Comparisons between the experimental pan and full scale industrial production (Lionnet, 1999) showed that the crystallisation rates in the experimental pan were considerably slower.

A laboratory pan based on the original 13 litre design was built for Tongaat Hulett sugar by the SMRI. The original purpose of the pan was to process higher purity products so as to provide molasses suitable for exhaustability tests as per Bruijn et al., (1972). It was this pan that was refurbished and automated with computer control to investigate the effect of purity on crystallisation rate as described in the following section.

## 6.3     Setting up a Laboratory Scale Pan

The first attempts of this research to measure crystal growth under tightly controlled conditions began using the Tongaat Hulett laboratory pan mentioned above. A sketch of the pan construction is shown in Figure 6.1.
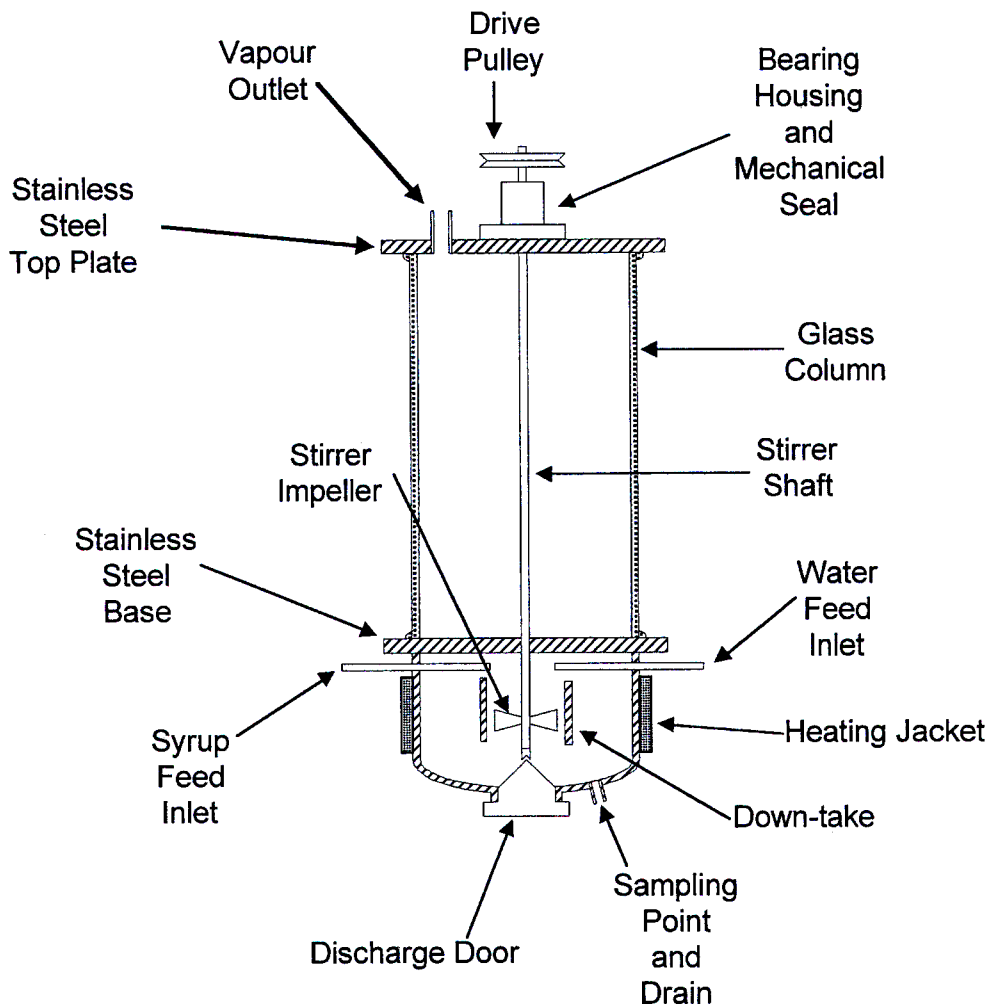
**Figure 6.1** Diagram of Laboratory Pan Body

The pan consists of a stainless steel base section with a dished end. This section has a volume of 4,9 litres and is fitted with a 2kW electric heating jacket on the outside of the cylindrical wall to achieve boiling on the inside wall. To promote circulation an axial flow stirrer is installed in a central downtake. The stirrer is driven by a variable speed motor, providing a maximum impeller speed of 120rpm. The pumping action is down the downtake so as to assist the upward flow adjacent to the outside wall caused by the vapour bubbles during boiling. Since the heating is electrical the metal temperature can rise to levels which can cause sucrose destruction if the base is not kept flooded at all times when the heating is on. The heat input can be manually regulated using a device which uses a time proportional on/off control with a frequency of 1 Hz or faster.

Above the metal base section, the rest of the pan volume is provided by a section of glass

column, 500mm in height, providing an additional volume of 15,5 litres. This section provides both additional volume for crystallisation and as well as space for disengagement of droplets of liquor from the vapour before it passes to the condenser. Figure 6.2 gives a schematic diagram of the pan with its ancillary equipment.
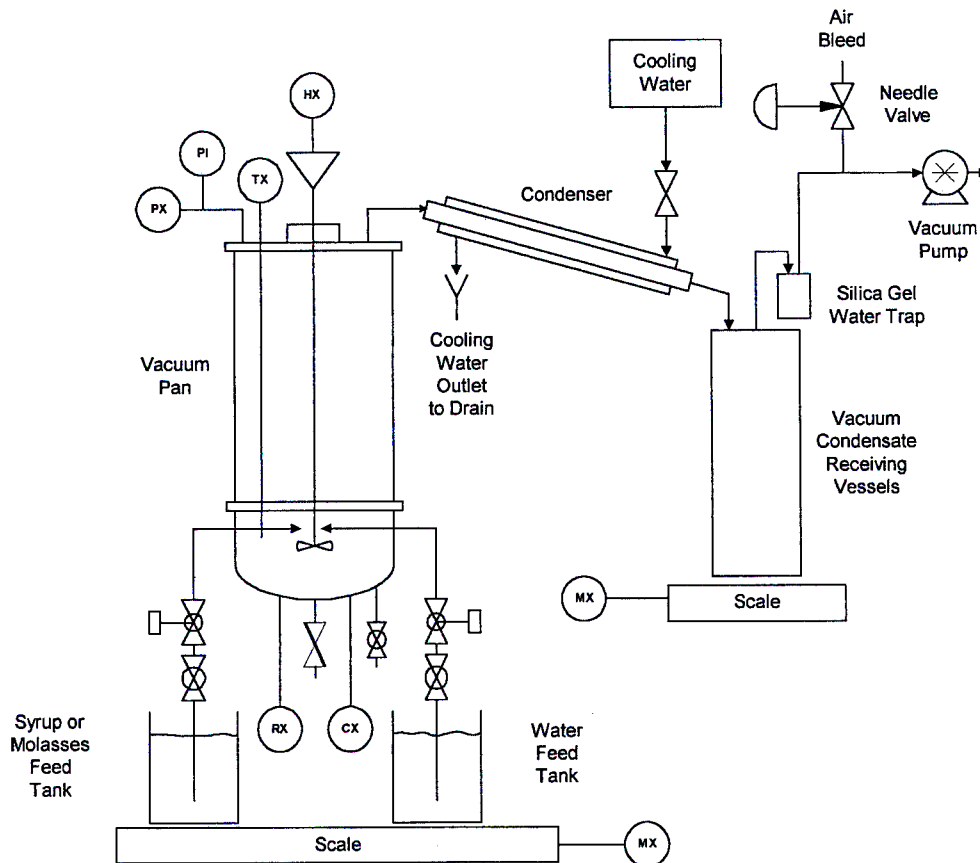


**Figure 6.2** Schematic diagram of Laboratory Pan with Instrumentation

A critical aspect of the design of the complete system was to ensure that accurate on-line mass balances could be achieved. This allows the contents in the pan to be estimated at any stage from a knowledge of the initial charge into the pan and measurements of the total feed into the pan and the total amount of material removed from the pan. Specifically the unmeasured holdup in feed lines and condenser had to be minimised.

The condenser is a double pipe heat exchanger mounted directly above the pan body and sloping downwards towards the vacuum condensate receiver which is mounted on an electronic balance. The balance is connected to the logging and control computer through an RS232 serial communications link. Water flow in the condenser is counter current to ensure the maximum

cooling of the incondensible gasses. The condensate is collected in a transparent condensate receiving vessel whilst the incondensible gasses pass on to the vacuum pump through a silica gel vapour trap to collect any remaining vapour.

A two-stage diaphragm vacuum pump is used to allow the pan to operate under vacuum. The absolute pressure in the pan is regulated by bleeding air into the suction of the vacuum pump. The air bleed requires a very small valve with a Cv out of the range of normal control valves (as an indication, the valve needs to throttle to less than the capacity of a 1mm orifice). An adequate bleed valve was constructed from a redundant chart recorder mechanism coupled to a home-made needle and seat arrangement which gives good control although the construction is not very robust.

Two means are provided for sampling from the pan whilst it is operating under vacuum. A "proof-stick" is installed in the upper section of the stainless steel pan base. This allows small samples (approx 0,4ml ) to be taken from the pan for microscopic analysis. A 15mm ball valve is provided in the base of the pan to allow larger samples (approx 100ml) to be removed for analysis using a vacuum sampling arrangement described below.

The massecuite boiling temperature is measured by a transmitter with a long probe inserted through the top of the pan. The measuring element is at the tip of the probe immersed in the massecuite with probe cooling by atmosphere minimised by the length of the probe body extending through the heated vapour. This positioning prevents over-reading which was suspected when the probe was installed through the heated side wall of the pan. The temperature probe was specially constructed (Anon,1986) for accurate measurements of massecuite temperature between 65 and 75°C. The probe uses a thermistor sensor which has a more pronounced variation in resistance with temperature than the conventional platinum resistance sensors. The combination of temperature probe and computer interface was calibrated against a high precision mercury in glass thermometer which had been calibrated by an accredited calibration laboratory.

The absolute pressure measurement is by a Yokogawa absolute pressure transmitter of modern digital design. A previously installed Rosemount transmitter of an older analog design was identified as the source of significant errors caused by drift during operation. The combination of

transmitter and computer interface was calibrated using a mercury in glass differential manometer against a full vacuum achieved using a high quality vacuum pump. The full vacuum was shown to be better than 0,015 kPa absolute by measurement with a Macleod gauge. The pressure transmitter is ranged with a maximum of 30 kPa abs so as to be sensitive to variations around the normal operating point. A vacuum gauge, ranged from 0 to -100kPa g is also installed, allowing the initial drop in pressure from atmospheric to be monitored.

Two small insulated probes are installed into the base of the pan to allow the measurement of electrical conductivity of the solution between them using a Siemens conductivity transmitter.

An adapted version of the radio frequency "Duotrac" conductivity probe (developed and marketed by Tongaat Hulett Sugar, Radford & Cox, 1986) is also installed through the base of the pan. This probe provides two outputs (the RS and the XS signals ) which, because of different sensitivities to both dielectric constant and conductance of the massecuite in the pan, are better able to sense changes in both mother liquor concentration and crystal content than a single conventional conductivity measurement.

There are two feed lines into the pan which enter through the side wall of the metal base of the pan and extend through to just above the downtake. This allows feed material to be rapidly mixed into the pan contents as it passes down the downtake and through the impeller of the stirrer. One feed line is allocated for feeding liquor (syrup or molasses) and the other is allocated for feeding water. A solenoid operated valve is installed on each feed line close to the pan to allow feed into the pan to be automatically regulated. A feed line extends from each valve to dip into a feed bucket containing liquor or water respectively. With a time-proportional on/off control system used to regulate the feed flow, a simple orifice flow restriction can be used to ensure a smooth control action without significant concern over the size of the control valve. The water flow requires a very small orifice restriction and consequentially is a potential blocking problem. The solution has been to manufacture a restriction from a segment of centrifugal screen, with all but two slots blocked providing an open area of approximately $1 mm^2$ .This is fitted to the end of the water feed line and can be easily removed for cleaning. Both feed buckets can be mounted on the feed balance which is also connected to the logging and control computer with an RS232 serial communications link.

The control and logging computer is fitted with an analog and digital interface card (PC30 card supplied by Eagle Electronics). This interface card provides the analog inputs to monitor the temperature, pressure and conductivity measurements. It also provides an analog output to regulate the air bleed valve and digital outputs to control the liquor and water feed valves. The computer also has two RS232 ports which are used for monitoring the condensate and feed balances.

The details of the multi-tasking computer control program (which was developed for this work) described in detail in Chapter 12. All the measurements and variables calculated by the control program (eg controller outputs and on-line mass balances) can be logged to disk for subsequent analysis. The logged data is in text file format and can be imported into a computer spreadsheet program for graph plotting and further calculations and analysis.

To facilitate the operation of the pan and make the necessary measurements during test boilings, a number of pieces of ancillary equipment are required. A steam heated vacuum evaporator has been refurbished to allow it to be used to pre-concentrate liquor before it is fed to the pan. This minimises the concentration period in the pan (which has a much lower maximum evaporation rate) and is also essential to de-aerate and eliminate foaming tendencies of factory syrups. The evaporator has a much larger disengagement space than the pan and is able to concentrate syrups to the point where foaming is minimised.

A high vacuum pump with water trap is available to create a vacuum in a glass sampling pot which can be connected to the valve positioned in the base of the pan for this purpose. This allows sufficient quantities of sample for analysis to be removed from the pan during boiling, without disrupting the pan operation or control.

Crystal growth can be monitored by measuring the increase in crystal size over time during the boiling. The "proof-stick" described above is able to remove small quantities of massecuite from the pan during boiling - just sufficient for microscopic analysis. A video camera connected to a computer through a dedicated interface (Snappy "frame grabber") allows images to be captured from the microscope onto computer disk for subsequent analysis to determine crystal size distribution. Attempts to automate the analysis of these images have not been successful (Schumann and Thakur, 1993) and a semi-automated method is still necessary. A description of

the software developed for this semi-automatic size analysis is given in Appendix E.

A full analysis of massecuite sampled from the pan requires that a sub-sample of mother liquor be separated from the massecuite immediately the sample has been taken. The conventional "nutch bombs" (Munsamy, 1980) used in the sugar industry are too large for this work and special centrifuge tubes are available to perform this separation. The tubes are designed to be used in a large laboratory centrifuge. The tubes have a fine screen, with a rigid backing screen, which is secured approximately half way along the length of the tube. Massecuite is placed in the tubes above the screen and then centrifuged. The crystal remains above the screen whilst the molasses drains under the "increased gravitational force" into the empty bottom section of the tube. The tubes can be unscrewed at the point where the screen is mounted to allow the molasses to be removed and the screen to be cleaned. By measuring the mass of massecuite added and the mass of molasses separated, it is possible to obtain a rapid estimate of crystal content.

## 6.4    Results Achieved with Laboratory Scale Pan

Considerable effort was necessary to achieve reliable operation and control of the laboratory pan. The description of the pan in the previous section is the result of many modifications made towards this end. For example, many attempts to pump condensate out of the condenser (which is under vacuum) to allow it to be collected and weighed in a collection vessel which was at atmospheric pressure were all less than successful, with intermittent problems frequently causing test runs to be aborted. The final solution was to collect the condensate in a vacuum vessel mounted on a scale, with the connections to the condenser and vacuum system made by flexible hoses carefully positioned to minimise any influence on the mass measurement.

The quality of the control finally achieved in the laboratory pan is demonstrated in Figure 6.3 below. In this test a sample of high purity liquor was first concentrated and then diluted in steps from approximately 76 % brix up to approximately 79 % brix and back again over a period of about three hours. It is clear from the graph, that after the pressure control had stabilised at the beginning of the test, the control was considerably better than ± 0.1kPa. The changes in concentration are reflected in the changes in boiling point elevation. Some manual intervention was necessary to minimise overshoot or undershoot on setpoint changes, but control at setpoint was better than ± 0.1°C.
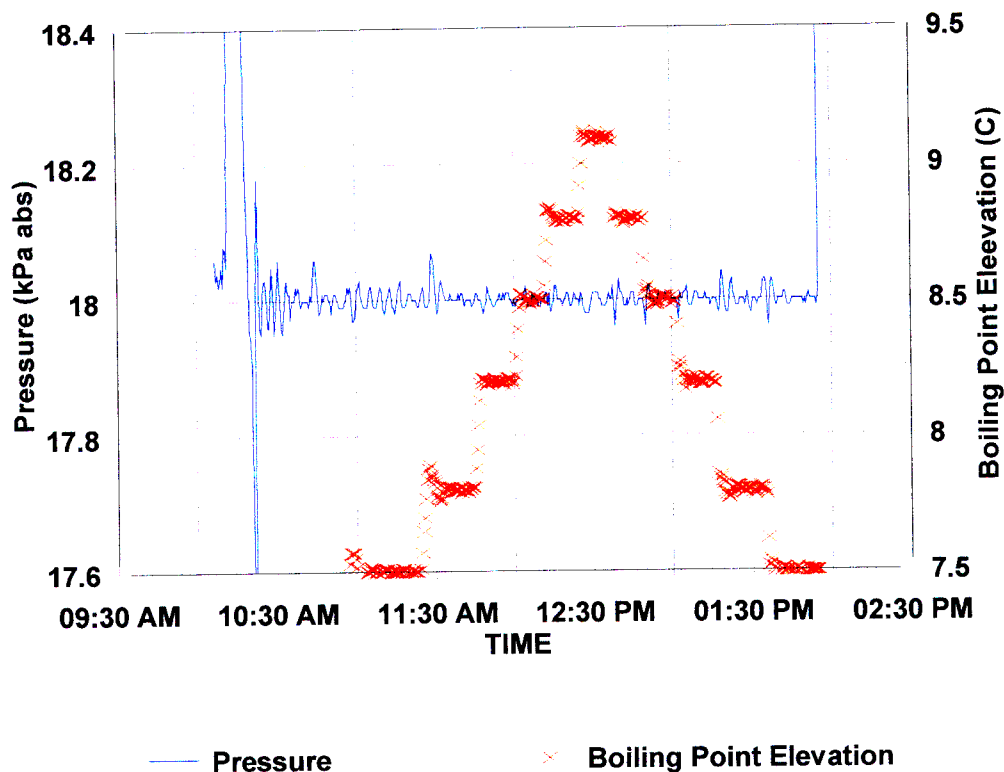
**Figure 6.3** Quality of control in Laboratory pan

The importance of this level of control can be determined by relating boiling point elevation to the level of supersaturation for a mother liquor of 74 % purity and at 70 °C, as typical of the A-massecuite boilings which are of interest. From equation 2.36, and assuming a crystal content of 45%, the supersaturation at the nucleation threshold limit is 1.17. Using equations 2.3, 2.4, 2.5 and 5.4 it is possible to calculate the solids concentration at saturation (supersaturation of 1.0) and at the nucleation threshold limit of 1.17. These are 80.10 and 82.32 % respectively, giving the width of the metastable zone (see Figure 2.1), within which the liquor must be maintained for controlled crystallisation, as 2.22 percentage units. These limits can be interpreted in terms of boiling point elevation (BPE) using the relationships of Batterham et al., (1973) :

$$BPE1 = 2.442 \cdot SW - 0.0757 + 3.333 \cdot IW \qquad \text{(6.1)}$$

$$BPEp = \frac{(273 + T)^2}{\dfrac{373^2}{BPE1} + (100 - T)} \qquad \text{(6.2)}$$

Where *BPE*1 is the boiling point elevation at one atmosphere pressure and *BPEp* is the boiling point elevation at any other pressure defined by the saturated temperature of water vapour at that pressure, *T*, in °C. Assuming a pressure of 18kPa abs which has a saturated vapour temperature of 57.8 °C, the metastable zone can be calculated to exist between a BPE of 7.903 °C and a BPE of 9.231 °C, giving a width of 1.328 °C. To control supersaturation to 10% of the width of the metastable zone thus requires that the BPE be controlled within a range of 0.1328 °C - demonstrating the importance of accurate pressure and BPE control during boiling.

The design and operation of the pan to perform an on-line mass balance provides direct estimates of the concentration (dry solids % ) of the massecuite in the pan during boiling. Obtaining reliable results from this feature required considerable attention to the equipment details and measurement accuracies. A test of the accuracy of the mass balance was achieved by analysing results from the concentration and dilution tests shown in Figure 6.3. Using BPE as a measure of concentration, if the contents of the pan are diluted back to the starting concentration, this should be reflected in the measurements from the on-line mass balance. The results of the test are shown in Figure 6.4 with different markers used to indicate the concentration and dilution phases.
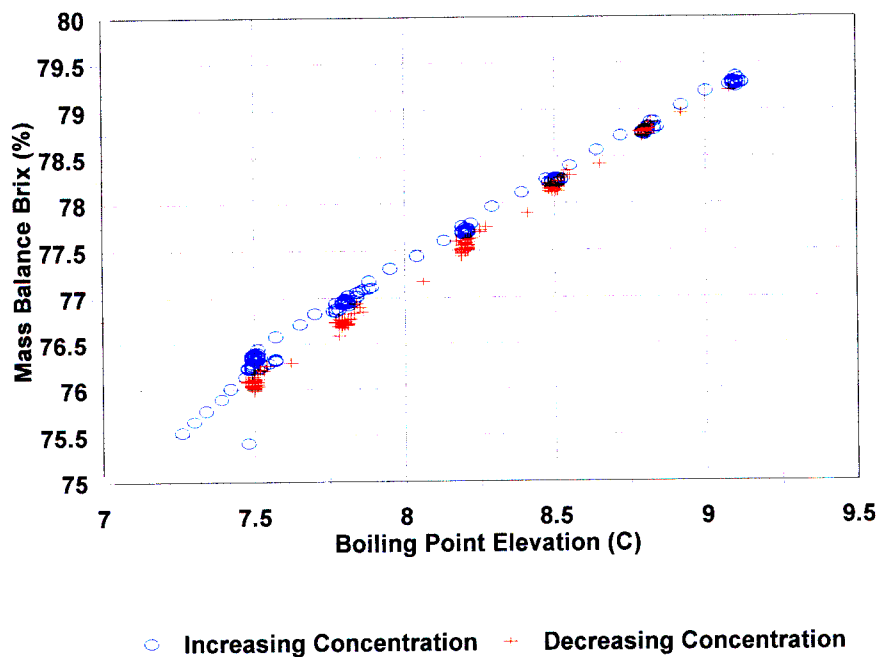


Figure 6.4 Test of on-line mass balance by concentration and dilution.

Figure 6.5 shows the level of agreement between BPE and the RS output of the RF probe, both being measures of the concentration of the pan contents.
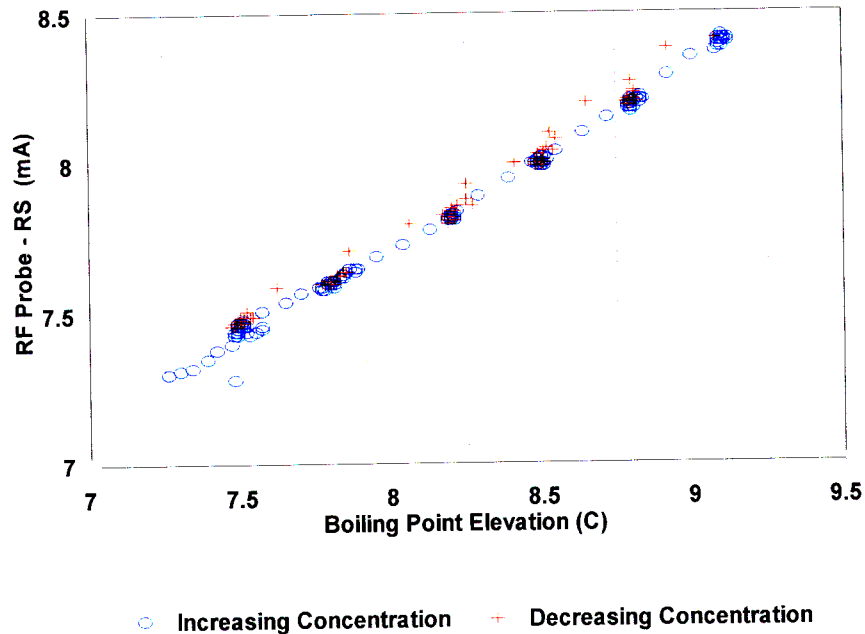


**Figure 6.5** Agreement between measurements reflecting changes in concentration

Over the three hour test period, the error in the mass balance relates to approximately 0.25 % in the brix reading. This is only slightly greater than the conventional 0.2% accuracy assumed for the analytical procedure used to measure brix.

With the tight control and reliable measurements that were finally achieved, it was hoped that it would be possible to achieve adequate simulation of industrial scale pan boiling. Attempts at creating "artificial" massecuites by mixing crystals with mother liquor were not successful. Adequate mixing and the exclusion of air bubbles were particular problems and crystals tended to bond together and form conglomerates when crystallisation began. In consequence, massecuites were created by conventional seeding with a small quantity (approximately 0.4 ml) of seed slurry. This slurry contains crystals of approximately 4 micron size , suspended in isopropyl alcohol, created by a standardised ball milling procedure (Anon.,1985). The seeding procedure, in terms of seeding point, holding time etc was developed by trial and error to generate massecuites with adequate numbers of crystals. An example of the data collected on crystal growth rates is shown in Figure 6.6. Massecuite samples were taken throughout the

boiling cycle and digital images of the crystals saved to computer disk. To obtain these images, each massecuite sample was spread onto a microscope slide and up to three images were captured (from different portions of the slide) before cooling of the slide caused crystallisation in the mother liquor and a substantial degradation of the image.

The images were subsequently analysed using the software described in Appendix E. Lionnet (1998) conducted tests to determine the number of crystals that needed to be counted to provide a reliable result. He found that the standard deviations of both length and width tended to constant values after about 140 crystals had been measured. He thus recommended that 200 crystals was a suitable sample size. Each of the images captured from the massecuite samples from the lab pan test contained between 100 and 270 crystals, with most exceeding the minimum requirement of 140 crystals. Rather than combining the results of images from the same massecuite sample, the results of each image are plotted to give some measure of the degree of variability in the tests.
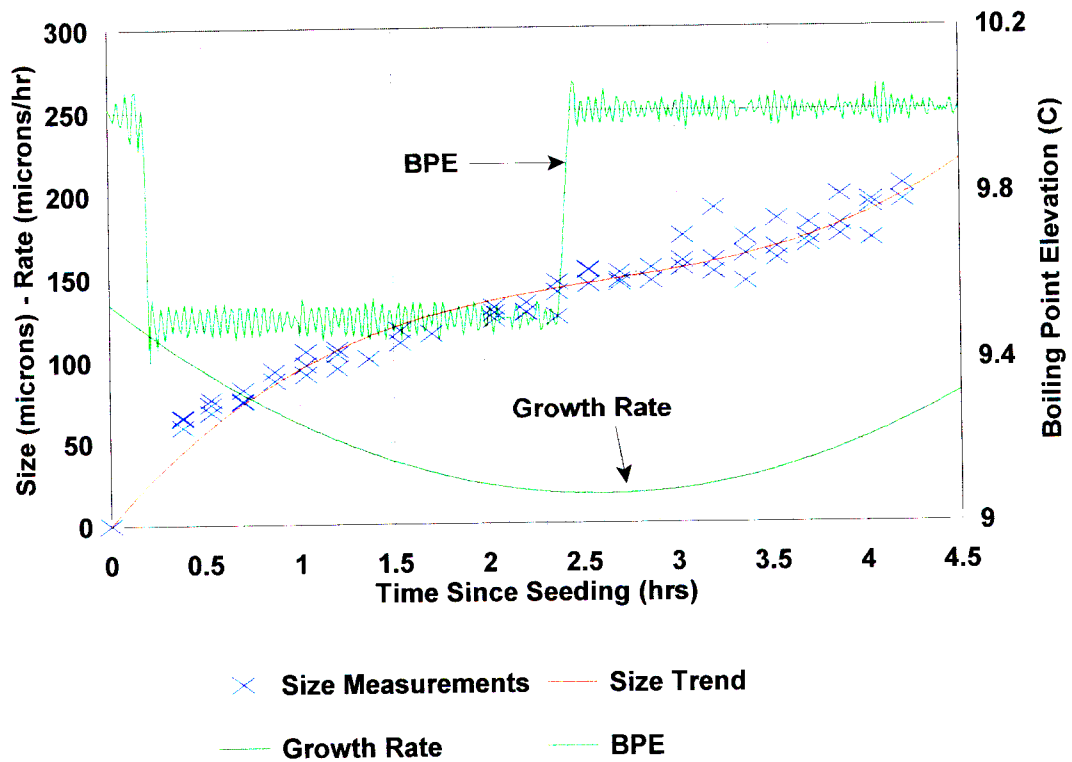


**Figure 6.6** Growth Rate of Crystals in Laboratory Pan

This boiling was performed on a raw sugar factory syrup of 84% purity. A polynomial was fitted to the relationship between crystal size and time, allowing the growth rate to be determined as the derivative of this polynomial. The boiling was controlled for the first 2.4 hours at a BPE of 9.5°C which was then increased to a BPE of 10.0°C. This is reflected in the increase in growth rate at that time. The constant BPE over the first portion of the boiling cycle would have resulted in an approximately constant concentration of mother liquor but a declining supersaturation, resulting in the decline in growth rate. The magnitude of the growth rates is within the range of those achieved in industrial scale pan boiling (as described in Chapter 2). Unfortunately it was evident that the crystal size distribution was poor by industrial standards and became worse as the boiling progressed. Examples of the images of crystals captured during the boiling are shown in Figures 6.7 to 6.10 below. Each image covers a region 4000 μm by 3000 μm.
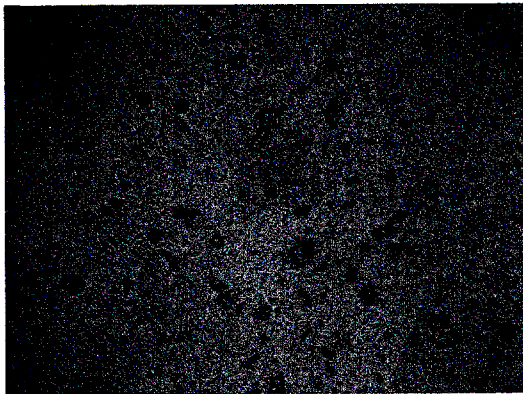


**Figure 6.7** 30 minutes after seeding
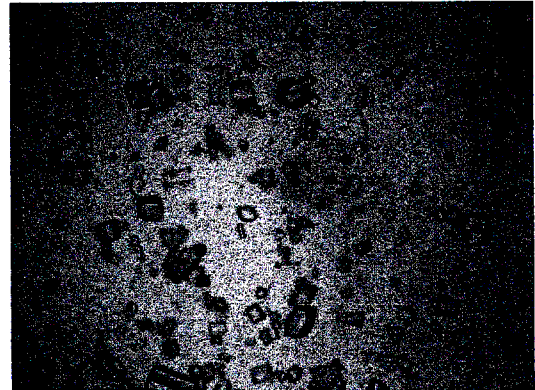


**Figure 6.8** 60 minutes after seeding
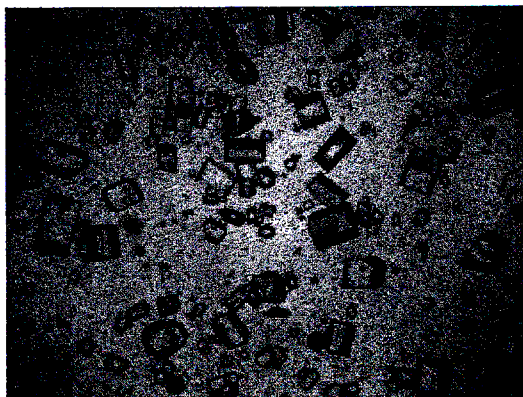


**Figure 6.9** 120 minutes after seeding
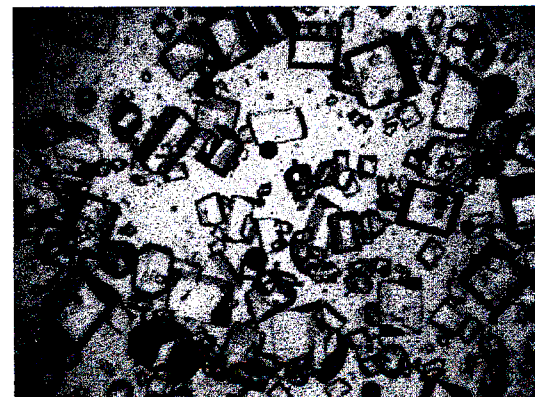


**Figure 6.10** 180 minutes after seeding

An appropriate measure of the spread of the size distribution is the Coefficient of Variation (CV) as described in Appendix A (equation A.44). To demonstrate the poor quality of the size distribution it is possible to plot the CV against the mean of the size distributions of the analysed images on a graph which includes data from industrial scale pan boiling ( the tests on the Felixton continuous A-pan reported in Appendix F). This graph (Figure 6.11) shows how the CV of the size distribution increases as the mean size increases (as the boiling process progresses). At the time when the crystals are first large enough to be analysed by the semi-automated technique (a mean size of about 0.06 mm) they have a CV of about 30%. By the time that the crystals have grown to approximately 0.18 mm, the spread in size has worsened to a CV of close to 70%.
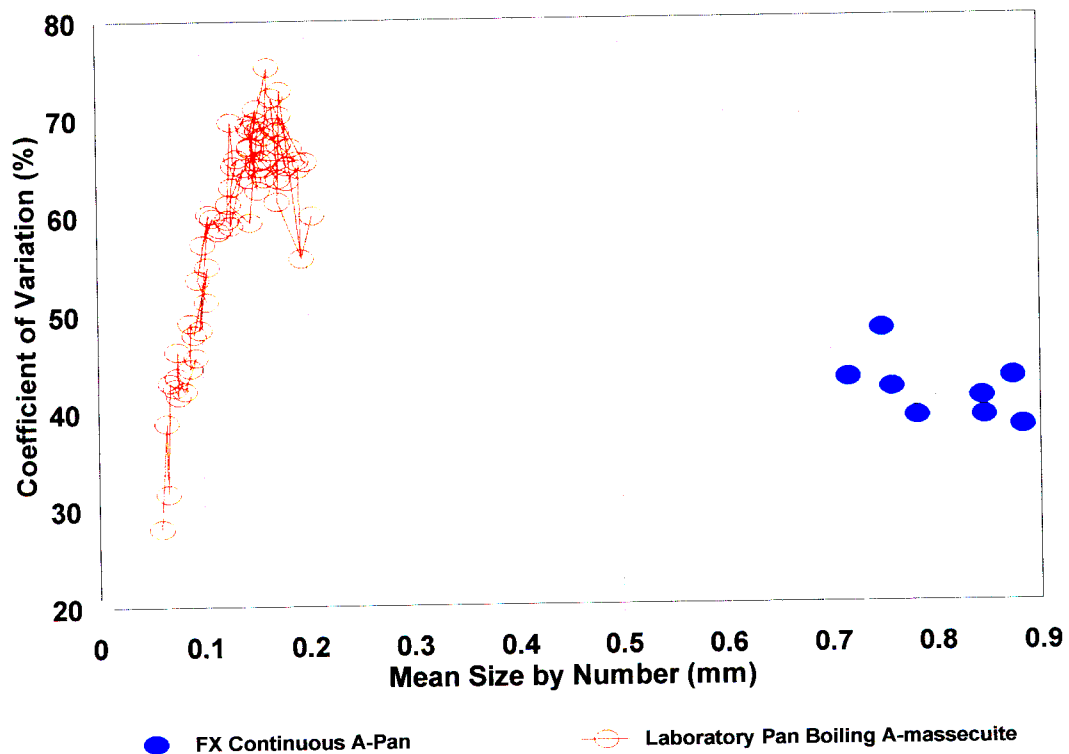


**Figure 6.11** Comparison of Laboratory Pan with full scale crystal size distributions

It is clear that the size distribution in the laboratory pan is rapidly deteriorating as the boiling progresses. There is also an increase in the variability of the CV measurement as the mean size increases, much of which can be ascribed to the measurement technique. The larger sizes correspond to higher crystal contents and an increased difficulty in separating the crystals to provide a clear image for crystal counting. Despite this variability, any reasonable extrapolation

of these data indicate that the CV will continue to worsen and will never achieve the quality of the size distribution achieved in industrial practice shown on the graph (a CV of approximately 40% at a mean size of approximately 0.8 mm). The discrepancy between the laboratory and industrial data is so severe as to cast considerable doubt on the applicability of any results obtained in the lab pan to full scale pan boiling.

Despite many attempts at altering boiling techniques and testing with high purity products (ie refined sugar boilings) no observable improvement in this aspect of the boiling could be achieved. The importance of pan design in obtaining good product sugar quality is well known (eg Donovan , 1988) and having both ensured good control and experimented with boiling technique, the design of the laboratory pan is the most likely cause of the poor performance.

The requirements of other research objectives of Tongaat Hulett provided an opportunity to utilise the knowledge and experience gained with the laboratory pan to design and build a larger, pilot scale, pan. The selection of the type of pan and the details of its design are described in the following sections.

## 6.5    Options for a New Pilot Scale Pan

Experience with the laboratory pan indicated that the following aspects of the design of the pilot pan should be given particular attention :

—    *Massecuite Circulation*

Good circulation is a major consideration in full -scale batch pan design and appears to be more difficult to achieve on small scale because of the relative increase in frictional drag resulting from the increased wetted perimeter to cross-sectional area of smaller pipes.

—    *Heating surface temperatures*

Insufficient heating surface and electrical heating can result in very high heating surface temperatures. This creates the possibility of areas of high temperature massecuite where crystal dissolution takes place. Steam heated tubes, as used in full scale equipment, limit the maximum temperature possible whilst the provision of good circulation and adequate heating surface reduces the maximum temperature necessary.

—    *Feed line blocking*

The blocking of the syrup feed line was a problem on the laboratory pan.

—    *Adequate vacuum system*

A vacuum system that was marginally adequate on the laboratory pan meant that both
frequent refurbishment of the vacuum pump and very tight control of air leaks into the
pan were necessary. A failure of the vacuum system during a boil often led to the
termination of the test and the discarding of the results.

The new pilot pan design needed to avoid the limitations of the laboratory pan whilst attempting
to approach the design and performance of a full scale pan as closely as possible. Industrial
batch pan designs have been iterated over a period of more than a hundred years and whilst
considerable design experience and information was available within Tongaat Hulett Sugar,
much of this information is empirical rather than fundamental and needed to be applied with
caution to the design of a small scale pilot pan. (It is an interesting reversal of conventional
chemical engineering practice to be using data from full scale installations to design a pilot
plant!)

Given the requirement of approximating full scale pans as closely as possible whilst keeping
quantities of massecuite manageable within the laboratory, possible design options were
investigated before proceeding with the detailed design.

An ideal pilot pan would be one based around a single standard pan tube (100mm diameter) with
a length equivalent to those used in industrial pan designs (approximately 1000mm long). The
difficulty with this design is that if the circulation ratio (ie the ratio of the total cross sectional
area of the tubes to the cross sectional area of down-take) is maintained at the value for a full
scale pan, circulation will be impeded by the disproportionate resistance of the down-take. This
is because the effect of frictional drag from the down-take wall is increasingly significant with
smaller pans whilst there is no equivalent effect of pan size on frictional drag through the tubes
(when using standard size pan tubes). Attempting to maintain the circulation by reducing the
velocity and thus the drag in the down-take will result in a disproportionately large down-take.

As a solution to this problem, the possibility of using a "pumped down-take" was investigated.
The high viscosities, presence of crystals and unacceptability of crystal damage leaves very few
choices for pump selection. A sliding vane positive displacement pump offered the possibility of

providing the necessary performance and a test rig was constructed to re-circulate massecuite through a pump on trial and allow crystal damage to be investigated. Unfortunately, a short test showed very clearly that there was excessive and unacceptable crystal damage caused by the pump. Whilst other pumping options may be possible these were not pursued.

Given the difficulties of the full length single tube design described above the design proceeded on the basis of using multiple 100 mm tubes but using shorter tubes to keep massecuite volumes small. The basis for the design is a set of tubes equally spaced around a central down-take with a circulation ratio approaching that of a full scale batch pan. Because of the significance of frictional drag in the down-take of small pans described above, the design requires a stirrer to promote circulation.

## 6.6    Design of a New Pilot Scale Pan

The photograph of Figure 6.13 (on page 6-28) and the instrumentation diagram of Figure 6.12 (on page 6-27) may assist in clarifying the descriptions of the aspects of the design of the new pilot scale pan which follow .

### 6.6.1    *Pan body*

The material of construction for both the pan body and calandria is stainless steel, using standard pipe and flanges where possible and standard 100mm stainless steel pan tubes. This approach eliminates the corrosion problems associated with intermittent pan operation and has the added benefit of shiny internal surfaces which improve lighting and thus visibility of the pan contents.

The design uses six (100 mm diam) tubes equally spaced around a central down-take as discussed below under the section on heating surface (on page 6-22). The pan body is constructed from standard 450 mm pipe and with the selected down-take diameter of 140 mm (see below) provides a strike volume of 51,4 litres and a graining volume of 21.3 litres. This ratio of strike volume to graining volume ration of 2.42 is higher than the value of 1.89 for Tongaat-Hulett's present design of 85 m$^3$ batch pan, but is achieved with a massecuite level only 200mm above the top tube plate. This low head will favour good circulation. Expressed differently, the graining volume is 41% of the strike volume, approximating the recommendation of Rouillard

(1987) of a value of 40% as a compromise between good circulation and number of cuts required to achieve the required final crystal size.

The base (saucer) of the pan was sized to minimise holdup of massecuite and eliminate stagnant regions whilst promoting good circulation. The base includes a fitting to allow a standard industrial model RF probe (short length) to be fitted into the pan and protrude into the down-take where the forced circulation past the probe will ensure a representative reading. A major advantage of the use of a full scale probe is that it should enable control settings determined during the pilot test work to be converted into appropriate settings for full scale equipment. (To achieve probe readings comparable to full scale boilings without recalibration of the probe it was found necessary to shorten the tip to compensate for the conduction path from the tip to the walls of the down-take).

The pan body is fitted with three (standard industrial size of 200 mm diameter) sight glasses above the calandria. Two are just above the calandria level to allow the massecuite level to be monitored during boiling and the other is positioned near the top of the pan body to provide extra light and to allow any foaming and potential carryover to be monitored. The sight glasses are not provided with any steam or water wash points as this would introduce added complexity to system for on-line mass balances. Natural condensation has proved to be sufficient to keep the glass clean in most instances but a wash system compatible with the mass balance requirements could be designed and fitted.

### 6.6.2   Heating Surface

The use of six 100mm tubes of 200mm length provides a heating surface area to volume ratio of $6.8 \text{ m}^{-1}$. For comparison, other appropriate figures are

| | |
|---|---|
| $6.07 \text{ m}^{-1}$ | Tongaat-Hulett design of 85 $\text{m}^3$ batch pan |
| $5 \text{ to } 6 \text{ m}^{-1}$ | quoted by Wright (1974) as normal range for batch pans |
| $8 \text{ to } 10 \text{ m}^{-1}$ | range of values used in Tongaat-Hulett continuous pan designs - this normally allows the pans to be boiled using sub-atmospheric vapour when they are clean. |

With the small size of the calandria, steam distribution was not considered to be a problem and the only special arrangement used was a tangential steam inlet to promote mixing in the steam

chest and reduce the possibility of stagnant pockets where incondensible gasses can accumulate. Since the calandria is only 200 mm high, only a single incondensible gas vent is installed (rather than the conventional top and bottom vents). The vent is positioned to remove incondensibles from close to the down-take.

In the calculation of surface area for heat transfer, the down-take surface area is not included. As presently designed, the down-take is only marginally different from the heating tubes and there will undoubtedly be heat transfer through this surface. If this heat transfer affects circulation (eg by the generation of vapour bubbles and cavitation of the impeller), it is possible to install an insulating sleeve within the down-take.

### 6.6.3    Pan Circulation

Whilst the importance of circulation in pans is well known, there is very limited data available on the actual circulation rates or velocities achieved in industrial equipment, making appropriate selection of a stirrer for the pan difficult.

In reviewing the literature it is important to take account of the error of Webre (1933) who proposed that no boiling takes place in the tubes and that natural circulation is due to the difference between the density of hotter massecuite in the tubes and colder massecuite in the down-take. The validity of this assumption was questioned by Allan(1962) and later demonstrated by the detailed measurements of Rouillard (1985) to be completely erroneous. Webre's error was propagated by Hugot and Jenkins (1959) in their elegant mathematical derivation of the optimum dimensions of a pan down-take. The details of this calculation were included in the first edition of Hugot's handbook (1960). The more recent edition of the handbook (Hugot, 1986) has simplified the optimisation of down-take dimensions to minimising the sum of the resistance to flow through both tubes and down-take, without any reference to the error in the previous calculation. Bubbles in the tubes are stated to be the driving force for circulation but this driving force is simply neglected in the optimisation calculations. A recent paper by Sheng (1993) makes no mention of this problem of quantifying the driving force for circulation and simply refines Hugot's calculations to allow for multiple down-takes and the non-Newtonian behaviour of massecuite.

The circulation velocity measurements of Webre (1933) quoted by Hugot (1986) were inferred from temperature measurements and based on his erroneous assumption of the absence of boiling in the tubes and must thus be disregarded. Rouillard (1985) estimated circulation in pan tubes by fitting a mathematical model of heat transfer to pilot plant results. One of the parameters estimated by the model is the circulation velocity. No measurements of circulation velocities were, however, made to check the validity of the model predictions. It is even more difficult to have confidence in the model when, as Rouillard demonstrates, the model predictions of evaporation rate are not applicable to A-massecuites and predict the **opposite** of the observed response of evaporation rate to operating pressure on B and C-massecuites. Rouillard did conduct some tests with pumped circulation of massecuite through a single tube and the flow rate for these tests is available from the calibration of the positive displacement pump used. Bosworth (1959) provides some data on direct measurements of circulation velocity obtained with an adaptation of a hot wire anemometer. Bosworth's measurements were unfortunately taken in the volume above the calandria and the direction of flow could only be inferred. They do not thus relate directly to the flow rate through the tubes or through the down-take.

For mechanically stirred pans, some data are available on the size and installed power of stirrers (Hoekstra, 1999). Bachan and Sanders (1987) describe the benefits of the Ekato design of impeller on the performance of refinery pans. Cox and Purdham (1989) demonstrated the benefits of a marine type of impeller over a Kaplan Turbine impeller for white massecuites. These authors do not provide any direct measurements of circulation rates.

The readily available data on pan circulation (which must obviously be treated with circumspection) can be summarised as follows:

*Circulation Ratio* (ratio of cross sectional area of the tubes to the down-take area)

      2,8     - average for South African Batch pans (Rouillard 1987)

      2,75   - Tongaat Hulett 85 $m^3$ pan design

      Rouillard (1987) used a mathematical model which predicted an optimal circulation at a circulation ratio of 3,5, although there is little variation between values of about 2,5 and 4,0. The model predicts that specific evaporation rates will drop slightly as circulation ratio increases.

*Circulation velocity* (inlet velocity at the bottom of the tube):

        0,14 to 0,61 m/sec. (Rouillard, 1985, estimates from mathematical model)

        0,03 to 0,13 m/sec (Rouillard, 1985, forced circulation tests )

*Mean Circulation rate in massecuite above calandria or coil* (Bosworth, 1959)

| | |
|---|---|
| 0,10 m/s | A-massecuite |
| 0,08 m/s | AB-massecuite |
| 0,04 m/s | B-massecuite |
| 0,02 m/s | C-massecuite |

*Installed Stirrer Power*

| | |
|---|---|
| 1,65 kW/m$^3$ | (Wright, 1974) |
| 0,97 to 1,57 kW/m$^3$ | (Hoekstra, 1999) |
| 1,06 kW/m$^3$ | (Bachan and Saunders, 1987) |

As discussed earlier in this report, small pans have a proportionally larger frictional drag in the down-take than larger pans with the same circulation ratio as a result of the increased wetted perimeter to cross-sectional area of the smaller downtake. Consequentially the laboratory pan is designed with a circulation ratio of 2,98, approximating that of full scale natural circulation pan but with a stirrer to promote circulation. The design circulation velocity was selected as 0.15m/s, based on Rouillard's pumped circulation tests.

Rather than use a simple Kaplan type impeller or a conventional marine impeller design, the stirrer selected was an available commercially designed impeller - a 134mm A103 impeller supplied by Aeromix. This is a complex aerofoil design and the suppliers provide limited information on its performance. The impeller appears to be the same as a unit described in the book by Oldshue (1983) - published by the company which designed and manufactured the impeller. The impeller has a pitch of 1,5 (implied by Oldshue and checked by measurement).

The spreadsheet calculations indicate that the design circulation velocity can be achieved with a reasonably low rotational speed of 150 rpm (assuming no slippage). To allow for slippage and the uncertainty in this aspect of design, the impeller is directly coupled to a variable speed DC

motor with sufficient extra speed capability (maximum speed of 1500 rpm). The motor is rated at 0,3 kW, giving an installed power of 5,8 kW/m$^3$ - more than sufficient when compared with the quoted design figures.

At the design speed of 150 rpm, the tip speed of the impeller is 1,04 m/s, well below the upper limit of 10 m/s quoted as the value above which secondary nucleation will be produced by the impeller blades (Cox and Purdham, 1989).

### 6.6.4    *Feed System*

With a stirrer in the pan down-take, good feed distribution can be achieved by simply directing the feed line into the top of the down-take. To eliminate the problem of the syrup feed line blocking whilst water is being fed through a separate feed line (as occurred on the laboratory pan) only a single feed line is provided into the down-take - connections outside the pan allow either water or syrup/molasses to be fed through this line.

### 6.6.5    *Sampling Facilities*

Two options are provided for sampling from the pan. A small proof-stick above the calandria allows small samples (approx. 0,4 ml) to be taken for microscopic examination. A second sampling point is provided in the base of the pan. By connecting this to a vacuum sampling system, sufficient quantities of sample can be taken for laboratory analysis.

### 6.6.6    *Ancillary Equipment*

The pan sizing is compatible with an available electrode boiler (Hamworthy Model ES 100 - full load of 30 kW) with an estimated capacity of 39 kg/hr of steam at 100 kPa abs., produced from water at 25 °C. With the pan operating at an assumed maximum specific evaporation rate of 90 kg/hr/m$^2$ the boiler needs to operate at approximately 87% of capacity.

The pan is provided with a condenser, a length of 150 mm pipe mounted horizontally and fitted with copper cooling coils, to condense the vapour generated in the pan. The condenser is capable of condensing 34kg/hr of vapour at 10kPa abs.

An accurate estimate of the quantity of incondensibles to be removed from the pan and associated equipment under vacuum is difficult to obtain without extensive calculation (Ryans and Croll, 1981). For industrial installations, Tongaat Hulett normally size vacuum systems based on a practically attainable leakage rate (defined by a standardised test) and estimates of the quantity of air which will enter with input streams. Following this calculation procedure, the estimated volumetric flow of water saturated incondensibles at 30 C and 10 kPa abs. is 2,3 $m^3$/hr. A single stage liquid ring vacuum pump with a nominal capacity of 40 $m^3$/hr was available on short delivery from a local supplier, providing a considerable safety margin for poor sealing of air leaks and deterioration in pump performance with time.

To allow the pan calandria to be operated under vacuum, the steam condensate and incondensibles removed from the calandria are collected in a condensate receiving tank held under vacuum. A small cooler/condenser cools these streams to minimise the load on the vacuum pump which would otherwise have to condense the vapour and vapour flash from these streams.

Two identical tanks are provided for collecting the condensed vapour from the boiling massecuite and the steam condensate from the calandria. These tanks operate under vacuum and are constructed from 2 m lengths of 300 mm polypropylene pipe fitted with sight glasses and drain valves. The volume of approximately 140 litres provides capacity for 9.4 hrs of operation at an average specific evaporation rate of 40 kg/$m^2$/hr (A massecuite). The vapour condensate tank is hung from a load cell, providing a mass reading which is fed to the control computer via an RS232 link.

Two feed tanks (for liquor/syrup/molasses and water) are provided. These are large buckets with removable lids (to minimise evaporation) from which feed to the pan is sucked through tubes which dip into each tank. The feed tanks are mounted on an electronic scale with an RS232 connection to the control computer.

6.6.7   *Schematic Diagram of Pan*

The schematic diagram of Figure 6.12 shows how the pan is connected to its ancillary equipment. The diagram also indicates the instrumentation and control valves but does not show individual control loops which are all implemented within the control computer.
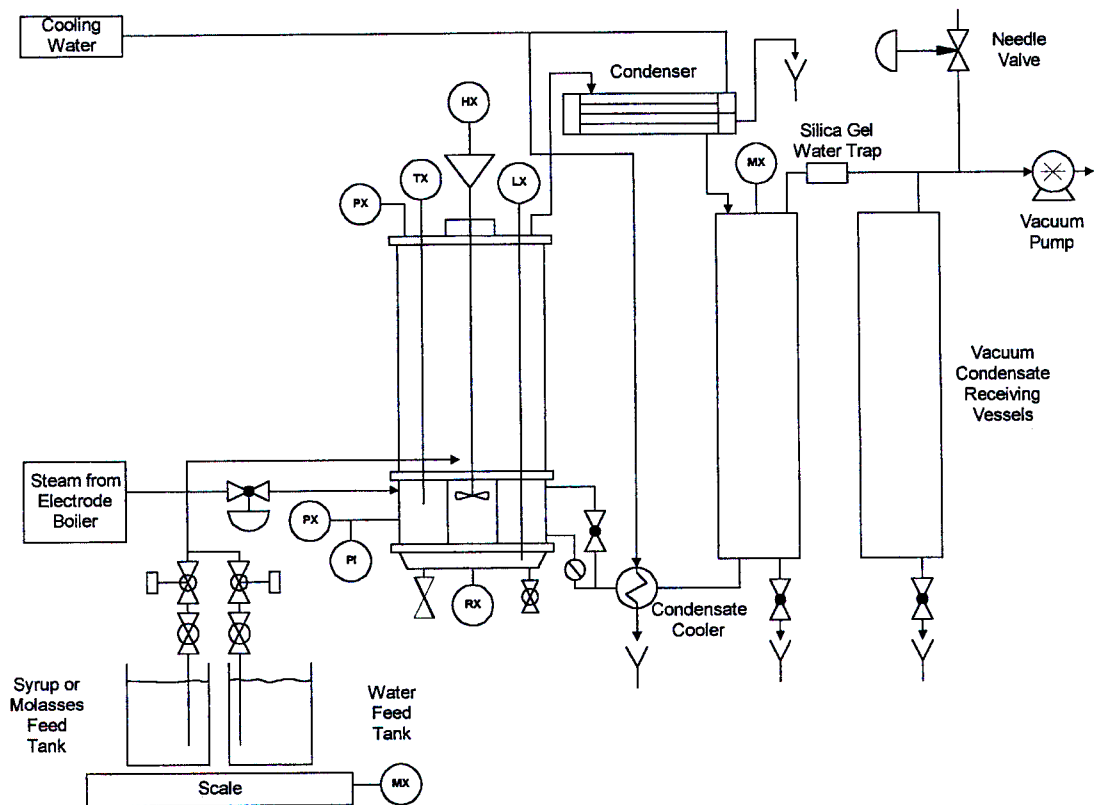


**Figure 6.12** Schematic diagram of pilot pan and instrumentation.

6.6.8    *Photograph of the Pilot Pan*
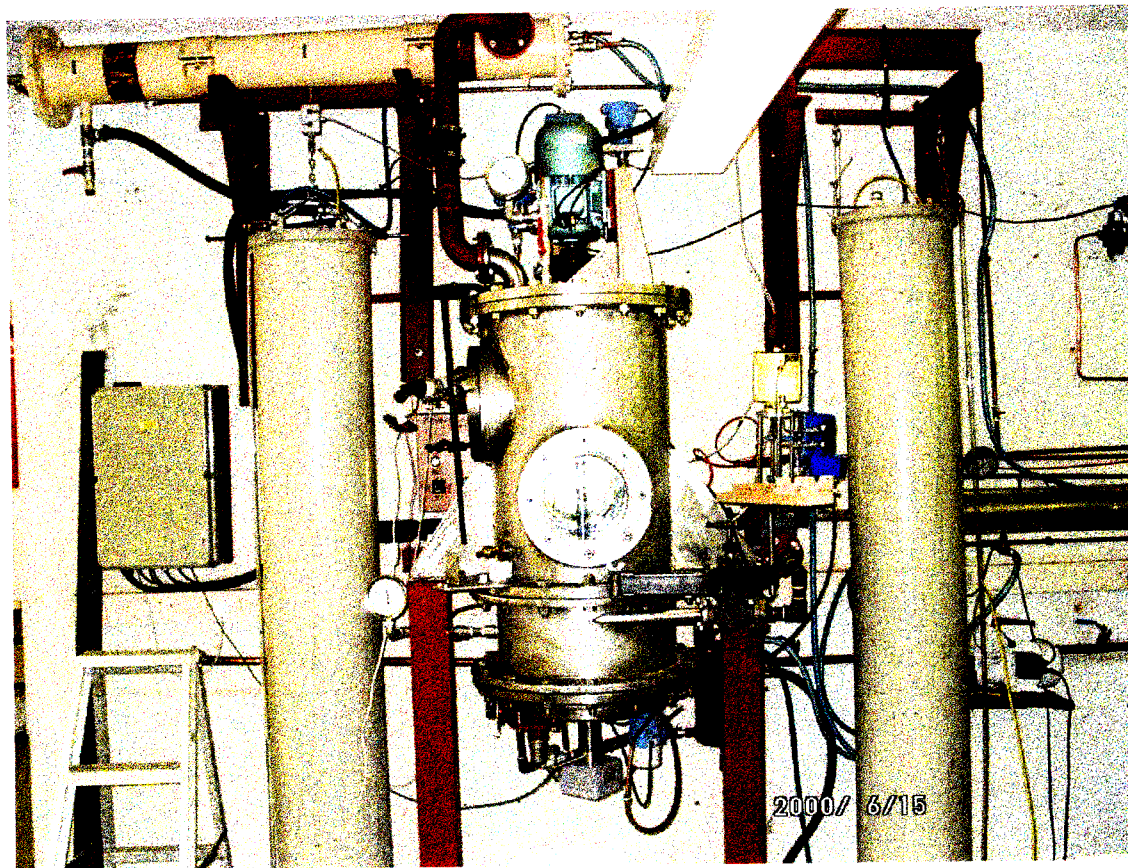


**Figure 6.13** Pilot pan with condensate receiving tanks on either side

## 6.7    Performance of New Pilot Scale Pan

After the solution of some instrumentation and equipment problems, the new pilot pan could achieve control and mass balance performance equivalent to that obtained on the laboratory pan. As with the laboratory pan, massecuites were created by seeding with slurry. Developing a suitable seeding procedure was achieved with a measure of trial and error. Once some experience had been gained with the seeding and boiling techniques, it was evident from simple visual observation that the spread in the crystal size distribution was considerably better than that obtained in the laboratory pan. To quantify the performance, the results of a boiling test on A-massecuite, are plotted in Figures 6.14 and 6.15 below, using the same format in which the results of the laboratory pan were presented.
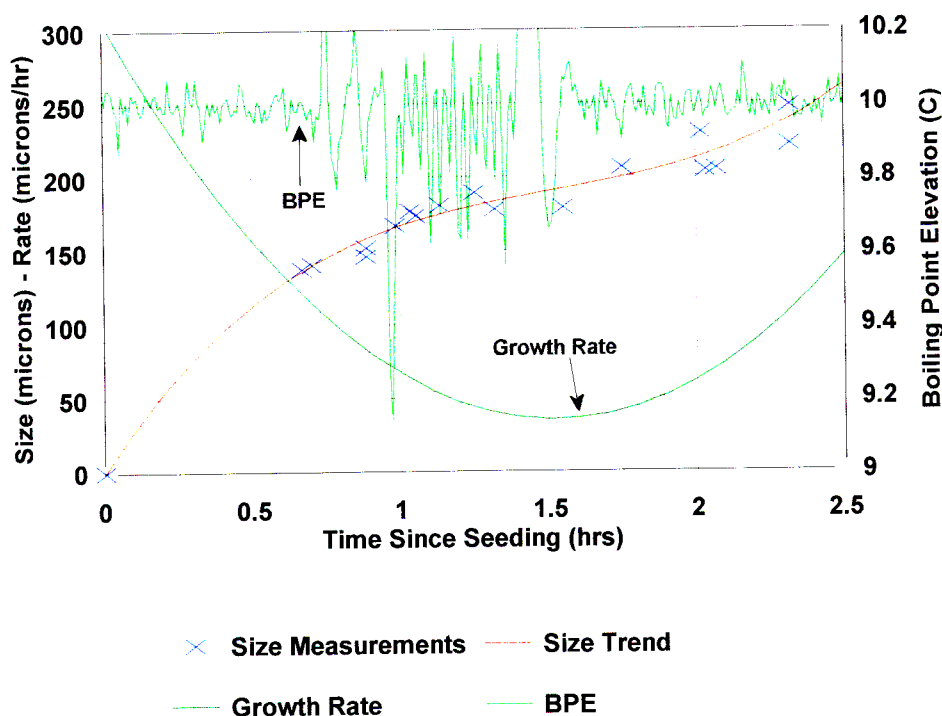
**Figure 6.14** Crystal Growth Rates in Pilot Pan - Boiling A-Massecuite

This test was on massecuitte of approximately 81 % purity. At this relatively low A-massecuite purity, the growth rates are relatively high (compared with the industrial data presented in Chapter 2). The inflection point in the growth rate in this graph cannot be explained by a change in the concentration of the mother liquor, as with the lab pan results of Figure 6.6, given the constant level of Boiling Point Elevation (BPE) over the test. The inflection is probably an artefact of the data, as a result of both the limited number of data points in the region between 1.4 and 2 hours and the concern over the accuracy of the last few data points where the number of crystals counted in each image is less than 100. A better understanding of how the on-line measurements relate to the nucleation boundary needs to be developed. This will then enable the operating conditions to be adjusted so as to maintain the maximum possible supersaturation driving force and achieve the maximum crystal growth rates.

The improved quality of the sugar produced, in terms of a narrower size distribution is evident from plotting the mean size vs CV data on the same graph as the data from the laboratory pan and from the full scale Felixton continuous A-pan.
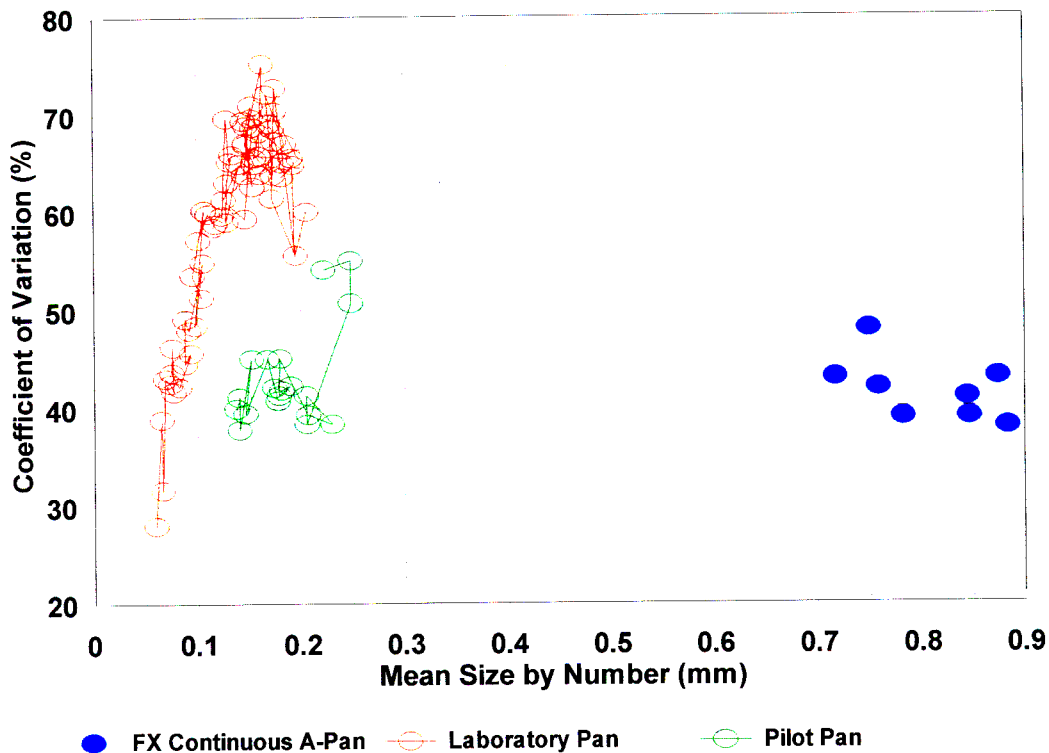
**Figure 6.15** Quality of crystal size distribution produced in Pilot Pan

It is clear that with a suitable boiling technique, the crystal size distribution achieved by the pilot pan is substantially better than that achieved in the laboratory pan. The increase in CV towards the end of the test could well result from the problem of measurement at higher crystal contents and larger crystal sizes where the numbers of crystals counted were below 100 per sample. Given this problem (which can be addressed by changes to the measurement technique), it appears as if the pan performance is achieving acceptable simulation of full scale operation.

The results of the considerable development effort discussed in this chapter have unfortunately not yet yielded any suitable data on the relationship between mother-liquor purity and crystal growth rate. The work has however highlighted the limitations of small laboratory scale pan boiling even when good quality control can be achieved. The new design of pilot pan that has been developed and constructed, has good crystallisation performance and shows considerable promise that it will be able to collect the necessary data on variations in growth rate with purity. It is hoped that a new research project will make use of the pan to continue this research and provide reliable, applicable data on the relationship between growth rate and purity appropriate for A-pan boiling in the South African cane sugar industry.

# CHAPTER 7

## 7. Measurements of Growth in a Full Scale Continuous Pan

### 7.1 General

A mathematical model of a continuous pan (as developed in Chapter 4) can only be considered to be of practical use if it has been shown capable of accurately modelling the behaviour of a real installation. A method of ensuring this correspondence between model and real behaviour is to determine some of the major parameters of the model by fitting the model predictions to experimental data from a full scale pan operating in a production environment. In taking this approach, it is important not to try to fit parameters that relate to conditions that do not vary significantly during the tests to gather experimental data..

For the continuous pan model developed in Chapter 4, the parameters which have been fitted in this way are :

$K_1$, the parameter which defines the linear dependence of growth rate on oversaturation,

and $p$, the parameter which describes the spread in growth rates.

The parameter $K_3$, which describes the dependence of growth rate on the purity of the mother liquor is specifically excluded since there is little variability in purity in the experimental data. Attempts to measure $K_3$ in experimental scale batch pan boilings unfortunately did not produce any usable results (Chapter 6) and it was necessary to use values taken from a review of the literature and available industrial data (Chapter 2). The parameters in the correlations for sucrose solubility in impure solutions were also not obtained by fitting the model to the experimental data, but rather they were obtained from the laboratory experiments specifically undertaken for this purpose (Chapters 5).

Hoekstra (1985) reported a similar approach of fitting a continuous pan model to experimental data on a Tongaat-Hulett continuous pan. His model did, however, not include the size dispersion parameter $p$. When fitting his model to experimental data (termed evaluation mode), to accommodate for insufficient experimental data, he was forced to assume equal supersaturation in each compartment and a linear dependence of heat transfer coefficient with compartment number. The assumed heat transfer coefficients were used to provide estimates of the evaporation rate in each compartment and thereby to estimate the feed flow to each compartment.

The approach taken for this thesis was to increase the scope of experimental measurements to eliminate the necessity for the type of simplifying assumptions used by Hoekstra. As has been described in Chapter 4, the steady state model of the continuous pan used here is derived as a simplification of a full dynamic model. The parameters determined in this analysis of data on steady state performance are thus applicable to the dynamic model.

The steady state model, validated against actual performance by this fitting process, has uses as a design tool in a simulation mode and as the mechanism for determining the optimum operating conditions for a continuous pan (Chapter 8)

## 7.2    Description of Plant

The basic design of the Tongaat-Hulett continuous pan has been described in Chapter 3. Figures 3.3 and 3.4 show the mechanical construction of the pan and Figure 3.8 shows the instrumentation and control scheme. The pan tested was one of the two continuous A-pans (the A1 pan) at the Felixton factory. This pan has a massecuite volume of $120m^3$ and is constructed with 12 compartments of equal volume and heating surface area.

When the Felixton factory was constructed in 1984, it was fitted with an early generation of distributed control system (DCS) which was used to implement the control strategy outlined in Figure 3.8. This system did not have facilities for data logging (for subsequent processing and analysis) nor facilities for advanced control. For this reason a version of the data logging and control program described in Chapter 12 was adapted to this task and implemented on a PC at Felixton to control and monitor the A1 pan. The system used analog and digital interfaces to the plant which were of a local design manufactured by the Conlog company (their Anaflex range) and connected to the control computer via a proprietary network (Conet) developed by the same company.

This PC based control and logging system was designed to monitor all of the process variables shown in Figure 3.8. Whilst the pressure and flow control loops were left to be implemented on the DCS, the feed control loops were removed from the DCS and implemented on the PC. The feed control was changed from using proportional settings of control valve openings to using time proportional on/off actuation of the feed valves. Whilst allowing a simpler digital interface to the

computer control system, this also provided a means of estimating the feed flow to each compartment by recording the control output to each compartment over the period of each test (as described in Appendix F).

Those compartments which were fed with water (compartments 11 and 12) were fitted with simple integrating water flow meters which could be read manually at regular intervals.

To provide extra information on the conditions in each pan compartment, special temperature probes (capable of providing a resolution of 0.01 °C) were fitted in each compartment of the pan and connected to the data logging system. An on-line measurement of the level in the seed receiver was also available, and logged.

## 7.3    Experimental Technique

An important aspect of the testing of a full scale pan is to ensure steady process operation (particularly given the long process time constants involved ) and good performance of the automatic control loops.

Throughout the period of each test, the computer control and logging system recorded all of the monitored process variables and the set points and outputs of the 12 feed control loops. The recording was to computer disk in a standard text file format, allowing the data to be subsequently imported into a spreadsheet for analysis and plotting. Special arrangements were made to measure product and seed massecuite flows by manually recording changes in level over time. The details of the vessel dimensions and procedures are given in Appendix F.

Massecuite samples were taken from each compartment during the duration of the test. Samples of seed massecuite and product massecuite were also collected. A portion of the sample was immediately separated in specially designed centrifuge tubes to generate samples of mother liquor (Nutsch molasses) and sugar for subsequent analysis. By weighing the sugar and molasses samples, it was also possible to calculate an approximate crystal content, determined as sugar as a mass percent of massecuite.

Samples of syrup feed during the test were collected for analysis of concentration and purity.

## 7.4    Results and Analysis

Four tests were performed on the A1 continuous A-Pan at Felixton. In the first two tests, the facility of recording control outputs to the feed valves was not implemented and as discussed, this required that the syrup flows were estimated as "parameters" when fitting the model to the collected data. This may appear to be an "over parameterisation" of the model which would allow a high level of fitting of the model to the data with little confidence in the statistical significance of the fitted parameters. An indication that this is not so, is that the syrup flows into the individual compartments (and the evaporation rate in each compartment) can be calculated directly from the plant measurements. This is done by assuming that the number of crystals flowing through the pan remains constant (equation B.39 at steady state) and then iteratively calculating the flow of masecuite out of each compartment from the massecuite flow into that compartment using equation B.10, starting with compartment 1 and the known seed flow. The procedure of determining syrup flows by estimating them as "parameters" during the fitting of the model will be an improvement on this technique in that it takes into account other requirements (eg that the sum of the syrup flows to the individual compartments is equal to the total syrup flow) in a best fit or least squares manner.

For clarity, the description of the procedure for analysing test results in this section applies to the tests in which the control outputs to the feed valves were recorded.

An example of a full set of data collected during one of the tests, and its interpretation, is given in Appendix F. The trends of the logged data over the two hour test period demonstrate the quality of control which was achieved. Of particular importance in achieving constant growing conditions during the test is the ability to maintain a constant absolute pressure in the pan. For the test reported in Appendix F, the average absolute pressure was 18.27 kPa with a standard deviation of 0.07 kPa and a maximum deviation of 0.24kPa. This level of attention to the quality of control of the fundamental parameters of pan boiling does not always appear to have been given sufficient attention in attempting to model pan performance. For example, de Azevedo et al. (1993) published data for a batch pan, to which they were fitting a mathematical model, where the absolute pressure showed oscillations with an amplitude greater than 10 kPa. Fluctuations of this type can affect results through a range of interacting mechanisms viz.

*Evaporation :*

A changing pressure will alter the massecuite temperature and in turn change the rate of evaporation from the massecuite. This change in evaporation rate will be influenced by :

—       the quantity of heat absorbed or released by the massecuite as a result of its change in sensible heat as it changes temperature.

—       the change in the temperature driving force for heat transfer.

—       the interacting effect of evaporation rate on heat transfer coefficient .

The magnitude of the effect on the evaporation rate will depend on the rate of change in pressure and the average rate of evaporation per unit mass of massecuite. A very rapid increase in pressure can suppress boiling entirely.

*Solubility :*

The changing massecuite temperature will result in a change in the solubility of sucrose of the mother liquor , as described by equation 2.2 or equation 2.3.

*Measurement and Control :*

Since there is no available instrument which measures supersaturation driving force directly, control of crystallisation is normally achieved using approximate measurements (eg electrical conductivity) as described in Chapter 3. To accommodate the changes in massecuite temperature it is necessary compensate for both the effect of temperature on the measurement (eg change in electrical conductivity at constant concentration) and the change in sucrose solubility with temperature. Even if it is possible to compensate for these effects at steady state, the results can be influenced by the different time constants of separate aspects of the process ( as demonstrated for boiling point elevation measurements in Chapter 9).

The complexity of these effects and their interactions is difficult to model and the use of average values will not adequately accommodate the nonlinear aspects of the effects of pressure and temperature fluctuations.

The first step in analysing the results of a test is to collate the logged data (converting measurements into appropriate engineering units where necessary) and have all the necessary laboratory analyses performed on the samples that were collected. The original intention had been to use pol and brix measurements as appropriate measurements of sucrose and dry solids content for A-massecuite. The review of appropriate data on the relationship between these types of approximate and accurate measurements in Chapter 3 showed that the differences were of

consequence and had an influence on the correlations which were developed for sucrose solubility in impure solutions (Chapter 5). In consequence all measurements of brix and pol are converted into estimated dry solids and sucrose measurements using equations 3.3 and 3.6.

The specific tasks of collating and preliminary data analysis can be summarised as follows :

—     Plot all logged data for the period of the test and examine for instabilities, excursions and anomalies.

—     Calculate averages and standard deviations of the logged variables.

—     For those compartments fed with syrup, estimate the individual flow to each compartment based on the average valve opening for the period, subject to the constraint that the sum of the flows is equal to the total syrup flow measured for the test period.

—     For those compartments fed with water, estimate the flow to each compartment by consolidating valve output readings and flow meter readings.

—     Consolidate seed flow measurements with seed pump speed measurements and determine the average seed flow for the period.

—     Estimate massecuite flow measurements from measurements of crystalliser levels.

—     Analyse all the sugar molasses and syrup samples for pol and brix.

—     Analyse sugar samples to determine average length and width and the standard deviations of these measurements.

—     Estimate the sucrose and dry solids contents of all the samples using the relationships presented in Chapter 3.

—     Calculate crystal contents for all streams from the analyses of massecuite and molasses

—     Calculate approximate crystal contents from the masses of sugar and molasses recorded during the centrifugal separation process.

—     Correct approximate crystal contents for molasses still adhering to the crystal, based on a representative analysis of sugar.

—     Compare crystal contents calculated by both techniques to check for anomalies.

—     Determine the average characteristic crystal dimension ( $Dc$ )and its variance for each sample based on the measurements of length and width (as described in Appendix A, equations A.49 and A.50).

An example of the collation of a set of laboratory analyses is given in Appendix F (page F-13).


The average data that are available from these procedures can be checked to see that it is internally consistent. Specifically all of the flows into and out of the pan must meet the

requirements of a mass balance over the pan. Since it is assumed that the purity is constant over the whole process (ie seed massecuite purity = syrup purity = product massecuite purity) it is only necessary to ensure that there is mass balance closure for total flow and solids flow. The water flow, sucrose flow and impurity flow will close because of their fixed relationships to the total flow and water flow balances. In performing this mass balance, it is assumed that the rate of evaporation of water from the massecuite is equal to the rate of condensation of steam in the calandria. This common assumption is approximate because of a range of factors whose combined effect is difficult to quantify (eg heat of crystallisation, superheat in steam condensing in calandria, sub-cooling of condensate in the calandria, superheat given up by jigger steam, superheat in vapour evaporated from the massecuite, heat losses and differences in enthalpy of evaporation for condensation and evaporation at different pressures).

This problem of reconciling the inconsistencies in process measurements when evaluated in terms of mass balances has been addressed by a number of authors as summarised by Crowe (1988) and by Howat in Perry and Green (1997). Much of this work appears to have a strong academic rather than practical bias and the theory is further complicated by the distinction of problems into two different types viz. linear and nonlinear (Crowe et al 1983, Crowe 1986). A simple technique has been developed to apply the principles of process flow reconciliation by using the non-linear optimisation techniques of modern spreadsheets. The details of this technique and its application to a problem of reconciling data collected during the evaluation of a high grade centrifugal is given by Hubbard and Love (1998). The principle behind the technique of reconciling process flows is the simple idea that the plant measurements must be adjusted to create a new set of measurements which meets the requirements of mass balance. In creating this new set of adjusted measurements, the more accurate measurements should be adjusted less than the less accurate measurements.

The relative adjustment of measurements according to their accuracy is achieved by the use of weighting factors. Beckman (1982) recommends that the weighting factor is the inverse of the variance (variance being equal to the standard deviation squared). Approximate values of the standard deviation are considered to be accurate, as the main purpose of the weighting factors is merely to indicate which data are "poor", "good" or "excellent". Kneile (1995) has recommended estimating the standard deviation from the concept of a confidence interval, $\pm a$, which includes 95% of all measured values. The relation to calculate the standard deviation from this more

intuitive measure of variability is :

$$\sigma = \frac{a}{1.96} \tag{7.1}$$

This technique has been applied to the data collected in the continuous pan tests. An example of the application to the results of a test, which shows the estimated confidence intervals used, is shown in Appendix F (page F-14). The standard non-linear regression routine of the Corel Quatro spreadsheet does not perform well when there is a variation in the scale of the variables being adjusted. To accommodate this, the measurements are not adjusted directly, but rather adjustments are made to multiplying factors (which are initially set at unity for no adjustment).

The data obtained from this process reconciliation becomes the basis for estimating the growth parameters by fitting of the mathematical model. Summaries of the reconciled and measured data for each of the tests (used as the basis for fitting to the pan model) are given in section F.4 of Appendix F.

## 7.5    Fitting Model to Data

The steady state model that was fitted to the results of the tests on the Felixton Continuous A-Pan is described in Chapter 4. The "best fit" is achieved by minimising differences between modelled and measured values. To compensate for the different scales of the variables and the varying accuracies of the different measurements, appropriate weighting factors are used to create a weighted sum of squares as the function to be minimised. Following the approach of Beckman (1982) discussed above for the reconciliation of process flows, the weighting factors are based on estimates of the accuracies of the measurements. The accuracy of a measurement is expressed as a standard deviation and the weighting factor is the inverse of the square of the standard deviation. In this way, a measurement with a small standard deviations (which correspond to a measurement with a high accuracy) will have a large weighting factor, forcing the modelled value to approach the measured value more closely than it will for less accurate measurements. (The fitting program , as described in Appendix E, Section E.5, is written to weight the error first and then square the weighted error, and thus the weighting factor is simply the inverse of the standard deviation.)

The estimates of the accuracies of the flow measurements were based of assumptions of the confidence intervals. To obtain estimates of the accuracies of measurements of massecuite properties, it was assumed that the measurements had no bias and the errors were simply random variations as a result of unsteady operation, sampling and analysis. To obtain an estimate of this level of variability, a set of eight samples was taken from a single compartment of the continuous pan and analysed. The time required for the sampling and Nutsching procedure meant that the samples were collected in pairs approximately 15 minutes apart. The standard deviations calculate from this set of tests thus reflects a combination of the variability associated with sampling, analysis and variations in plant operating conditions about steady state.

The weighting factors obtained by this procedure as well as those derived from estimates of the accuracy of the flow measurements are summarised in Table 7.1 below. All units are converted to SI units, as used in the modelling, before calculating the weighting factors.

| Measurement | Confidence Interval | | Standard Deviation | | | | Weighting Factor |
|---|---|---|---|---|---|---|---|
| | Value | Units | Value | Units | Value | Units | |
| Nutch Purity | - | - | - | - | 0.219 | % | 4.6 |
| Mean Size | - | - | 33.3 | $\mu$m | 3.3e-05 | m | 30000 |
| Variance in Size | - | - | 10139 | $\mu$m$^2$ | 1.0e-08 | m$^2$ | 100000000 |
| Total Evaporation | 2 | ton/hr | 1.02 | ton/hr | 0.283 | kg/s | 3.5 |
| Final Massecuite Flow | 2 | ton/hr | 1.02 | ton/hr | 0.238 | kg/s | 3.5 |
| Seed Massecuite Flow | 1 | ton/hr | 0.51 | ton/hr | 0.142 | kg/s | 7.1 |
| Total Syrup Flow | 2 | ton/hr | 1.02 | ton/hr | 0.238 | kg/s | 3.5 |

**Table 7.1** Weighting Factors for Fitting Continuous Pan Model to Measured Data.

The computer routine used to perform the fitting is described in Appendix E. As described in section 7.1 the parameter $K_3$ was not fitted but assumed. The table below summarises the results of the fits of the model to the experimental data for different assumed values of $K_3$.

| Assumed $K_3$ | Fitting Result | Test 1-A | Test 1-B | Test 2-A | Test 2-B |
|---|---|---|---|---|---|
| 1.0 | $K_1$ (μm/sec) | 0.187 | 0.187 | 0.378 | 0.369 |
| | $p$ (mm) | 0.375 | 0.276 | 0.213 | 0.215 |
| | Weighted Sum Sq. | 69 | 100 | 45 | 157 |
| 1.25 | $K_1$ (μm/sec) | 0.252 | 0.239 | 0.499 | 0.497 |
| | $p$ (mm) | 0.355 | 0.297 | 0.200 | 0.227 |
| | Weighted Sum Sq. | 66 | 102 | 45 | 163 |
| 1.5 | $K_1$ (μm/sec) | 0.342 | 0.366 | 0.674 | 0.634 |
| | $p$ (mm) | 0.338 | 0.189 | 0.187 | 0.218 |
| | Weighted Sum Sq. | 64 | 107 | 45 | 159 |
| 1.75 | $K_1$ (μm/sec) | 0.437 | 0.479 | 0.870 | 0.850 |
| | $p$ (mm) | 0.369 | 0.208 | 0.199 | 0.224 |
| | Weighted Sum Sq. | 65 | 108 | 45 | 162 |
| 2.00 | $K_1$ (μm/sec) | 0.614 | 0.604 | 1.145 | 1.076 |
| | $p$ (mm) | 0.319 | 0.253 | 0.214 | 0.253 |
| | Weighted Sum Sq. | 63 | 110 | 45 | 165 |
| 2.25 | $K_1$ (μm/sec) | 0.787 | 0.734 | 1.500 | 1.301 |
| | $p$ (mm) | 0.359 | 0.326 | 0.209 | 0.339 |
| | Weighted Sum Sq. | 66 | 120 | 45 | 180 |
| 2.45 | $K_1$ (μm/sec) | 1.038 | 0.804 | 1.820 | 1.933 |
| | $p$ (mm) | 0.320 | 0.477 | 0.208 | 0.235 |
| | Weighted Sum Sq. | 65 | 136 | 46 | 176 |

**Table 7.2** Effect of assumed value of $K_3$ on quality of fit to model data.

Tests 1-A and 1-B did not include measurements of syrup flow to the individual compartments so, for these tests, the flows are fitted by the nonlinear regression routine and an extra term is added to the weighted sum of squares to ensure that the total syrup flow to the continuous pan matches the measured flow. The "weighted sum of squares" values for tests 1-A and 1-B are thus not directly comparable with the results from tests 2-A and 2-B.

Owing to the difficulty in obtaining a reliable value for the factor $K_3$ which defines the dependence of growth rate on levels of impurity, the model has been fitted for a range of possible values. The range of values is based on the review of published data reported on in Chapter 2 (section 2.5), covering the highest value ($K_3 = 2.45$) and extending to a comparatively low dependence of growth rate on purity ($K_3 = 1.0$). The "weighted sum of squares" results indicate, as expected, that the quality of the fits shows very little relationship to the value of $K_3$ assumed. There is however some indication that the quality of fit deteriorates for values of $K_3$ above 2.0.

In the absence of a good quality measurement of the value of $K_3$ obtained specifically for the conditions of A-pan boiling in the South African sugar industry, it is necessary to assume a most appropriate estimate for further calculations and analysis. The value of 1.75 is well supported by both laboratory (Broadfoot and Steindl, 1980) and plant measurements (Wright and White, 1974) for Australian conditions. Although it appears to predict a stronger dependence of achievable growth rates on purity, than is evident from average industrial crystal growth rate measurements for the South African sugar industry (Figure 2.8), it predicts a weaker dependence than the measurements of Morel du Boil (1985) for specific impurities occurring in South African factories. In the absence of a better estimate, $K_3$ is assumed to be equal to 1.75.

Using this assumed value of $K_3$, the major results of fitting the pan model to the results of the tests on the Felixton continuous A-pan are tabulated in the following table. A range of performance factors, which are useful in interpreting the results and comparing them with other reported data, have also been calculated. these are :

—        Crystal retention time : the sum of the crystal retention time in each compartment. This compartment retention time is calculated from the massecuite flow out of each compartment and the total mass in each compartment.

—        The average growth rate : the change in size from seed to masssecuite divided by the crystal retention time.

—        The nominal retention time: the total mass in the pan divided by the mass flow of massecuite leaving the pan.

—        The average supersaturation : a simple arithmetic average of the supersaturation in each compartment as an indicator of the average driving force for crystallisation.

—        Crystal deposition rate: the mass of crystal sucrose deposited in the pan per hour, divided by the pan volume - a useful comparative figure of the crystallisation work performed.

| Test | $K_1$ (μm/sec/°os) | $p$ (mm) | Average Growth Rate (μm/hr) | Average Super Saturation. | Crystal Retention Time (hr) | Nominal Retention Time (hr) | Ratio Crystal to Nominal Retention | CDR kg/hr/m³ | Massecuite to Seed Ratio | CV of Seed (%) | CV of Massecuite (%) |
|------|------|------|------|------|------|------|------|------|------|------|------|
| 1-A | 0.437 | 0.369 | 54 | 1.156 | 4.22 | 2.78 | 1.52 | 211 | 4.36 | 31 | 48 |
| 1-B | 0.479 | 0.208 | 72 | 1.182 | 4.01 | 2.72 | 1.47 | 218 | 4.5 | 33 | 43 |
| 2-A | 0.870 | 0.199 | 73 | 1.104 | 4.10 | 2.64 | 1.55 | 196 | 3.54 | 37 | 41 |
| 2-B | 0.850 | 0.224 | 74 | 1.111 | 3.96 | 2.62 | 1.55 | 195 | 3.42 | 36 | 39 |

**Table 7.3** Summary of results of fitting model to data.

The values of $p$ calculated for these tests are about five times greater than the value of 0.044 mm reported by Rein, Cox and Love (1985).This increase is in line with the overall observation that these tests do not show the improvement in CV from seed to massecuite reported by Rein, Cox and Love. Whilst this may indicate poorer pan performance or growth characteristics of the particular massecuite, the result may be the consequence of a different analytical technique. The tests reported here used size distribution by number measured directly by semi-automatic counting of crystals in microscopic images, whilst, the previous tests used size distributions by number calculated from the measurements of size distribution by mass using the relationships developed by Hoekstra (equations A.45 and A.46).

Equations A.45 and A.46 predict that although the mean size by mass may be different from the mean size by number, the coefficient of variation (CV) by mass should be the same as that by number. The CV data presented in table 7.3 are number based measurements obtained by semi-automatic counting of crystals in digital images as described in Appendix A. Although size distributions by mass were not evaluated for the tests on the Felixton continuous pan reported here, average monthly data for product sugar are available for the time of the tests. These data show CV results for the mass distribution which are substantially lower than measured for the product massecuite in these tests :

Tests 1-A and 1-B :

| | |
|---|---|
| CV of mass distribution during this period | 28 |
| CV of number distribution for test 1-A | 48 |
| CV of number distribution for test 1-B | 43 |

Tests 2-A and 2-B :

| | |
|---|---|
| CV of mass distribution during this period | 31 |
| CV of number distribution for test 2-A | 41 |
| CV of number distribution for test 2-B | 39 |

The results from the tests on the Felixton continuous pan reported here thus need to be treated with caution when comparing them with size measurements determined by different means. The reliability of the CV measurement by semi-automated counting of microscopic images requires further investigation to assist in comparisons of data across the industry.

Although all four tests were achieving similar rates of crystallisation (CDR values of around 200

kg/hr/m$^3$) tests 2-A and 2-B showed values of the growth parameter $K_1$ of almost double that for tests 1-A and 1-B. A major cause of this difference is that the crystallisation in tests 1-A and 1-B was achieved with a considerably higher average supersaturation driving force. Test 1-A is different from the other tests in that it has a value of the dispersion parameter p of between 65 and 85% greater than that for the other three tests. This is associated with growth that is made up of a smaller change in average size and a larger increase in CV.

## 7.6    Interpretation of Fitting Results

The tests on a full scale continuous pan have provided measures of the growth parameters $K_1$ and p of the mathematical model of a continuous pan. The parameters determined in this way are particularly useful in that they include the effects of practical aspects of pan design and operation such as circulation and quality of control. The parameters can be used in the model for design, optimisation and simulation studies. Unfortunately the values of $K_1$ determined in these tests are dependent on the assumed value of $K_3$ and it is important to note that a value of 1.75 has been assumed for $K_3$ to calculate $K_1$.

The parameter $K_1$ describes the dependence of the growth rate on the degree of oversaturation and was found to vary between 0.44 and 0.87 $\mu$m/sec/$^\circ$os.

The parameter p describes the degree of growth rate dispersion which takes place and was found to vary between 0.20 and 0.37 mm.

All the tests were conducted on massecuite purities between 87 and 88 and the results must be used with circumspection for purities outside of this range. It is also important to note that the parameters relate to crystal size measurements determined by semi-automated counting of individual crystals in digital images. The results must thus be treated with caution when comparing with data that use size distributions by mass (as obtained by sieving tests).

# CHAPTER 8

## 8.     Optimal Operating Profile for a Continuous Pan

### 8.1     General

The fundamental question on which this thesis is based, is the need to know what the optimum operating conditions for a continuous pan should be. This is not a question that can be answered in isolation but must apply to a specific size/design of pan processing a specified quantity and quality of product.

In designing a continuous pan to meet a specified production quality and quantity, the bases for the major design decisions are largely defined as follows :

| | |
|---|---|
| pan volume : | based on the quantity of sucrose to be crystallised and an estimate of the average crystallisation rates which can be expected. |
| pan heating surface : | based on the quantity of water to be evaporated and the expected heat transfer coefficients. |
| number of compartments : | based on the available seed quality and the specifications for the product crystal size distribution. |

Whilst there are numerous opportunities for optimising these aspects of pan design, given a pan designed in accordance with these principles, there remains the question of what operating conditions will yield the best performance from a given pan.

A means for determining the optimal operating policy for a continuous pan will be of benefit for maximising the performance of existing continuous pans enabling operation to be tailored to the prevailing conditions (i.e. growth kinetics, throughput etc). It would also greatly assist the design process, enabling the limiting factors in designs to be identified and eliminated and allowing different designs to be properly compared (since different designs may well have their maximum performance at different operating conditions).

Expressed simply as "what are the optimum operating conditions for a continuous pan ?", the question is too broad to be answered directly. The question needs to be formulated more specifically and is done so in this investigation, to address the practical situation which

prompted this research ( as discussed in Chapter 1). Consequently, the problem has been formulated for the multi-compartment type of continuous pan ( the THS-FS continuous pan being the particular model of interest) as described in Chapter 3.

A portion of the research described in this chapter has been published in a paper which concentrated primarily on the technique of determining an optimum pan profile whilst providing some preliminary results on optimum profiles for assumed growth kinetics (Love, 1991).

## 8.2     Formulation of the Problem

The problem of determining the optimal operating policy of a continuous pan is ultimately a multi-dimensional non-linear optimisation problem. Problems of this type increase greatly in complexity as the number of dimensions (i.e. operating variables) increases. It is thus important in formulating the problem to use sound process judgements to fix as many variables as possible, consequently minimising the dimension of the problem. This process is particular to the situation being considered, and is applied in this instance to a A-pan boiling within the conventional South African "three boiling partial remelt" scheme described in Chapter 3.

Within this boiling scheme there is a strong incentive to achieve high A massecuite exhaustions, which have the benefit of minimising the reprocessing of sugar in the B and C boilings. This in turn reduces sucrose destruction in the process and also reduces steam usage and installed plant requirements. The flow chart in Figure 8.1 shows the position of a continuous A Pan within a simplified representation of the boiling scheme, showing the components of the "A-station" whilst the components of the "B- and C-stations" are lumped together..

The objective of the A station is to maximise A exhaustion (within certain constraints such as steam usage and product crystal size). The exhaustion of the A station can be defined as the fraction of sucrose entering in the combination of "total pan feed syrup" and "B-magma" which appears in product sugar. This "A station exhaustion" is the result of the combined performance of the pans, crystallisers and centrifugals. However, by making reasonable process judgements it should be possible to optimise the A continuous pan independently of the seed preparation, crystallisers and centrifugals.
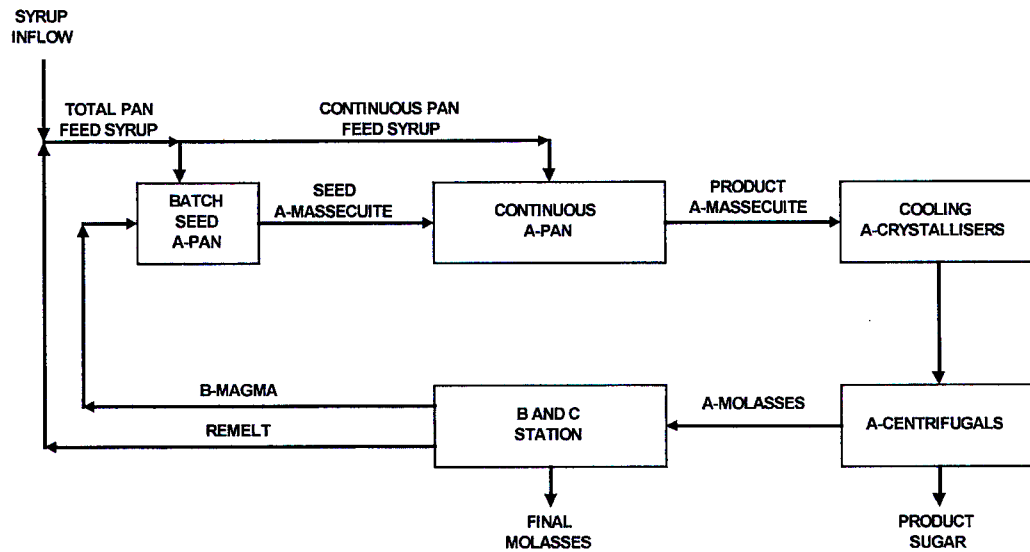
**Figure 8.1** Simplified South African "three boiling partial remelt" boiling scheme


The optimisation problem can thus be stated as follows:

| | | |
|---|---|---|
| Given : | i) | The seed flow to the continuous pan. |
| | ii) | The crystal content of the seed |
| | iii) | The crystal size distribution in the seed. |
| | iv) | The purity of the seed. |
| | v) | The Brix of the pan feed syrup. |
| | vi) | The purity of the pan feed syrup. |
| | vii) | The quantity of pan feed syrup. |
| | viii) | The operating absolute pressure (vacuum) for the pan. |
| Determine : | i) | The required evaporation rate in each compartment. |
| | ii) | The required feed rate to each compartment. |
| Constrained by : | i) | Not producing any secondary nucleation of crystals (false grain). |
| | ii) | Maintaining good circulation by preventing excessively high crystal contents. |
| | iii) | Processing all of the available feed syrup. |

| | |
|---|---|
| Which Achieves : | The highest fraction of sucrose in crystal form in the product massecuite (i.e. the highest "pan exhaustion"). |

The assumptions implicit in this formulation of the optimisation problem are:

i)     The product crystal size is achieved by correctly specifying the seed fed to the pan. (The dependence of product crystal size on pan exhaustion, within normal operating limits, is small compared with the effects of seed flow and properties).

ii)    The purity of the remelt and the B magma are assumed to be equal to the purity of the syrup inflow. Thus the massecuite purity at any point in the A continuous pan will be constant and equal to that of the syrup inflow.

iii)   The operating absolute pressure of the pan, and thus boiling temperature, will be determined by a compromise between high crystallisation rates (high temperature) and low product degradation (low temperatures). A boiling temperature in the range of 65°C to 70°C is considered a reasonable compromise for raw cane sugar A-massecuite.

iv)    This is a steady state optimisation.

In this formulation of the problem, other than the specification of the pan pressure, seed flow and properties, there is no presupposition of what the optimum operating conditions might be. The optimum policy determined from this specification will uniquely define the operating conditions in each compartment, giving the optimal profiles of all variables including supersaturation and crystal content.

## 8.3     Formulation As A Dynamic Programming Problem

### 8.3.1   *Previous work on Optimal Conditions for Crystallisation in Pans*

The equations which describe sucrose crystallisation are detailed in Chapter 4 and Appendix B.

In his classic study, Frew (1973) used optimal control theory to determine a set of rules or operating principles to achieve the optimum performance from a batch pan. Other researchers have used this batch pan problem for evaluating alternative techniques for solving the problem (eg Chew and Goh, 1989). Broadfoot (1980) approached the problem of optimal operating conditions for a continuous pan as a conventional multi-dimensional optimisation problem. He found that the dimensions of the problem made

the optimisation problem intractable for a pan with more than 5 compartments.


### 8.3.2  *Dynamic Programming as a Technique for Optimisation*

Dynamic Programming, originally developed by Bellman (1957), is a technique for solving optimisation problems where an optimal profile or trajectory is sought. It is particularly well suited to problems of a multistage nature, making it an ideal technique for applying to continuous pans. Dynamic Programming converts a large optimisation problem into a sequence of smaller problems by breaking the system down into a number of "stages". At any stage, the condition of the system is uniquely defined by its "state".

The fundamental principle of the dynamic programming method is the principle of optimality : "The optimal path from a particular stage-state point remains the same, regardless of how the system got to the particular point." (Rhinehart and Beasley, 1987) The use of this principle allows the stage-wise calculation of an optimal policy, greatly reducing the complexity of the optimisation problem and providing solutions to what would otherwise be an intractable problem. In contrast to the simple, and almost obvious nature of the principle of optimality, the complexity of dynamic programming lies in the *application* of the principle to multi-dimensional optimisation problems. Bellman's standard computational algorithm was only useful for relatively simple problems but there are however, a number of methods developed subsequently which can substantially reduce the computational requirements and help to solve "the curse of dimensionality". These "methods, techniques and subterfuges" (Larson and Casti, 1982) cover not only the computational algorithm on a formulated problem, but extend to the problem formulation, with "clever problem formulation" being recommended as "one of the most important factors in successful dynamic programming"(Larson,1967). Dynamic programming and its application to a range of optimisation problems is well described in the literature. ( eg Rhinehart and Beasley, 1987, Larson and Casti, 1982, Larson,1965) and has been used locally in the sugar industry for determining an optimum cane crushing program (Hoekstra, 1978).

### 8.3.3    *Standard Formulation of Dynamic Programming Problem*

Larson (1967) gives the general case of the discrete-time variational control problem as follows (using the conventional terminology and notation of dynamic programming):

Given:    1.    A system described by the non-linear difference equation:

$$X(k+1) = \Phi\Big(X(k), U(k), k\Big) \tag{8.1}$$

where   $X$ is an n dimensional state vector,

$U$ is an m dimensional control vector,

$k$ is an index for the stage variable,

and    $\Phi$ is an n dimensional function.

2.    A variational performance criterion

$$J = \sum_{k=0}^{K} L\Big(X(k), U(k), k\Big) \tag{8.2}$$

where   $J$ is the total cost (i.e. $J$ is the objective function)

$L$ is the cost for a single stage

$K$ is the total number of stages

3.    Constraints

$$X(k) \in X'(k)$$
$$U(k) \in U'\Big(X(k), k\Big) \tag{8.3}$$

where   $X'(k)$ is a set of admissible states at stage $k$,

and    $U'(X(k),k)$ is a set of admissible controls at state $X(k)$ and at stage $k$.

4.    An initial state

$$X(0) = c \tag{8.4}$$

Find:

The control sequence $U(0)$, $U(1)$, . . . ., $U(K)$ such that $J$ in (8.2) is minimised (or maximised) subject to the system equation (8.1), the constraint equations (8.3), and the initial condition (8.4).

As mentioned above, there is a range of techniques which can be applied to solve this problem, however, the common fundamental principle is that the state and control variables (i.e. the elements of the state and control vectors) are quantised to a set of possible values. The optimal path (in terms of both states and control actions) is then calculated stage-wise. At the stage under consideration, the optimal path to each possible state is calculated by considering the combined cost of the optimal path to each state of the previous stage and the cost of the transition to the state under consideration. In building up the optimal path in this manner, the constraints are very easily accommodated by simply excluding any state that would violate any of the constraints (either on the states themselves or on the control actions required to achieve them). This procedure is described for a number of simple processes in the literature (Rhinehart and Beasley, 1987, Larson, 1967 and Hoekstra, 1978)

### 8.3.4    Formulation of a System Description for the Continuous A-Pan Optimisation

The "stages" in the formulation of the dynamic programming problem in this instance are clearly the compartments of the continuous pan and thus the system difference equation must describe the massecuite leaving a compartment based on the massecuite entering the compartment and the control applied to the compartment. The difficulty in applying dynamic programming to a continuous pan is that the states (the variables which uniquely define the massecuite flowing from one compartment to the next) are not independent of the performance of the pan. For example, the performance of the pan (exhaustion) is uniquely defined by the state of the massecuite leaving the last compartment (crystal content and flow rate). It is here that careful problem formulation is necessary in the selection of the state and control vectors.

The state vector must uniquely define the massecuite flowing from one compartment to the next. From the numerous possible sets of state variables which would constitute an adequate state vector, it is possible to select a set so that the state variables fall into three distinct groups, viz:

i)     State variables which are independent of the crystallisation performance of the pan

$X_1(k)$ = total massecuite flow out of compartment $k$.

$X_2(k)$ = flow of water in massecuite leaving compartment $k$.

ii)    State variables which describe the crystallisation performance of the pan.

$X_3(k)$ = flow of dissolved sucrose out of compartment $k$.

iii)   State variables which describe the size distribution of the crystals in the massecuite.

$X_4(k)$ = 1st moment of crystal size distribution leaving compartment k.

$X_5(k)$ = 2nd moment of crystal size distribution leaving compartment k.

(Assuming that the size distributions can be described by a two parameter distribution).

We may now argue heuristically as follows:

For a given massecuite flow (in terms of solids and water) it is optimal to maximise the amount of sucrose in crystal form. Thus for massecuite leaving compartment $k$, which is specified by $X_1(k)$ and $X_2(k)$, the optimal path can be determined by selecting the control actions which minimise $X_3(k)$ thereby maximising the amount of sucrose as crystal. Implicit in this argument is that $X_4(k)$ and $X_5(k)$ play no part in the choice of the optimal path, but are merely a consequence of it. This is a reasonable assumption since the relationship between the mean crystal size ($X_4(k)$) and the spread in crystal sizes (of which $X_5(k)$ is a measure) is predominantly dependent on the seed massecuite quality and such design features as good circulation in the compartments and the number of compartments in the pan. This has been demonstrated both theoretically (by treating residence time distribution and growth rate dispersion as independent random variables) and experimentally in the work of Rein, Love and Cox (1985). The operating policy will have a minimal effect on the relationship between the mean crystal size and the spread in crystal sizes.

This approach of using a state variable as the variational performance criterion has been

used previously in deriving minimum fuel trajectories for supersonic aircraft. (Larson, 1965).

Quantisation of the state variables is thus only 2 dimensional, with a matrix of possible values for $X_1(k)$ and $X_2(k)$ being evaluated at each stage $k$. The control actions applied to each compartment are ultimately the evaporation rate and the syrup flow rate. However to simplify the system equation, the control variables are specified as:

$U_1(k)$ =     flow of sucrose in syrup into the $k$th compartment.

$U_2(k)$ =     net water feed rate into the $k$th compartment.

(In raw cane sugar practice, where surplus fuel is available, water may be fed to a compartment to achieve an effectively lower evaporation rate, thus:

$U_2(k)$ =     water added directly + water in syrup feed - water evaporated).

These control variables can be determined by simple mass balance from the massecuite leaving the compartment $(X_1(k), X_2(k))$ and the massecuite entering the compartment $(X_1(k-1), X_2(k-1))$.

### 8.3.5    *Formulation of a System Equation for the Continuous A-Pan Optimisation*

The system equation is required to describe the massecuite leaving a compartment in terms of the massecuite entering the compartment and the control actions applied to the compartment (at steady state). As is clear from the discussion of crystal growth in Chapter 2 and the details of the formulation of a steady state model discussed in Chapter 4 and Appendix B, the complexity does not allow for a simple explicit equation as used in simpler dynamic programming problems. The computer routines which numerically solve the sets of non-linear equations to determine steady state pan operation (Appendix E) become the effective system equation.

### 8.3.5    *Formulation of a Variational Performance Criterion for the Continuous A-Pan Optimisation*

As has already been argued, the variational performance criterion is simply the state variable $X_3(k)$. The exhaustion achieved by the first k compartments of the continuous pan can be calculated from $X_1(k)$, $X_2(k)$, $X_3(k)$, the massecuite purity, *pty*, and the

quantity of sucrose in "total pan feed syrup" and magma, $T$.

$$\textit{Exhaustion after k compartments} = \frac{\frac{pty}{100}\cdot\left(X_1(k)-X_2(k)\right)-X_3(k)}{T}\cdot 100 \quad \% \quad (8.5)$$

Note that this variational performance criterion applies specifically to this particular formulation of the problem. In practice it is possible to achieve a low flow of dissolved sugar out of the pan with a low exhaustion by decreasing the amount of syrup fed to the pan. This however violates the assumption of a fixed quantity of total pan feed syrup.

### 8.3.6    Constraints for the Continuous A-Pan Optimisation

The admissible states, for all pan compartments, must be constrained to prevent both the formation of false grain and excessively viscous massecuites which inhibit circulation. In the specific example discussed in section 8.7, an upper limit of a 55% crystal content (all crystal contents are expressed as mass % on massecuite, the convention for the South African sugar industry as defined on page 3-1) was used to exclude massecuite conditions which would impede circulation and an upper limit on supersaturation was set at 1.2 to exclude conditions which would result in false grain formation.

The total solids flow out of the final compartment must be constrained to be equal to the total solids flow in B magma and "total pan feed syrup".

If necessary, constraints of a practical nature can be applied to the control actions, e.g. specify a maximum syrup flow to each compartment.

### 8.3.7    Initial State for the Continuous A-Pan Optimisation

The initial state, $X(0)$, is the specification for the seed to be fed into the first compartment of the continuous pan. This must be estimated to give the required product crystal size when the continuous pan is operated at optimum operating conditions. Some iteration may be necessary if the initial assumption of pan performance leads to a result where the specification for the product crystal size distribution is not met. Rein, Cox and Love (1985) have shown both theoretically and experimentally that there is a relatively simple and direct relationship between the size distribution of the crystals in the product massecuite and that of the crystals in the seed. The graphs presented in this paper can be

used to assist in specifying a seed crystal size distribution which will ensure that the required massecuite crystal size distribution is achieved.

## 8.4    Solution of Dynamic Programming Problem

As discussed in the formulation of the problem, it is necessary to consider the performance of the pan at each stage (compartment) over a range of quantized state variables, $X_1(k)$ and $X_2(k)$. From a conceptual point of view it is more convenient to quantize massecuite solids flow and massecuite concentration (brix), from which $X_1(k)$ and $X_2(k)$ can be calculated without any loss of generality. (In this instance, brix is taken to be synonymous with mass percent dry solids.)
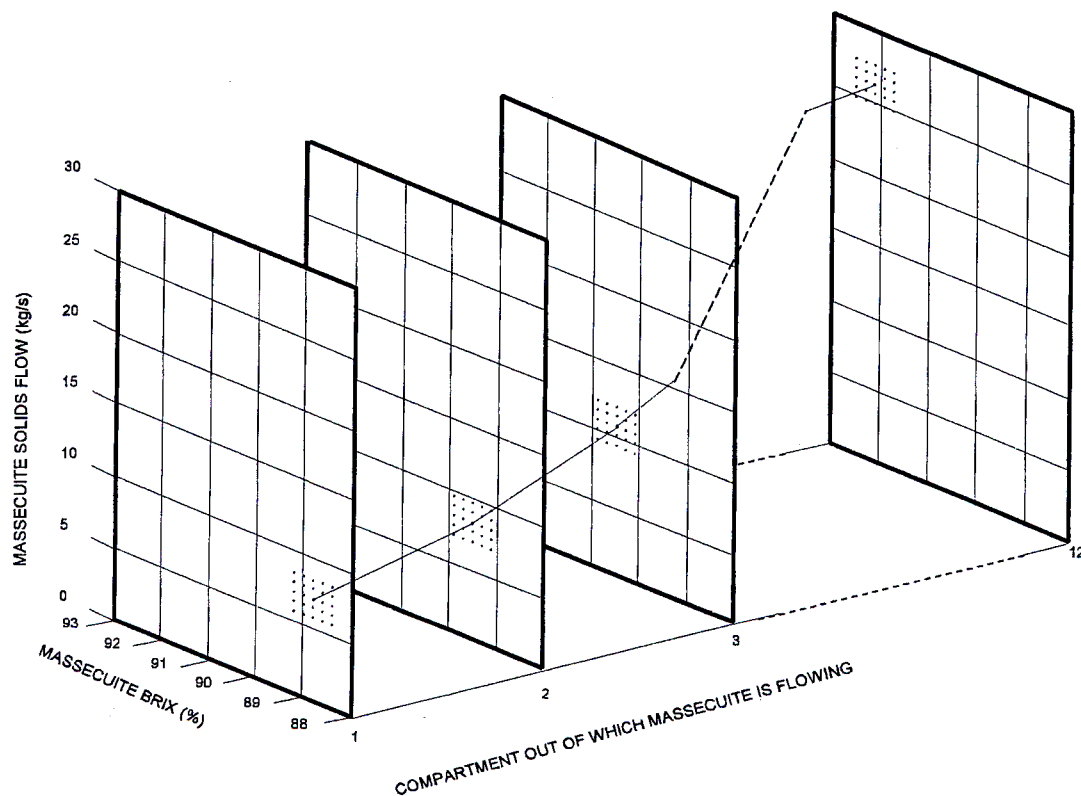


**Figure 8.2** Nominal trajectory and search grid

Figure 8.2 shows how, for each compartment, there is a matrix or grid of states which must be considered. The solids flow in massecuite must fall between that entering with the seed and the total solids flow which results once all of the syrup has been added. Experience dictates the approximate range of massecuite brixes which can be expected. If a fine grid of values was

considered over the full range of possible values for each compartment, the dimensions of the problem would become so large as to make it intractable. The use of the concept of a "nominal trajectory" greatly reduces the dimensions of the problem.

A "nominal trajectory" is an estimate of what the optimal trajectory might be. An option, based on operating practice, is to set the "nominal trajectory" initially to start at a low brix and solids flow from compartment 1 increasing to a high brix and solids flow from the last compartment. The solids flow from the last compartment is defined by the need to process all of the available syrup. The range of quantized states can then be constrained to an area around this nominal trajectory, as indicated in the diagram of Figure 8.2.

Starting from compartment 1, an improved trajectory is sought by checking the variational performance criterion (the minimum value for $X_3(k)$) of each state, for each of the possible previous states, and recording only the best performance and the previous state which was necessary to achieve it. By proceeding in this way from the first to the last compartment, an improved trajectory is built up on the basis of the best trajectories to the previous compartment.

The improved trajectory achieved in this way will not be the optimal trajectory unless the nominal trajectory and grid surrounding it happen to include the optimal trajectory. By resetting the nominal trajectory to the improved trajectory and restarting the search, the search area will move closer to the optimal trajectory. This process can be repeated until there is no improvement in the nominal trajectory, at which point the nominal trajectory is the optimal trajectory.

Judicious selection of the spacing between the quantized states forming the search grid around the nominal trajectory, and the dimensions of the grid is necessary for this optimisation procedure to work correctly. A computer program was developed to perform this process. The program allows the operator to set the nominal trajectory and the size and spacing of the grid around it. Normally a coarse grid would be chosen for rapid convergence of the initial searches, with a finer grid used to improve the accuracy of the final search.

## 8.5    Application of the Computer Program

The Computer program developed to perform the search for an optimal profile according to the method outlined above, is described briefly in Appendix E. The program provides a tool which allows a user to specify :

&mdash;    the size of the pan

&mdash;    the flow rate and properties of the seed massecuite fed to the pan

&mdash;    the growth and solubility characteristics resulting from the particular impurities present

&mdash;    the quantity of syrup to be processed

and the program will determine the optimum operating policy for the pan so as to achieve the maximum massecuite exhaustion (ie proportion of total sucrose in crystal form). The optimum policy is expressed as a profile of syrup flows and effective evaporation rates for each compartment. (Note that whilst the actual evaporation rate in each compartment cannot be varied individually in the THS-FS continuous pan, the effective evaporation rate can be reduced in individual compartments by the addition of water).

The computer optimisation program can be used for different objectives.

&mdash;    At the design stage, it can be used to guide decisions such as the appropriate allocation of heating surface to individual compartments.

&mdash;    For a factory with an existing pan and a fixed throughput it can specify the profile necessary to give the best massecuite exhaustion.

&mdash;    For an expansion investigation, it can be used in an iterative manner specify the maximum throughput compatible with achieving a desired exhaustion from an existing pan, and the operating profile necessary to achieve this.

A particular kind of problem that will be encountered in most factories operating a continuous A-pan can be stated as follows :

An installed pan of fixed capacity is required to process a given quantity of syrup, given that batch pans are available to produce a limited quantity of seed massecuite ( the crystal size in the seed having been selected to give the required crystal size in the product massecuite ). With an un-optimised operating profile (set by the pan boilers) the pan is able to process the required quantity of syrup, but the level of exhaustion achieved is below the desired level of at least 68%. What maximum level of exhaustion can be

achieved or could throughput be increased whilst also achieving a minimum exhaustion of 68%? What is the optimum profile necessary to achieve this improvement and in what way is it different (qualitatively) from that conventionally selected by pan boilers.

Given the complexity of the optimisation, and the range of possible inputs to the optimisation, the technique of dynamic programming and the computer program developed to implement it do not specify a "generic optimum policy", but rather an optimum specific to the particular conditions which are specified.

## 8.6     Principles Underlying Optimisation

Whilst the computer program is capable of solving a specific steady state optimisation problem, the complexity of the model obscures the principles involved in the optimisation. The program tends to become a "black box" which simply gives specific answers to specific questions without a qualitative explanation of the rationale behind the answer. Before presenting results from the computer when applied to a specific problem of this kind it is important to understand, qualitatively, one of the major components of the optimisation.

The major component of the optimisation to be understood is the trade off between growth rate and retention time or crystal content, within the constraints of fixed quantities of seed and massecuite. There are two ways of conceptualising this, which are equally valid.

One way is to view the continuous pan crystallisation from the view point of an average crystal. What is its residence time through the pan and what is its growth rate at each instant over that time? The increase in size of the crystal will be the integral of the growth over the total retention time and it is this that must be maximised. More syrup added in the earlier pan compartments will reduce the average crystal retention time but by decreasing crystal content and increasing mother liquor purity, will increase growth rates. The optimisation seeks to trade off retention against growth rate to get the maximum increase in size.

The other way is to view the continuous pan from the perspective of a compartment operating at steady state. What is the total mass of crystal in the compartment and what is the average growth rate defined by the mother liquor conditions? Assuming that the mother liquor concentration is at

the super-saturation boundary (ie evaporative capacity is not limiting), the fact of constant massecuite purity means that as crystal content drops, mother-liquor purity increases and the growth rate will increase. In this conceptual format, the optimisation is finding the crystal content which maximises the product of crystal growth rate and crystal content.

The view of the optimisation from the point of view of the steady state pan compartment is the most convenient to use and can be investigated further with a simple spreadsheet model of a compartment. The major factor affecting this simple form of optimisation will be the extent to which growth rate varies with purity. This is defined by the factor $K_3$ in the growth equation (equation 2.30) and for the present purpose can be used to specify a relative growth rate as follows:

$$Growth = \frac{\exp(-K_3 \cdot IW)}{\exp(-K_3 \cdot 1.2)} \tag{8.6}$$

where    $IW$ is the impurity to water ratio of the mother liquor

This provides a relative measure of growth rate at constant super-saturation, with the same purity dependence as the full equation 2.30, and normalised to give a relative growth of 1 at an impurity to water ratio of 1.2.

Using this growth equation and the equation for solubility coefficient (equation 5.2), it is possible to estimate how the growth rate varies as crystal content varies for a compartment of massecuite of a fixed purity ( taken as 85 in this simulation ). The quantity of primary interest is a relative measure of total rate of sucrose crystallisation in the compartment. This is the product of crystal content and growth rate given by equation 8.6. Performing this calculation for a range of values of the growth parameter $K_3$ provides the data which are plotted in Figure 8.3 below. Crystal contents above about 56% are not considered as this is an approximate upper limit defined by the flow characteristics of massecuite.
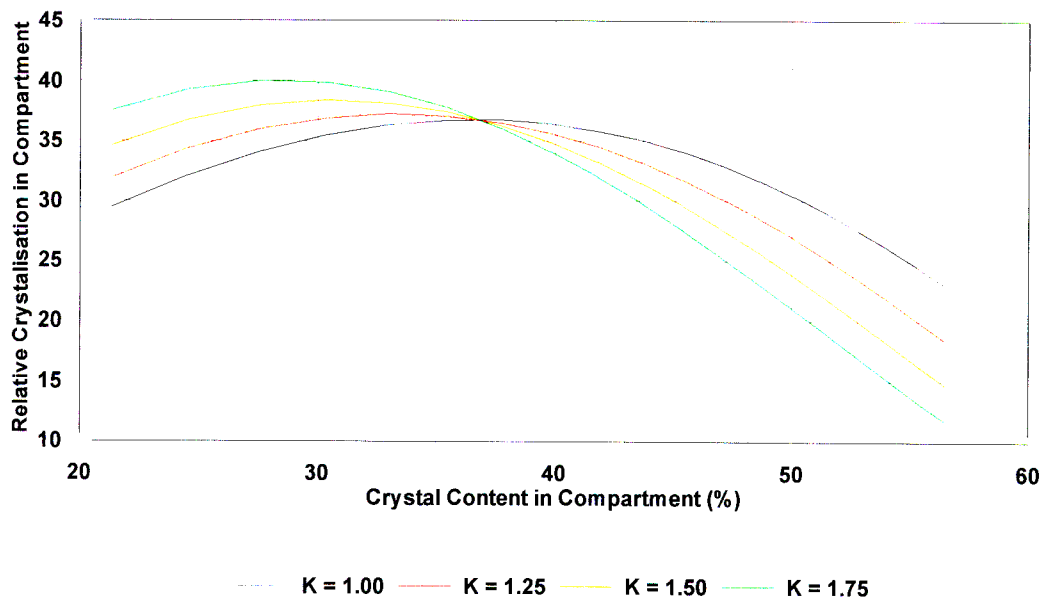
**Figure 8.3** Variation of total crystallisation with crystal content in a continuous pan compartment

It is clear that there is an optimum crystal content which maximises the total amount of crystallisation which takes place in a compartment and that this optimum depends on the growth parameter $K_3$ .

For the strongest dependence of growth on purity shown ,ie $K_3$ = 1.75 (as reported by Wright and White, 1974 and by Broadfoot and Steindl, 1980) the maximum crystallisation in the compartment occurs at about 29% crystal content. This maximum rate is about double that for a crystal content of 50%. This is a particularly interesting insight as conventional practice is to operate with high levels of crystal content in continuous pan compartments (in the range of 45 to 50%, rising to 55% in the last compartment ) in the belief that this will maximise crystallisation. If the dependence of growth rate on purity is less pronounced, as indicated by the other curves plotted for smaller values of $K_3$ , the optimal crystal content increases and the variation in total crystallisation with crystal content becomes less pronounced.

It is interesting to note that, as discussed in Chapter 2, that the data of du Boil(1985) indicates a value of $K_3$ = 2.33 and Li Wu and Corripio (1985) determined a value of $K_3$ = 2.45. Both of figures thus predict an even stronger dependence of growth on purity than considered above, implying maximum growth rates would be achieved at even lower crystal contents!

This simple simulation provides the background to understanding the optimal profiles calculated by the full dynamic programming algorithm.

## 8.7    Application of Dynamic Programming Optimisation

The dynamic programming optimisation technique has been applied to the specific instance of a continuous A-pan at the Felixton factory of Tongaat-Hulett Sugar.

The pan has a total massecuite volume of 120 m³ comprising 12 compartments of equal volume. The conditions selected for the optimisation (based on the results of test 2-A) are:

Purity of Seed, Syrup and Massecuite    = 87.74        %

Seed Massecuite into first compartment:

| | | |
|---|---|---|
| Total Flow | $X_1(0)$ | = 5.17 kg/s |
| Water Flow | $X_2(0)$ | = 0.523 kg/s |
| Dissolved Sucrose Flow | $X_3(0)$ | = 1.446 kg/s |
| 1st moment of crystal size distribution, | $X_4(0)$ | = $6.31 \times 10^{-4}$ m |
| 2nd moment of crystal size distribution, | $X_5(0)$ | = $4.51 \times 10^{-7}$ m² |

( this seed can be calculated to have a crystal content of 48.4 %)

Continuous Pan Feed Syrup:

Total Flow    =    18.17 kg/s

Brix         =    66.27%

Constraints:

The maximum crystal content limit recommended by Broadfoot (1980) for Australian conditions is significantly lower than normal South African practice, and thus an upper limit of 55% crystal content has been used.

Whilst it is possible to use equations such as 2.34 and 2.35, to define the maximum permissible super-saturation, running the program with this feature appears to create strange local optima in the search for the global optimum profile. As a simplification, it is assumed that for this A-massecuite boiling, a constant value for the maximum supersaturation is set at 1.2.

The evaporation in the pan is set at 0.6 kg/s in each compartment, giving a total evaporation rate for the pan of 25.9 tons/hr, a realistic practical value.

Growth Kinetics :

The growth kinetics are based on the parameters determined by fitting the model to full scale experimental data, with the purity dependence according to the parameter of Wright and White (1974) ie $K_3 = 1.75$ :

$$K_1 = \quad 0.000\,000\,87 \quad m/sec/°os$$

$$K_2 = \quad 0.578$$

$$K_3 = \quad 1.75$$

$$K_4 = \quad 3.254$$

$$K_5 = \quad 0.08$$

$$P = \quad 0.000\,199 \qquad m$$

The computer program was used to determine the profile which would achieve the maximum performance from the pan for these conditions. The optimum profiles of operating variables determined by the program are presented in the graphs below.
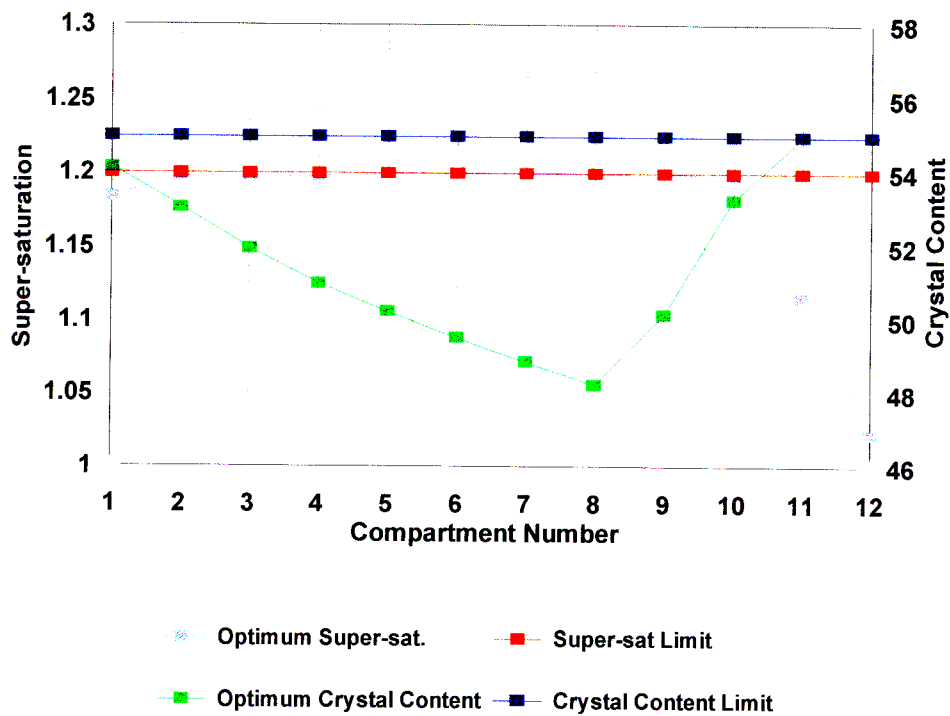


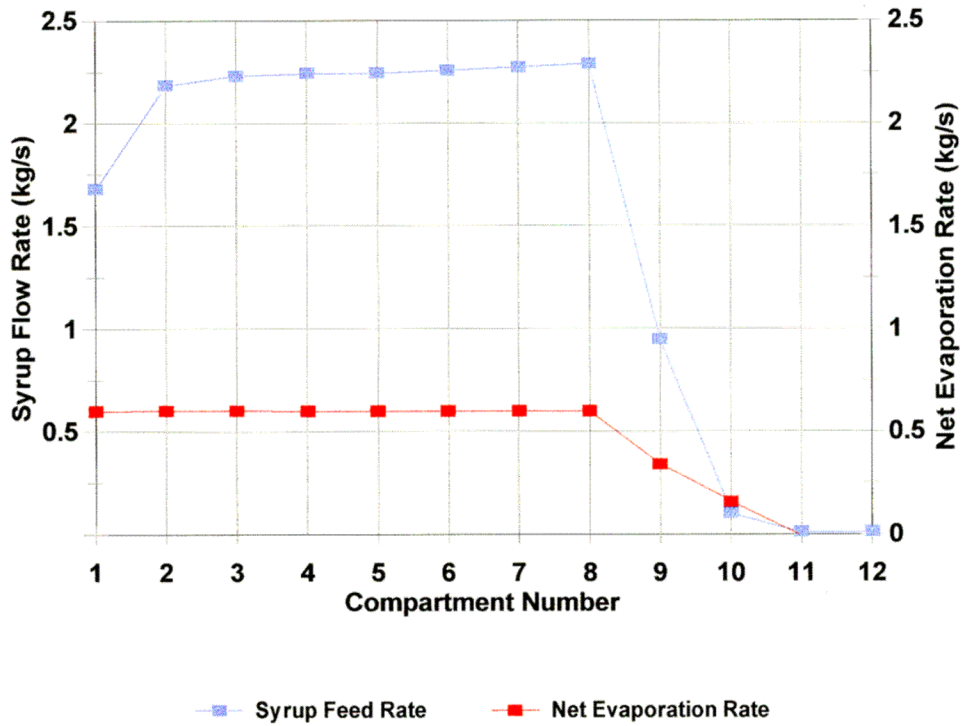**Figure 8.4** Optimum profile of Supersaturation and Crystal Content - limited evaporation

**Figure 8.5** Optimum profile of Syrup Feed and Effective evaporation - limited evaporation
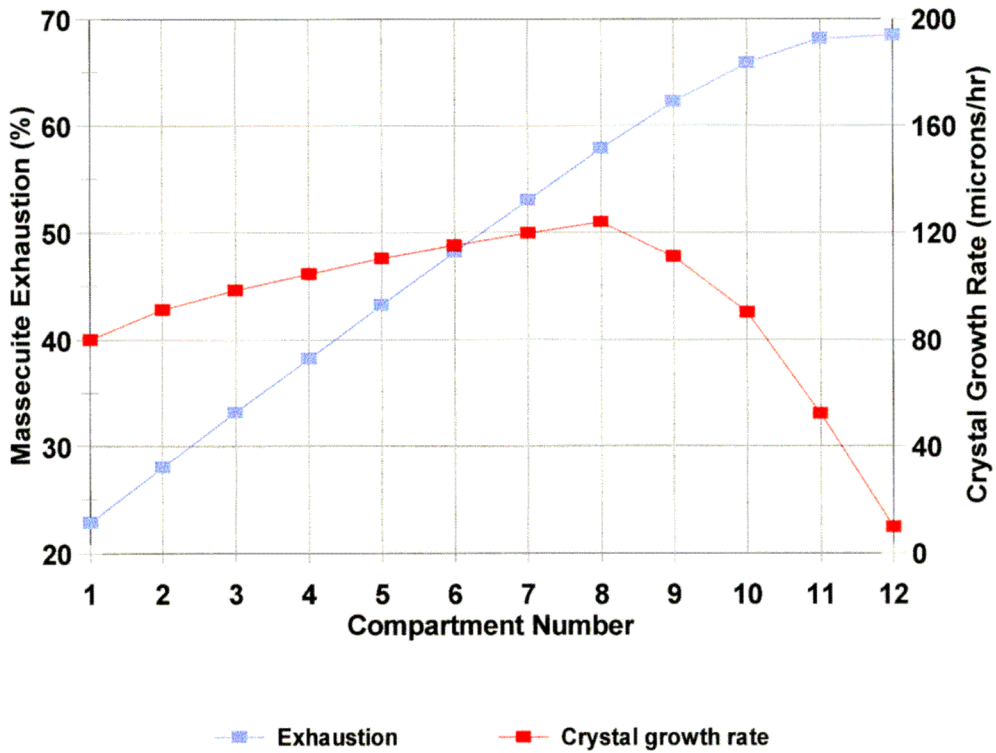


**Figure 8.6** Exhaustion and crystal growth rates for optimum profile - limited evaporation

When operating at this optimum profile, the pan clearly has excess capacity - the maximum crystal content limit is reached in compartment 11 with all the syrup already added. This tends to drive the optimisation to focus on finer aspects of the optimisation which would be of no consequence in a factory struggling to maximise performance at high throughputs. (Specifically, this particular optimisation attempts to achieve maximum performance by exhausting the mother liquor whilst holding the crystal content on the limit as the supersaturation tends towards unity.)

Accepting the limitations of optimisation on a pan with excess capacity described above, a feasible interpretation of the implications of these graphs, guided by the simple optimisation calculation described in section 8.6 , is as follows :

- The high crystal content of the seed (48.4 %) corresponds to a low crystal growth rate. To maximise performance, this crystal content must be reduced as early as possible in the pan. The apparently anomalous increase in crystal content from the seed to that in the first compartment (to approximately 54%) is an indication of the fact that the seed mother liquor has been reasonably well exhausted no doubt assisted by cooling to temperatures below pan operating temperature. When this seed is added to compartment 1 and its temperature increases, the mother liquor will be undersaturated and immediate concentration is necessary to provide a positive supersaturation driving force. It is this concentration which produces the anomalous increase in crystal content.

- The importance of this need to reduce the crystal content, results in syrup being fed to the first compartment at a rate large enough to result in a super-saturation level below the maximum allowable. This is because of the limited evaporation rate in each compartment. With an unlimited evaporation rate for the first compartment, it would be possible to reduce the crystal content in the first compartment to any desired value whilst maintaining the super-saturation on its maximum value.

- Further reductions in crystal content are achieved slowly by feeding the syrup at the maximum rate to each subsequent compartment, compatible with maintaining the supersaturation at its maximum level. (ie no water should be added to reduce the effective evaporation rate.)

- Once all the syrup has been consumed the remaining compartments are used to increase the crystal content by feeding water to keep the super-saturation at its maximum level.

- The growth rate is sufficiently fast to ensure that the crystal content limit is reached before the last compartment. Once this limit is reached a slight further increase in

exhaustion is achieved by maintaining the massecuite at the crystal content limit whilst the mother liquor is allowed to exhaust towards a supersaturation of unity.

Assuming this to be a correct interpretation of the principles underlying the calculated optimum profile, the two major implications of this analysis are that:

–       The seed crystal content should be fed to the pan at the value which matches the optimum profile (ie there should be an insignificant difference between the seed crystal content and the crystal content in the first compartment).

–       The evaporation rate of the continuous pan should be sufficient (and the syrup brix high enough) to ensure that when controlled at the maximum supersaturation driving force, sufficient solids are added to the earlier compartments to prevent the crystal content in these compartments from rising above their optimum value.

To test this hypothesis the optimisation was re-run with effectively unlimited evaporation allowed in each compartment (achieved by setting the maximum evaporation rate in each compartment to 10 kg/s). The results of this optimisation are shown in the equivalent set of three graphs below (Figures 8.7 to 8.9).
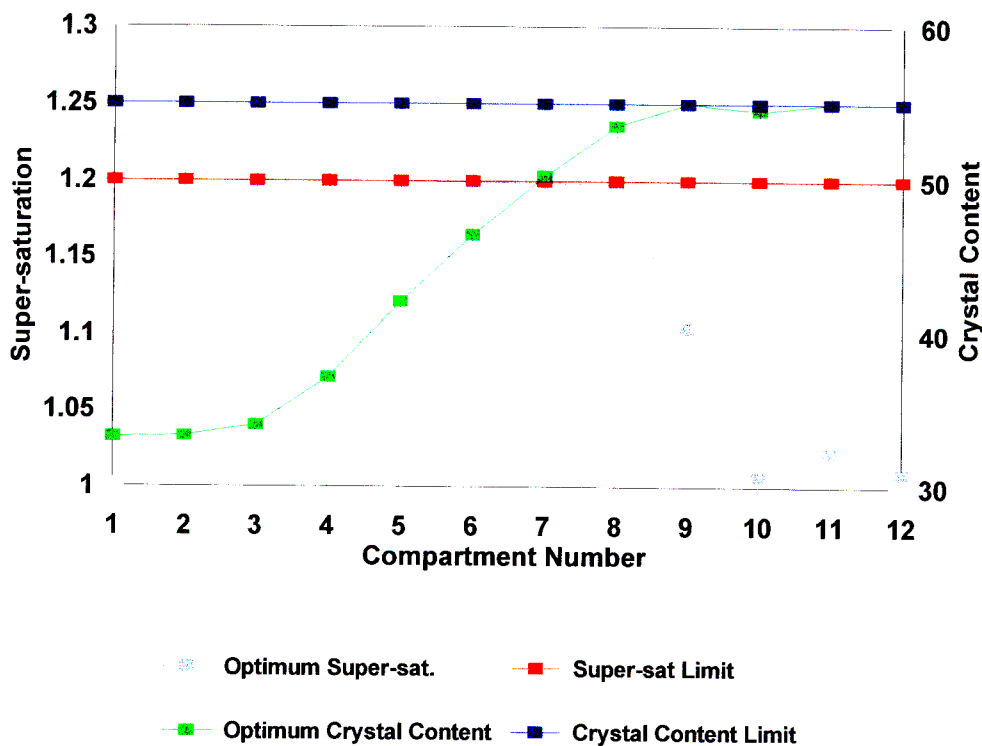


**Figure 8.7** Optimum Profile of Supersaturation and Crystal Content - unlimited evaporation
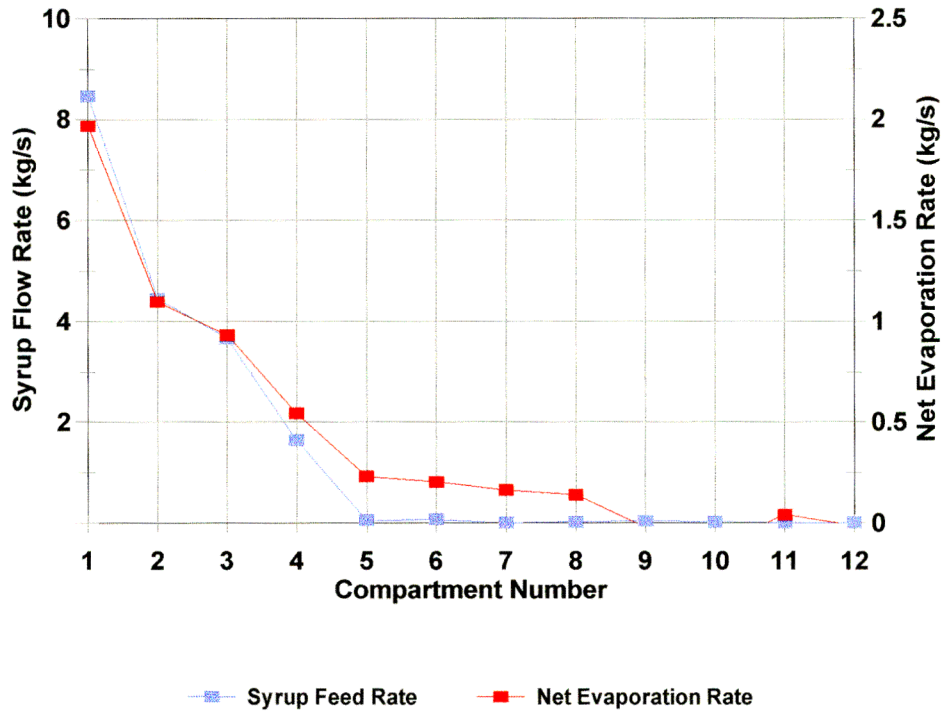
**Figure 8.8** Optimum profile of Syrup Feed and Effective Evaporation- unlimited evap.
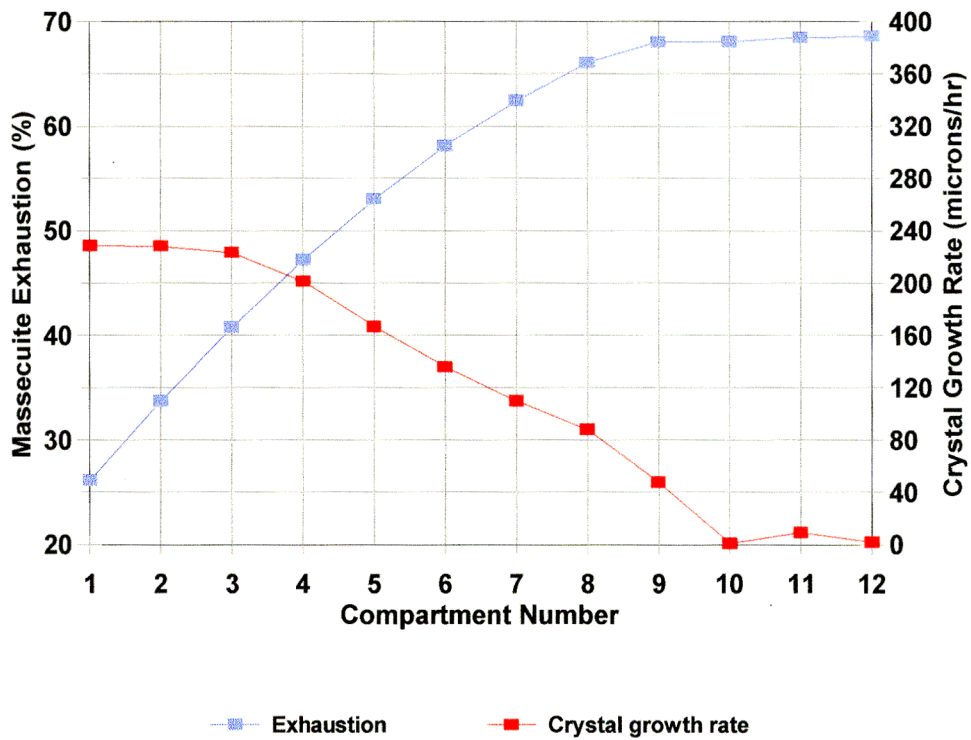


**Figure 8.9** Exhaustion and Crystal growth rates for optimum profile - unlimited evaporation

These graphs support the hypothesis presented above. They indicate the requirement to reduce the crystal content to a relatively low value in the first compartment and hold it at this optimum level ( approximately 33 % , which is slightly higher than the value of approximately 29 % indicated by the simple optimisation procedure discussed in section 8.6) by feeding the required quantity of syrup. The effective evaporation rate in each compartment is adjusted to hold the supersaturation at the maximum level. Applying this principle, all the syrup is added in the first four compartments. In the subsequent compartments, the crystal content is first raised to the maximum limit by adjusting the effective evaporation rate to maintain the supersaturation at its maximum limit. When the maximum crystal content has been achieved (in compartment 9) the last small increment in exhaustion is achieved by holding the crystal content at the limit in the final compartments whilst allowing the mother liquor to exhaust towards a supersaturation of unity.

This second simulation requires substantially increased evaporation rates in the first three compartments, which would be impractical to try and achieve in a real application. The simulation should rather be interpreted as an indication of the critical importance of low crystal contents (in the range of 33%) in the initial compartments of the pan. This should be addressed in a practical situation by preparing seed which matches this requirement rather than preparing a high crystal content seed which requires a drastic adjustment when it enters the continuous pan.

Whilst the particular optimum requirements can be determined for any practical situation by applying the computer optimisation to the specific details of the problem it is useful to try and draw some practical operating guidelines from the application of the technique to the instance studied in this chapter.

A generalised set of guidelines is :

–       Produce a seed massecuite at a crystal content slightly above the value indicated by the
        simple optimisation of section 8.5 ( 33 % for massecuite where parameter $K_3$ is 1.75).

–       Feed syrup into the first and subsequent compartments , with controls set to operate
        close to the supersaturation boundary (just below the onset of false grain).

–       Set as many compartments on syrup as is necessary to match the syrup supply to the

—    Compartments subsequent to those fed on syrup are all fed with water, again with

controls set to operate close to the supersaturation boundary.

—    The crystal content should remain constant for those compartments fed with syrup and

only start to increase in the final set of compartments fed with water.

—    If the crystal content increases in those compartments fed with syrup, this can be

countered by increasing the evaporation rate in the pan and ensuring that the brix of the

syrup fed to the pan is as high as practically possible. The opposite approach can be

applied if the crystal content is found to drop over these compartments.

The simple optimum condition for a single compartment derived in section 8.6 does shows a

rather flat optimum peak (Figure 8.3) with little change in performance over about five

percentage units of crystal content. this indicates that precise control of the crystal content is not

that critical in the compartments fed with syrup. Since the objective is ultimately to increase the

crystal content to a maximum value by the last compartment, the incentive is to operate on the

high side of the simple optimum peak.

In applying this approach to existing installations, some practical compromises will undoubtedly

need to be made to meet equipment requirements. Examples are limitations on seed pump

capacity, the ability of the stirrer to maintain the crystals in suspension whilst in the seed receiver

at the required lower crystal contents.

# CHAPTER 9

## 9.    Measurement of the Dynamic Behaviour of a Compartment

### 9.1    General

As discussed in Chapter 2, one of the advantages of continuous pan boiling over batch pan boiling is that the process can be operated at steady state. The intention is that the pan can be maintained at a fixed optimum operating condition without the dynamic adjustments to operating conditions which are necessary in batch pan boiling.

Operation at steady state does, however, not imply that the time dependent (dynamic) behaviour is unimportant. As discussed in detail in Chapter 4, the behaviour of a continuous pan is determined by the mechanisms of heat and mass flows. Steady state occurs when these processes are in balance resulting in a dynamic equilibrium. For an individual compartment of a continuous pan, this equilibrium is achieved by the adjustment of the feed (of either water or syrup) into the compartment to balance the effects of evaporation and crystallisation so as to attain the desired steady state conditions for optimum crystallisation (as discussed in Chapter 8). The feed to each compartment is conventionally controlled by a standard single loop Proportional Integral Derivative (PID) controller which adjusts the feed valve in response to the deviation of the condition in the compartment (usually an approximate measurement such as electrical conductivity, as discussed in Chapter 3) from the specified set point.
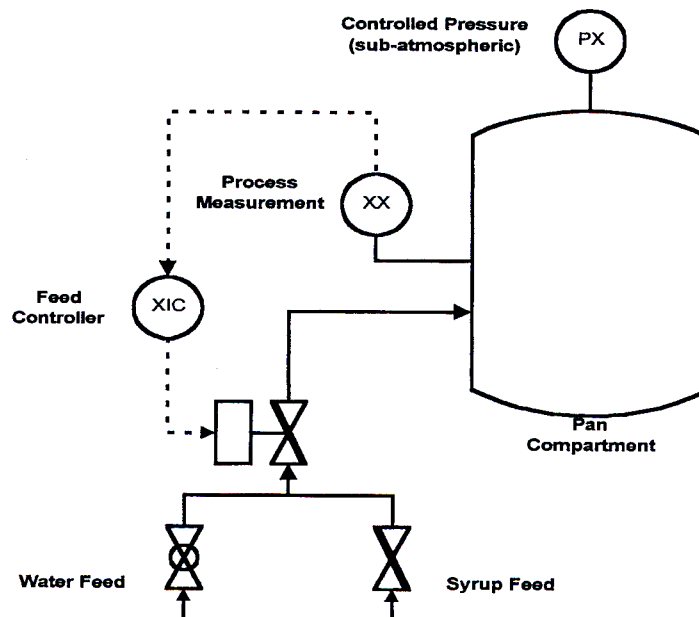


**Figure 9.1** : Feed control on a Continuous Pan compartment

The important aspects of a conventional feed control loop are summarised in the schematic diagram shown in Figure 9.1. For controlling continuous A-Pans in this study, the process measurement was the RS output of an RF conductivity probe.

The time dependent or dynamic behaviour of a pan compartment (ie unsteady deviations from steady state) is important for the following purposes:

- As a quantitative measure of the pan circulation ( a useful tool for comparisons and trouble shooting).

- As an aid to determining the most appropriate tuning parameters for the feed control loop.

- As a basis for understanding the dynamics of the entire pan and how it will behave when adjusted from one steady state operating point to another.

The construction of the Felixton sugar factory (Rein 1983) with the unique situation of continuous pans on all grades of massecuites provided new commissioning challenges. The unstable commissioning environment and large number of feed loops prompted some preliminary work on trying to understand the dynamic behaviour of pan compartments. This resulted in the development of a simple and rapid method for tuning feed control loops (Love and Chilvers, 1986) . This work identified that conventional loop tuning techniques were not appropriate. The closed loop cycling test (Ziegler & Nichols, 1942) was very time consuming because of the long time constants of the system whilst the conventional step test (Cohen & Coon, 1953) could not be performed as the process did not exhibit any first order stabilisation within normal operating limits.

Plant tests showed that the dynamics of a pan compartment approximated a pure integrating process with dead-time. Simple modelling of the process indicated that this was to be expected. Love and Chilvers (1986) proposed a simple two step test which could be rapidly applied to a pan compartment to estimate the dead-time and the effective capacitance of the pure integrating process. The details of the two step test can be explained by considering the process as seen by the controller in the following terms :

**Input to Process**
**r(t)**

**PROCESS**

**Output from Process**
**c(t)**

**(Output from Controller)**

**(Input to Controller)**
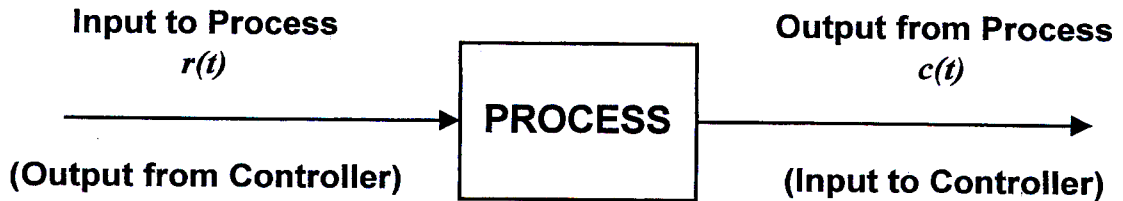
**Figure 9.2** Diagram showing the definition of signals to and from the process under control

The behaviour of the process is given by :

$$c(t) = \frac{1}{C_p} \cdot \int_{t_0}^{t-t_d} \left( r(t) - r_0 \right) dt + c(t_0)$$

(9.1)

Where :

$r_0$      is the process input which holds the process output constant

$C_p$      is the effective capacitance of the process (with units of time)

$t_d$      is the process dead time

$t_0$      is an initial reference time

The process behaviour can, alternatively, be expressed as :

$$\frac{dc(t + t_d)}{dt} = \frac{1}{C_p} \cdot \left( r(t) - r_0 \right)$$

(9.2)

To implement the two step test, the input to the process *r(t)* must first be held for a period at a constant input $r_1$ less than $r_0$ then held for a second period at a constant input $r_2$ greater than $r_0$ (the reverse order is equally suitable). A constant input will result in a constant rate of change of the output *c(t)*. Expressed mathematically,

For    $t \in [t_0, t_1)$    $r(t) = r_1$   where   $r_1 < r_0$

For    $t \in [t_1, t_2]$    $r(t) = r_2$   where   $r_2 > r_0$

(9.3)

will result in :

$$\frac{dc(t)}{dt} = S_1 \quad \text{for} \quad t \in [t_0, t_1 + t_d)$$

$$\frac{dc(t)}{dt} = S_2 \quad \text{for} \quad t \in [t_1 + t_d, t_2]$$

This is best illustrated graphically as :



r(t) ———— c(t)
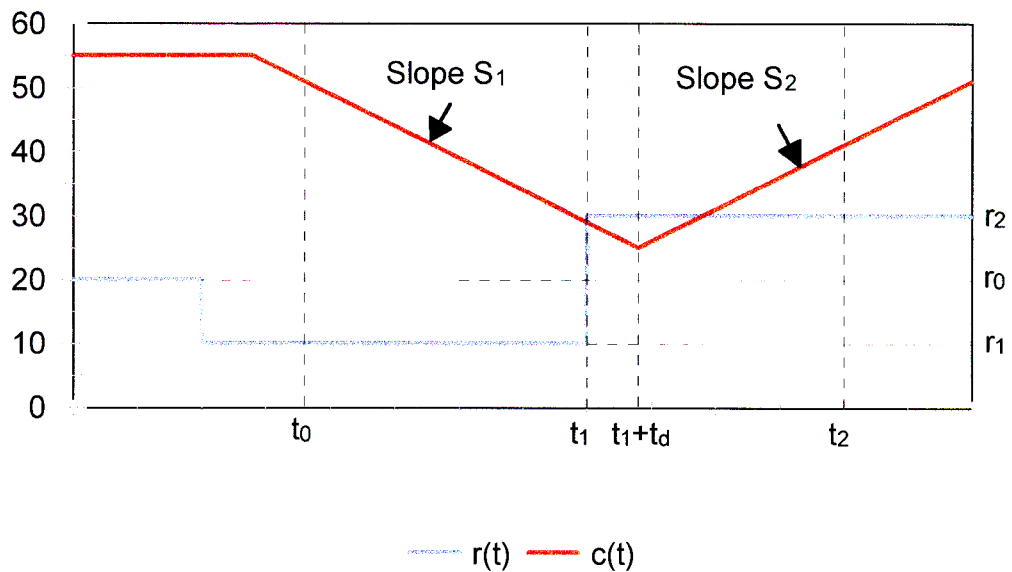
**Figure 9.3** Response of integrating process with dead time to the "two step" test

The slopes of the process output, $S_1$ and $S_2$, which can be estimated from the data recorded during the test, can be related to the process input by the following equations :

$$S_1 = \frac{r_1 - r_0}{C_p}$$

$$S_2 = \frac{r_0 - r_2}{C_p} \tag{9.5}$$

These equations can be combined to solve for $C_p$ which can then be calculated from :

$$C_p = \frac{r_1 - r_2}{S_1 - S_2} \tag{9.6}$$

The process dead time can be determined by finding time corresponding to the intersection point between the two lines with slopes $S_1$ and $S_2$. Subtracting $t_1$ from this time yields the dead time. It can be shown that if a process with these characteristics is subjected to the standard closed loop cycling test, the process will cycle with constant amplitude if the controller gain $G_c$ is given by :

$$G_c = \frac{\pi \cdot C_p}{2 \cdot t_d}$$

(9.7)

The period for the constant cycling, $T_0$ can be shown to be given by :

$$T_0 = 4 \cdot t_d$$

(9.8)

These relationships enable the Ziegler-Nichols rules for determining the tuning parameters for PID controllers to be converted from their conventional expression in terms of $G_c$ and $T_0$ into expressions in terms of $C_p$ and $t_d$ as shown in the Table 9.1 below.

| Type of Test | Gain | Integral Time | Derivative Time |
|---|---|---|---|
| Constant Cycling | $0,602 \cdot G_c$ | $0,5 \cdot T_0$ | $0,125 \cdot T_0$ |
| "Two Step" | $(0,946 \cdot C_p) / t_d$ | $2 \cdot t_d$ | $0,5 \cdot t_d$ |

**Table 9.1** Calculation of PID tuning parameters from test results

This technique proved to be an effective tool in a production environment. For situations where feed control is by time proportional operation of an on/off valve it has been found suitable to simply set $r_1 = 0$ % (ie valve closed) and $r_2 = 100$ % (ie valve open).

To investigate dynamic behaviour in more detail and evaluate options for automatic tuning which could be incorporated into continuous pan control systems, the research for this present work included the dynamic testing of compartments of a continuous A-Pan at the Felixton factory, using this two step test.

## 9.2    Computerised Testing System

A dedicated control and data collection system was configured to allow control and testing of a single compartment independently of the pan control system. The system consisted of a Personal Computer running dedicated control software (as described later in Chapter 12) connected via a proprietary network (Conlog's CONET) to a remote interface (Conlog SmartBox) which provided the link to the analog signals from the plant.

The signals recorded were :

      massecuite temperature

      the RS signal from the RF probe

      the XS signal from the RF probe

      Absolute pressure (from a second absolute pressure transmitter, which did not interfere with the absolute pressure measurement and control of the plant control system )

The program provided features for

      data logging

      conventional control

      manual operation

      Pseudo Random Binary Noise (PRBN) testing

Data analysis was off-line, using both a conventional spreadsheet and the MathCad computer program (see Appendix E for details of computer software used in this research).

## 9.3    Sensitivity to Absolute Pressure Stability

The importance of stability of the absolute pressure control on the pan was investigated, particularly with respect to its effect on the use of Boiling Point Elevation (BPE) measurements and their suitability as control signals. The absolute pressure can be controlled independently of the feed control of individual compartments and is dependent on proper design and operation of ancillary equipment.

Previous use of BPE as a signal for feed control (as described in Chapter 3) was observed to be

particularly sensitive to fluctuations in absolute pressure. To investigate this in some detail, a single compartment of a continuous A-Pan was operated for a period with manual throttling of the feed control valve (to eliminate periodic fluctuations in the massecuite temperature that could be caused by the feed control system). A significant fluctuation in absolute pressure at the beginning of the test demonstrates an undesirable effect as shown in the graph below. To assist in quantifying the effect of the pressure variations, the saturated vapour temperature corresponding to the measured pressure is plotted rather than the pressure itself.:
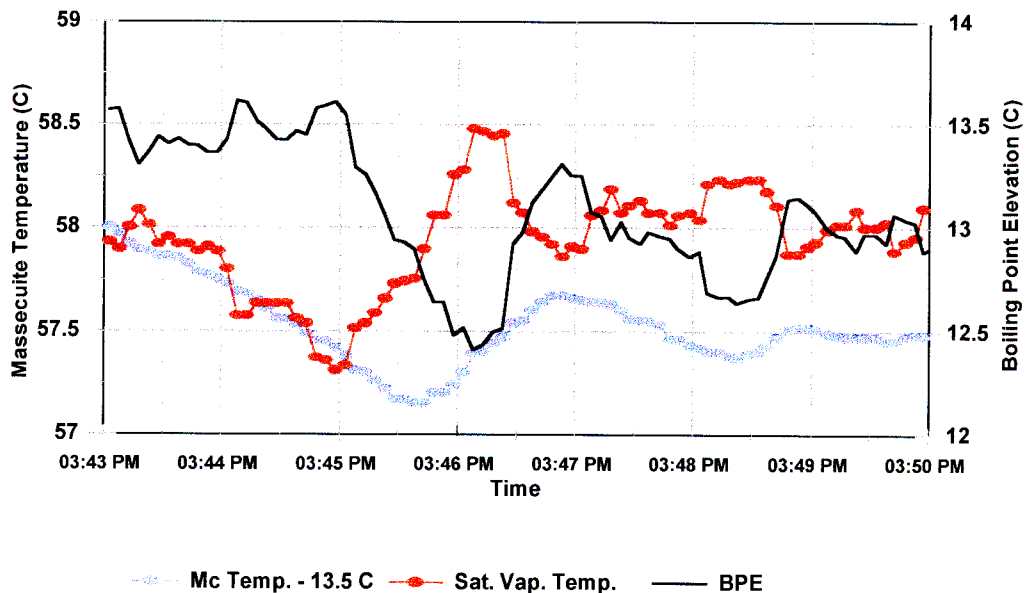


**Figure 9.4** Effect of fluctuations in pan absolute pressure on massecuite temperature

There is an indication in this graph that the "thermal inertia" of the massecuite in the pan is causing an approximately 35 second delay (7 sample intervals of 5 seconds in the logged data) from the time that changes in pressure occur until the massecuite temperature responds. This causes a variation in the calculated BPE which is simply a function of this dynamic behaviour and not a reflection of a variation in massecuite properties as intended. The effect of the delay can be demonstrated in the following graph which shows how the calculated BPE is affected when the pressure signal shifted forward by this estimated time delay of 35 seconds.
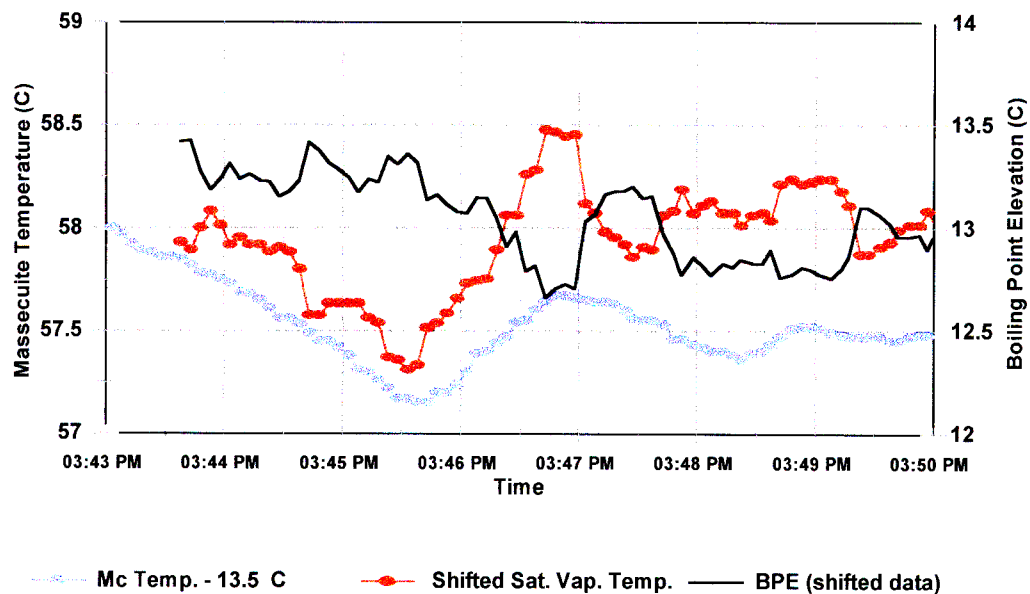
**Figure 9.5** Demonstration of effect of shifting saturated vapour temperature by 35 seconds

The variability in the BPE can be shown to have reduced from a standard deviation of 0,32 °C to a standard deviation of 0,20 °C by implementing this shift.

The indications of this time lag in the response of massecuite temperature was investigated in further detail over a longer period (3500 seconds) using techniques of auto-correlation, cross-correlation and Fourier Transforms. The details of this analysis are provided in Appendix F (section F.1). This analysis of small variations in absolute pressure (approximately ± 0,2 kPa) confirms the presence of a delayed response in massecuite temperature to variations in absolute pressure. The calculations reveal a time delay of between 25 and 39 seconds, depending on the frequency of the oscillation, confirming the magnitude of the delay estimated "by eye" from Figure 9.4.

Whilst these results indicate that it should be possible to implement some form of dynamic compensation in the estimation of BPE, this is probably an unwarranted complication. Rather these results should provide extra impetus to ensuring stable absolute pressure control as a fundamental requirement for good performance of a continuous pan. Careful attention to the design, sizing and operation of the ancillary equipment required to control the absolute pressure in the pan ( direct contact condenser, cooling water supply system, cooling water control valve , automatic control system and vacuum pump) can achieve control to within ± 0,1 kPa.

## 9.4     Step Tests

The automatic tuning tests described in section 9.6 below produce results which can be analysed in terms of the two step test described above. An added advantage of these automatic tuning tests is that they produce a sequence of two-step tests which can be evaluated to determine the repeatability of the two-step test. Figure 9.6 plots a portion of the recorded measurements. The details of the test were :.

| Factory : | Felixton | Pan Number : | A1 |
| Duty : | A-Massecuite | Compartment : | 1 |
| Feed : | Syrup | | |
| Process Measurement : | RS output from the RF Probe | | |
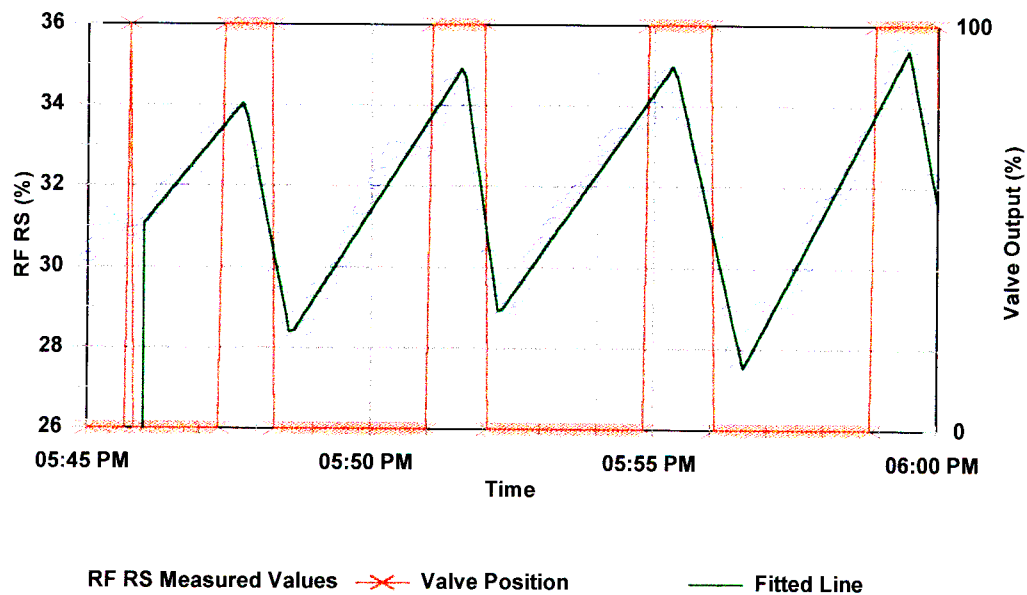


Figure 9.6 Step tests on Compartment 1 of the A1 Continuous pan at Felixton with syrup feed

To analyse the results, the nonlinear regression capabilities of a spreadsheet (Corel Quattro Pro) were used to fit segments of straight lines to the process measurement with the objective of minimising the sum of squares error between fitted and measured values. The results of the fitting process are tabulated below.

| Turning points for fitted line | | | Slope (% / sec) | "Capacitance" (sec) | Time of Step | Dead time (sec) |
|---|---|---|---|---|---|---|
| Ref. | Time | RS | | | | |
| 0 | 05:46:00 PM | 31.09 | | | | |
| 1 | 05:47:46 PM | 34.10 | 0.0285 | | 05:47:25 PM | 20.84 |
| 2 | 05:48:35 PM | 28.30 | -0.1184 | 680 | 05:48:19 PM | 15.87 |
| 3 | 05:51:37 PM | 34.99 | 0.0367 | 645 | 05:51:04 PM | 33.16 |
| 4 | 05:52:15 PM | 28.84 | -0.1644 | 497 | 05:52:04 PM | 10.54 |
| 5 | 05:55:21 PM | 35.03 | 0.0333 | 506 | 05:54:54 PM | 26.69 |
| 6 | 05:56:34 PM | 27.52 | -0.1027 | 736 | 05:56:04 PM | 29.77 |
| 7 | 05:59:30 PM | 35.41 | 0.0448 | 678 | 05:58:54 PM | 35.67 |
| 8 | 06:00:27 PM | 28.15 | -0.1259 | 586 | 06:00:04 PM | 23.31 |
| 9 | 06:03:05 PM | 34.83 | 0.0423 | 594 | 06:02:39 PM | 26.22 |
| 10 | 06:03:49 PM | 28.40 | -0.1475 | 527 | 06:03:34 PM | 14.79 |
| 11 | 06:06:50 PM | 35.02 | 0.0365 | 543 | 06:06:09 PM | 41.05 |
| 12 | 06:07:41 PM | 27.90 | -0.1403 | 565 | 06:07:24 PM | 16.77 |
| 13 | 06:10:00 PM | 33.53 | 0.0404 | 553 | | |
| Average : | | | | 593 | | 25 |
| Standard Deviation : | | | | 73 | | 9 |

**Table 9.2** Analysis of step tests on Compartment 1 of Felixton A1 continuous pan, syrup feed

The values of "capacitance" and dead time estimated by the fitting process show reasonable repeatability. It is however clear from an observation of the recorded trends, that instabilities in the absolute pressure cause small fluctuations in the RS reading, adding a noise component to the reading. This noise particularly affects the estimation of the dead time, adding to the spread in the estimated values, although it should not add any bias to the result.

Love and Chilvers (1986) measured a similar dead time (30 sec) but a "capacitance" of 1727 sec for the same application. The "capacitance" is not a measure of the mixing or circulation in the pan, but rather a measure of the overall gain of the process. The differences between the measured "capacitance" results is probably due to the fact that the step tests used by Love and Chilvers were between valve positions of 10% and 30% (as feed control at that time was by proportional setting of valve position) whilst, these tests were done between valve positions of 0% and 100% (to make the results applicable to feed control using time-proportional on/off control). The dead time is a reasonable measure of the circulation characteristics of the pan since it must approximate the time for the massecuite diluted by the feed liquor to pass up through the pan tubes and then part of the way down the down-take to where the measurement probe is positioned.

A similar set of tests was performed on the same pan compartment with the feed changed from

syrup to water. A portion of the results are shown in Figure 9.7 below.



RF RS Measured Values ─✕─ Valve Position          ──── Fitted Line
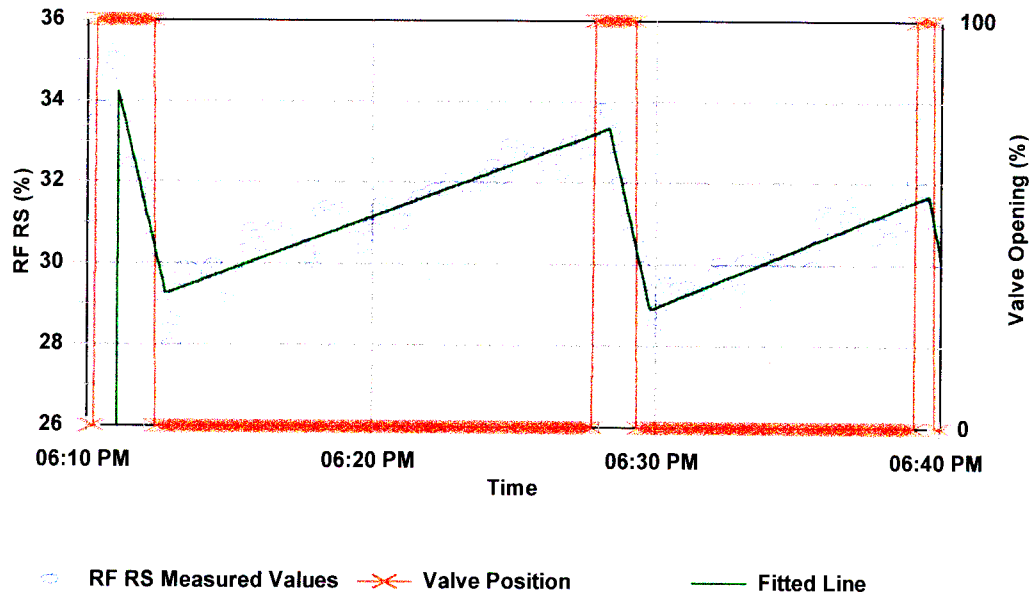
**Figure 9.7** Step tests on Compartment 1 of the A1 Continuous pan at Felixton with water feed

A water flow meter on the feed line showed that there was significant water leakage through the feed valve when fully closed, which resulted in the increased time to concentrate the massecuite between the lower and upper limits from approximately 3 minutes to approximately 8 minutes.

The results obtained by the same procedure of fitting straight line segments to the recorded data from the RS output of the RF probe are :

| Turning points for fitted line | | | Slope (%/sec) | "Capacitance" (sec) | Time of Step | Dead time (sec) |
|---|---|---|---|---|---|---|
| Ref. | Time | RS | | | | |
| 0 | 06:11:00 PM | 34.42 | | | | |
| 1 | 06:12:44 PM | 29.25 | -0.0495 | | 06:12:24 PM | 20.38 |
| 2 | 06:28:19 PM | 33.35 | 0.0044 | 1856 | 06:27:49 PM | 29.93 |
| 3 | 06:29:46 PM | 28.90 | -0.0513 | 1794 | 06:29:19 PM | 26.68 |
| 4 | 06:39:35 PM | 31.70 | 0.0048 | 1782 | 06:39:08 PM | 26.97 |
| 5 | 06:40:11 PM | 29.40 | -0.0645 | 1444 | 06:39:48 PM | 22.73 |
| 6 | 06:52:55 PM | 33.42 | 0.0053 | 1434 | 06:52:28 PM | 27.42 |
| 7 | 06:54:01 PM | 29.20 | -0.0639 | 1445 | 06:53:53 PM | 8.33 |
| 8 | 07:05:56 PM | 33.26 | 0.0057 | 1437 | 07:05:33 PM | 23.49 |
| 9 | 07:07:29 PM | 28.90 | -0.0470 | 1897 | 07:07:03 PM | 26.20 |
| 10 | 07:12:00 PM | 31.46 | 0.0095 | 1770 | | |
| | | Average : | | 1651 | | 24 |
| | | Standard Deviation : | | 192 | | 6 |

**Table 9.3** Analysis of step tests on Compartment 1 of Felixton A1 continuous pan, water feed

The average value for the "capacitance" of the process is significantly different from that for syrup feed but with a similar relative level of variability in its estimation indicated by the standard deviation. The estimated dead time shows a very small difference in average value compared with that measured with syrup feed, indicating that the circulation characteristics are not affected by the type of feed.

A test of the same type performed on Compartment 6 of the same pan yielded the following results :

| Turning points for fitted line | | | Slope (%/sec) | "Capacitance" (sec) | Time of Step | Dead time (sec) |
|---|---|---|---|---|---|---|
| Ref. | Time | RS | | | | |
| 0 | 12:53:00 PM | 38.31 | | | | |
| 1 | 12:56:32 PM | 32.41 | -0.0279 | | 12:56:15 PM | 16.73 |
| 2 | 12:58:24 PM | 38.78 | 0.0565 | 1185 | 12:57:54 PM | 30.43 |
| 3 | 01:02:47 PM | 32.79 | -0.0228 | 1260 | 01:02:24 PM | 23.08 |
| 4 | 01:04:29 PM | 39.23 | 0.0630 | 1166 | 01:03:59 PM | 30.35 |
| 5 | 01:08:50 PM | 32.23 | -0.0269 | 1113 | 01:08:19 PM | 30.51 |
| 6 | 01:10:35 PM | 38.67 | 0.0612 | 1136 | 01:09:59 PM | 35.81 |
| 7 | 01:13:55 PM | 32.14 | -0.0327 | 1066 | 01:13:34 PM | 20.58 |
| 8 | 01:15:52 PM | 38.29 | 0.0526 | 1173 | 01:15:19 PM | 32.67 |
| 9 | 01:19:10 PM | 32.45 | -0.0295 | 1219 | 01:18:39 PM | 30.91 |
| 10 | 01:20:52 PM | 39.44 | 0.0687 | 1018 | 01:20:24 PM | 27.67 |
| 11 | 01:25:37 PM | 32.31 | -0.0250 | 1067 | 01:25:14 PM | 22.78 |
| 12 | 01:27:34 PM | 39.30 | 0.0596 | 1182 | 01:26:59 PM | 35.20 |
| 13 | 01:31:00 PM | 36.55 | -0.0134 | 1371 | | |
| | | | Average : | 1163 | | 28 |
| | | | Standard Deviation : | 91 | | 6 |

**Table 9.4** Analysis of step tests on Compartment 6 of Felixton A1 continuous pan, syrup feed

These results show another different value for "capacitance" but an average dead time similar to the other tests, indicating a similar degree of circulation in the compartment.

This type of testing and analysis has the capability to be used for on-line automatic tuning of control loops which is discussed in more detail in section 9.6 .

## 9.5     Testing with Random Signals

Whist the two step test does appear to give reasonably repeatable results for measurements of plant dynamics, the techniques for estimating plant dynamics from the analysis of response to random signals offers the possibility of perhaps a more robust, average measurement.

The techniques for estimating plant dynamics from dynamic signals require significant numerical computation and, despite the relative scarcity of computers at that time, their successful application to process equipment was reported in the 1960's (Murrill et al., 1969a, Murrill et al., 1969b, Gallier et al., 1961). More recent summaries of these "system identification" techniques have been given by Levine (1996) and Ljung (1996).

The application of this type of technique in the sugar industry has been reported (McWhinney, 1973,a and b) for use in investigating frequencies of oscillations and time delays in a crushing train. It is surprising that the sugar industry literature does not appear to indicate any major increase in the use of these techniques with the advent of powerful personal computers and the availability of digitally recorded plant data.

The particular calculation techniques used in this research for estimating plant dynamics follow the method outlined by Murrill et al., (1969 a and b) and are based on determining the auto-correlation of the input signal and the cross-correlation between the input and output signals. It can be shown mathematically that the relationship between the auto-correlation and cross-correlation variables (which are functions of time) is identical to the relationship between the conventional time dependent input and output signals. It is thus possible to determine the dynamic response of the process from an analysis of the auto- and cross-correlation signals.

A major advantage of this procedure is that the correlation signals may be calculated from relatively long records of input and output signals, thereby providing an "average" response which minimises the influence of random fluctuations which might affect the results of conventional time response tests. If suitable noise is present (usually as an addition) in the input signal, the auto-correlation of the input signal will approximate an impulse function.

The particular characteristics of the impulse function have important implications for the analysis of the dynamic response. The constant power spectral density of the impulse function, can be interpreted as meaning that the (time domain) input signal is comprised of an infinite combination of sinusoidal signals of every possible frequency, all of constant amplitude (Papoulis, 1965). This in turn implies that the process is being tested equally at all possible frequencies. The Laplace transform of the impulse function is unity, implying that the output (in this instance the cross-correlation) is simply the inverse transform of the transfer function.

If the auto-correlation only approximates the impulse function, it is still relatively simple to analyse the results by applying Fourier transforms to the auto- and cross-correlation functions and to calculate the plant dynamics in terms of the amplitude ratio and phase shift at each frequency. Effective application of Fourier transforms to this type of non-periodic data requires the use of window functions. Based on a review of the wide range of window functions which are available (Harris,1978) a Blackman-Harris function was selected for this work.

A particular type of random signal which approximates white noise and can be simply generated and added to the input signal is the Pseudo Random Binary Noise (PRBN) signal. The signal has two possible values (eg 0 and 1) and is generated by making a random decision at a regular, fixed, minimum time interval. The random decision is whether to keep the signal at its present value, or to change it to its other possible value. A description of how this type of signal can be generated and applied to a simulated pure integrating process is given in Appendix C.2. This simulation, to investigate the suitability of applying the technique to a pan compartment, demonstrates that the technique is suitable for estimating the capacity of the process from the analysis of the amplitude ratio of oscillations in input to output. It also demonstrates that the capacity cannot be estimated by studying the phase shift, because of ambiguities in estimating phase lead and phase lag.

With an understanding of the difficulty of interpreting the phase shift data, the technique was applied to data collected by applying a PRBN signal to the feed valve of the continuous pan compartment. Since the valve could only be actuated either on or off, the standard PRBN signal would result in a valve that was, on average, 50% open. This would not necessarily be a suitable feed to the compartment, causing either excessive concentration or dilution. To address this problem, an option was created to manually adjust the random decision making process of generating the PRBN signal. Whilst still maintaining the random nature of the decision, it was possible to specify a bias to achieve any desired average opening. Used infrequently this manual adjustment was able to prevent the conditions in the compartment from drifting too far away from normal operation without affecting the desirable random characteristics of the signal (as could be subsequently verified by evaluating the shape of the autocorrelation function).

The results and analysis of the test are presented in Appendix C.3. They demonstrate a dead time

of approximately 25 to 30 seconds - in agreement with that measured using the two step procedure described in the previous section.

## 9.6    Automatic Tuning

Astrom and Wittemark (1989) proposed a "relay feedback" method for auto tuning. The technique is simple to implement and involves specifying a dead band around the process set point. The control output is then set to toggle between two values when the process variable moves from one side of the dead band to the other. This should settle into a sustained oscillation whose amplitude and frequency can be measured. Assuming that the control action is a symmetric periodic square wave, Astrom and Wittemark then consider the amplitude of the first harmonic component of this square wave (as defined by a Fourier analysis ) with a frequency equal to the square wave frequency and use it to determine tuning parameters according to the standard Ziegler-Nichols rules for constant amplitude closed loop cycling.

When this procedure was applied to the control loop of a pan compartment, with a valve that was only either full open of full closed, the results were those shown in Figures 9.6 and 9.7. These are clearly not symmetric square waves, showing shorter open and longer closed times. The fundamental assumption of the method proposed by Astrom and Wittemark thus did not hold and the method does not thus calculate appropriate tuning parameters.

The relay feedback method is however successful in generating regular cycles. The calculation procedures used in section 9.4 can be programmed into a control system along with the relay feed back to develop an automatic tuning system based on the two step method.

## 9.7    Interpretation of Results of Measurements of Dynamic Behaviour

Based on the measurements of the dynamic behaviour of an individual continuous pan compartment presented in this chapter it is possible to conclude the following :

–       Good absolute pressure control of a continuous pan is essential (and possible) if Boiling Point Elevation is to be used as a signal for automatic control of the condition of the massecuite in the pan.

- Both the two step test of Love and Chilvers (1986) and tests using Pseudo Random Binary Noise (PRBN) have confirmed that the short term dynamic behaviour of a pan compartment can be described as a pure integrating process combined with a dead time.

- The two step test and the PRBN test provide similar measurements of effective capacitance (of the pure integrating as pect of the process) and dead time when testing the same compartment under the same operating conditions. These measurements can be used to calculate tuning parameters for the compartment feed control loop.

- The pure integrating aspect of the compartment behaviour is predicted as the short term response in the dynamic simulation of compartment behaviour described in Chapter 10. The longer term responses predicted by the dynamic simulations are probably obscured by measurement noise and drift.

- The dead time measured as part of the compartment response is not predicted by the dynamic model. This aspect of the behaviour can be explained by the time taken for the feed to circulate from the feed distribution manifold, up the heating tubes and then down the down-take to the measurement sensor. This is not taken into account by the dynamic model which assumes the compartment to behave as a fully mixed tank or CSTR. The dynamic model can be modified to mimic this behaviour by treating the dead time as a simple delay on the measurement signal.

- The "relay feedback" automatic tuning procedure suggested by Astrom and Wittemark (1989) is not appropriate for use on pan feed controls. The technique can however be modified to create an automatic version of the two step test to achieve automatic control loop tuning.

# CHAPTER 10

# 10. Simulation of Dynamic Behaviour of a Continuous Pan

## 10.1 General

Using the equations developed in Chapter 4 to describe the behaviour of a continuous pan, it is possible to investigate the dynamic behaviour by numerical simulation. This type of simulation has a range of possible uses:

−       The simulation of particular changes in operating conditions to investigate the effects of the operation of the pan, eg if a pan compartment is operating at steady state with a mother liquor supersaturation of 1.15, to what level will the supersaturation increase if the feed flow is reduced by 20% and how long will it take to reach this value?

−       Simulations can be used to elucidate the nature of the mechanisms (in qualitative terms) which determine the dynamic behaviour. This is the approach taken in section 10.4 below.

−       The simulated dynamic behaviour can be compared with that measured on operating equipment. This is useful both as a confirmation of the applicability of the model and to assist in interpreting plant results.

## 10.2 Techniques for Solution of Differential Equations

Once the modelling of the pan has been achieved in codifying the behaviour into equations, the simulation of the dynamic behaviour of the pan reduces to the solution of a set of simultaneous first order differential equations with defined initial conditions. A range of techniques is available for solving this type of problem and the approach used in this work follows the recommendations of Press et al., (1989).

Whilst more sophisticated solution techniques (such as the the Bulirsch-Stoer or predictor-corrector methods) can be very much more efficient procedures, the Runge-Kutta method is known to be an appropriate method for situations where particularly high accuracy is not essential and the desire is to tabulate results at equally spaced intervals and plot them as a graph. Although adaptive stepsize control can be added to Runge-Kutta techniques, it is not necessary in this type of application where the suitability of the chosen stepsize can be checked by halving the

stepsize, rerunning the simulation and checking that there is no significant change to the results. The fourth order Runge-Kutta technique is reported to be generally superior to both lower and higher order Runge-Kutta schemes, when considered in conjunction with altering the stepsize.

Whilst Press et al., (1989) provide computer algorithms in Pascal for developing programs to solve differential equations using the Runge-Kutta method, this work uses the convenience of the facilities of the Mathcad program (Appendix E gives details of the computer software used in this research). Mathcad provides the fourth order Runge-Kutta method as a built in function and has the advantage of its self documenting nature and the ability to include graphical presentation of results with minimal extra complexity.

## 10.3    Simulation of a Pulse Test

Appendix H presents the results of a simulation of the dynamic behaviour of a single compartment of a continuous pan in the form of a MathCad spreadsheet, suitably annotated to explain the solution procedure and including graphs to illustrate the time trends of the important characteristics.

The simulation is based on the first compartment of the Felixton Continuous A-Pan as measured in Test 2-A (summarised in Appendix F). The evaporation rate is selected to approximate average conditions. The feed rate was selected to achieve a steady state supersaturation of approximately 1.1. The steady state condition was determined by repeatedly running the simulation with a fixed feed flow, and resetting the initial conditions to the final conditions of the previous simulation until there was minimal change in final conditions.

The equations, and thus the simulations, assume a constant evaporation rate. This is clearly an approximation and it is conventional to expect that evaporation will reduce as the concentrations of solids and crystal in the pan increase. Unfortunately there are very limited data on the nature and magnitude of the relationship between evaporation and massecuite properties (eg Rouillard, 1985), making it difficult to add any extra reality to the simulations by including some form of concentration dependence of evaporation rate into the simulation. The magnitude of the variations in massecuite properties in the simulations presented here are small and are unlikely to

play a significant role in the dynamic behaviour. When evaporation rate control is implemented on a continuous pan (as shown in Figure 3.8) this will tend to hold the evaporation rate constant in spite of variations in massecuite properties, although the effect will be limited if the variation in massecuite properties occurs in only one compartment of a multi-compartment pan.

The simulation presented in Appendix H calculates the consequences of a pulse input applied as a short period (10 seconds) of increased feed flow to the compartment. The simulation uses a 5 second step for the calculations. The suitability of this stepsize was confirmed by rerunning the simulation with a 2.5 second stepsize to check that there was no significant change in the calculated process response.

The graphs included in the Mathcad printout demonstrate the time behaviour of the following variables in response to the pulse input:
—       average crystal size
—       crystal content
—       mother liquor supersaturation
—       massecuite brix.
These trends are analysed qualitatively in the next section.

The relationship between crystal content and feed flow has been investigated using Fourier transforms in a manner similar to that used for analysing plant measurements in Chapter 9. Without the noise associated with plant measurements it is not necessary to use random signals and averaging over long periods of time, and the Fourier transform techniques are thus applied directly to the time responses rather than to autocorrelation and crosscorrelation functions. This analysis produces a Bode plot which shows trends similar to those calculated from measurements in Appendix C. Over the frequency range of 6 to 600 cycles per hour, the magnitude Bode plot shows the proportional drop in amplitude with frequency (of one decade per decade) of a pure integrating process ( or at least the response of a first order operating well above its corner frequency). This particular range of frequencies covers the frequencies of interest in controlling compartment conditions by manipulating the feed valve, and confirms the appropriateness of assuming the process to be a pure integrating process in control studies and the development of tuning rules. The simulation does not include any modelling of the dead time observed in plant measurements. This can be added as a pure delay in the measurement when necessary.

Both the time trends and the Bode plots indicate that the pan compartment does display a first order (self-regulating) behaviour, but that this is a very slow acting effect with a time constant of the order of 2000 seconds. This relates to the lowest frequencies of the Bode plot which are of limited accuracy as a result of end effects and the application of the windowing function. The self regulating nature of the process is discussed in more detail in the following section.

## 10.4    Qualitative Understanding of Dynamic Behaviour

As has been demonstrated, the complexity of the processes which combine to describe the behaviour of a continuous pan compartment are effectively handled by the formulation of the appropriate equations and their numerical solution. Handled in this way, it is easy to simulate any specific behaviour which is of interest but the qualitative nature of the behaviour is obscured.

The combined behaviour can be considered to be made up of three separate mechanisms viz.:

–        Concentration and dilution. At steady state, the evaporation from a compartment is closely balanced by feed into the compartment. Any imbalance causes the concentration in the compartment to ramp away from steady state as an integral of the imbalance.

–        "Wash-out". The flow of massecuite into and out of a pan compartment produces a stabilising effect. Fluctuations in compartment conditions will be "washed-out" by this massecuite flow.

–        Crystallisation. In addition to the two processes described above, crystallisation takes place as a function of the prevailing supersaturation driving force, purity and temperature dependent growth rate and the available crystal surface.

A very simple model of a continuous pan compartment was presented by Love and Chilvers (1986) who demonstrated that the "wash-out" effect was small in relation to the concentration/dilution effect and that the concentration/dilution effect (neglecting the "wash-out") behaved as a pure integrator. The appropriateness of this simplification and the relative influences of the three mechanisms can be investigated by an examination of the results of the simulation presented in Appendix H.

It is possible to eliminate the effect of crystallisation by considering the response of massecuite brix which is merely a product of balances between water and solids flows and is independent of

crystallisation. Over the short time scales of interest for tuning of pan feed controls, massecuite

brix approximates the response of a pure integrator to a pulse input (ie a step function) as shown

in Figure 10.1 below.
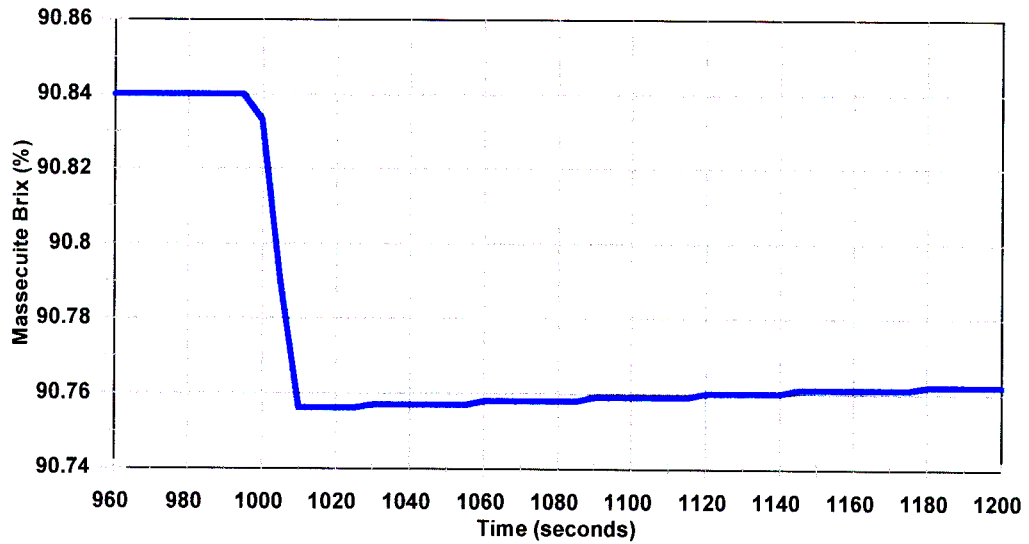


**Figure 10.1** Approximate step response of massecuite brix to feed pulse

If observed over the full time period of the simulation, the consequences of the "wash-out"

mechanism are evident.
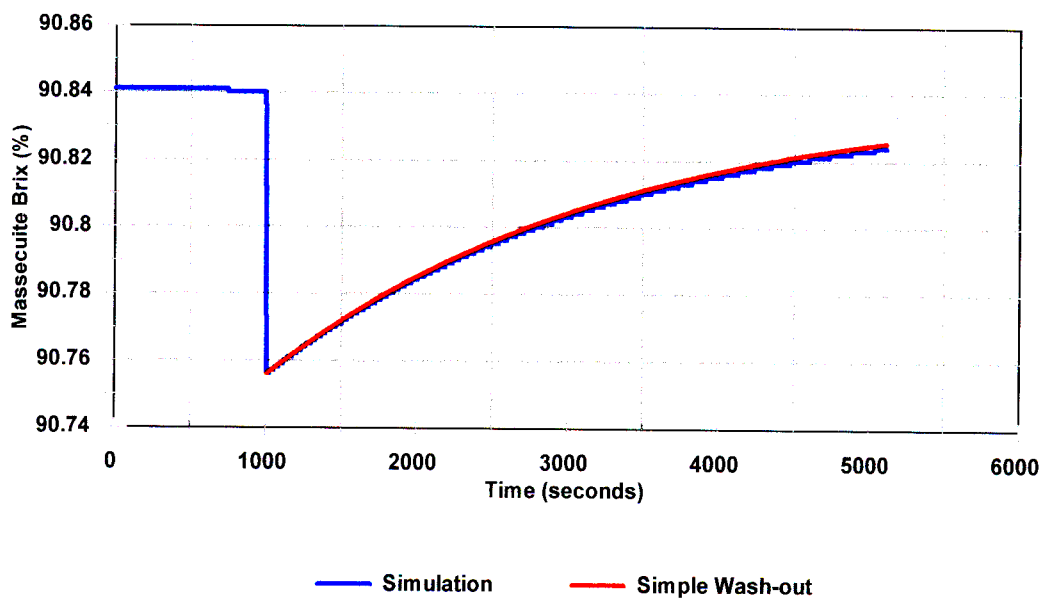


**Figure 10.2** Massecuite brix response showing "wash-out" effect

The "wash-out" effect shows the conventional asymptotic exponential response of a first order process. The time constant of the compartment in relation to the massecuite flow can be determined from the massecuite flow leaving the compartment and mass of massecuite in the compartment.

Thus:          mass of massecuite in compartment, $CT$  =       14500 kg

                       massecuite leaving compartment          =       $u1 + u6 - u8$

                                                                                       =       6.21 kg/s

          and     retention time                                        =       14500 / 6.21

                                                                                       =       2335 s

Simulating a simple first order response with a time constant equal to the compartment retention time matches the behaviour of the full simulation very closely, as shown by the red line in Figure 10.2.

The crystal content measurement includes the effects of crystallisation. This is illustrated very clearly in Figure 10.3 which also includes a curve to demonstrate the expected behaviour if "wash-out" was the ONLY mechanism bringing the compartment back to steady state as happens for massecuite brix.
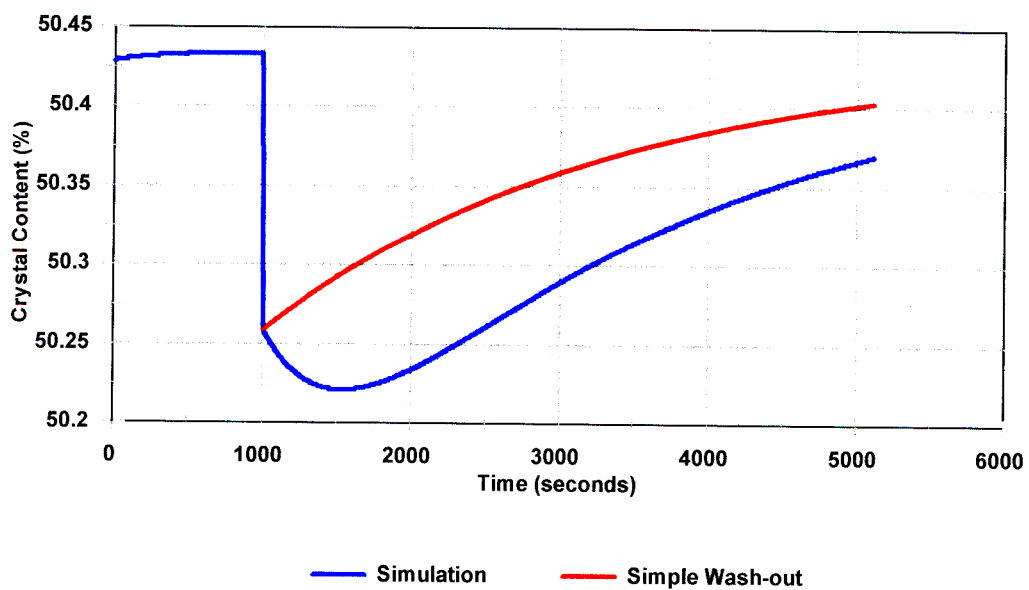


**Figure 10.3** Crystal content response to feed pulse.

The simple wash-out mechanism is clearly insufficient to explain the compartment behaviour. The difference between the simulated behaviour and the simple wash-out mechanism can be interpreted as the effect of crystal growth. This "growth effect" has been calculated and plotted in Figure 10.4. The nature of this effect is clearly more complicated than a simple first order system. The combination of a supersaturation driving force with the crystallisation process which it propells, suggests a mechanism of two first order processes in series. An appropriate model can thus be developed based on the equation for the impulse response of $N$ tanks in series as presented by Levenspiel (1972):

$$E = \frac{N \cdot (N \cdot \theta)^{N-1}}{(N-1)!} \cdot e^{-N \cdot \theta} \qquad (10.1)$$

where $\theta$          is the dimensionless time calculated as the ratio of the actual time to the mean residence time for all the tanks

A curve based on this equation and scaled by eye to provide a reasonable approximation to the magnitude of the effect is plotted in Figure 10.4
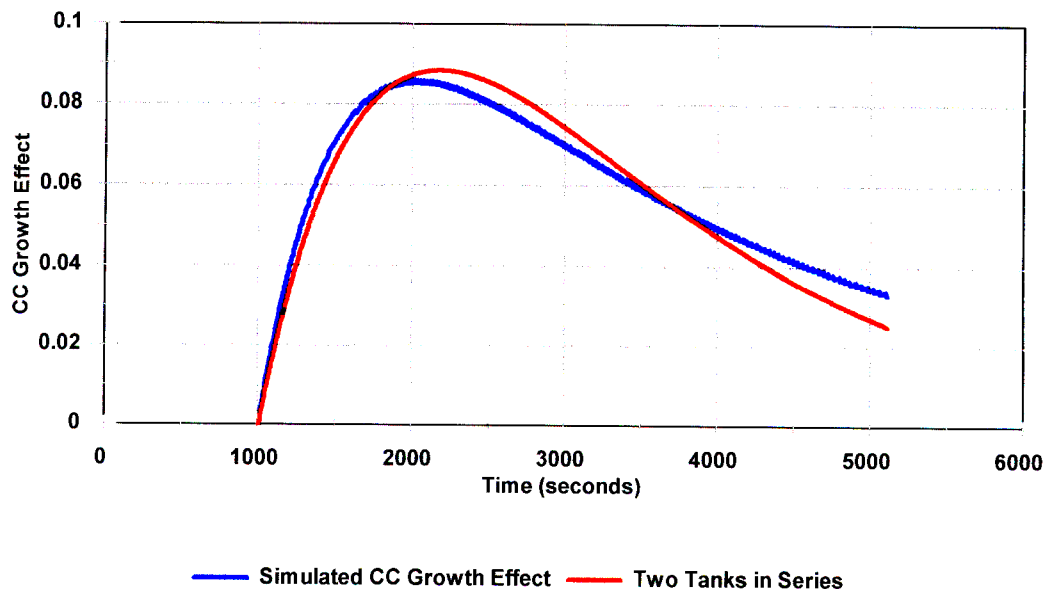


**Figure 10.4** Growth effect of impulse response on crystal content

These evaluations of the simulated dynamic behaviour of a single compartment of a continuous pan to a pulse input on the feed flow have demonstrated that the behaviour can be described in the following qualitative terms :

—       the short term behaviour can be described as a pure integrating process.

—       the longer term behaviour of variables unaffected by crystallisation can be described by a first order process with a time constant equal to the retention time in the compartment

—       the longer term behaviour of variables affected by crystallisation can be described by combining this same first order process but with an added effect described by two first order processes in series with an overall time constant equal to the compartment retention time.

# CHAPTER 11

## 11.    Stabilisation of Continuous Pan Throughput

### 11.1    General

The advantages of continuous pans over batch pans have been discussed in some detail in chapter 3. However, if these advantages of continuous processing are to be achieved then the continuous pan has to be run as close to steady state as possible. The multi-compartment continuous pan is particularly sensitive to varying throughput since it is designed to provide a practical approximation to plug flow conditions. This plug flow behaviour causes disturbances to be propagated through the pan. For example, a change in the seed flow rate into the pan will require at least the retention time of the vessel before its full effect is present in the product massecuite leaving the pan. In practice there is some spread in residence times about the mean value which increases the time taken to reach steady state to a value greater than the mean . The mean residence times for continuous pans are designed to accommodate the slow crystal growth rates and in consequence are relatively long. Even in the relatively fast growing conditions of "A" continuous pans, residence times are approximately 5 hours, increasing to about 10 hours for "C" continuous pans (Rein et al., 1985). It is thus important to make optimal use of the buffer tank which is conventionally provided to filter out fluctuations in total feed flow and allow the continuous pan to operate at conditions as close to steady state as possible. To place this problem in its context it is necessary to explain how the conventional operating procedures that have developed in factories where all processing takes place in batch pans contrast with the requirements for continuous operation.

With little loss of generality, the problem can be specified for the requirements of "A" massecuite boiling within the conventional South African "three boiling partial remelt" boiling scheme as described in Chapter 3. Conventionally a syrup tank is provided after the evaporators to provide buffer storage from which the batch pans may draw syrup as required.

In a traditional factory, where all syrup is processed in batch pans, any variation in syrup supply can be accommodated by adjusting the time that the pans remain idle between successive batch boilings. (There is obviously a maximum processing rate defined by the conditions when there is no idle time between batches.) Furthermore, if no syrup is available, batch pans can be stopped and restarted, usually with little or no negative effect on the crystallisation process. It is also

possible to "hold a pan on water" until syrup is available, causing a minimum of interruption to the batch process. This process of holding on water (matching the evaporation rate with an equivalent addition of water through the feed system) does carry a cost in terms of steam usage, but this is often not of concern in cane sugar factories with an energy surplus. In contrast to these minor penalties for emptying the syrup buffer tank, allowing the tank to fill completely has much more severe consequences. Either the tank will overflow with a consequential loss of sucrose or to prevent this the upstream processes will have to be slowed down. The situation of slowing down or stopping the crushing process to accommodate an inability to process the syrup ("factory full" condition) is often a cause for severe sanction of operating staff by management. Thus with the flexibility to alter the syrup processing rate, and the contrasting consequences of the buffer tank running either full or empty, it is not surprising that plant operators will often attempt to operate with the syrup tank level as low as practically possible. This policy of maintaining a low level in the syrup buffer tank provides the maximum buffer for unexpected increases in syrup flow or for equipment downtime should any of the batch pans need maintenance.

Some work has been done on achieving automatic scheduling of batch pan cycles (Merensky, 1985) but the major objective of this has been to achieve a more steady steam demand from the entire pan floor.

If only part of the "A" station capacity is provided by a continuous pan, and the balance is provided by batch pans, then a strategy similar to that for a completely batch station can be adopted. The continuous pan can be set to operate at a constant throughput whilst the batch pans are used to process the variable balance of the syrup flow. The strategy for the batch pans must now be slightly different. Rather than attempting to keep the buffer tank empty, the target should be to maintain a level in the tank to provide a buffer for the continuous pan in the case when the syrup supply from the evaporators drops below the demand of the continuous pan. The actual tank level to aim for will be a compromise between providing a buffer to allow steady operation of the continuous pan and providing a buffer against having to slow down the upstream processes if the tank fills up.

When the "A" station consists entirely of continuous pans, it is no longer clear what operating strategy should be followed to achieve the closest possible approach to steady state operation of

the continuous pans (ie a steady demand of syrup from the buffer tank). What is clear is that some form of trade-off is required between holding the syrup demand constant and varying the syrup demand to prevent the tank from either emptying or overflowing.

When Tongaat-Hulett constructed a completely new factory at Felixton with continuous pans used on all three grades of massecuite (Rein, 1983), the problem of maintaining steady throughput through the continuous pans was significant. The operators, whose (extensive) experience was in factories using batch pans exclusively, found it particularly difficult to adapt to requirements of continuous process equipment. This absence of local experience in dealing with this issue, prompted the research described in this chapter.

## 11.2    Definition of Standard Buffer Control Problem

The problem of smoothing out the flow to a continuous pan by effective use of an upstream buffer tank is essentially the classical surge or buffer tank problem, illustrated diagrammatically in Figure 11.1 .
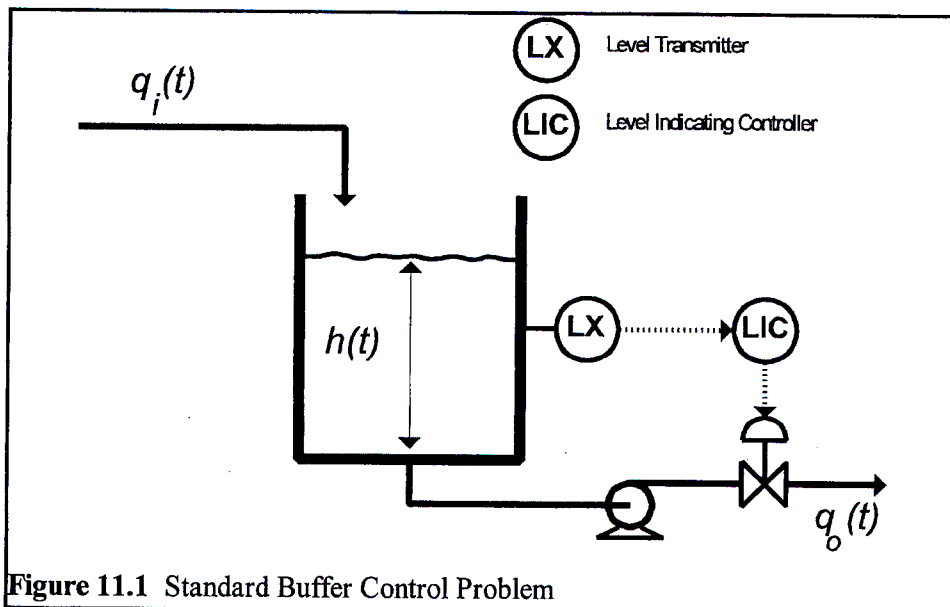


**Figure 11.1**  Standard Buffer Control Problem

A variable inflow , $q_i(t)$, enters a buffer tank of cross-sectional area, $A_t$, and height, $h_{max}$. The flow out of the tank, $q_o(t)$, must be adjusted in some optimal manner to satisfy two conflicting requirements:

- Tank Level Control ; to prevent the tank from either overflowing or running empty and also to return the level to some midpoint so as to accommodate future variations in inlet

flow.

- Outlet Flow Control ; to have the smoothest possible outlet flow from the tank to minimise the effect on the downstream process.

The behaviour of the system can be easily modelled as follows:

Defining deviation variables about steady state initial conditions,

$$q_o'(t) = q_o(t) - q_s \qquad (11.1)$$

$$q_i'(t) = q_i(t) - q_s \qquad (11.2)$$

$$h'(t) = h(t) - h_s \qquad (11.3)$$

which will all be zero at the steady state initial conditions of nominal (expected) flow, $q_s$ and nominal (desired average) tank level, $h_s$.

By mass balance,

$$\frac{dh'(t)}{dt} = \frac{1}{A_t} \cdot \left( q_i'(t) - q_o'(t) \right) \qquad (11.4)$$

Taking Laplace transforms,

$$s \cdot H(s) = \frac{1}{A_t} \cdot \left( Q_i(s) - Q_o(s) \right) \qquad (11.5)$$

Which can be written as,

$$H(s) = G_L(s) \cdot Q_i(s) - G_L(s) \cdot Q_o(s) \qquad (11.6)$$

where,

$$G_L(s) = \frac{1}{A_t \cdot s} \qquad (11.7)$$

If the controller has a transfer function $G_C(s)$ then,

$$Q_o(s) = G_c(s) \cdot H(s) \tag{11.8}$$

Substituting equation 11.8 into equation 11.6 yields ;

$$H(s) = G_L(s) \cdot Q_i(s) - G_L(s) \cdot G_C(s) \cdot H(s) \tag{11.9}$$

$$\therefore H(s) = \frac{G_L(s)}{(1 + G_L(s) \cdot G_C(s))} \cdot Q_i(s) \tag{11.10}$$

The characteristic equation for the closed loop system is thus :

$$1 + G_L(s) \cdot G_C(s) = 0 \tag{11.11}$$

In contrast to more complex systems where mathematical models are often necessary for a clear understanding of dynamic behaviour , the surge tank system is simple enough that a conceptual model is sufficient in most instances. The mathematical model of the surge tank system, whilst necessary to prove optimum behaviour and analyse stability, does unfortunately often obscure the simple principles involved. For example, after having derived an optimal buffer tank control strategy, Campo and Morari (1989) remark that, "Whilst notationally involved, this solution is easy to understand".

An important aspect of the behaviour of a controlled buffer tank, which is fundamental to most analyses of this system, can easily be understood intuitively. Consider the system operating at steady state, with the outflow equal to the inflow. If there is a step change in the inlet flow, the tank level will begin to rise. To counteract this rise in the tank level the outlet flow must be increased. When the outlet flow matches the inlet flow the tank level will stabilise but the level will have increased (the tank has effectively integrated the imbalance between the inlet and outlet flows during the period when the outlet was increasing to match the inlet flow). To return the tank to its original level requires that the outlet flow rate is increased above the inlet flow rate before being reduced to finally match the inlet flow rate. The consequence is that any strategy to return the tank level to its original position will give a response with a peak in the outlet flow when stimulated with a step change in inlet flow rate. This applies even if the control strategy is selected to ensure an overdamped system.

To compare different control strategies, a number of researchers have used a standard tank system with the following characteristics :

| | | | |
|---|---|---|---|
| Cross-sectional area of tank, | $A_t$ | 1.0 | m$^2$ |
| Tank height, | $h_{max}$ | 2.0 | m |
| Steady state level in tank, | $h_s$ | 1.0 | m |
| Steady state flow, | $q_s$ | 1.0 | m$^3$/min |
| Range of level transmitter, | $\Delta h$ | 2.0 | m |
| Range of flow control, | $\Delta q$ | 4.0 | m$^3$/min |
| Tank holdup time | $\tau_v$ | 0.5 | min |

where the tank holdup time is defined as ;

$$\tau_v = \frac{\Delta h \cdot A_t}{\Delta q} \tag{11.12}$$

The valve controlling the flow out of the tank is assumed to have linear installed characteristics. Thus the controller output of 0 to 100% is converted linearly into a flow between 0 and 4.0 m$^3$/min.


## 11.3    Overview of Control Options

Before reviewing the work of other researchers into the buffer control problem (sections 11.4, 11.5 and 11.6) and describing the development of a technique based on Linear Quadratic Gaussian control (section 11.7) it is perhaps useful to discuss the problem of control strategy selection in general terms.

Shinskey (1979) reports that, if the time constant of the tank is long enough, the buffer process will often be operated on manual. This can perhaps give performance superior to automatic control if the operator has knowledge of upstream processing conditions, can predict future variations in the inflow to the tank and is capable of providing the constant supervision necessary to implement this type of manual control. The challenge is to provide an automatic control system that is cheaper, better and more reliable than manual control.

The definition of the buffer control does not suggest what form the control strategy should take, nor does it provide a clear indication of how the quality of the control can be evaluated once it

has been implemented. The published work on the buffer problem which is presented in this chapter addresses the situation where the tank is subjected to a step change in the flow into the tank. Whilst this is convenient for analysis of the behaviour of the controlled system it has only limited application to the real demands of buffer control. The planned production schedule of a sugar factory (as for most continuous processes) requires that the production staff attempt to maintain a steady throughput. Thus a buffer control strategy in this environment should be concerned with damping out random fluctuations in throughput about a predefined average value rather than damping the infrequent changes in the average throughput rate. The published work has to be viewed critically with regard to its application to the requirements of a sugar factory because of its emphasis on step changes in flow.

Classical control techniques also have limited application because they are primarily concerned with forcing one or more variables to a desired value (setpoint) rather than handling the conflicting requirements of level and flow control posed by the buffer control problem . Despite these limitations, de-tuned classical controllers (Proportional and Proportional Integral) have been used for buffer control and their use is described in section 11.4.

It is possible to bypass some of the limitations of classical linear control strategies by using nonlinear control strategies. These nonlinear strategies are easy to define, based on an intuitive understanding of the control requirements, but are difficult to tune for best performance, to analyse for stability or to determine whether they are in any way optimal. A number have been reviewed in the literature and are briefly described in section 11.5.

The more modern techniques of optimal control hold some promise, if the control requirements can be framed in such a way that they match the format of the technique. However, the fact that a control can be shown mathematically to be "optimum" is no guarantee that it provides the best solution. Astrom and Wittenmark (1990) summarise the limitations of optimal techniques as follows:

"Much of the arbitrariness of design seems to disappear when design problems are formulated as optimisation problems. The model and the criteria are stated and the control law is obtained simply as the solution to an optimisation problem. The simplicity is deceptive because the arbitrariness is then transferred to the modelling and the formulation of criteria. A successful application of optimisation theory requires insight into how the properties of the model and the

criteria are reflected in the control law."

Model Predictive Control (MPC) is a concept that has been used by some researchers to provide improved control algorithms. The basic concept is that a model is used to predict the expected future behaviour of the process over some finite time horizon. A control law is selected which optimises a performance criterion over this time horizon subject to system constraints. The first step of the control law is implemented and then at the next time instant, the whole process is repeated. These algorithms have clearly attracted interest for the buffer control problem because they have the ability to handle constraints (viz the maximum and minimum tank levels) in an optimal way. A number of schemes for implementing this type of control have been developed eg Model Algorithmic Control (MAC) (Richalet et al., 1979), Dynamic Matrix Control (DMC) (Cutler and Ramaker, 1979), Internal Model Control (IMC) (Garcia and Morari, 1982) and, in an effort to unify a number of these schemes whilst adding nonlinear capabilities, Generic Model Control (GMC) (Lee and Sullivan, 1988). The application of some of these optimal techniques to the buffer control problem which have been reported in the literature are reviewed in section 11.6

Linear Quadratic Gausian (LQG) control, whilst an older and more established optimal technique than Model Predictive Control does not appear to have been applied to the buffer control problem. In section 11.7 a control strategy is derived using LQG techniques.

A further dimension to the buffer control problem is the behaviour of a cascade of buffer tanks. Whilst it would seem that a cascade of tanks should result in improved filtering in the flow out of the last tank in the cascade, the contrary is often the case. The control of a single buffer tank which returns the tank level to its original value after a step increase in flow into the tank results in a peak in the outlet flow which is greater than the inlet flow (as explained above). Consequently a cascade of tanks with independent level controls will amplify this peak in outlet flow rather than damp the flow step. Cheung and Luyben (1979) quantified this amplification effect and also reported on a method of using feed forward control to counteract the effect. They do not however provide any quantitative information on how the controllers with the added feed forward action should be tuned. In section 11.7 the Linear Quadratic Gausian Control approach is extended to two tanks in series to show how this technique can accommodate the problem of a cascade of tanks in an optimal manner.

Within the sugar industry, Hale and Whayman (1972) described their work on smoothing juice flow at an Australian sugar factory and emphasised the importance of sufficient surge (buffer) tank capacity and correct control valve sizing. They experimented with both proportional only control and versions of non-linear control (gap-action) that were available on the pneumatic controllers that were installed. They were unable to provide any clear recommendations on which option was the most appropriate. Miller (1988) demonstrated how stochastic process methods could be used to forecast the levels in molasses tanks feeding batch pans but only mentioned the possibility of using this information as part of a control strategy to adjust processing rates, without describing how it might be implemented .

In a review of juice flow control systems in the South African sugar industry, Meadows (1996) reported that comparatively simple systems were being used for stabilising juice flow, despite the universal agreement of process staff that good control was fundamental to good process performance. The systems in place were :

—       Flow control with a manually selected set point.

—       Heavily damped level control.

—       Gap action level control

—       Cascade control where a level controller provides a set point to the flow control.

Meadows (1996) also reported that despite the importance of flow control and the limited success in implementing good flow stabilisation, the subject had not been addressed in the previous 50 years of proceedings of the South African Sugar Technologists association.

## 11.4    Classical Buffer Control Strategies ( P and PI )

Shinskey (1979) reports on the simple system of using the level in the tank to set the flow out of the tank directly. The outlet flow will thus vary from zero when the tank is empty to maximum when the tank is full. This very simple system is equivalent to a proportional controller with a gain of unity in terms of instrument signal scales. Cheung and Luyben (1979) investigated in some detail the use of conventional proportional (P) and proportional-integral (PI) controllers for use in this application. The controllers must necessarily be de-tuned as their objective is not to provide tight level control.

For a proportional only (P) controller, the transfer function of the controller is ;

$$G_C(s) = K_L \tag{11.13}$$

and the characteristic equation (11.11) reduces to,

$$A_t \cdot s + K_L = 0 \tag{11.14}$$

The characteristic equation has only one real root, and the system will thus not display any oscillatory behaviour. In a proportional only controller the tank level is not returned to any midpoint and at steady state the level in the tank will depend on the flow into the tank. By solving for the time domain response to a step change in input flow of magnitude $B$, Cheung and Luyben (1979) showed that the controller gain to prevent the tank from overflowing is given by:

$$K_K = \frac{B}{h_{max} - h_s} \tag{11.15}$$

The controller gain, $K_L$, used here, has units of m³/min/m and as such includes the gains of the level transmitter and the control valve. The true, dimensionless, controller gain $K_C$ is given by:

$$K_C = K_L \cdot \frac{\Delta h}{\Delta q} \tag{11.16}$$

For a proportional plus integral (PI) controller, the transfer function of the controller is ;

$$G_C(s) = K_L \cdot \left( 1 + \frac{1}{\tau_I \cdot s} \right) \tag{11.17}$$

The characteristic equation of the closed loop system (11.11) then reduces to ;

$$\frac{A_I}{K_L} \cdot \tau_I \cdot s^2 + \tau_I \cdot s + 1 = 0 \tag{11.18}$$

By comparison with the standard form of a second order system, the damping factor is given by ;

$$\xi = \frac{1}{2} \cdot \sqrt{\frac{\tau_I \cdot K_L}{A_t}} \tag{11.19}$$

Cheung and Luyben (1979) provide charts to assist in the selection of controller settings by

considering their effect on the damping coefficient, peak height and rate of change of flow. They also show that for a critically damped system, ie $\xi = 1$, to prevent the tank level from exceeding a height of $h_{peak}$ for a step change in input flow of magnitude $B$, the controller gain is given by :

$$K_C = 0,736 \cdot \frac{B \cdot \Delta h}{(h_{peak} - h_s) \cdot \Delta q} \qquad (11.20)$$

and the integral time is given by ;

$$\tau_I = 5,43 \cdot \frac{(h_{peak} - h_s) \cdot A_t}{B} \qquad (11.21)$$

or alternatively ;

$$\tau_I = \frac{4 \cdot \tau_v}{K_C} \qquad (11.22)$$

## 11.5    Nonlinear Control Strategies

One of the schemes which has been used in the South African sugar industry for smoothing the flow of cane juice into the factory is to have a direct but nonlinear relationship between tank level and outlet flow as shown in Figure 11.2.
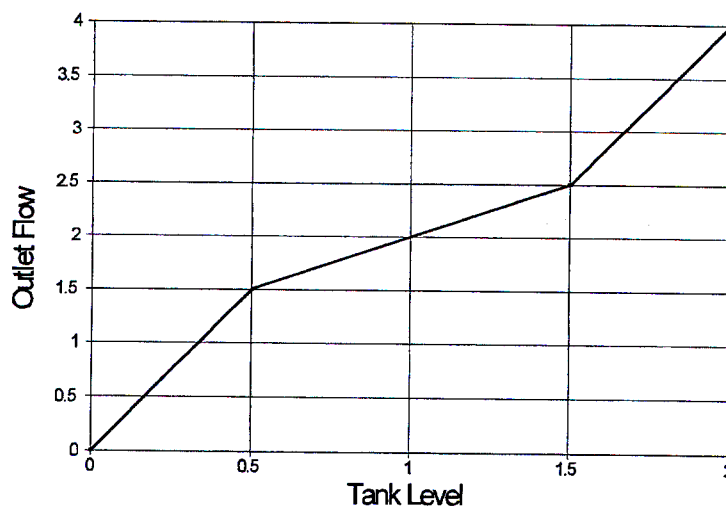


**Figure 11.2** Nonlinear Control of Outlet Flow

This controller is defined by the position of two break points, and thus requires 4 parameters (or

only 2 parameters if it is designed to be symmetrical about its average value). This example is configured for an expected flow of 2 and an average tank level of 1.

Cheung and Luyben (1980) reviewed a range of nonlinear controllers . The general principle behind these controllers appears to be an attempt to achieve fast control action for large disturbances and slow control action for small disturbances. In that sense they are similar to the rudimentary system depicted in figure 11.2 .

The Wide-Range Controller is a PI controller where the gain and the integral time are dependent on the magnitude of the error. The controller is tuned by specifying the gain and integral time for zero error (which defines the damping coefficient for the system) and a rangeability factor which affects the rate at which the gain changes with the error. The integral time varies with the gain in such a way as to keep the damping coefficient constant.

The Proportional-Integral/Proportional Controller (PIP) uses an override system to switch between a proportional only controller when the error is inside a specified band and a proportional-integral controller when the error goes outside of that band. The integral action is set up so that only the error outside of the specified band is integrated. This controller has better filtering than a PI controller of small variations in flow, but it does have a steady state offset in level.

The Dual Range Integral/Proportional Controller (DRIP) is similar to the PIP controller but uses PI control both inside and outside of the specified error band. Only the integral time is varied when the error varies between in and out of the band. A large integral time is used inside the band to provide overdamping for small errors whilst a small integral time is used for errors outside of the band to give an underdamped response for large errors.

Limited Output Change (LOC) Control is the principle of constraining the output of any controller to have less than a specified maximum rate of change. It can be used to eliminate the uncertainties in tuning nonlinear controllers. It also allows conventional P and PI controllers to be tuned quite differentially, enhancing their flexibility.

It is clear from this range of nonlinear controllers that a designer can add any type of nonlinear

elements to produce a nonlinear controller which may enhance some aspect of the performance of a linear controller. The limitations of this approach are that it is difficult to specify how the controller should be tuned to give the best performance and that the improvements in performance in one aspect (eg flow filtering of small sinusoidal disturbances) may result in a degradation in performance in another aspect (eg the controller may not return the tank level back to the desired 50% full condition after responding to the disturbance).

## 11.6    Continuous Time Optimal Control Strategies

McDonald et al. (1986) investigated optimal control strategies to achieve the smallest maximum rate of change in the outlet flow (MRCO), subject to the maximum and minimum tank levels not being violated.  Their initial analysis was of the system at steady state being subjected to a step in inlet flow of magnitude B. If no control action is taken, the level will rise and overflow at time given by :

$$t_{max} = \frac{A_t \cdot (h_{max} - h_s)}{B} \qquad (11.23)$$

The control action to minimise the rate of change of outlet flow (MRCO) is to ramp the outlet flow linearly from its steady state value up to the new inlet flow so that the tank level just reaches its maximum level as the flows become equal. Under these circumstances the average imbalance in flow (ie inlet - outlet) during the time taken for the tank to fill will be half of that for the situation where no adjustment is made to the outlet flow. Consequently the tank will take twice as long to fill.  After that, any change in outlet flow that is slower than this ramp will is acceptable as it does not affect the maximum rate of change criterion. This is the core of the strategy determined by McDonald et al., and expressed mathematically as :

$$q_o(t) = q_s + \frac{B}{t_{full}} \cdot t \qquad \text{for} \quad t \in \left[0, t_{full}\right] \qquad (11.24)$$

$$t_{full} = 2 \cdot t_{max} \qquad (11.25)$$

and, generalising for both positive and negative values of B which would cause the tank to overflow or empty respectively :

$$q_o(t) = q_s + \alpha \cdot t \quad \text{for} \quad t \in \left[0, t_{\lim}\right] \tag{11.26}$$

where :

$$\alpha = \frac{B^2}{2 \cdot A_t \cdot (h_{\lim} - h_s)} \tag{11.27}$$

and :

$$t = \frac{2 \cdot A_t \cdot \left|h_{\lim} - h_s\right|}{B} \tag{11.28}$$

$$h_{\lim} = h_{\min} \quad \text{if} \quad B < 0 \tag{11.29}$$

$$h_{\lim} = h_{\max} \quad \text{if} \quad B > 0 \tag{11.30}$$

If this control is implemented there will be a determinable relationship between the time, $t$, and the level in the tank, $h$. Thus by suitable manipulation the control law can be expressed in terms of $h$ instead of $t$.

$$q_o(t) = q_s + B \cdot \left(1 - \sqrt{1 - \frac{|h'|}{h'_{\lim}}}\right) \tag{11.31}$$

where :

$$h'_{\lim} = h_{\max} - h_s \quad \text{if} \quad B > 0 \tag{11.32}$$

$$h'_{\lim} = h_{\min} - h_s \quad \text{if} \quad B < 0 \tag{11.33}$$

This scheme will not bring the tank level back to its original level and McDonald et al., recommend adding some integral action to achieve this objective. They report that an integral time constant of $\tau_I = 10 \cdot t_{\lim}$ ( with $t_{lim}$ as defined in equation 11.28 ) gives acceptable results in terms of avoiding a large overshoot in outlet flow. This scheme is of little practical value as it requires the magnitude (and direction) of the step in the inlet flow, $B$, to be known. Whilst the authors suggest that $B$ could simply be set to the maximum expected disturbance, yielding sub-optimal performance for smaller steps, this still implies that the direction of the step is known. They refer to this controller as the ramp controller (RC).

Using the ramp controller as a basis McDonald et al. developed an optimal predictive controller (OPC). This controller has both feedforward and feedback modes, using measurements of both tank level and inlet flow. The controller is developed by an analysis of the buffer system, beginning at time $t_0$ with the system not necessarily at steady state. The tank level is $h(t_0)$, the inlet flow $q_i(t_0)$ and the outlet flow $q_o(t_0)$. The flow imbalance, $B$, is estimated from the difference in inlet and outlet flows :

$$B = q_i(t_0) - q_o(t_0)$$

(11.34)

Following the same arguments as for the ramp controller, the optimal solution is a ramp in the outlet flow given by :

$$q_o(t) = \frac{B^2 \cdot (t - t_0)}{2 \cdot A_t \cdot (h_{\lim} - h(t_0))} + q_o(t_0)$$

(11.35)

where:

$$h_{\lim} = h_{\max} \quad \text{if} \quad B > 0$$

(11.36)

$$h_{\lim} = h_{\min} \quad \text{if} \quad B < 0$$

(11.37)

Re-arranging and substituting for $B$ gives:

$$\frac{q_o(t) - q_o(t_0)}{(t - t_0)} = \frac{\left(q_i(t_0) - q_o(t_0)\right)^2}{2 \cdot A_t \cdot \left(h_{\lim} - h(t_0)\right)}$$

(11.38)

Taking the limit as $t$ tends to $t_0$ gives the optimal predictive control law (OPC) in terms of the rate of change in outlet flow that the controller must implement :

$$\frac{dq_o(t)}{dt} = \frac{\left(q_i - q_o\right)^2}{2 \cdot A_t \cdot \left(h_{\lim} - h\right)}$$

(11.39)

There are two problems with this control scheme. Firstly, if there is any error in the measurement of either inlet or outlet flow, then at steady state the controller will drive the measured inlet and outlet flows to be equal but there will be an imbalance in the actual flows.

This imbalance will cause the tank level to drift, eventually causing the tank to either empty or overflow. Secondly, the scheme has no integral action and the tank level will not return to its average value after an upset even if the flow measurements are exact. To eliminate these two shortcomings, McDonald et al. recommend adding proportional and integral action to the optimal control $q_0(t)$ calculated from equation 11.37 .The gain and integral time are set to the following proportions of the values determined from equations 11.20 and 11.21 for a conventional PI controller :

$$K_{C,OPC} = 0{,}05 \cdot K_{C,PI} \qquad\qquad (11.40)$$

$$\tau_{i,OPC} = 1{,}4 \cdot \tau_{i,PI} \qquad\qquad (11.41)$$

In a practical implementation, selecting the value of $h_{lim}$ by calculating $B$ from equation 11.34 is unwise since a bias in the measurement of either $q_i$ or $q_o$ can result in the wrong value being selected. The preferred method is to measure the rate of change in tank level to determine whether the flow imbalance, $B$, is positive or negative. To avoid toggling between $h_{min}$ and $h_{max}$ McDonald et al recommend filtering the level measurement before applying this criterion.

## 11.7   Discrete Time Optimal Control Strategies

Campo and Morari (1989) extended the work of McDonald et al., described above, by determining a discrete time version of the optimal averaging level controller (DTOALC). Campo and Morari provide a proof of the control law which they describe as "straight forward but tedious". For clarity, a "common sense" description of the basis for their control law is provided in this section particularly as the DTOALC forms the basis for their further work.

Equation 11.23 gives the time taken, $t_{max}$, for the tank to fill to capacity in response to a step change in inflow of magnitude $B$ if no change is made to the outlet flow. Expressed as a number of discrete time intervals, the tank will overflow after $k_{max}$ intervals, where :

$$k_{max} = \frac{t_{max}}{T}$$

$$= \frac{A_t \cdot (h_{max} - h)}{B \cdot T}$$

(11.42)

and      $T$ is the length of a time interval

If $t_{max}$ is an exact number of time intervals, then $k_{max}$ is an integer. In this instance, the optimal solution is to ramp the outlet flow in equally sized steps so that the outlet flow matches the inlet flow as the tank reaches its maximum level. The average imbalance in flow over the period that the tank takes to fill will be reduced to half that for the situation where no adjustment is made to the outlet flow. The tank will thus take twice as long to fill and the tank will reach its maximum level after $2 \cdot k_{max}$ time intervals. There are thus $2 \cdot k_{max} + 1$ steps in outlet flow required, and the optimal control action is given by :

$$q_o(t + k) = q_o(t + k - 1) + \Delta q_o$$

$$\text{where}\quad \Delta q_o = \frac{B}{2 \cdot k_{max} + 1}$$

(11.43)

$$\text{for}\quad k = 0 \quad \text{to}\quad k_{max}$$

If $2 \cdot k_{max}$ is not an integer, then the outlet flow must be ramped slightly faster, so that the tank reaches its maximum level at the end of $k^*$ time intervals where :

$$k^* = N\left[2 \cdot k_{max}\right]$$

$$= N\left[\frac{2 \cdot A_t \cdot (h_{max} - h)}{T \cdot B}\right]$$

(11.44)

and N[x] indicates the smallest integer greater than or equal to x .

The outlet flow must then be stepped in $k^* + 1$ equal increments of size $\Delta q_o^*$ . The average outlet flow over the period of $k^*$ time intervals is given by :

$$\frac{(1 + 2 + 3 + \ldots .k) \cdot \Delta q_o^*}{k^*} = \frac{k^* \cdot \left(\dfrac{k^* + 1}{2}\right)}{k^*} \cdot \Delta q_o^*$$

$$= \left(\frac{k^* + 1}{2}\right) \cdot \Delta q_o^* \tag{11.45}$$

The average flow imbalance over the period is thus given by :

$$\text{Ave. Flow Imbalance} = B - \left(\frac{k^* + 1}{2}\right) \cdot \Delta q_o^* \tag{11.46}$$

The increase in level in the tank over this time period can be equated to the average imbalance in flow multiplied by the time period, as follows :

$$A_t \cdot (h_{max} - h) = \left(B - \left(\frac{k^* + 1}{2}\right) \cdot \Delta q_o^*\right) \cdot k^* \cdot T \tag{11.47}$$

Solving for $\Delta q_o^*$ yields:

$$\Delta q_o^* = \frac{2 \cdot B}{k^* + 1} - \frac{2 \cdot (h_{max} - h) \cdot A_t}{k^* \cdot (k^* + 1) \cdot T} \tag{11.48}$$

For the case where ;

$$k^* = \frac{2 \cdot A_t \cdot (h_{max} - h)}{T \cdot B} \tag{11.49}$$

equation 11.48 is equal to equation 11.43, showing that this solution applies for the case where the time taken for the tank to fill is an exact number of time intervals.

For the general case of either positive or negative steps in inlet flow, the discrete time optimal control strategy is given by :

$$q_o(t+k) = q_o(t+k-1) + \Delta q_o^* \qquad \forall \ k \in \left[0, k^*\right]$$

$$\text{where } \Delta q_o^* = \frac{2 \cdot B}{k^* + 1} - \frac{2 \cdot (h_{\lim} - h) \cdot A_t}{k^* \cdot (k^* + 1) \cdot T}$$

$$k^* = N\left[\frac{2 \cdot A_t \cdot (h_{\lim} - h)}{T \cdot B}\right] \qquad\qquad (11.50)$$

$$h_{\lim} = h_{\max} \quad \text{if} \quad B > 0$$

$$h_{\lim} = h_{\min} \quad \text{if} \quad B < 0$$

As previously, N[x] indicates the smallest integer greater than or equal to x .

As with the continuous time case, for values of $k \geq k^*$ , $\Delta q$ can be chosen somewhat arbitrarily as long as $\Delta q \leq \Delta q^*$ and the tank level does not violate its constraints. For the value of $B$, Campo and Morari use the flow imbalance at the previous time interval, estimated from the change in level over one time interval. Their calculation of $B$ is based on their internal model formulation of the problem, which can be shown to be equal to what would be expected from a simple analysis viz :

$$B = \frac{A_t}{T} \cdot \left(h(t) - h(t-T)\right) \qquad\qquad (11.51)$$

Campo and Morari used the formulation of equation 11.50 as the basis for developing a model predictive controller ( the Discrete Time Model Predictive Optimal Averaging Level Controller, DTMPOALC). Here the decision on what control action to take is not based on an estimation of the behaviour of the tank over an infinite future time horizon, but rather over a finite future time horizon of P sample periods. The optimal control action is implemented, and then the whole process is repeated at the next time interval. The solution to this model predictive controller is very similar to that given in equation 11.50 for the DTOALC.

For the DTMPOALC the control option is selected from one of three possible options, based on the value of $k^*$, the number of time intervals for the tank level to reach a limit at the same time that the inlet and outlet flows match, assuming the outlet flow is ramped steadily to match the inlet flow :

1      If, $P \leq k^* /2$ the tank level is not estimated to reach a limit within the prediction horizon of P intervals even if no control action is taken, so make no adjustment to the outlet flow.

2      If, $P \geq k^*$, the tank level is estimated to reach a limit within the prediction horizon even with the application of DTOALC, so implement the control action defined by equation

11.50.

3        If, $P$ falls between these values, adjust the outlet flow at a rate predicted to match the inlet flow and have the tank level reach a limit at the end of the prediction horizon. This is achieved by using equation 11.50 with $k^*$ replaced by P.

This formulation still requires the addition of some form of integral action for it to be of any use in a practical situation, as the controller's response to a step change is simply to drive the tank level to a limiting value and remain there. An integral action could simply be added to the optimal solution, as done by McDonald et al. (1986), but this will obviously create a non-optimal solution.

To provide a practical and optimal control strategy, Campo and Morari developed an alternative formulation of the DTMPOAL Controller using what they call box level constraints. These box level constraints are to force the level back to its steady state at the end of the prediction horizon. This allows the derivation of an optimal strategy with integral action that is included in the derivation rather than added on as a non-optimal afterthought. The control strategy derived to meet this specification can best be described by the following procedure :

1        Estimate the flow imbalance , $B$, from equation 11.51

2        Evaluate $k^*$ (as per equation 11.50)

3        Evaluate the required rate of change in outlet flow , $\Delta q_o^*$, for the DTOALC (as per equation 11.50)

4        Evaluate the required rate of change in outlet flow , $\Delta q_o^0$, necessary to force the tank level back to its nominal level at the end of the prediction horizon using the modified form of equation 11.50 given as equation 11.52 below.

5        Implement the change in outlet flow given by $\Delta q_o^*$ or $\Delta q_o^0$, depending on which has the larger magnitude.

$$\Delta q_o^0 = \frac{2 \cdot B}{P+1} - \frac{2 \cdot (h_s - h) \cdot A_t}{P \cdot (P+1) \cdot T} \qquad (11.52)$$

Compo and Morari investigated an even further level of complexity, by proposing a formulation of the problem with embedded feedback to stabilise the plant and constraints on the outlet flow. There is no explicit solution to this problem but they show how this can be formulated as an optimisation to be solved on-line by linear programming at each time interval.

## 11.8    Development of A Linear Quadratic Gaussian Control Strategy

Whilst the control strategies described in the previous section have demonstrated a rigorous approach to determining optimality, their value must be viewed critically in the light of the comments of Astrom and Wittemark (1990) quoted in section 11.3. The optimal character of these solutions applies only to the definition of the problem in terms of the response of the system to step changes in inlet flow. For practical implementation in stabilising continuous pan throughput, what is required is a strategy that is optimal in terms of the type of random fluctuations in inlet flow that can be expected. This is a much more complex, and perhaps unquantifiable, definition of "optimum" and indicates the opportunity for an alternative approach to determining a buffer control strategy.

Linear Quadratic Gaussian (LQG) control does not appear to have been applied to the buffer tank problem but, as will be shown in this section, it provides an approach which has a number of advantages over other techniques and can also be extended to cover a sequence of buffer tanks in an optimal way. It does not however address the issue of constraints. LQG control, although not widely used in industrial practice, is frequently described in the more modern texts on control theory. (eg Richards 1979, Astrom and Wittemark 1990, Ogata 1987) The formulation of the LQG problem requires that the plant behaviour be expressed in state space format as :

$$\dot{x} = A \cdot x + B \cdot u \qquad (11.53)$$

$$y = C \cdot x \qquad (11.54)$$

where :

$x$        is a vector of plant states

$u$        is a vector of control actions

$y$        is a vector of plant outputs

$A$, $B$, and $C$ are matrices with constant coefficients

The control action must minimise the performance index, $J$, given by

$$J = \int_0^\infty \left( y^T \cdot Q \cdot y + u^T \cdot R \cdot u \right) dt \qquad (11.55)$$

where $Q$ and $R$ are suitable weighting matrices. The matrix $Q$ must be positive semi-definite and matrix $R$ must be positive definite.

The solution to this problem is a linear control given by

$$u = K \cdot x \tag{11.56}$$

where the gain matrix $K$ is given by

$$K = R^{-1} \cdot B^T \cdot P \tag{11.57}$$

and $P$ is the solution to the Riccati equation :

$$-\left(P \cdot A + A^T \cdot P\right) - C^T \cdot Q \cdot C + P \cdot B \cdot R^{-1} \cdot B^T \cdot P = 0 \tag{11.58}$$

The performance index used in deriving LQG control was selected mainly because it allows an analytical solution. However it does have some intuitive appeal.

*       It penalizes large deviations much more heavily than small deviations.

*       Positive and negative deviations are penalized equally.

*       The weighting matrices can be used to give any desired balance between penalizing control actions and penalizing process deviations.

*       The closed loop control using the optimal gain matrix, $K$, can be shown to be stable.

To apply LQG control to the buffer control problem requires a small contrivance; an integrator is included as part of the plant, as shown in Figure 11.3 below.
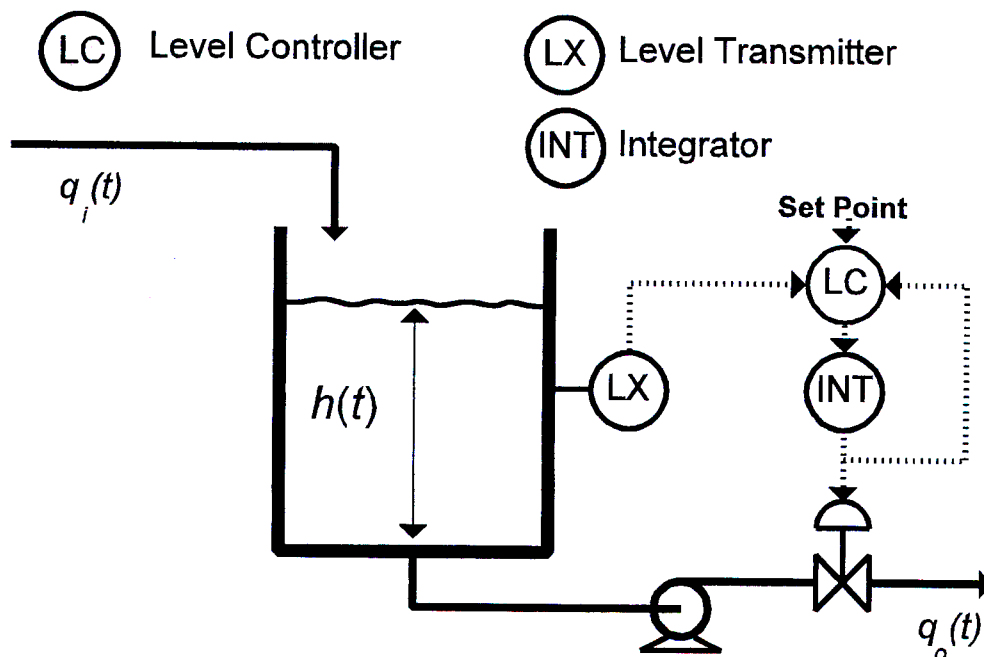


**Figure 11.3**   Inclusion of Integrator into Buffer Control Problem

This enables the output of the controller to be the rate of change in output flow since it is this rate of change of flow that we would wish to penalise in the design of an optimum buffer control strategy.

The equations derived in section 11.2 to describe the buffer control must be modified to include the integrator as part of the process. Expressed in terms of deviation variables, the integrator converts the output of the controller into an output flow according to the equation :

$$q_o'(t) = q_o'(0) + \int_0^t u(t) \, dt \tag{11.59}$$

or

$$\frac{dq_o'(t)}{dt} = u(t) \tag{11.60}$$

By mass balance (as in equation 11.4)

$$\frac{dh'(t)}{dt} = \frac{1}{A_t} \cdot \left( q_i'(t) - q_o'(t) \right) \tag{11.61}$$

Since in this instance the objective is to accommodate random fluctuations in input about the steady state value $q_s$, then on average $\quad q_i'(t) = 0 \quad$ and ;

$$\frac{dh'(t)}{dt} = -\frac{1}{A_t} \cdot q_o'(t) \tag{11.62}$$

Defining the two state variables as:

$$\begin{aligned} x_1(t) &= q_o'(t) \\ x_2(t) &= h'(t) \end{aligned} \tag{11.63}$$

The equations describing the system may be written as:

$$\begin{aligned} \dot{x}_1 &= u(t) \\ \dot{x}_2 &= -\frac{1}{A_t} \cdot x_1(t) \end{aligned} \tag{11.64}$$

Writing this in matrix format:

$$\begin{pmatrix} \dot{x}_1 \\ \dot{x}_2 \end{pmatrix} = \begin{pmatrix} 0 & 0 \\ -\dfrac{1}{A_t} & 0 \end{pmatrix} \cdot \begin{pmatrix} x_1 \\ x_2 \end{pmatrix} + \begin{pmatrix} 1 \\ 0 \end{pmatrix} \cdot u \tag{11.65}$$

The variable to be controlled is the level in the tank $h'(t)$ so:

$$y = \begin{pmatrix} 0 & 1 \end{pmatrix} \cdot \begin{pmatrix} x_1 \\ x_2 \end{pmatrix} \tag{11.66}$$

The matrices of the standard format are thus:

$$A = \begin{pmatrix} 0 & 0 \\ -\dfrac{1}{A_t} & 0 \end{pmatrix} \qquad B = \begin{pmatrix} 1 \\ 0 \end{pmatrix}$$

$$C = \begin{pmatrix} 0 & 1 \end{pmatrix} \tag{11.67}$$

For this system the weighting matrices are simply scalar values $Q$ and $R$.

Whilst it is common to use numerical techniques to determine the gain matrix, $K$, this system is simple enough to allow an algebraic solution to be determined analytically. Although the algebra is a little tedious, the advantage is that solution provides a simple control law which includes a single tuning parameter dependent on the relative values of $Q$ and $R$. The derivation is described in detail in Appendix D, where it is shown that if we define a weighting factor $W = \dfrac{Q}{R}$ then the gain matrix is given by:

$$K = \begin{pmatrix} \left( \dfrac{4 \cdot W}{A_t^2} \right)^{\frac{1}{4}} & -\sqrt{W} \end{pmatrix} \tag{11.68}$$

And the control law can be expressed in terms of measured plant variables as :

$$u = -\left( \dfrac{4 \cdot W}{A_t^2} \right)^{\frac{1}{4}} \cdot \left( q_o(t) - q_s \right) + \sqrt{W} \cdot \left( h(t) - h_s \right) \tag{11.69}$$

There is an intuitive appeal to this solution in that at steady state (ie $u = 0$), if the outflow is greater than the expected value, the tank level will also be greater than its nominal level. The tank

would thus appropriately have a greater capacity to cope with reductions in flow rather than increases in flow - since flow reductions would be expected as most likely at high flow rates.

This single buffer tank strategy can be applied to stabilising the production rate of a continuous A-Pan (defined by the control of evaporation rate as discussed in Chapter 3) in terms of the level in the syrup storage (buffer) tank. The strategy is unfortunately compromised when the syrup tank also supplies batch pans producing seed for the continuous pan. This is particularly so when a single large batch pan is used, as at the Felixton factory. Continuous seed production, which may become a viable production process in the future, would eliminate this problem.

## 11.9    Extension of LQG Control to Multiple Tanks in Series

Rather than simply address the problem of stabilising the throughput of the continuous pan in isolation, an improved strategy is to stabilise the production rate through the factory. If all the available buffer tanks can be used in an optimal way, without the flow amplification effects described in section 11.3, an improved throughput stabilisation will be achieved for the continuous pan. The added benefit will be optimum throughput stabilisation for other processes.

Within a conventional cane sugar factory, this concept of optimal throughput stabilisation over multiple buffer tanks can be applied to the front end of the factory as shown in Figure 11.4 below.
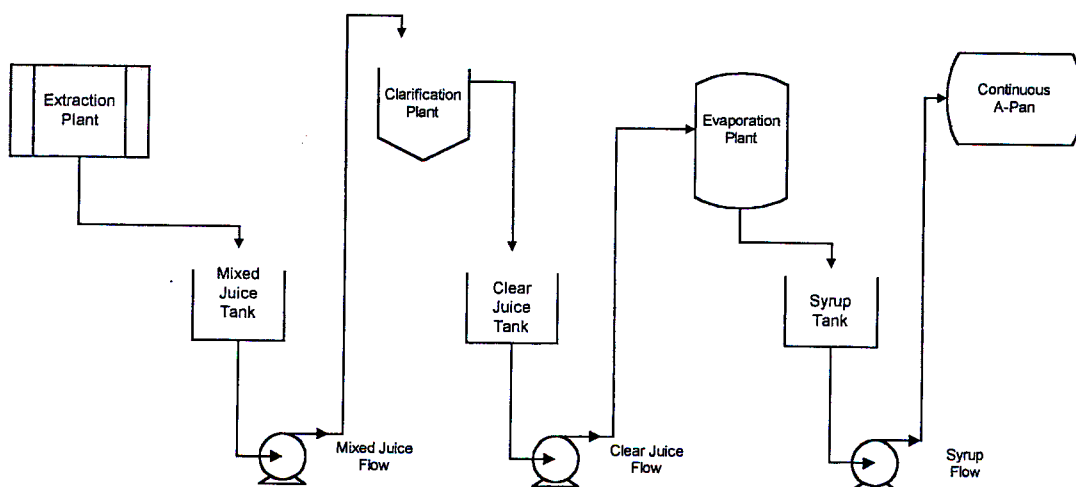


**Figure 11.4** Multiple Buffer Tanks in Series in a Cane Sugar Factory

The derivation of the control law for the extension of the LQG Control to two tanks in series is given in Appendix D. Whilst the implementation of this control is simple, determining the numerical values for the gain matrix is significantly more complex than for the single buffer tank problem. This complexity can be addressed by using standard numerical techniques to solve the Riccati equation and determine the gain matrix. In this work, the specific solution routine of the MATRIX$_X$ Computer package was used to evaluate the gain matrix, $K$, for different values of the weighting matrices $Q$ and $R$.

Using the same approach, the technique can be extended to larger numbers of tanks in series. Each extra tank will introduce two extra state variables and one extra control variable. This will increase the dimensions of the matrices $A$, $B$, $C$, $Q$ and $R$ whose dimensions will be :

| | | | |
|---|---|---|---|
| $A$ | $2n$ | by | $2n$ |
| $B$ | $2n$ | by | $n$ |
| $C$ | $n$ | by | $2n$ |
| $Q$ | $n$ | by | $n$ |
| $R$ | $n$ | by | $n$ |

where $n$ is the number of tanks in series.

For any practical number of tanks in series (estimated as a maximum of 10 tanks) the size of the matrices should not present any significant problems to computerised numerical techniques for solving the matrix Riccati equation. The major challenge will be the "tuning" of the controller by selecting appropriate values for the elements of the weighting matrices $Q$ and $R$.

Whilst the limitations of installed control hardware prevented this system of flow stabilisation from being evaluated in a full scale production environment, the potential of the strategy is demonstrated in the simulations presented in section 11.10. The simulations also demonstrate the added complexity of "tuning" the system with two tanks in series over the simple single buffer tank control problem.

## 11.10   Comparison of Buffer Control Strategies

A comparison between alternative control strategies is particularly difficult because of the need to define the disturbances that the control must respond to, the tuning parameters that need to be specified and the criteria by which the strategies are to be compared. Ideally, both a much clearer definition of the criteria for "optimal" performance and a more realistic specification (probably statistical) of the expected inlet disturbances are required. Given these difficulties, its is not possible to make a sensible and unbiased comparison between the Linear Quadratic Gausian Control developed in this work and the strategies developed by other research workers. The intention of this section is merely to demonstrate that LQG Control applied to single buffer tank, whilst unable to take account directly of maximum and minimum limits on level and flow, does provide a suitable solution to the buffer control problem even compared to the DTMPOAL Control (as formulated with level constraints) when the inlet flow is random in nature. This is done using simple spreadsheet simulations of the two strategies.

The simulations of the two control strategies are based on the standard buffer control problem as specified in section 11.2. A time period of 20 minutes and a sampling time of 0,2 minutes are used, for direct comparison with the work of Campo and Morari (1989). The "random" inlet flow was simulated by adding random fluctuations (positive and negative) to an initial flow of $1,0 \ m^3$ /min and then applying a first order filter to the resulting signal. This provides a signal which has the appearance of the type of random flow fluctuations seen in sugar factories. Applying the DTMPOAL Control strategy with tank level constrained between 0.6m and 1.4m in a spreadsheet simulation, yielded the following results for different values of the prediction horizon, $P$ :

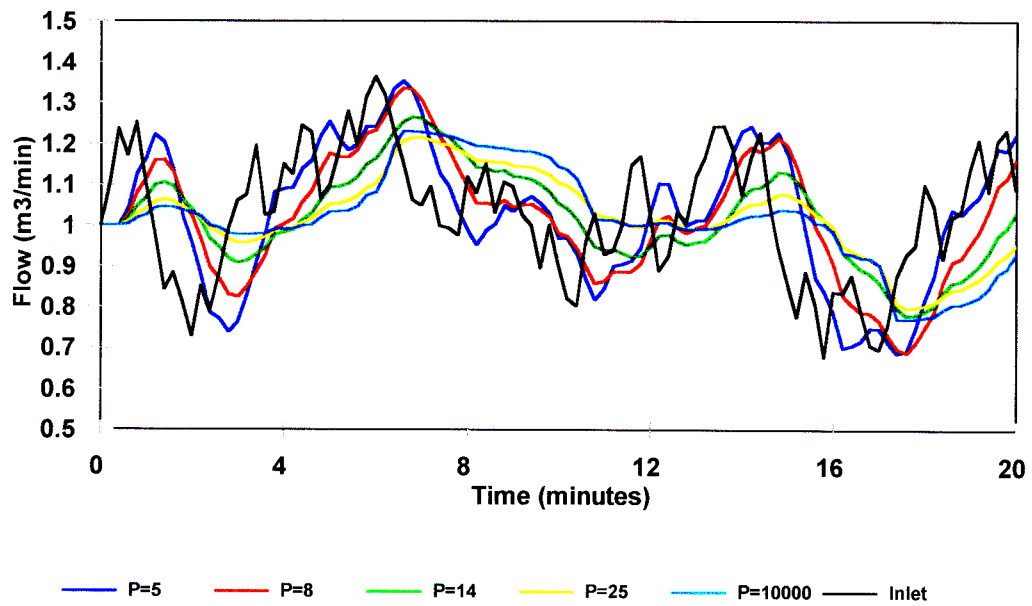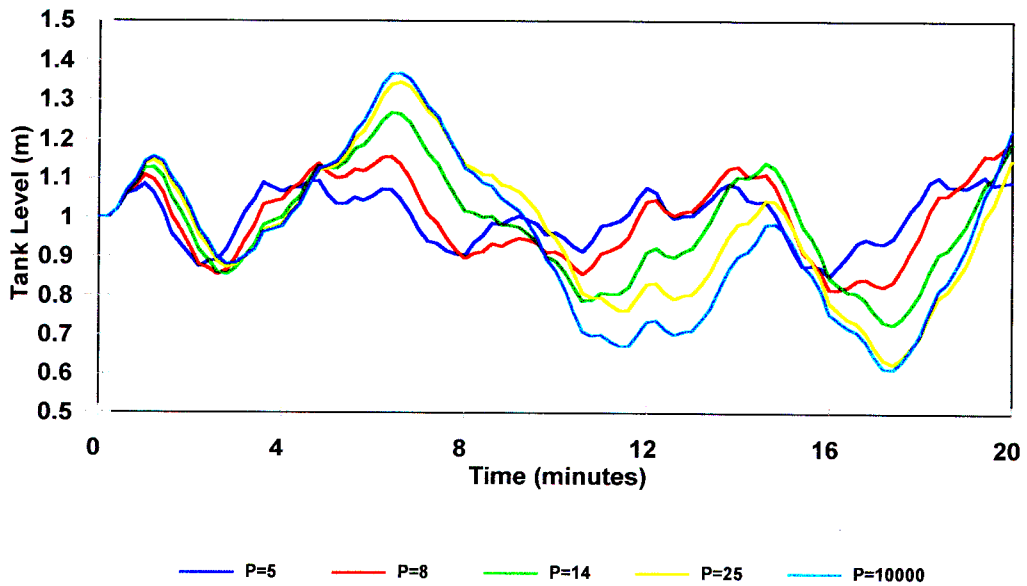**Figure 11.5** : Flow fluctuations with DTMPOAL Control



**Figure 11.6** : Level Fluctuations with DTMPOAL Control

Applying the LQG Control strategy to the same input signal in a similar spreadsheet simulation, yielded the following results for different values of the tuning parameter, $W$:
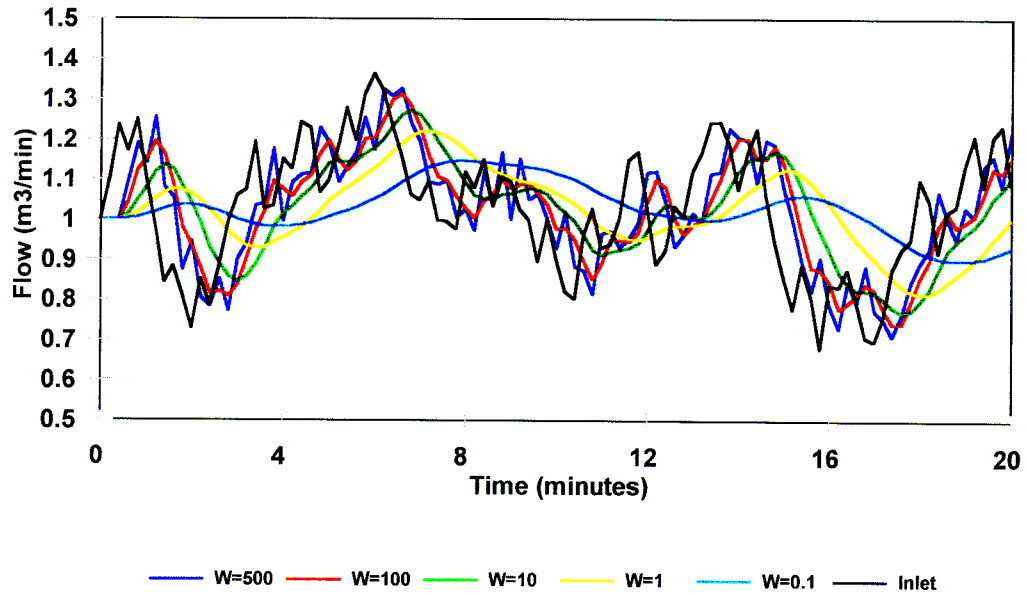


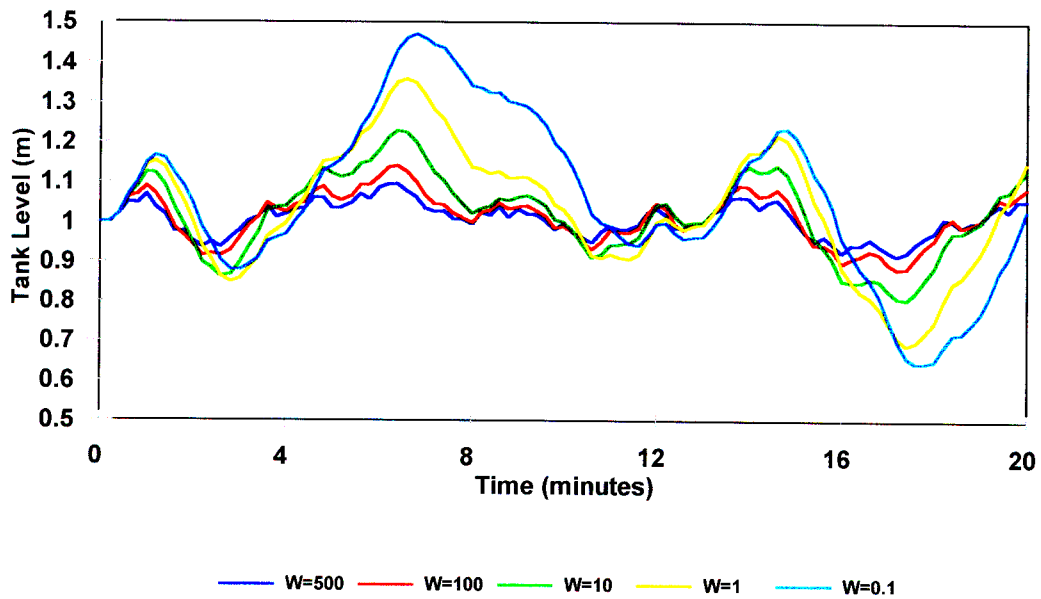**Figure 11.7** : Flow Fluctuations with LQG Control.



**Figure 11.8** : Level Fluctuations with LQG Control

Analysing these trends, it is clear that the DTMPOAL Control does not violate the level limits, but requires large values of the prediction horizon to maximise its use of the available buffer capacity. In comparison, LQG Control requires a value of $W \geq 1$ to prevent violation of level limits in this simulation, but there is no guarantee that with a different random signal the level constraints would not be violated for the same value of W.

The issue of the violation of level constraints, is probably one that should not be left entirely to the control strategy which can only base decisions on the signals it has available. With an appropriate control strategy to respond to the majority of the flow fluctuations, operator intervention is probably the most appropriate strategy when the tank level approaches the constraints. This should only occur in unusual circumstances and the operator can then make an appropriate decision using extra information which is unavailable to the control strategy, for example a maintenance worker's estimate of the time still required to complete a repair and restart a pump.

It is also evident from the simulations, that for similar "levels of damping" of the larger, lower frequency flow fluctuations (eg $P = 25$ and $W = 1$ ), LQG control provides better filtering of the smaller, higher frequency fluctuations. Campo and Morari (1989) deem that "suboptimal filtering of small disturbances (as determined by the selection of P) is not a practical concern". This may be true with regard to equipment sizing and the effects on downstream buffer tanks but is not true in terms of the effect on some control loops (eg juice pH control) and perhaps on some processes (eg clarification) which are less affected by large slow variations in flow than they are by small fast variations in flow.

The major advantage of the LQGC approach is not in this application to a single buffer tank but rather in the ability of the technique to be extended to multiple tanks in series as described in section 11.9. The performance of this type of control is demonstrated in the following graphs which show the results of a spreadsheet simulation of a random inflow to two identical tanks (of the same detail as used in the single tank simulation) in series. The simulation uses the same random input flow as used in the single tank simulations.
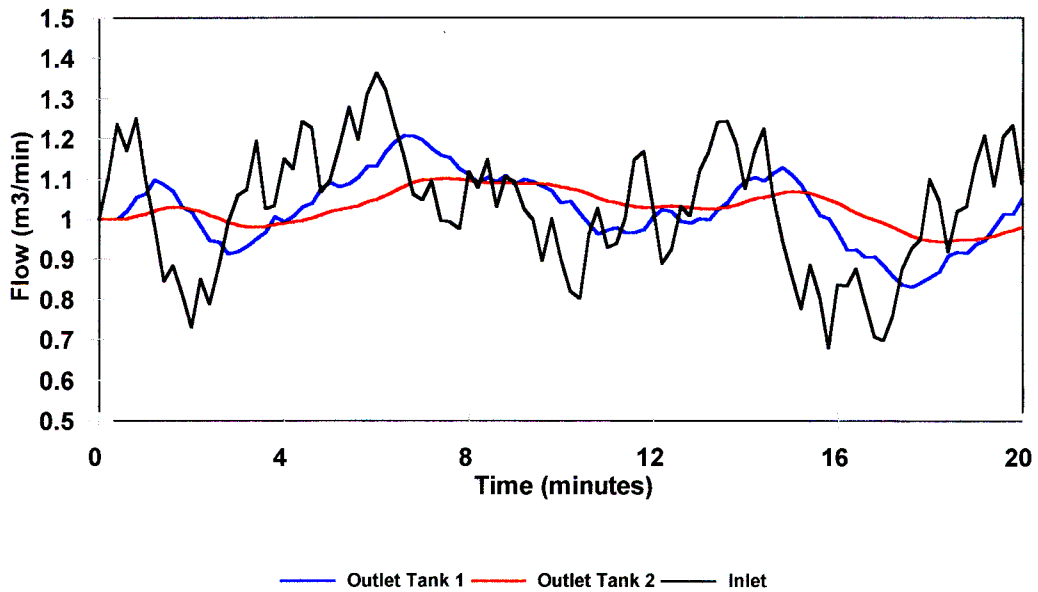
**Figure 11.9** : Linear Quadratic Gaussian Control applied to two identical tanks in series



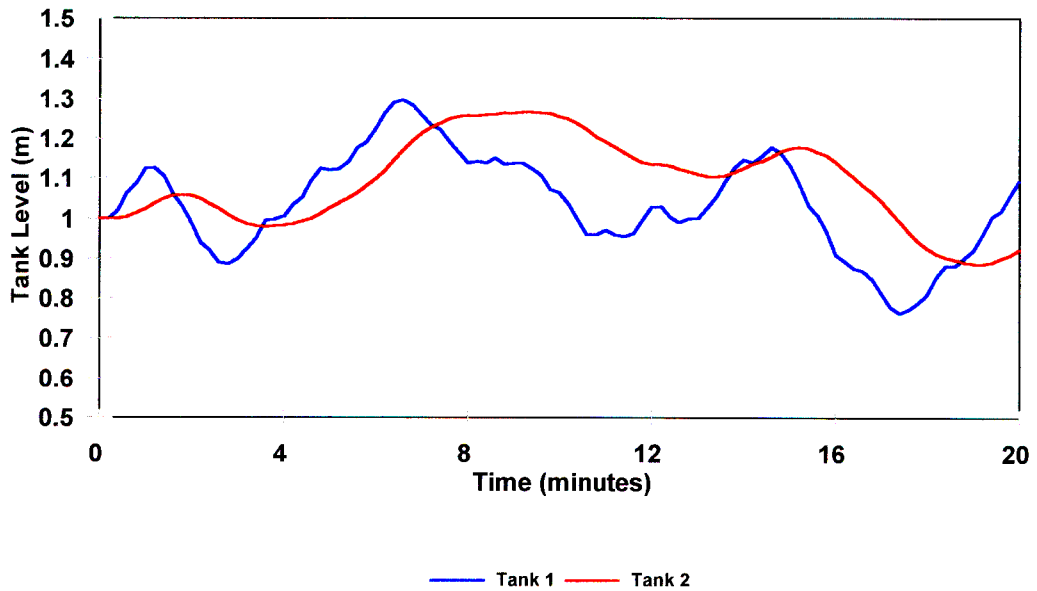**Figure 11.10** : Linear Quadratic Gaussian Control applied to two identical tanks in series

To determine the gain matrix, $K$, for this simulation, it was necessary to specify the weighting matrices $Q$ and $R$ and to solve the matrix Riccati equation (equation 11.58) numerically. Conventionally, only the diagonal elements of the $Q$ and $R$ matrices are specified, with the rest of

the elements set to zero. This weights the individual outputs and control actions and not the products of pairs of outputs or control actions (represented by the off-diagonal elements).

As with the single tank simulation, it is only the relative values of the elements of the $Q$ and $R$ matrices that define the overall performance. For the simulation shown here the weights for the level and rate of change of flow for the first tank were selected as unity, making it equivalent to the single tank simulation with $W = 1$. To achieve the increased flow stabilisation in the second tank, it was necessary to set the weighting factor for the level in this tank to 0.01 whilst keeping the weighting on the rate of change of flow at unity. Further improvements in performance could probably be achieved by more experimentation with the selection of these weighting factors.

It is clear from these graphs that this multivariable control strategy has the ability to improve the smoothing of flow fluctuations down a train of buffer tanks.

Although the formulation, and tuning of this type of multivariable control is reasonably complex (involving the numerical solution of the matrix Riccati equation), the details of the calculations can be automated, allowing a user to simply select different weighting values to achieve the appropriate balance between flow stabilisation and fluctuations in buffer tank level.

## 11.11   Application of the LQG Control Strategy

Unfortunately a number of factors have mitigated against the successful application of the LQG strategy in industrial practice, some of which were shown up in a test of the simple single input single output version of the LQG strategy on juice flow control in a production environment.

The single input single output verison could not be applied to the control of continuous A-pan throughput at Felixton because of the existence of a considerable batch A-pan capacity used for producing seed. The batch pans produce periodic fluctuations in syrup flow and tank level which should not be treated as mere random fluctuations to be damped out - making the LQG control inappropriate. This limitation may well disappear in the future. As confidence in continuous pan boiling grows, future factory installations are likely to have relatively much smaller batch seed pan capacities (with a larger portion of the crystallisation taking place in the continuous pans)

making the size of the periodic fluctuations which they cause to be of much less significance. The production of seed for the continuous pans by cooling crystallisation (already practised in the beet sugar industry) will have the same benefits of minimising batch process induced syrup flow and level fluctuations.

The maximum flow stabilisation benefits will be achieved by applying the multivariable strategy to the full sequence of processes and buffer tanks as described in section 11.9. This will produce benefits for all the processes whilst reducing the fluctuations to be damped out at each successive stage. The factors which need to be addressed for successful application of this strategy are :

−     Control hardware : The control hardware needs to have sufficient capabilities to be able to program the multivariable control strategy. To provide both operators and control technicians with assistance in understanding the control strategy and confidence in its ability to make sensible control decisions, the algorithm should not simply be programmed as a "black box". The control hardware should thus be able to display intermediate results (such as the desired rates of changes of the individual flows) demonstrate the basis for these decisions (eg by showing the contributions of the individual tank level measurements to these control decisions). Ideally the control system should be able to accept new weighting factors as inputs and calculate the necessary gain matrix for control by solving the matrix Riccati equation.

−     Staff training: Given the unusual nature of this control algorithm compared with the conventional PID algorithms normally used in sugar mills, both instrumentation and operating staff will need training to provide them with confidence in the system and enable them to tune the performance by adjusting the weighting factors.

−     Minimisation of effects of batch processes : the extension of the LQG control algorithm to flows through the pan boiling process requires that the intermittent flows to batch pans are minimal. (Although the batch pans produce level and flow fluctuations, these fluctuations will occur according to a regular cycle and should thus not be treated merely as random disturbances to be damped out by the control strategy). Whilst the minimisation of the size and importance of batch pans is only likely to occur with considerable changes from present operating practice, improved flow stabilisation in the earlier stages of the process (eg mixed juice flow and clear juice flow) will reduce the fluctuations in syrup flow presented to the continuous pans - the original objective of this specific investigation.

# CHAPTER 12

## 12. Development of a Computer Control System

### 12.1 General

The scope of the research undertaken for this thesis dictated the need for a computer system for data collection and control. The applications were diverse, covering

- Operation and testing of an industrial scale continuous pan to measure practical sucrose crystallisation rates

- Operation of laboratory and pilot scale batch pans to quantify effects of operating parameters on sucrose crystal growth rates.

- Cooling crystallisation experiments to determine solubility of sucrose in the impure solutions found in South African factories .

- Testing of industrial scale pan compartments to measure dynamic behaviour, using step tests and Pseudo-Random Binary Noise (PRBN) Signals.

The control and data collection system had to be capable of accommodating a range of different plant interfaces, viz.

- Analog and digital inputs an outputs on a proprietary Local Area Network (CONET).

- A plug-in interface card with analog to digital (A/D) , digital to analog (D/A) and digital input and output interfaces.

- Electronic balances connected via standard serial interfaces (RS232).

This wide range of requirements dictated a need for a high level of flexibility of programming, ruling out commercial options whose design was orientated to standard PID control and data logging. Given the open ended nature of research the ideal system would have the ability to implement any desired advanced computational feature on-line (eg matrix algebra, nonlinear regression). This need for an appropriate system for developing and testing advanced control options, addressed at the beginning of this research has continued to be an issue for control specialists ( MacLeod, 1998).

Whilst computer hardware and software have undergone enormous evolution over the period during which the research took place, the decision to develop a data-logging and control system, based around the IBM Personal Computer has proved to be a good one and provided a reliable

research tool with flexibility and cost unmatched by commercial systems.

The details of the development of the control system described in this chapter have been published in conference proceedings (Love, 1991).

## 12.2    Control Requirements

It is difficult to be general about the requirements of a computer control system as these will depend to some degree on the application. There are however two basic requirements which are often identified in the literature viz. multi-tasking and real time behaviour (Kompass, 1985, Kompass, 1988, Astrom and Wittemark, 1990, Stewart, 1987, Sandoz, 1982, Edwards 1982, Stirling, 1982, Pyle, 1982).

### 12.2.1   *Multi-Tasking*

Anything more than a rudimentary control task requires that the computer should perform multitasking. Multitasking is the ability to perform effectively a number of separate tasks simultaneously. For example, a computer control system might need to read data from the plant interface (A/D card), perform control calculations, monitor the keyboard for operator instructions and write data to the plant interface (D/A card). There must also be a means for the tasks to communicate between each other and co-ordinate their functions.

Multitasking is usually implemented by "time slicing", a procedure where each task is allocated a "slice" of time on the central processing unit (CPU). At the end of each time slice, the current state of the executing task, known as its context, is stored, and the next task is given a time slice to execute, using its previously stored context.

### 12.2.2   *Real Time Performance*

The control computer needs to respond to events as they happen (e.g receive a message sent to the serial port from some remote instrument) and to perform some actions at specified times (e.g log data to disk every five seconds). For a computer with only one

CPU, this requires a feature that allows a task to be interrupted to allocate CPU time to a more crucial task.

## 12.3    The Personal Computer (PC) and its Control Limitations

The Personal Computer (PC) has provided, since its introduction, an enticingly cheap source of computing power when selecting hardware to perform process control. The wide range of affordable software and plug-in interface cards that is available, makes it even more attractive. Furthermore the compatibility between the control computer and a PC in the conventional role of a desktop machine used for program development, data analysis and report generation has made the PC an almost irresistible choice. Unfortunately both the PC and its original operating system, MS-DOS, were designed for the commercial office environment, and this legacy has resulted in significant limitations for application as the basis of a process control computer.

### 12.3.1 *Hardware Limitations*

Given the intended application for IBM PC's as the office environment, the conventional PC has the following limitations :

- The cooling system may be inadequate, e.g fan too small, dust filter inadequate.
- There is minimal protection against dirt and liquid spills, particularly of the keyboard.
- The unit has limited ability to withstand mechanical shock, the hard disk in particular.
- The PC is constructed with a "motherboard" processor mechanical design in which the PC bus is implemented on the motherboard itself. Whilst any of the modules plugged into the bus may be easily removed and replaced, any failure on the processor board itself will require the complete machine to be dismantled.

Industrially hardened PCs are available, designed to eliminate these limitations, at a significant cost premium.

### 12.3.2 *Software Limitations*

The operating system is the fundamental software component. It provides the interface between the hardware of the computer and any other software. The original MS-DOS operating system for the PC was also designed for the office environment, where it

would normally only be expected to perform one task at a time. Whilst it is possible to achieve multitasking with MS-DOS, the non re-entrant nature of the MS-DOS code limits the performance of the resulting operating system. Despite the limitations of the original MS-DOS operating system , a wide range of commercial software was developed to perform process control on a PC, whilst maintaining some level of compatibility with MS-DOS. The different options varied widely in price and performance, with the more comprehensive software packages costing an order of magnitude greater than the PC itself.

The need to maintain compatibility with the original MS-DOS has perpetuated many of the limitations of this software into the newer operating systems developed by Microsoft, with some control system vendors even deeming Microsoft's most advanced operating system (Windows NT) not suitable for real-time control.

## 12.4    Options for a PC-Based Control System

There is a range of software products available to enable process control on a Personal Computer. They vary widely in price and performance but may be grouped into some broad categories :

• Operator interface and Supervisory Control

> These systems use the graphics and data storage capabilities of the computer to provide an operator interface to a process, without needing to cope with the rigours of direct digital control. They require extra hardware to perform the actual control (e.g a programmable logic controller).

• Integrated Control Package

> These are systems which provide a range of control features such as sequence control, PID loops, data logging, trending and an operator interface. They are usually easy to program but limited in their flexibility.

• Computer languages for process control

> There are computer languages which have the necessary multitasking features to enable a control system to be written. Examples are FORTH, MODULA2 and ADA.

• Multitasking operating systems

> The operating system provides all the necessary features to enable real time multitasking. The control tasks are developed in a conventional computer language which can make use of the features of the operating system.

## 12.5    Criteria for Selecting A PC-Based Control System

The criteria which were considered when evaluating the options for selecting a particular software route for developing a control and data logging system were :

- Cost - this includes the cost of the control software, the cost of special hardware and the programming costs to configure the system to the specific application.

- Hardware requirements - the required specification of the CPU (processor) of the PC, the requirements for additional hardware in the form of peripheral processors, interfaces, storage devices etc., compatibility with locally available or installed equipment.

- DOS compatibility - The compatibility with Microsoft's DOS operating system enables recorded data files to be analysed by standard spreadsheets. The availability of a vast array of compilers and software tools available for DOS provided a significant advantages when building a system from a multitasking operating system.

- Speed - Whilst speed of operation can be increased by using faster processors, a simple control system may provide sufficient features and be fast enough to operate on simpler cheaper hardware.

- Reliability/track record - whilst this is an important criterion in selecting products and suppliers for most purchases, it is particularly difficult to assess in the rapidly changing environment of computer software and hardware.

- Features - Increased features usually require greater memory, faster processors or a reduction in speed on the control tasks.

- Flexibility/Ease of Programming - There is often a direct trade off between the flexibility of a system and its ease of programming.

- Technical Support - This is an important aspect in the selection of many technical products but it is particularly difficult to assess the reliability of continuing quality support for products in the rapidly changing environment of computer hardware and software. Technical support is often not readily available within South Africa where informal support networks can be more important as a source of assistance.

## 12. 6    A PC Control System Based on A Multi-tasking Operating System

It is unlikely that there is a "right" choice from the bewildering array of options for a PC-based control system. The system that was developed as part of this research was driven by the primary requirements of cost and flexibility. To meet these requirements, the system is based on a low cost multitasking operating system (MULTI-DOS PLUS) with tasks written in a popular compiled language with structured programming features (TURBO PASCAL)™. The use of a popular computer language provides access to a comprehensive range of cheap and reliable software for implementing numerical techniques (Press et al., 1989) The alternative of using a language which provides multitasking features (MODULA2) was considered but not selected because of lack of widespread support for the language.

A number of variations of this control system were developed, tested and used. The variations were to accommodate different control requirements, a range of plant interfaces and were programmed with different operator interfaces.

### 12.6.1    The MULTI-DOS PLUS Operating System and its Multitasking Features

MULTI-DOS PLUS does not replace MS-DOS but must be loaded into the computer after MS-DOS to operate in conjunction with it. MULTI-DOS PLUS provides the extra features necessary for multitasking, whilst still using MS-DOS to provide the conventional interface to the PC hardware, i.e disk handling, keyboard and screen interface etc. This ensures that the operating environment created by MULTI-DOS PLUS is compatible with MS-DOS. MULTI-DOS PLUS provides a range of features which can be used in building up a control system. Once MULTI-DOS PLUS has been loaded into the computer, a number of its features are available to the user as commands executed from the keyboard or from a batch file (much as MS-DOS uses *.BAT files). These include the ability to:

- reserve areas in memory;
- load tasks (i.e files with EXE or COM extensions) into these reserved areas;
- run , suspend or remove tasks which reside in memory;
- swap tasks between foreground, (where they have control over the keyboard and screen) and background, (where they can continue to execute, transparent to the user).

Once the tasks are running they may access the services of the multitasking operating system by making use of "software interrupts". Executing a software interrupt is effectively making use of a subroutine or procedure provided by the operating system (Claff, 1986). TURBO PASCAL provides the necessary command to execute a software interrupt. Since the use of software interrupts results in rather cryptic program code, a number of procedures were developed to provide clear and easy access to the services provided by MULTI-DOS PLUS. (Appendix E).

The common services used by the tasks are :

- Communication by messages

  Tasks can send and receive messages through 64 different message queues. Tasks can either be suspended whilst waiting for a message or test regularly for the arrival of a message whilst continuing to execute. Messages are simply sequences of bytes and must be interpreted by their context.

- Communication by resources

  Tasks can coordinate their operations by the use of resources (sometimes referred to as semaphores or tokens). Tasks may acquire, release or test the availability of 64 resources. This is an efficient means of communicating simple yes/no messages between tasks and implementing access control to common devices such as printers or serial ports.

- Control of time slicing

  Normally MULTI-DOS PLUS will assign CPU time slices to the various tasks in a round robin manner. Tasks can alter this procedure when necessary. A task performing a critical operation may suspend time slicing, complete its operation and then allow time slicing to resume. A task with only a quick operation to perform, may give up the remaining portion of its time slice once it has completed its operation.

- Control of tasks

  Tasks can be suspended, allowing their time slices to be allocated to other tasks , and then later resumed. This suspension can be either on command or for a specified interval. Priorities of tasks can be set, with high priority tasks getting more time slices than low priority tasks.

### 12.6.2   Structure of the Control Program

The danger in writing a large computer program without a structure is that it quickly becomes unintelligible to anyone other than the programmer, and shortly thereafter, unintelligible even to the programmer. Comments throughout the program, explaining its operation, do help but they are not sufficient. Unstructured programs quickly end up as "spaghetti code" with the program flow weaving a tortuous path through the lines of program code with "GOTO" statements marking each twist or turn.

The first level of structure built into this program is the specification of a set of tasks that are to run in concert under the multi-tasking operating system. These tasks have been selected as the major function areas of the control system, rather than individual control loops.
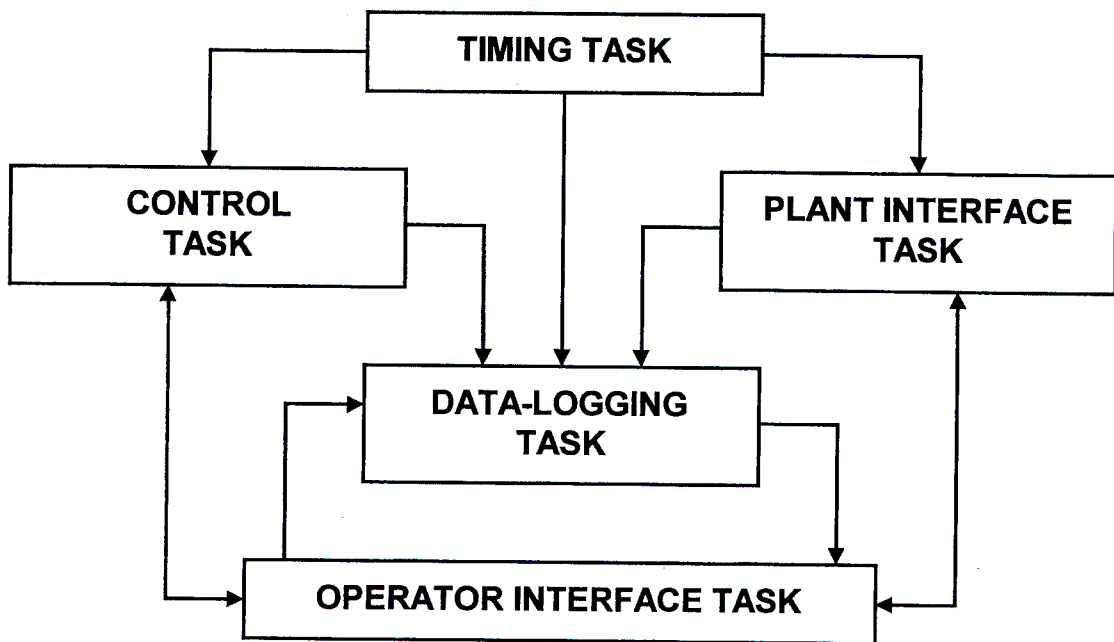


**Figure 12.1** Communications between the individual tasks which constitute the control system

Figure 12.1 shows the tasks and the lines of communication between them. The tasks are programs written in Pascal and compiled to files which will execute under MS-DOS (i.e files with the extension EXE).

The Pascal language was designed to facilitate structured programming with the

intention of producing clear and manageable code. It has a number of features which encourage good programming practice. Looping structures such as REPEAT... UNTIL... and WHILE....DO... enable programs to be written without any "GOTO" statements. Procedures and functions allow the artful hiding of detail where any segment of the program that does a specific task can be separated as a sub-program with a name that describes (or at least hints at) its purpose. The ability to build complex structured variables can greatly facilitate writing code that is both concise and clear. A well structured program built using these features will be easy to debug, adapt or modify.

### 12.6.3   *Sharing data between tasks*

Sharing data between tasks is crucial to the performance of the control system. For example, data read from the plant interface must be available to the control task where, amongst other calculations , the raw data are converted into engineering units. The data in engineering units must then be available to the datalogging task.

Some early experiments to share variables by sending messages (which contained all the shared data) between tasks, placed an enormous overhead on the system resulting in unacceptably slow performance. A more efficient method of sharing variables is to have a single area in memory where the common variables are located, and to have all tasks use this one set of data. This was achieved by using the PASCAL feature of "pointer variables".

The following code shows how a complex variable type, All, can be defined to hold all the common data and then be referenced by a pointer variable of type ^All (i.e pointer to type All). The purpose of this demonstration code is to create a common variable which contains the necessary information on 12 PID control loops, 96 integer variables intended for the input and output of analog data and details necessary for the data logging task.

```
type
  String10 = string[10] ;
  LogInfo  = record                        { for Datalogger   }
                  period : Integer  ; { Sample Period    }
                  nosamp : Integer  ; { Number of Samples}
                  logname: string10 ; { File Name        }
               end ;
```

```
OneLoop   = record                          { For single control loop}
                        tag  : String10 ;   { Describing Name           }
                        pv   : Real ;       { Process Variable          }
                        sp   : Real ;       { Set Point                 }
                        vo   : Real ;       { Valve Output              }
                        auto : Boolean ;    { auto/manual setting       }
                        gain : Real ;       { Gain                      }
                        taui : Real ;       { Integral Time             }
                        taud : Real ;       { Derivative Time           }
                        filt : Real ;       { Filter Time Constant      }
              end ;


  All =   record
              loop : array[1..12] of OneLoop ;
              ioin : array[1..96] of Integer ; { for analog I/O }
              thislog : Loginfo ;
            end ;
  AllPtr = ^All ;


var
  common : AllPtr ;
```

The variable, common, contains an address which points to a dynamic variable of type All which is created at run time (using the **new** command) in the free memory. The variable, common, thus provides access to all of the shared data specified in the type definition. For example the setpoint of loop 7 is held in the variable group^.loop[7].sp.

To ensure that all tasks use the same data, they must all define a variable, common, of type AllPtr. Only one task must create the dynamic variable by using the **new** command, and then inform the other tasks where the variable resides by sending them messages containing the value of common (which is simply a four byte address). The other tasks must wait to be informed where the dynamic variable exists before beginning to execute.

### 12.6.4 *Operator Interface Task*

An effective operator interface is an important component in providing a flexible control system for a research and development environment. It is as necessary in a production environment to ensure operator acceptance.

The operator interface task provides access to the system by allowing data and commands to be entered from the keyboard whilst providing a variety of possible data displays on the screen. This link to the screen and the keyboard is achieved by having the operator interface task as the foreground task.

Examples of features which have been provided by this task in various versions of the control program are :

- Individual "faceplates" for PID control loops.
- Summary display of a group of PID loops.
- A configurable graphic display built up from the extended ASCII character set.
- The ability to configure, start and stop the data logger.
- An input/output display which displays the raw data to and from the plant interface.
- The ability to configure, start and stop a simple "chart recorder" to run on a text printer.
- The ability to save the configuration of the system to be used on restarting, (includes all controller settings etc.).

The operator interface task also performs a number of initialisation functions when the system is started up viz:

- Create the dynamic variable for shared data.
- Send messages to all other tasks giving the location of this variable.
- Load a "configuration file" to initialise all variables and configure the system to a previously saved state.
- Load an ASCII file for the MIMIC screen.

### 12.6.5  Timing task

The objective of the timing task is to provide timing signals to the other tasks which have time dependent functions (i.e the datalogging task and the control task).  With the timing task sending simple one byte dummy messages to the time dependent tasks, these other tasks can simply wait for a message, perform their function, clear the message from the queue and then wait for the next message.

The system was programmed to operate with timing signals every second, which was adequate for the processes being controlled.

One method of obtaining timing signals is by measuring elapsed time on the system clock which can be accessed through MS-DOS. This is cumbersome and time consuming, and a more effective method is to make use of the hardware timer interrupt which interrupts the processor 18,2 times per second.

When the timer interrupt occurs the processor will normally execute interrupt routine 08Hex. It is possible to write a new interrupt routine which intercepts this interrupt and performs the required timing functions before continuing to execute the original interrupt routine. TURBO PASCAL provides the necessary features to program such a task. The timing task must thus :

- define the necessary new interrupt routine;

- direct interrupt 08Hex to this new routine;

- suspend itself (it must stay in memory but does not need any time slices as it will be activated by the hardware).

The pseudo-code, shown below, illustrates how this is achieved.

```
program TimingTask ;

  procedure EveryTimeTick ;
  interrupt ;
   begin
     Count := Count + 10 ;
     if Count > 182 then
       begin
         count := count - 182 ;
         SendTimingMessages ;
       end ;
     ExecuteOriginalRoutine ;
   end ;

begin
  SaveOriginalRoutine ;
  DirectInterruptToNewRoutine ;   { as defined above }
  SuspendTask ;
end .
```

### 12.6.6  *Control task*

The control task is required to do all of the control calculations, including the conversion of the raw data into engineering units and digital first order filtering of signals. Because of the importance of performing these calculations on time, time slicing is suspended while the calculations are in progress. It is important when programming to ensure that a divide by zero can never occur in the calculations as this will cause the task to abort.

```
program ControlTask ;
begin
 while true do
 begin
  CheckForTimingMessage ;
  if message = true then
  begin
   ClearMessageFromQueue ;
   StopSlicing ;
   PerformCalculations ;
   ResumeSlicing ;
  end ;
  GiveUpRestOfTimeSlice ;
 end ;
end .
```

### 12.6.7  *Datalogging task*

The datalogging task can store all of the plant data to disk at time intervals specified by the operator. The data is stored as lines of ASCII data which can be subsequently imported into a spreadsheet for analysis and display. The task has checks to prevent existing data files from being overwritten. The task also performs the function of writing data to the printer to provide a simple chart recorder. The following simplified code demonstrates how the task performs the logging of data to disk.

```
program DataloggingTask ;
begin
 while true do
 begin
  WaitToBeSwitchedOn ;
  AcquireResource ;     { to indicate that logger is on }
  OpenDiskFile ;
```

```
     Loggeron := true ;
     while Loggeron do
     begin
      WaitForTimingMessage ;
      ClearMessageFromQueue ;
      Seconds := Seconds + 1 ;
      if Seconds = Period then
      begin
       Seconds := 0 ;
       WriteDataToDisk ;
       Samples := Samples + 1 ;
       if Samples = Requiredno then
        begin
         Samples := 0 ;
         CloseDiskFile ;
         Loggeron := false ;
         ReleaseResource  ; { to indicate that logger is off }
        end ;
      end ;
      GiveUpRestOfTimeSlice ;
     end ;
    end ;
   end .
```

### 12.6.8  Plant interface task

The detail of the plant interface task is dependent on the particular hardware used to provide the physical connections to the sensors and actuators on the plant . Writing this task is usually a matter of following the suppliers instructions on how to write to and read from the output and input ports respectively. This task need not be synchronised with the timing signals but can be left to run as fast as possible, which will then provide the operator display with the most rapid update of plant data possible.

Laboratory instrumentation often provides an interface through a serial port (RS-232). This adds special complications since the TURBO PASCAL language does not support serial ports directly. Experiences with trying to use text file device drivers with BIOS calls and with various public domain routines to access the serial ports proved unsuccessful. A commercial package which provided PASCAL routines for interrupt handling of the serial ports (BLAISE ASYNCH PLUS)™ solved this problem.

## 12.7    Use and Performance of the Control System

A number of variations of this control system were applied in separate aspects of this research, viz.

Laboratory and pilot scale batch pans (Chapter 6 ).

Full scale continuous pan (Chapter 7).

Sucrose solubility measurements (Chapter 5).

Dynamic behaviour of full scale continuous pan compartments (Chapter 9).

The program was also applied to a number of other unrelated projects, controlling pilot plants for climbing film evaporation, hydrocarbon distillation and boiler plant simulation.

The program was difficult to debug during development as errors would often only show up when all the tasks were running together, but once debugged, it was relatively easy to modify the system for the different applications.  The program has numerous protections to prevent the system from crashing as a result of unusual operator commands or plant interface performance and proved to be a reliable tool.

The processes monitored and controlled have moderately long time constants (usually 10 seconds or greater) and the one second update time has been sufficient.  The low overheads of a relatively simple operating system and the ability to tailor tasks to minimise time wastage, meant that even the earliest models of PC (PC XT) were adequate for the control tasks undertaken.

The structure and techniques which were developed in this research to produce a working control system are not specific to the language and type of multi-tasking operating system used, but could be applied using alternative languages and operating systems which provide the same basic features. This may not be cost effective in the face of more recent commercial offerings of PC based control systems (particularly the concept of "soft PLCs" - a Programmable Logic Controller based on standard PC hardware running suitable software) and recent advances in standards for programming control systems (in particular IEC 1131 part 3).  An area where these techniques could, however, be beneficial is that of embedded systems. These embedded systems combine cheap microprocessors which operate with software that is transparent to the user, to provide systems tailored to specific applications. Embedded systems can  provide users with cost effective control solutions with advanced features but which do not require any ability to maintain or modify program code.

# CHAPTER 13

## 13. Conclusions

### 13.1 General

The objective of this thesis was to determine how to operate a continuous pan so as to obtain optimal performance. The primary focus has been on the specific case of a high grade (A-massecuite ) continuous pan in the South African sugar industry, but the approach has been kept as general as possible to allow the work to be extended to other instances. The broad approach to answering this question has been as follows

1    to review published data on the fundamentals of crystal growth and sucrose solubility, particularly those relating to the high grade boilings in a South African raw sugar factory.

2    to undertake laboratory and pilot scale experiments to confirm available data and determine unavailable data on these fundamentals of sucrose solubility and growth

3    to develop a mathematical model of a continuous pan which can be used for evaluation, simulation and optimisation

4    to set the appropriate parameters of the continuous pan model by fitting the model to data from detailed experiments on a full scale installation, thereby checking the validity of the model and ensuring that it provides realistic quantitative predictions of industrial performance

5    to use the model as the basis of an optimisation to determine the steady state operating conditions which maximise the pan performance.

6    to investigate the factors necessary to maintain a continuous pan at steady state in a dynamic operating environment. This involves how to best stabilise the pan throughput by the effective use of buffer tanks and studies of the control dynamics of maintaining stable absolute pressure in the pan and stable crystallising conditions in each compartment by the regulation of feed to the compartment.

### 13.2 Sucrose Solubility and Growth Kinetics

The review of sucrose solubility in impure solutions revealed a lack of data pertaining to the local South African conditions of interest. In consequence, an experimental procedure was developed to measure sucrose solubility on these local syrups/molasses at the temperature and range of

purities of interest for pan boiling. The data from these tests showed discrepancies from Australian data which had previously been used in the absence of local solubility data.

An evaluation of the discrepancies led to an investigation into the differences between the approximate analyses used for soluble solids and sucrose (viz brix and pol) which are often used interchangeably (on high purity streams) with the more accurate analytical methods (viz vacuum oven drying and high pressure gas-liquid chromatography). Correlations which can estimate the accurate measurements from the approximate measurements, were investigated and appropriate correlations confirmed as being applicable to the area of this study. These corrections to approximate measurements have been shown to have a significant influence on the solubility calculations.

The published growth rate data and correlations showed significant variations between the predictions and measurements of different researchers (as great as a factor of 10). Accurate data is particularly difficult to gather on industrially applicable growth rates and as a result researchers often use the published correlations of others. This has led to the propagation of errors and misprints in earlier work and the uncritical acceptance of inappropriate correlations. An attempt has been made in this work to cross-check earlier work and evaluate it against experiments in the present work.

## 13.3 Mathematical Modelling of Continuous Pan Performance

A modular dynamic mathematical model of a continuous pan has been developed. It is based on growth and solubility correlations which have been checked against experimental data which are directly applicable to local conditions.

This model has been used to simulate the dynamic behaviour of a single compartment (by numerical solution of the differential equations). The simulation results have been used to demonstrate that the behaviour can be described by three processes viz.

- concentration and dilution
- "wash-out"
- crystallisation.

Using the dynamic model as the basis, a steady state simplification has been developed which can be used for evaluation, simulation and optimisation. Three separate computer programs which solve the model numerically have been written and used for these purposes.

## 13.4 Optimum Steady State Operating Conditions

The dynamic programming optimisation technique has been applied to a continuous pan. Based on the validated mathematical model, it is able to determine the optimum steady state operating conditions for a continuous pan, given an appropriate specification of the pan and the material to be processed. This is a tool which can be applied to improving the performance of existing installations and optimising the design of new installations.

Applying the technique to a typical installation at the Felixton factory, the optimisation indicates that the traditional operating practice of maintaining relatively high crystal contents in all compartments is not conducive to maximising growth. The optimum profile requires lower crystal contents in the earlier compartments, rising to a maximum crystal content in the final compartment.

To clarify the reasons why the optimum profile requires these lower crystal contents, a simplified analysis of the conditions which are necessary to maximise crystallisation in a single compartment has been used. This analysis demonstrates the importance of relationship between crystal growth rate and the levels of impurity present in the mother liquor (specifically the parameter $K_3$ in the growth equation) in determining the crystal content which achieves maximum crystallisation. Expressed simply, the more rapid the drop in growth rate with increasing levels of impurity, the lower the optimum crystal content.

These techniques for determining optimum performance have provided a novel insight which has the potential for substantially increasing the performance and/or capacity of existing continuous pans. They also indicates that the design of new installations could be optimised, with the potential to reduce capital costs and increase sales of the pan.

## 13.5 Stabilisation of Throughput

Given the long crystal retention times in continuous pans, of between 5 and 12 hours, it is important to maintain a steady crystallisation load. Without a stable operating condition, the steady state assumed for the optimisation does not exist.

The effective use of buffer tanks is an appropriate method of smoothing fluctuations to provide a stable feed to a continuous process. In this work, alternative strategies for the effective use of buffer tanks have been investigated and a novel strategy based on Linear Quadratic Gaussian (LQG) control theory has been developed. This strategy has been shown in simulations to give sensible flow filtering when presented with the type of fluctuations encountered in industrial practice.

A major advantage of the LQG control strategy is that it can be extended to apply to a series of tanks in series, maintaining its optimal formulation and avoiding the amplification of disturbances that occurs with other published techniques. An optimum controller of this type has been demonstrated for two tanks in series in a computer simulation. The method does not account for constraints, but suggestions in this regard are given.

## 13.6 Achievement of Stable Control

The importance of stable absolute pressure control has been demonstrated. The dynamics of feed control have been investigated both by step tests and by the use of random signals. There is close agreement on the dynamics measured by both methods. Good control can be achieved by using control parameters derived from either of these test methods. A proposal is made for an automatic tuning procedure for the pan feed control loops.

# REFERENCES

## R. References

Acharya, G.N., Kapur P. and Patil V.L.(1984) Interrelationships among process variables in low-grade strikes, Int. Sug. Jnl., Vol. 86, No. 1025, 131 - 135.

Albon, N. and Dunning W.J. (1959) Factors influencing the growth of sucrose crystals, Proc. Int. Soc. Sugar Cane Technol., 10th Congress, 310 - 315.

Allan, C.J. (1962) Some suggested revisions of pan circulation theory, Proc. Qld. Soc. Sugar Cane Technol., 29th Congress, 89 - 94.

Allen, A.J., Wood, R.M. and McDonald M.P. (1974) Molecular association in the sucrose-water system, Sugar Technology Reviews, Volume 2, 165 - 180, Elsevier, Amsterdam.

Anon (1985) Laboratory manual for south african sugar factories, 3rd Edition, South African Sugar Technologists Association, Mount Edgecombe.

Anon (1986) Sugar Milling Research Institute annual report 1995-1996, Sugar Milling Research Institute, Durban.

Anon (1991) The standard laboratory manual for Australian sugar mills, Bureau of Sugar Experiment Stations, Brisbane.

Anon. (1994) The determination of the particle size distribution of white sugar by sieving - Accepted, Method GS2-37, ICUMSA.

Archibald, R.D. and Smith I.A.(1975) The effect of low juice purities at Darnall on boiling house capacity, Proc. S. Afr. Sug. Technol. Assoc.: 49, 63 - 73.

Astrom K.J. and Wittenmark, B. (1989) Adaptive Control, Addison-Wesley, Reading, Mass..

Astrom K.J. and Wittenmark, B. (1990) Computer-Controlled Systems, Second Ed., Prentice-Hall, Englewood Cliffs, N.J..

# REFERENCES

Austmeyer, K.E., Schliephake D., Hempelmann R. and Frankenfeld T. (1990) Process control of continuous evaporation crystallisation based on experiences with an ECT, Zukerind. Vol 115, No. 1, pp 15 - 18.

Bachan, L. and Sanders R.R. (1987) Evaluation of a refinery pan stirrer, Proc. S Afr Sug Technol Ass 61 : 65 - 69.

Batterham, R.J., Frew, J.A. and Wright P.G. (1973) The use of boiling point rise for the control of pans, Proc. Qld. Soc. Sugar Cane Technol.: 40, 187 - 192.

Batterham R.J. and Norgate T.E. (1975) Boiling point elevation and superheat in impure cane sugar solutions, Int. Sug. Jnl., Vol. 77, No. 924, 359 - 364.

Beckman, J. R. (1982) Data adjustment for non-reactive batch or steady-state processes, Chem. Eng. Commun., 15 :357 - 365.

Bellman, R. (1957). Dynamic Programming, Princeton University Press, Princeton, NJ.

Boas, M.L. (1966) Mathematical Methods in the Physical Sciences, John Wiley, New York, 142 -143.

Bohn, K., Schick, R., Schult, W. and Barthel, D.(1991) Determination of the oversaturation during the afterproduct cooling crystallisation, Zukerind. Vol 116, No. 11, 967 - 971.

Bonnenfant, Ph. (1985) Application of numerical analyses for pan automation, Paper B4, 27th Tech. Conf., British Sugar plc.

Bosse, D. (1996) A review of results obtained in more than 10 years of operation with the vertical continuous vacuum pan - VKT, Proc. Sug. Ind. Technol.: 55, Durban 1996, 71 - 94.

Bosworth, R.C.L. (1959) Evaporation and circulation in the crystallisation process, in Honig (Ed.) Principles of Sugar Technology, Vol II, pp 149 - 184, Elsevier, Amsterdam.

# REFERENCES

Broadfoot, R. (1980) Modelling and optimum design of continuous pans, PhD Thesis, University of Queensland, Brisbane, Australia.

Broadfoot, R. (1984) Viscosity limitations on massecuite exhaustion, Proc. Aust. Soc. Sugar Cane Technol., 279.

Broadfoot, R. (1999) Energy efficient design and operation of continuous pans, Proc. Aust. Soc. Sugar Cane Technol.: 21, 373 - 380.

Broadfoot, R., Miller, K.F. and Bartholomew, H.C. (1996) Improving the quality of C-sugar magma, Proc. Int. Soc. Sugar Cane Technol., 22nd Congress, 132 - 136.

Broadfoot, R. and Steindl, R.J. (1980) Solubility - crystallisation characteristics of queensland molasses, Proc. Int. Soc. Sugar Cane Technol., 17th Congress, 2557 - 2581.

Broadfoot, R., and Wright, P.G. (1972) Nucleation studies, Proc. Qld. Soc. Sugar Cane Technol.: 39, 353 - 363.

Brown, D.J., Alexander, K. and Boysan, F. (1991) Crystal growth measurement and modelling of fluid flow in a crystalliser, Proc. 19th Gen. Assembly of CITS, Cambridge, 1991.

Browne, C. A. and Zerban, F. W. (1948). Physical and Chemical Methods of Sugar Analysis, Third Ed., John Wiley & Sons Inc., New York.

Broyden, C.G. (1965) A class of methods for solving nonlinear simultaneous equations, Math. Comp., Vol. 19, 577 - 593.

Bruijn, J. (1964) Laboratory vacuum pans, Proc. S. Afr. Sug. Technol. Assoc.: 38, 102.

Bruijn, J. (1977) Exhaustion of molasses - equipment to determine target purities, Proc. S. Afr. Sug. Technol. Assoc.: 51, 123 - 124.

Bruijn, J., Fitzgerald, J.R., Koenig, S. and McGillivray, A.W. (1972) Exhaustion of South

# REFERENCES

African final molasses, Proc. S. Afr. Sug. Technol. Assoc.: 46, 103.

Bruijn, J., Koenig, S. and Wolf, M.(1980) Influence of gum on molasses exhaustion, Proc. Int. Soc. Sugar Cane Technol., 17th Congress, 2429 - 2441.

Brunner, H.R., Geckert, K., Frankenfeld, Th., Tschersich, J. and Nitsche W. (1992) II. Process engineering of the new continuous crystallisation system, Zukerind., Vol. 117, No. 6, 446 - 454.

Bubnik, Z. and Kadlec, P.(1992a) Sucrose crystal shape factors, Zukerind., Vol. 117, No. 5, 345 - 350.

Bubnik, Z. and Kadlec P. (1992b) Solubility of sucrose in impure sugar solutions, Zukerind. Vol 117, No. 8, 619 - 625.

Bubnik, Z., Vaccari, G., Mantovani, G., Sgualdino, G. and Kadlec, P.(1992) Effect of dextran, glucose and fructose on sucrose crystal elongation and morphology, Zukerind., Vol. 117, No. 7, 557 - 561.

Burden, R.L., Faires J.D. and Reynolds A.C. (1981) Numerical analysis, second edition, Prindle, Weber & Schmidt, Boston.

Burton, W.K., Cabrera, N. and Frank, F.C. (1951) Phil. Trans. Royal Soc. London, A243, 299.

Caceci, M.S. and Cacheris W.P. (1984) Fitting curves to data - the Simplex algorithm is the answer, Byte, May 1984, 340 - 362.

Campo, P.J. and Morari, M. (1989) Model predictive optimal averaging level control, AIChE Journal, Vol. 35, No. 4, pp 579 - 591.

Carnahan, B., Luther, H.A. and Wilkes, J.O. (1969) Applied numerical methods, John Wiley, New York.

Charles, D.F. (1960) Solubility of pure sucrose in water, Int. Sugar Journal, 62:126.

# REFERENCES

Chen, J.C.P. and Chou, C. (1993) Cane Sugar Handbook, 12th Ed., John Wiley, New York.

Cheung, T.F. and Luyben, W.L. (1979) Liquid-level control in single tanks and cascades of tanks with proportional-only and proportional-integral feedback controllers, Ind. Eng. Chem. Fund., Vol 18, No. 1, 15 - 21.

Cheung, T.F. and Luyben, W.L. (1980) Nonlinear and non-conventional liquid level controllers, Ind. Eng. Chem. Fund., Vol 19, No. 1, 93 - 98.

Chew, E.P. and Goh, G.J. (1989) On minimum time optimal control of batch crystallisation of sugar, Chem. Eng. Comm., Vol 80, 225 - 231.

Clark, S.J. (1999) Data interpretation 3, more color, Sugar Journal, December 1999, p12.

Cohen, G.H. and Coon, G.A. (1953) Theoretical considerations of retarded control, Trans. ASME, 75: 827 - 834.

Coulson, J.M. and Richardson, J.F. (1968) Chemical Engineering Volume Two Unit Operations, Second Edition, Pergamon, Oxford.

Cox, M.G.S. and Purdham, P.R. (1989) Design and evaluation of a refined pan stirrer at Hulett refinery, Proc. S. Afr. Sug. Technol. Assoc.: 63, 56 - 63.

Crowe, C.M., Garcia Campos, Y.A. and Hrymak, A. (1983) Reconciliation of process flow rates by matrix projection, Part I: linear case, A.I.Ch.E. Journal 29 (6): 881 - 888.

Crowe, C.M. (1986) Reconciliation of process flow rates by matrix projection, Part II: The nonlinear case, A.I.Ch.E. Journal, 32 (4): 616 - 623.

Crowe, C.M. (1988) Progress in the reconciliation of process flow measurements, Proc. S.A.Inst.Chem.Engrs., 5th National Meeting, August 1988.

Culp, E.J. (1981) The magic of small numbers - molecules of water per molecule of sucrose, The

# REFERENCES

Sugar Journal, September 1981, 7 - 10.

Cuttler, C.R. and Ramaker, B.L. (1979) Dynamic matrix control - a computer control algorithm, Paper No. 51b, A.I.Ch.E., 86th National Meeting (1st April, 1979).

Davies, L.W., Knight, J.F. and O'Loughlin, D.J. (1989) Control systems of the SRI continuous high grade pan at Maryborough, Proc. Aust. Soc. Sugar Cane Technol., pp 162 - 167.

de Azevedo, S.F., Chorao, J., Goncalves, M.J. and Bento, L.S.M. (1993) On-Line monitoring of white sugar crystallisation through software sensors, Proc. SIT 53rd Annual Meet., Honolulu Hawaii, 1994, Paper 646, 217 - 250.

de Azevedo, S.F., Chorao, J., Goncalves, M.J. and Bento L.S.M.(1993) Monitoring crystallisation : Part I, Int. Sug. Journal, Vol. 95, No. 1140, 483 - 488.

de Azevedo, S.F., Chorao, J., Goncalves, M.J. and Bento, L.S.M. (1994) Monitoring crystallisation : Part II, Int. Sug. Journal, Vol. 96, No. 1141, 18 - 26.

de Robillard J.P.M. and van Hengel, A. (1984) Preliminary results of a modified boiling system at Illovo factory, Proc. S. Afr. Sug. Technol. Assoc.: 58, 47 - 50.

Debbas, S. and Rumpf, H.(1966) Chem. Eng. Sci., 21, 583 - 607.

Depeyre, D., Isambert, A., Ducloux, P., Chribi, H., Dauvois, P., Kuipers, S. and Roy, D.(1989) Using a dynamic simulation model of discontinuous crystallisation in sugar industry as process control tool, Dechema-Monographs, Vol. 116, 293 - 300.

Dijkstra, J.J.F.M., de Nie, L.H. and Pot, A. (1996) In-line measurement of crystal size, campaign experience with the Lasentec M200 system, Int. Sug. Jnl., Vol 98, No. 1174, 521 - 523.

Ditl, P., Beranek, L. and Rieger, F.(1990) Simulation of a stirred sugar boiling pan. Zukerind. Vol 115, No. 8, 667 - 676.

# REFERENCES

Donovan, M.(1988) Sensors for computer control of white sugar vacuum pans . Proc. SIT 47th Annual Meet., Savannah 1988, 78 - 89.

Edwards, J.B. (1982) Process control by computer, in Computer control of industrial processes. Linkens, D. A. Editor, IEE Control Engineering, Series 21. The Institution of Electrical Engineers, London.

Ehrenberg, J. and Kessler, K. (1997) Application of a high frequency measurement technique to the determination of dry substance content in solutions and suspensions as well as for the control of evaporating crystallisers. Zukerind. Vol 122, No. 2, 100 - 108.

Evans, L.B., Trearchis, G.P. and Jones, C.(1970) Simulation study of a vacuum pan sugar crystalliser, Part I, Sugar y Azucar, Vol. 65, No. 10, 19 - 37.

Evans, L.B., Trearchis G.P. and Jones C.(1970) Simulation study of a vacuum pan sugar crystalliser, Part II, Sugar y Azucar, Vol. 65, No. 12, 19 - 25.

Fitzgerrald, J.R., Koenig, S. and MacGillivary, A.W. (1972) Exhaustion of South African final molasses, Proc. S. Afr. Sug. Technol. Assoc.: 69, 146 - 151.

Foster, D.H., Sockhill B.D. and Wright P.G.(1960) Variations of supersaturation coefficient in high grade boilings, Proc. Qld. Soc. Sugar Cane Technol.: 27, 111 - 120.

Foust, A.S., Wenzel, L.A., Clump, C.W., Maus, L. and Andersen, L.B. (1960) Principles of Unit Operations, John Wiley, London.

Frew, J.A. (1973) Optimal control of batch raw sugar crystallisation, Ind. Eng. Chem. Process Des. Develop., Vol. 12, No. 4, 460 - 467.

Gallier, P.W., Sliepcevich, C.M. and Puckett, T.H. (1961) Some practical limitations of correlation techniques in determining process frequency response, Chem. Eng. Prog. Symp. Ser. No. 36, 57, 59.

# REFERENCES

Garcia, C.E. and Morari, M. (1982) Internal model control 1. A unifying review and some new results, Ind. Eng. Chem. Process Des. Dev., 21, 308.

Garside, J., Mersmann, A. and Nyvlt, J. (1990) Measurement of crystal growth rates, European Federation of Chemical Engineering Working Party on Crystallisation.

Gebler, J. and Bubnik Z. (1997) Czech continuous evaporating crystalliser, Zukerind. Vol 122, No. 2, 112 - 116.

Goddard, J.M. (1991) Development in Continuous pan boiling, Int. Sug. Jnl., Vol. 93, No. 1107, 48 - 51.

Golovin, P.V. and Gerasimenko A.A. (1959) Crystallisation of sucrose at higher temperatures, Proc. Int. Soc. Sugar Cane Technol., 10th Congress, 248 - 262.

Grabka, J. and Wawro, P. (1998) Study on the growth rate of sucrose crystals in heated pure solutions, Zukerind., Vol. 123, No. 8, 610 - 613.

Graham, W.S. and Radford, D.J. (1977) A preliminary report on a continuous C pan, Proc. S. Afr. Sug. Technol. Assoc.: 51, 107 - 111.

Grimsey, I.M. and Brown D.J. (1994) Superheating effects during sucrose crystal growth in an evaporating crystalliser, Zukerind., Vol 119, No. 9, 769- 775.

Grut, E.W. (1936/37) Z. Zukerind., Czech. Rep., 61, 373.

Guimaraes, L., Sa, S., Bento, L.S.M. and Rocha, F. (1995) Investigation of crystal growth in a laboratory fluidized bed, Int. Sugar Jnl., Vol. 97, No. 1157, 199 - 204.

Hale,D.J. and Whayman, E. (1972) Forecasting pan stage tank levels, Proc. Aust. Soc. Sugar Cane Technol., 203 - 209.

Harman, R.W. (1933) Saturation temperature of sucrose solutions, The Int. Sug. Journal, July

# REFERENCES

1933, 261 - 263.

Harris, F.J. (1978) On the use of windows for harmonic analysis with the discrete Fourier transform, Proc. IEEE, Vol.66, No. 1, 51 - 83.

Hashimoto, H., Kawamura, T., Chigusa, T. and Satori, T. (1985) Automatic pan boiling control using rheometer and microprocessor, Proc. SIT Vol. XLIV, paper 528.

Heffels, S.K. (1986) Product size distributions in continuous and batch sucrose crystallisers, Delft University of Technology, Delft.

Herdan G. (1960) Small particle statistics, Second revised edition, Butterworths, London.

Herrera F, F. (1990) Application of modern theory to boiling control, C.Centro Azuc., Vol. 17, No. 2, 59 - 66.

Herzfeld, Z. (1892) Ver. Rubenzuckerind., 42, 182.

Hoekstra, R. G. (1978). Optimisation of the crushing programme for the season by dynamic programming, Proc. S. Afr. Sug. Technol. Ass.: 52, 26 -32.

Hoekstra, R.G. (1985) Program for simulating and evaluating a continuous A-sugar pan, Proc. S. Afr. Sug. Technol. Assoc.: 59, 48 - 57.

Hoekstra, R. G. (1986) Simulation of effect of different values of operating variables in a continuous pan, Proc. S. Afr. Sug. Technol. Assoc.: 60, 84 - 93.

Hoekstra, R.G. (1989) Solubility coefficients of impure sucrose solutions, Tongaat- Hulett Sugar Internal Report, 2nd June 1989, Ref. T/MP/08,T/MP/12.

Hoekstra, R.G. (1999) Comparison of stirred pans supplied by Tongaat-Hulett Sugar, Personal Communication.

# REFERENCES

Hogg, J.S., McCarey, S.C.H., Wilkie, J.D.F., Brown, D. and Weatherby, E.J. (1986) Crystal sizing, Int. Sug. Jnl., Vol. 88, No. 1054, 193 - 197.

Hogg, J.S., McCarey, S.C.H., Wilkie, J.D.F., Brown, D. and Weatherby, E.J. (1986) Crystal sizing, Int. Sug. Jnl., Vol. 88, No. 1055, pp 207 - 210.PM18

Hubbard, G. and Love, D. (1998) Reconciliation of process flow rates for a steady state mass balance on a centrifugal, Proc. S. Afr. Sug. Technol. Assoc.: 72, 290 - 299.

Hugot, E. and Jenkins G.H. (1959) Circulation in vacuum pans, Proc. Int. Soc. Sugar Cane Technol., 10th Congress, 232 - 241.

Hugot, E. (1960) Handbook of Cane Sugar Engineering, first edition, Elsevier, Amsterdam.

Hugot, E. (1986) Handbook of Cane Sugar Engineering, third edition, Elsevier, Amsterdam.

Jensen, E.D. (1967) True seeding - let's be critical!, Proc. Qld. Soc. Sugar Cane Technol.: 34, 61 - 67.

Jesic, V.M. (1977) Variables affecting saturation coefficient in cane final molasses, Int. Sugar Journal, 274 - 277.

Journet, G.(1999) One design, three pans, a large flexibility of use, Proc. Int. Soc. Sugar Cane Technol., 23rd Congress, 104 - 114.

Jullienne, L.M.S.A. and Munsamy, S. (1981) Assessment of the Gledhow and Tongaat Fives-Cail Babcock continuous pans, Proc. S. Afr. Sug. Technol. Assoc.: 55, 79 - 84.

Kapur, P., Patil V.L. and Acharya G.N. (1986) A microprocessor based system for regulation of low-grade sugar strikes, Int. Sug. Jnl., Vol. 88, No. 1049, 94 - 98.

Kapur, P., Patil, V.L., Gautam, G.K., Vasudeva, T.R., Agarwal, A.K., Sai Kumar, K.S. and Bajaj, V.D. (1991) On-line estimation of crystallisation parameters and automatic pan feed

# REFERENCES

control, Int. Sug. Jnl., Vol 93, No. 1112, 161 - 165.

Kelly, F.H.C.(1959) The solubility of sucrose in impure solutions, in P.Honig (Ed.) Principles of Sugar Technology, Volume II, 67 - 112, Elsevier, Amsterdam.

Kelly, F.H.C. (1982) The morphology of sugar crystals, Sugar Technology Reviews, Vol. 9, Elsevier, Amsterdam, 271 - 323.

Kneile, R. (1995) Wring more information out of plant data, Chem. Eng., Vol.102, 3, 110 - 116.

Kompass, E. J. (1985) Industrialising the personal computer, Control Engineering, August 1985, 70.

Kompass, E. J. (1988a) The importance of control operating system specs, Control Engineering, March 1988, 39.

Kompass, E. J. (1988b) The role of personal computers in control, Control Engineering, May 1988, 14.

Kruger, G.P.N. (1983) Continuous 'A' pan boiling trial at Maidstone sugar factory, Proc. S. Afr. Sug. Technol. Assoc.: 57, 46 - 51.

Langreney, F. (1977) True continuous crystallisation, Proc. Int. Soc. Sugar Cane Technol., 16th Congress, 2427 - 2443.

Larson, R.E. (1965). Dynamic programming with reduced computational requirements, IEEE Transactions on Automatic Control, Vol.AC -10, 135-143.

Larson, R.E.(1967). Survey of dynamic programming computational procedures, IEEE Transactions on Automatic Control, Dec. 1967, 767 - 774.

Larson, R.E. and Casti, J.L. (1982). Principles of dynamic programming, Part II: Advanced theory and applications, Marcel Dekker Inc., New York.

# REFERENCES

Lee, P.L. and Sullivan, G.R. (1988) Genreric Model Control (GMC), Comput. Chem Engng., Vol. 12, No. 6, 573 - 580.

Levenspiel, O. (1972) Chemical reaction engineering, Second Edition, John Wiley, New York.

Levine, W.S. (1996) System identification when noise is negligible, in The Control Handbook, W.S. Levine Editor, 108 - 112, CRC Press, Boca Raton, Florida.

Li-Wu, Q. and Corripio, A.B. (1985a) Experimental verification of a dynamic model of a vacuum pan, J Amer. Soc. Sugar Cane Technol., Vol. 5, 77 - 84.

Li-Wu, Q. and Corripio A.B. (1985b) Dynamic Matrix Control of cane sugar crystallisation in a vacuum pan, ISA Paper 85-0734.

Lines, R. (1990) Sizing up the options for particle characterisation, Process Engineering, November 1990, 56 - 61.

Lionnet, G.R.E. (1987) Impurity transfer during A-massecuite boiling, Proc. S. Afr. Sug. Technol. Assoc.: 61, 70 - 75.

Lionnet G.R.E. (1998a) Impurity transfer rates during the crystallisation of sucrose, Proc. S. Afr. Sug. Technol. Assoc.: 72, 261 - 267.

Lionnet, G.R.E. (1998b) The incorporation of impurities into sucrose crystals during the crystallisation process, PhD Thesis, Natal University.

Lionnet, G.R.E. (1999) A continuous vacuum pan for refinery massecuites, Technical Report No. 1823, Sugar Milling Research Institute, Durban.

Lionnet, R.E. and Rein, P.W. (1980) Pilot plant studies on the exhaustion of low grade massecuites, Proc. Int. Soc. Sugar Cane Technol., 17th Congress, 2329 - 2350.

Ljung, L. (1996) System Identification, in The Control Handbook, W.S. Levine Editor, 1033 -

# REFERENCES

1054, CRC Press, Boca Raton, Florida.

Love, D.J. (1980) Tracer testing in clarifiers, Proc. S. Afr. Sug. Technol. Assoc.: 54, 93 - 98.

Love, D.J. and Rein, P.W. (1980) Percolation Behaviour in a cane diffuser, Proc. Int. Soc. Sugar Cane Technol., 17th Congress, 1900 - 1920.

Love, D.J. and Chilvers, R.A.H. (1986) Tuning of pan feed controls, Proc. S. Afr. Sug. Technol. Assoc.: 60, 103 - 111.

Love, D.J. (1991a) The use of dynamic programming for determining optimum profiles of operating conditions in continuous pans, Proc. 19th Gen. Assembly of CITS, Cambridge, 1991.

Love, D.J. (1991b) Multitasking on a personal computer for data logging and process control, Proc. 6th National Meeting, S. Afr. Inst. Chem. Eng., Durban, Aug. 1991.

MacLeod, I.M. (1998) Design and evaluation of advanced automation and control strategies, Elektron, February, 1998, 8 - 9.

Matthesius, G.A., Graham, W.S. and Pillay, J.V. (1978) An application of the fractional factorial experiment to continuous pan boiling, Proc. S. Afr. Sug. Technol. Assoc.: 52, 89 - 92.

Matthesius, G.A. and Mellet, P. (1976) An exhaustion formula for South African molasses, Proc. S. Afr. Sug. Technol. Assoc.: 50, 206 - 211.

Maudarbocus, S.M.R. and White E.T. (1978) Computer modelling of a cooling crystalliser, Proc. Queensland. Soc. Sugar Cane Technol.: 45, 45 - 52.

Maudarbocus, S.M.R. and White, E.T. (1983) Cooling policies for batch crystallisers, Proc. Int. Soc. Sugar Cane Technol., 18th Congress, 1282 - 1293.

Maurandi, V (1989) Mass transfer in pure sucrose solutions, Zukerind. 114 (1989) Nr. 12, 976 - 979.

# REFERENCES

Maurandi, V., Mantovani, G., Vaccari, G. and Rossi, A. (1988) Kinetics and technology of low boiling massecuite exhaustion, Zukerind., Vol. 113, No. 9, 791 - 794.

Maurandi, V., Mantovani, G. and Vaccari, G.(1988) Kinetic studies on low grade boiling, Sugar Technology Reviews, Volume 14, 29 - 118, Elsevier, Amsterdam.

McDonald, K.A., McAvoy, T.J. and Tits, A. (1986) Optimal averaging level control, A.I.Ch.E. Journal, Vol. 32, No.1, 75 - 86.

McDougall, E.E. and Wallace, G.A. (1982) The racecourse continuous vacuum pan, Proc. Aust. Soc. Sugar Cane Technol., 383 - 388.

McGinnis, R.A. (1971) Beet-Sugar Technology, 2nd Edition, Beet Sugar Dev. Foundation, Fort Collins.

McGinnis, R.A. (1978) Exhaustion of Beet Molasses, Sugar Technology Reviews, Volume 5, 155 - 286, Elsevier, Amsterdam.

McWhinney, W. (1973a) Frequencies and time delays observed in a crushing train - Part I, Int. Sug. J., Vol. 75, No. 899, 331 - 334.

McWhinney, W. (1973b) Frequencies and time delays observed in a crushing train - Part II, Int. Sug. J., Vol. 75, No. 900, 363 - 368.

Meadows, D.M. (1996) Raw juice flow control, screening, heating and liming, Proc. S. Afr. Sug. Technol. Assoc.: 70, 272 - 276.

Medawar, P.B. (1984) The limits of science, Oxford University Press, Oxford.

Merensky, H. (1985) Strike sequence control, Proc. S. Afr. Sug. Technol. Assoc.: 59, 102 - 107.

Mersmann, A. (1995) Crystallisation Technology Handbook, Marcel Dekker, New York.

# REFERENCES

Miller, K.F. (1988) Forecasting pan stage tank levels, Proc. Aust. Soc. Sugar Cane Technol., 203 - 209.

Miller, K.F. (1992) Maximising the Information Available from Sugar Sieve Test Data, Proc. Aust. Soc. Sugar Cane Technol.: 14, 297 - 302.

Miller, K.F. and Beath A.C. (2000) The measurement of raw sugar crystal size by sieving and by laser diffraction, Proc. Aust. Soc. Sugar Cane Technol.: 22, 393 - 398.

Miller, K.F. and Broadfoot, R. (1997) Crystal growth rates in high grade massecuite boilings, Proc. Aust. Soc. Sugar Cane Technol., 441 - 447.

Moller, G.R. (1984) Recent developments in pan boiling automatics, Int. Sug. Jnl., Vol. 86, No. 1023, 73 - 78.

Morel du Boil, P.G. (1980) Practical tracers for the sugar industry - the analytical feasibility of using Lithium, Chloride or Potassium, Proc. S. Afr. Sug. Technol. Assoc.: 54, 99 - 104.

Morel du Boil, P.G. (1985) Sucrose crystal habit in a refinery, Proc. S. Afr. Sug. Technol. Assoc.: 59, 33 - 38.

Morel du Boil, P.G. (1991) The role of oligosaccharides in crystal elongation, Proc. S. Afr. Sug. Technol. Assoc.: 65, 171 - 178.

Morel du Boil, P.G. (1995) Cane deterioration - oligosaccharide formation and some processing implications, Proc. S. Afr. Sug. Technol. Assoc.: 69, 146 - 151.

Morel du Boil, PG (1996) Theanderose - a characteristic of cane sugar crystals, Proc. S. Afr. Sug. Technol. Assoc.: 70, 140 - 144.

Morera, R. and Mischuk, R. (1978) Exhaustion of final molasses, Int. Sugar Journal 80: 73.

Moritsugu, T. (1974) Exhaustibility of cane molasses, Sugar Technology Reviews, Volume 2, 73

# REFERENCES

- 93, Elsevier, Amsterdam.

Mullin, J.W. (1992) Crystallisation, Third Edition, Butterworth Heinemann, Oxford.

Munsamy, S. (1980) The new SMRI Nutsch bomb, Proc. S. Afr. Sug. Technol. Assoc.: 54, 79 - 81.

Murril, P.W. Pike, R.W. and Smith, C.L. (1959a) Random inputs yield system transfer functions, Chem. Eng., April 7 1959, 151 - 154.

Murril, P.W., Pike, R.W. and Smith, C.L. (1959b) Frequency response data from statistical correlations, Chem. Eng., May 19, 1959, 195 - 200.

Nees and Hungerford (1936), Ind. Eng. Chem., 28 :893.

Newell,G.M.(1979) A preliminary investigation into factors affecting gas formation in massecuite and molasses, Proc. S. Afr. Sug. Technol. Assoc.: 53, 62 - 65.

Nicol, W.M. and Parker, J.S. (1971) The rates of sucrose crystal growth and dissolution, Int. Sug. J., Vol. 73, No. 876, 355 - 356.

Nikolic, S. and Valcic, A. (1991) Kinetics and mechanism of saccharose crystal growth, J. Serb. Chem. Soc., Vol. 56, No. 5, 289 - 301.

Ogata, K. (1987) Discrete-Time Control Systems, Prentice-Hall, Englewood Cliffs, NJ.

Oldshue, J.Y. (1983) Fluid Mixing Technology, McGraw-Hill Publications, New York.

Papoulis, A. (1965) Probability, Random Variables and Stochastic Processes, McGraw Hill, New York.

Pautrat, C., Genotelle, J. and Mathlouthi, M. (1996) The effect of some polysaccharidic non-sugars on the rate of sucrose crystal growth. Proc. Sug. Proc. Research Conf., New Orleans,

# REFERENCES

1996, 82 - 102.

Peacock, S. and Starzak, M. (1995) The effect of sucrose inversion on boiling point elevation, Zukerind., Vol 120, No. 12, 1051 - 1054.

Penklis, P. and Wright, P.G. (1963) Nucleation in sugar boiling, Proc. Qld. Soc. Sugar Cane Technol. : 30, 177 - 182.

Perry, R.H. and Green, D.W. (1997) Perry's Chemical Engineers' Handbook, Seventh Edition, McGraw-Hill, New York, 30-1 - 30-36.

Powers, H.E.C. (1948) The determination of the grist of sugars, Int. Sugar Jnl., 50, 149-150.

Press, W.H., Flannery, B.P., Teukolsky, S.A. and Vetterling, W.T. (1989) Numerical recipies in Pascal - The art of scientific computing, Cambridge University Press, Cambridge.

Pyle, I. C. (1982) Languages for computer control, in Computer control of industrial processes. Linkens D A Editor, IEE Control Engineering, Series 21. The Institution of Electrical Engineers, London.

Quin, G.F. and Wright, P.G. (1992) Infrared photometric measurement of the saturation temperature and supersaturation of syrups, Proc. Int. Soc. Sugar Cane Technol., 21$^{st}$ Congress, 671 - 685.

Radford, D.J. and Cox, M.G.S. (1986) The use of electrical properties measured at radio frequencies for pan boiling and brix control, Proc. S. Afr. Sug. Technol. Assoc.: 60, 94 - 102.

Radford, D.J., Tayfield, D.J. and Cox, M.G.S. (1988) Further developments in automated white pan boiling using radio frequency control, Proc. SIT 47$^{th}$ Annual Meet., Savannah 1988, 90 - 107.

Randolph, A.D. and Larson, M.A. (1962) Transient and steady state size distributions in continuous mixed suspension crystallisers, A.I.Ch.E. Journal, 8, 639 - 645.

# REFERENCES

Randolph, A.D. and White, E.T. (1977) Modelling size dispersion in the prediction of CSD, Chem. Eng. Sci., 32, 1067 - 1076.

Reichard, SR and TL Vidler (1975) Contactless conductivity measurement in massecuite, Proc. Qld. Soc. Sugar Cane Technol.: 42, 249 - 253.

Reid, M.J. and Rein, P.W. (1983) Steam balance for the new Felixton II Mill, Proc. S. Afr. Sug. Technol. Assoc.: 57, 85 - 91.

Rein, P.W. (1980) A study of continuous low grade crystalliser performance, Proc. Int. Soc. Sugar Cane Technol., 17th Congress, 2309 - 2327.

Rein, P.W. (1983) Continuous vacuum pans for Felixton II, The S.A. Sug. Journal, Vol. 67, 366 - 367.

Rein, P.W. (1986) A review of experience with continuous vacuum pans in Tongaat-Hulett sugar, Proc. S. Afr. Sug. Technol. Assoc.: 60, 76 - 83.

Rein, P.W. (1990) Encrustation and scaling in continuous sugar vacuum pans, Proc. S. Afr. Sug. Technol. Assoc.: 64, 204 - 208.

Rein, P.W. (1992) Recent developments in continuous pan boiling, Proc. Int. Soc. Sugar Cane Technol., 21st Congress, CV - CXVII.

Rein, P.W. and Archibald, R.D. (1989) Crystal breakage in continuous B-centrifugals, Proc. S. Afr. Sug. Technol. Assoc.: 63, 94 - 99.

Rein, P.W., Cox, M.G.S. and Love, D.J. (1985) Analysis of crystal residence time distribution and size distribution in continuous boiling vacuum pans, Proc. S. Afr. Sug. Technol. Assoc.: 59, 58 - 67.

Rein, P.W. and Msimanga, M.P. (1999a) A review of continuous pan development in the Southern African sugar industry, Proc. Int. Soc. Sugar Cane Technol., 23rd Congress, 124 - 136.

# REFERENCES

Rein, P.W. and Msimanga. M.P. (1999b) A review of continuous pan development in the Southern African sugar industry, Zuckerindustrie, Vol. 124, No. 6, 462 - 467.

Rein, P.W. and Smith I.A. (1981) Molasses exhaustability studies based on sugars analysis by gas-liquid chromatography, Proc. S. Afr. Sug. Technol. Assoc.: 55, 85 - 91.

Renton, R.H. (1985) Felixton - A new sugar mill in Zululand, Proc. S. Afr. Sug. Technol. Assoc.: 59, 1- 4.

Reuter, W., Klute, U., Burk, O., Weber, J.M. and Rosler, A. (1998) Microwave measurement in sugar manufacturing, Zukerind., Vol. 123, No. 12, 951 - 955.

Rhinehart, R.R. and Beasley, J. D. (1987) Dynamic Programming for chemical engineering applications, Chem. Eng, 94, 18.

Richalet, J., Rault, A., Testud, J.L. and Papon, J. (1979) Model predictive heuristic control: applications to industrial processes, Automatica, 14, 413.

Richards, R.J. (1979) An introduction to dynamics and control, Longman, Singapore.

Rodriguez, B.M. and Torres R, M.E. (1990) The quasi-linearisation and Gauss-Newton methods used for identification of the pan boiling process, C.Centro Azuc., Vol. 17, No. 2, 10 - 17.

Rodriguez, R., Consuegra R, R. and Riesgo E, J.(1989) Analysis of the boiling process in continuous vacuum pans based on mathematical modelling, CubaAzucar, July/Dec 1989, 78 - 82.

Rouillard, E.E.A. (1978) The crystallisation of high grade massecuite in crystallisers, Proc. S. Afr. Sug. Technol. Assoc.: 52, 73 - 79.

Rouillard, E.E.A. (1980) Mathematical modelling of A, B, and C crystallisers, Proc. Int. Soc. Sugar Cane Technol., 17th Congress, 2279 - 2295.

# REFERENCES

Rouillard, E.E.A. (1985) A study of boiling parameters under conditions of laminar non-newtonian flow with particular reference to massecuite boiling. PhD Thesis, Natal University.

Rouillard, E.E.A. (1987) Some ideas on the design of batch and continuous pans, Proc. S. Afr. Sug. Technol. Assoc.: 61, 76 - 82.

Rouillard, E.E.A. (1988) Development of the continuous vacuum pan 1932 - 1987 a literature survey, Communications from the SMRI, No. 148.

Rouillard, E.E.A. and Smith, I.A.(1981) A look a tracer testing in the sugar industry, Proc. S. Afr. Sug. Technol. Assoc.: 55, 75 - 78.

Rozsa, L. (1996) On-line monitoring of supersaturation in sugar crystallisation, Int. Sug. Jnl., Vol. 98, No. 1176, 660 - 675.

Rush, G. and Meredyth, C. (1959) Improved saturation cell and a laboratory vacuum pan for research work, Proc. Int. Soc. Sugar Cane Technol., 10th Congress, 263 - 269.

Ryans, J.L. and Croll, S. (1981) Selecting vacuum systems, Chemical Engineering, Dec 14th 1981, 73 - 90.

Sahadeo, P. (1998) The effect of some impurities on molasses exhaustion , Proc. S. Afr. Sug. Technol. Assoc.: 72, 285 - 289.

Sandoz, D. J. (1982) A survey of computer control, in computer control of industrial processes. Linkens, D. A. Editor, IEE Control Engineering, Series 21. The Institution of Electrical Engineers, London.

Saska, M. and Oubrahim, Y. (1989) Crystallisation rate of sucrose at high impurity concentrations, Int. Sugar Jnl., Vol. 91, No. 1086, 109 - 116.

Schneider, F. (Ed.) (1979) Sugar Analysis, Official and tentative methods recommended by the international commission for uniform methods of sugar analysis (ICUMSA), ICUMSA,

# REFERENCES

Peterborough.

Schukow, Z. (1900) Ver. Dtsch. Zuckerind., 50, 291.

Schorn, P.M. and Meadows, D.M. (1998) The use of a continuous pan to boil low grade refined massecuites at the Malelane refinery. Proc. SIT 57th Annual Meet., Marseille 1998, 193 - 208.

Schumann, G.T. and Thakur, C.S. (1993) The use of a video camera and PC for crystal image analysis, Proc. S. Afr. Sug. Technol. Assoc.: 67, 135 - 139.

Sheng, L.Q. (1993) Determining the circulation ratio of pans, Int. Sug. Jnl., Vol. 95, No. 1133, 183 -186.

Shinskey, F.G. (1979) Process Control Systems, McGraw-Hill, New York.

Smith, I.A. (1995) Exhaustability of molasses with very low reducing sugar levels, Proc. S. Afr. Sug. Technol. Assoc.: 69, 163 - 165.

Smythe, B.M. (1959) Measurements of crystallisation rates of sucrose from pure and impure solutions, Proc. Int. Soc. Sugar Cane Technol., 10th Congress, 323 - 336.

Smythe, B.M. (1971) Sucrose Crystal Growth, Sugar Technology Reviews, Volume 1, Elsevier, Amsterdam.

Sockhill, B.D. and Wright, P.G. (1960) Factors affecting supersaturation control in massecuites, Proc. Qld. Soc. Sugar Cane Technol.: 27, 121 - 130.

Sterling, M. J. H. (1982) Requirements for Real time computing, in Computer control of industrial processes, Linkens D. A. Editor, IEE Control Engineering Series 21, The Institution of Electrical Engineers, London.

Stewart, A.B. (1987) Problems relating to the use of personal computers in process control, Elektron, March 1987, 9.

# REFERENCES

Tayfield, D.J., Rein, P.W. and Proome, S.R. (1980) The application of a microprocessor based system for automatic pan boiling control, Proc. S. Afr. Sug. Technol. Assoc.: 54, 56 - 62.

Torres R., M.E., Herrera F, F. and Hernandez C, M.C. (1990) Results from identification of the pan boiling process in a sugar factory, C.Centro Azuc., Vol. 17, No. 2, 28 - 32.

Vaccari, G., Mantovani, G., Sgualdino, G. and Andreoli, F. (1993) Cooling crystallisation of raw juice: determination of sucrose solubility, Zukerind. Vol 118, No. 10, 778 - 782.

van Hengel A. (1983) Modified boiling system for better sugar quality, Proc. S. Afr. Sug. Technol. Assoc.: 57, 38 - 41.

van Hook, A. and van Hook, W.A. (1959) Rate of growth of sucrose crystals at very low supersaturations, Proc. Int. Soc. Sugar Cane Technol., 10th Congress, 305 - 309.

van Hook, A. (1977) How crystals grow (and dissolve), Proc. Int. Soc. Sugar Cane Technol., 16th Congress, 2613 - 2618.

van Hook, A. (1980) Size dependancy of growth of sugar crystals, Proc. Int. Soc. Sugar Cane Technol., 27th congress, Manila, 1980, 2244 - 2247.

van Hook, A. (1981) Growth of sucrose crystals, a review, Sugar Technology Reviews, Volume 8, 41 - 79, Elsevier, Amsterdam.

van Hook, W. A., Mantovani, G. and Mathlouthi, M. (1997) Sucrose Crystallisation Science and Technology, Bartens, Berlin.

Vavrinecz, G. (1962) Z. Zukerind., Vol. 12, 481.

Vavrinecz, G. (1978/79) The formation and composition of beet molasses, Sugar Technology Reviews, Volume 6, 117 - 305, Elsevier, Amsterdam.

# REFERENCES

Vigh, S.N. and Hurtado, C.E. (1999) Impact of crystal growth rate function on model predicted pan operation, Proc. Aust. Soc. Sugar Cane Technol., Poster Paper 21, 507 - 508.

Wagnerowski, K., Dobrowska, B. and Dobrowski, C. (1961) Gaz. Cukrov., 63, 262.

Wagnerowski, K., Dobrowska, B. and Dobrowski, C. (1962), Z. Zuckerind.,12, 664.

Webre, A.L. (1933) Experiments on the working of the calandria vacuum pan. Int. Sug. Jnl., 184 -186 and 227 - 229.

White, E.T., Mackintosh, D.L., Butler, B.K., Zhang, H. and Johns, M.R. (1998) Modelling growth rate dispersion (GRD) in sugar crystallisation, Proc. Aust. Soc. Sugar Cane Technol.: 20, 524 - 531.

White, E.T. and Wright, P.G. (1971) Magnitude of size dispersion effects in crystallisation, Chem. Eng. Prog. Symp., Vol. 67, No. 110, 81 - 87.

Wienese A., Schaffler, K.J. and Bachan, L. (1987) Personal computers as data loggers in the South African sugar industry, Proc. S. Afr. Sug. Technol. Assoc.: 61, 111 - 113.

Wiklund, O. (1946) Socker. Handl. ,2, 65.

Wright, P.G. (1974) Vacuum Pans - Batch and Continuous, Sugar Technol. Reviews, Vol.2, 137 - 163, Elsevier, Amsterdam.

Wright, P.G. (1978) The Determination of the saturation temperature of sugar syrup by a photometric method, Int. Sugar Journal, Feb 1978, 40 - 46.

Wright, P.G. (1980) The photometric saturation temperature method, Proc. Int. Soc. Sugar Cane Technol., 17th Congress, 2264.

Wright, P.G. (1983) Pan and Pan Stage Control, Sugar Technology Reviews, Volume 10, 39 -

# REFERENCES

96, Elsevier, Amsterdam.

Wright, P.G. (1984) Characteristics of conductivity transducers for pan control, Proc. Aus. Soc. Sugar Cane Technol.: 6, 301 - 307.

Wright, P.G. and White, E.T. (1968) A digital simulation of the vacuum pan crystallisation, Proc. Int. Soc. Sugar Cane Technol., 13th Congress, 1697 - 1710.

Wright, P.G. and White, E.T. (1969) Size distribution studies in sugar crystallisation, Proc. Qld. Soc. Sugar Cane Technol.: 36, 299 - 309.

Wright, P.G. and White, E.T. (1971) Crystal size distribution by direct weighing, Proc. Int. Soc. Sugar Cane Technol., 14th Congress, Louisianna, 1601 - 1611.

Wright, P.G. and White, E.T. (1974) A mathematical model of vacuum pan crystallisation., Proc. Int. Soc. Sugar Cane Technol., 15th Congress, 1546 - 1560.

Ziegler, JG and NB Nichols (1942) Optimum settings for automatic controller, Trans. A.S.M.E., 64: 759 - 768.

# NOMENCLATURE

## N.  Nomenclature

This list covers the nomenclature used in the body of the thesis. The nomenclature used in the appendices is defined as used in each appendix.

Roman Symbols

| | | |
|---|---|---|
| $a$ | confidence interval for experimental measurements | |
| $A$ | matrix in state space equations | |
| $A_t$ | cross-sectional area of buffer tank | $(m^2)$ |
| | | |
| $b$ | constant in solubility coefficient equation | |
| $b_0$ | constant in solubility coefficient equation | |
| $b'$ | constant in solubility coefficient equation | |
| $brix$ | solids mass as percent of total mass | $(\%)$ |
| $B$ | matrix in state space equations | |
| $B$ | step change in flow into a buffer tank | $(m^3/min)$ |
| $BPEp$ | boiling point elevation at a pressure different from 1 atmosphere | $(^\circ C)$ |
| $BPR1$ | boiling point elevation at 1 atmosphere. | $(^\circ C)$ |
| | | |
| $c$ | constant in solubility coefficient equation | |
| $cc$ | crystal content of massecuite (crystal mass percent total mass) | $(\%)$ |
| $C$ | matrix in state space equation | |
| $C_{s,p}$ | pure sucrose solution concentration at saturation (sucrose mass percent solution) | $(\%)$ |
| $Cp$ | effective capacitance of a process which behaves as a pure integrator | $(s)$ |
| $CT_n$ | total mass in continuous pan compartment $n$ | $(kg)$ |
| $CV$ | coefficient of variation of a particle size distribution | $(\%)$ |
| | | |
| $D$ | diffusivity | $(m^2/s)$ |
| $Dc$ | characteristic dimension of a sugar crystal | $(m)$ |
| $DS$ | dry solids concentration (mass dry solids percent total mass) | $(\%)$ |

| | | |
|---|---|---|
| $E$ | impulse response of $N$ tanks in series | |
| $Ea$ | activation energy | (kJ/mol) |
| $f_n$ | generalised nonlinear function | |
| $F$ | vector of generalised non-linear functions, $f_n$ | |
| $g0(x,u)$ | prevailing supersaturation in a continuous pan compartment | |
| $g1(x,u)$ | number flow rate of crystals into a continuous pan compartment | $(s^{-1})$ |
| $g2(x,u)$ | number of crystals in a continuous pan compartment | |
| $g3(x,u)$ | linear growth rate of the crystals in a continuous pan compartment | (m/s) |
| $G$ | crystal growth rate | (m/s) |
| $Gc$ | controller gain which produces sustained cycling | |
| $G_C(s)$ | transfer function of a buffer tank controller | |
| $G_L(s)$ | transfer function of a buffer tank | |
| $h$ | constant in solubility equation | |
| $h(t)$ | height of liquid in buffer tank at time t | (m) |
| $h_s$ | steady state height in buffer tank | (m) |
| $h_{lim}$ | limiting tank level used in MRCO buffer control strategy | (m) |
| $h_{max}$ | maximum height in buffer tank | (m) |
| $h_{peak}$ | peak height in buffer tank, in response to step change in input flow | (m) |
| $\Delta h$ | range of level transmitter used in buffer tank control | (m) |
| $IW$ | impurity to water ratio (kg impurity / kg water) | |
| $J$ | Jacobian matrix used in solution of set of simultaneous nonlinear equations | |
| $J$ | variational performance criterion used in dynamic programming | |
| $J$ | performance index used in Linear Quadratic Gaussian (LQG) control | |
| $k$ | index for stages in dynamic programming | |
| $k$ | number of time intervals in discrete time buffer tank control strategy | |
| $k^*$ | number of time intervals until buffer tank overflows (rounded up) | |
| $k_d$ | constant in growth rate equation | |

## NOMENCLATURE

| | | |
|---|---|---|
| $k_d$ | mass transfer coefficient | (m/s) |
| $k_I$ | constant used BCF growth expression | |
| $k_{max}$ | number of time intervals until buffer tank overflows | |
| $K$ | constant in equation to estimate sucrose from pol and brix | |
| $K$ | total number of stages in dynamic programming | |
| $K$ | gain matrix in LQG control | |
| $K_0$ | Offset defining level of supersaturation above which linear growth exists | |
| $K_1$ | Proportional dependence of growth on supersaturation | |
| $K_2$ | Factor adjusting growth rate for variation of temperature from a "normal" value | |
| $K_3$ | Factor defining exponential dependance of growth rate on impurity/water ratio | |
| $K_4$ | SW ratio of pure sucrose solution at saturation and at compartment temperature | |
| $K_5$ | Constant relating solubility coefficient to impurity/water ratio. | |
| $K_C$ | dimensionless controller gain | |
| $K_K$ | controller gain to prevent overflow of buffer tank | |
| $K_L$ | gain of proportional level controller | |
| | | |
| $l$ | length | (m) |
| $L$ | cost function for single stage in dynamic programming | |
| | | |
| m | constant in solubility coefficient equation | |
| m | dimension of control vector in dynamic programming | |
| | | |
| $n$ | dimension of state vector in dynamic programming | |
| $N$ | water to sucrose molecular ratio | |
| $N$ | number of tanks in series | |
| | | |
| os | oversatuation | |
| | | |
| $p$ | Size dispersion parameter | (m) |
| $p$ | prediction horizon, in number of steps, used in discrete time buffer tank control | |
| $pol$ | sucrose mass percent total mass estimated by polarisation | (%) |
| $pur$ | Common purity of the massecuite and the pan feed syrup | (%) |

# NOMENCLATURE

| | | |
|---|---|---|
| $P$ | matrix solution of the Riccati equation | |
| $q_s$ | steady state flow through buffer tank | (m³/min) |
| $q_i(t)$ | flow into buffer tank as a function of time, $t$ | (m³/min) |
| $q_o(t)$ | flow out of buffer tank as a function of time, $t$ | (m³/min) |
| $\Delta q$ | range of flow variation achievable by buffer tank controller | (m³/min) |
| $Q$ | weighting matrix in LQG control | |
| $Q_i(s)$ | Laplace transform of flow into buffer tank | |
| $Q_o(s)$ | Laplace transform of flow out of buffer tank | |
| $r$ | process input in control studies | (%) |
| $r_o$ | process input which holds process output constant (used in "two step" tuning technique) | (%) |
| $R$ | universal gas constant | (kJ/mol°K) |
| $R$ | constant in equation to estimate sucrose from pol and brix measurements | |
| $R$ | weighting matrix for LQG control | |
| $Re$ | Reynolds number | |
| $RSA$ | reducing sugar to ash ratio | |
| $s$ | complex variable in Laplace transform | |
| $ss$ | supersaturation | |
| $Sc$ | Schmidt number | |
| $SC$ | solubility coefficient | |
| $Sh$ | Sherwood number | |
| $Suc$ | sucrose mass percent total mass | (%) |
| $S_1, S_2$ | slopes measured in "two step" tuning technique for controllers | (%/s) |
| $SW_{s,p}$ | sucrose to water ratio of pure sucrose solution at saturation | |
| $SW_{i,p}$ | sucrose to water ratio of impure sucrose solution at saturation | |
| $t$ | time | (s) |
| $t_d$ | process dead time | (s) |
| $t_0$ | initial reference time | (s) |

# NOMENCLATURE

| | | |
|---|---|---|
| $t_{full}$ | time at which buffer tank will be full | (s) |
| | ( used in MRCO buffer control strategy) | |
| $t_{max}$ | time at which buffer tank will overflow | (s) |
| $T$ | Temperature | (°C) |
| $T$ | total mass of sucrose in pan feed syrup and magma | (kg) |
| $T$ | length of time interval in digital buffer control strategy. | (s) |
| $T_0$ | period of oscillation with constant amplitude, used for controller tuning | (s) |
| | | |
| $u$ | velocity | (m/s) |
| $\boldsymbol{u}$ | vector of plant inputs | |
| $u1$ | total mass flow of massecuite into continuous pan compartment | (kg/s) |
| $u2$ | mass flow of water in massecuite into continuous pan compartment | (kg/s) |
| $u3$ | mass flow of dissolved sucrose in massecuite into continuous pan comp. | (kg/s) |
| $u4$ | first moment of crystal size distribution entering continuous pan comp. | (m) |
| $u5$ | second moment of crystal size distribution entering continuous pan comp. | (m²) |
| $u6$ | total mass flow in feed  into continuous pan compartment | (kg/s) |
| $u7$ | mass flow of dissolved sucrose in feed into continuous pan compartment | (kg/s) |
| $u8$ | evaporation rate from continuous pan compartment | (kg/s) |
| $U$ | control vector used in dynamic programming | |
| $U\,'$ | set of admissible control vectors used in dynamic programming | |
| $U_1(k)$ | flow of sucrose in syrup into the $k$th compartment of a continuous pan | (kg/s) |
| $U_2(k)$ | net water feed rate into the $k$th compartment of a continuous pan | (kg/s) |
| | | |
| $W$ | weighting factor used in LQG buffer tank control strategy | |
| | | |
| $x$ | vector of plant states | |
| $x1$ | mass of dissolved sucrose in continuous pan compartment | (kg) |
| $x2$ | mass of water in continuous pan compartment | (kg) |
| $x3$ | first moment of crystal size distribution in continuous pan compartment | (m) |
| $x4$ | second moment of crystal size distribution in continuous pan comp. | (m²) |
| $X$ | state vector used in dynamic programming | |
| $X_1(k)$ | total massecuite flow out of continuous pan compartment $k$. | (kg/s) |
| $X_2(k)$ | flow of water in massecuite leaving continuous pan compartment $k$. | (kg/s) |

| | | |
|---|---|---|
| $X_3(k)$ | flow of dissolved sucrose in massecuite leaving continuous pan comp. $k$. | (kg/s) |
| $X_4(k)$ | 1st moment of crystal size distribution leaving continuous pan comp. $k$. | (m) |
| $X_5(k)$ | 2nd moment of crystal size distribution leaving continuous pan comp. $k$. | (m$^2$) |

| | | |
|---|---|---|
| $y$ | vector of plant outputs | |
| $y1$ | total mass flow of massecuite leaving continuous pan compartment | (kg/s) |
| $y2$ | mass flow of water in massecuite leaving continuous pan compartment | (kg/s) |
| $y3$ | mass flow of dissolved sucrose in massecuite leaving cont. pan comp. | (kg/s) |
| $y4$ | first moment of crystal size distribution leaving continuous pan comp. | (m) |
| $y5$ | second moment of crystal size distribution leaving continuous pan comp. | (m$^2$) |

Greek Symbols

| | | |
|---|---|---|
| $\alpha$ | constant used in MRCO buffer control strategy | |
| $\alpha_v$ | Volume shape factor of crystals | |
| $\eta$ | viscosity | (kg/m s) |
| $\Phi$ | generic function used in description of dynamic programming | |
| $\Phi$ | constant used in Frossling equation | |
| $\rho_x$ | Density of crystal sucrose | (kg/m$^3$) |
| $\sigma$ | standard deviation | |
| $\theta$ | dimensionless time | |
| $\tau_v$ | buffer tank hold up time | (min) |
| $\tau_I$ | integral time of a PI controller | (sec) |
| $\xi$ | damping factor for a second order system | |

Conventions

| | |
|---|---|
| $'$ | the prime symbol is used to indicate variables which describe deviation from steady state, used in control studies |
| $\cdot$ | the dot above a variable is used to indicate the time derivative |

# APPENDIX A

## A. Crystal Size Distributions
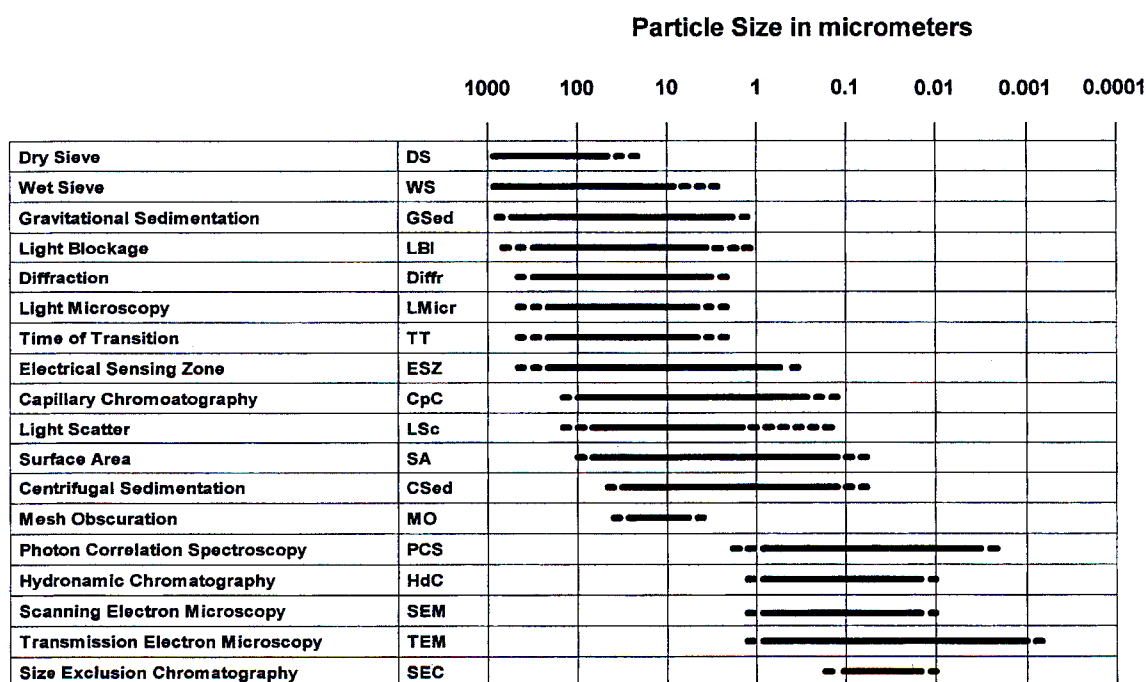
### A.1 General

Any analysis of practical sucrose crystallisation requires quantitative measures of the range of particle sizes present in the process. It is seldom possible to begin the crystallisation process on a seed of uniform size and the spread in crystal sizes will change during the crystallisation process. Techniques are required for both measuring and quantifying the distributions in crystal sizes to monitor or predict crystal growth.

### A.2 Measurement of Size Distribution

There are numerous techniques available for determining size distributions, described either in standard chemical engineering texts (Foust et al., 1960, Coulson & Richardson, 1968), or more comprehensively by Herdan (1960) in a text specifically devoted to the subject. A review by Lines (1990) gives a useful diagrammatic representation of available measurement techniques and their ranges of applicability, reproduced below as Figure A.1.

**Particle Size in micrometers**

| Method | Code | 1000 | 100 | 10 | 1 | 0.1 | 0.01 | 0.001 | 0.0001 |
|---|---|---|---|---|---|---|---|---|---|
| Dry Sieve | DS | | | | | | | | |
| Wet Sieve | WS | | | | | | | | |
| Gravitational Sedimentation | GSed | | | | | | | | |
| Light Blockage | LBl | | | | | | | | |
| Diffraction | Diffr | | | | | | | | |
| Light Microscopy | LMicr | | | | | | | | |
| Time of Transition | TT | | | | | | | | |
| Electrical Sensing Zone | ESZ | | | | | | | | |
| Capillary Chromoatography | CpC | | | | | | | | |
| Light Scatter | LSc | | | | | | | | |
| Surface Area | SA | | | | | | | | |
| Centrifugal Sedimentation | CSed | | | | | | | | |
| Mesh Obscuration | MO | | | | | | | | |
| Photon Correlation Spectroscopy | PCS | | | | | | | | |
| Hydronamic Chromatography | HdC | | | | | | | | |
| Scanning Electron Microscopy | SEM | | | | | | | | |
| Transmission Electron Microscopy | TEM | | | | | | | | |
| Size Exclusion Chromatography | SEC | | | | | | | | |

**Figure A.1** Particle size analysis methods - applicable size ranges

Lines (1990) also provides a chart to assist in the selection of the appropriate technique, the relevant portion of which is reproduced below as Figure A.2 :
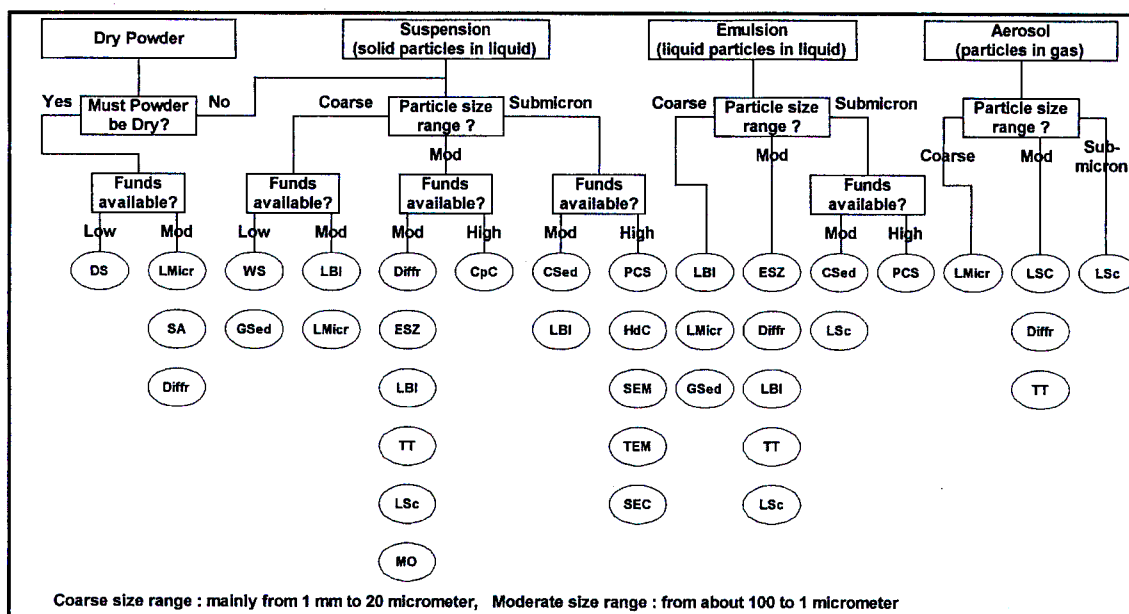


**Figure A.2**   Particle size analysis methods flow chart

High purity (A massecuite) boilings can include particle sizes from 1 to 1000 μm, with continuous pan boiling typically covering the range of 100 to 1000 μm. For these relatively large particle sizes, the tables of Lines indicate that a limited range of techniques are applicable, even if the crystals can be separated to a dry powder, viz.

    1.      Sieving (wet or dry)

    2.      Gravitational sedimentation

    3.      Light blockage

    4.      Light microscopy

    5.      Diffraction

A number of factors specific to sucrose crystals growing in impure mother liquor from raw cane syrup further complicate or limit the techniques which can be used to measure particle size distributions, viz:

    i)      The high colour of the mother liquor limits optical methods.

    ii)     The high viscosity of the mother liquor and small density difference between crystals and mother liquor limits techniques based on the sedimentation of particles.

iii)     The size of the crystals (at the required final product size) limits the use of size-dependent light dispersion.

iv)     The equilibrium between the crystal and its mother liquor (growth or dissolution) requires that special care be taken to ensure no change in crystal size during the measurement process.

v)      Transparent crystals complicate the identification of crystals by optical means.

Whilst success has been achieved elsewhere with other methods (Brown, 1991, Hogg et al., 1986a and 1986b, Wright and White, 1971) the South African sugar industry has standardised on measuring sugar grain size distributions either by sieving or by semi-automated counting of crystals under microscopic imaging (Schumann and Thakur, 1993). The microscopic counting method has the advantage, for crystal growth rate modelling, that the distribution by number is determined directly. Growth rate models (in the absence of nucleation and breakage) utilize number distributions as they assume a constant number or number flow of crystals.

## A.3     Mathematics of Particle Size Distribution

The basis of the mathematics of particle size distributions is standard statistical theory, with the frequency distribution function (or probability density function) used to describe the spread in particle sizes. An appropriate system of mathematics of this type, for handling size distributions, was developed by Rumpf and his co-workers at the Institute Verfarhenstechnic at Karlruke University( Debbas & Rumpf, 1966).

The distribution in particle sizes can be equally well described in a number of different ways. In particular, the frequency distribution can be expressed either in terms of the relative mass of particles or the relative number of particles of a particular size, both of which are in common usage. Different methods for measuring particle size distributions can provide their results in these different formats. For example sieving provides size distributions by mass, whilst optical counting provides size distributions by number. This can be an advantage, allowing, at times, the most appropriate measurement technique to be selected depending on the form in which the results are required. Furthermore, it is possible to choose the method of analysis to provide results applicable to the process under study (e.g. sedimentation analysis produces results that are directly applicable to particle-fluid interactions). A complication of these different methods

of determining size distributions is that the results may be in a format inconsistent with the requirements for further analysis or calculation. A method is thus required for mathematically transforming size distributions of one type into a different type.

Hoekstra (1984) developed a useful summary of these transformations for use in analysing the performance of Tongaat-Hulett Sugar's continuous pans (Hoekstra 1985).

*Size Distribution by Number:*

The probability density function (PDF) (sometimes referred to as the frequency distribution) for size distribution by number, $f_0(x) \cdot dx$ is defined by:

$$f_0(x) \cdot dx \quad = \quad \text{fraction of the number of crystals within the size interval } (x, x + dx)$$
relative to the total number of crystals in the sample.

The cumulative frequency distribution (CFD) for size distribution by number, $F_0(x)$, is defined by:

$$F_0(x) \quad = \quad \text{fraction of the number of crystals in sample with sizes } \le x \text{ relative to}$$
the total number of crystals in the sample.

The relationship between these two functions is given by:

$$F_0(x) = \int_0^x f(t) \cdot dt$$
$$where \quad 0 \le x$$
$$and \quad 0 \le F_0(x) \le 1$$

(A.1)

*Size Distribution by Length, Area or Mass/Volume:*

These distribution functions (PDF and CFD) can also be used to describe distributions by length, area or mass/volume (mass and volume distributions are identical for particles of constant

density) and can be identified by using the following notation:

$$F_r(x) = \int_0^x f_r(t) \cdot dt \tag{A.2}$$

where  $r$  =  0 indicates size distribution by number

$r$  =  1 indicates size distribution by length

$r$  =  2 indicates size distribution by area

$r$  =  3 indicates size distribution by mass/volume

Thus, for example:

$f_3(x) \cdot dx$     is the mass/volume fraction of particles in the size interval $(x, x + dx)$

and     $F_3(x)$     is the mass/volume fraction of particles of size less than $x$

The relationships between these different expressions for the distribution of particle sizes can be generalised for the case of converting from a distribution $f_m(x)$ to a distribution $f_r(x)$ as:

$$f_r(x) = \frac{x^{r-m} \cdot f_m(x)}{\int_0^\infty x^{r-m} \cdot f_m(x) \cdot dx} \tag{A.3}$$

Thus the distribution by mass/volume can be determined from the distribution by number as ;

$$f_3(x) = \frac{x^3 \cdot f_0(x)}{\int_0^\infty x^3 \cdot f_0(x) \cdot dx} \tag{A.4}$$

Alternatively, the distribution by area can be determined from the distribution by mass as:

$$f_2(x) = \frac{x^{-1} \cdot f_3(x)}{\int_0^\infty x^{-1} \cdot f_3(x) \cdot dx} \tag{A.5}$$

(These transformations assume that any shape factors which must be used are independent of particle size).

## A.4    Mathematical Forms of Distribution Functions

To assist in the analysis of crystal size distributions, it is common to assume that the distribution in crystal sizes matches a standard mathematical form. A number of these standard forms are detailed below, all of which are defined by only two parameters. These parameters of the mathematical descriptions can be estimated by fitting the standard forms to the results of particle size measurements. With a full mathematical description of the size distribution, it is a simple matter to calculate any of the other parameters or moments which describe the distribution (as described in sections A-6 and A-7 below).

Rather than attempting to follow any of the conventional norms for naming the parameters of the distributions described below, all simply use the Greek letters $\alpha$ and $\beta$.

*Gaussian or Normal Distribution :*

$$f(x) = \frac{1}{\beta\sqrt{2\pi}} \exp\left( \frac{-(x-\alpha)^2}{2 \cdot \beta^2} \right) \tag{A.6}$$

The Gaussian or Normal distribution is probably the most widely known of the distribution functions. It has an intuitive appeal in that the mean size and spread in size are easily related to the parameters. Despite the limitation that it predicts a finite number of particles of zero size (and the existence of particles of negative size) it forms the basis of the method of Powers (1948) for measuring sugar size distributions. The existence of standard graph paper specifically designed for this distribution function allows results to be analysed graphically by plotting the results- the basis of the Powers method , and also the standard method of the South African Sugar Technologists Association, SASTA (Anon., 1985). The method is also one of four recommended by International Commission for Uniform Methods of Sugar Analysis, ICUMSA (Anon., 1994).

A further limitation of the Normal distribution function, is that it describes a symmetrical

distribution, a characteristic not always encountered in actual distributions of particle sizes.

*Log-Normal Distribution :*

$$f(x) = \frac{1}{\beta \cdot x \cdot \sqrt{2\pi}} \cdot \exp\left( - \frac{(\ln x - \alpha)^2}{2 \cdot \beta^2} \right)$$                    (A.7)

The Log-Normal distribution addresses both the limitations (negative particle sizes and the assumption of a symmetrical distribution) inherent in the Normal distribution. It does this by assuming that the logarithm of the particle size is normally distributed. The availability of standard Log-Normal graph paper allows the graphical techniques of SASTA and Powers to be easily modified to accommodate this non-symmetrical distribution, as done by Rein and Archibald (1989).

*Rosin-Rammler Distribution :*

$$f(x) = \left( \frac{\alpha}{\beta} \right) \cdot \left( \frac{x}{\beta} \right)^{\alpha-1} \exp\left( - \left( \frac{x}{\beta} \right)^{\alpha} \right)$$                    (A.8)

Based on work on analysing ground coal, this distribution is the basis of one of the methods recommended by ICUMSA (Anon., 1994) and was used by Hoekstra (1986) for analysing the performance of continuous pans. Specialised graph paper is available to allow a graphical method of analysis.

*Generalised Negative Exponential Distribution :*

$$f(x) = \frac{\alpha}{\beta \cdot \Gamma\left( \frac{1}{\alpha} \right)} \exp\left( - \left( \frac{x}{\beta} \right)^{\alpha} \right)$$                    (A.9)

This distribution function was used by Hoekstra (1985) to analyse the results of continuous pan tests.

*Gamma Distribution :*

$$f(x) = \frac{x^{\alpha-1} \exp\left(-\frac{x}{\beta}\right)}{\beta^{\alpha} \cdot \Gamma(\alpha)}$$

(A.10)

This distribution was considered by Hoekstra (1985) but not used. Despite this it has a number of advantages when used for describing particle size distributions viz. :

−       It is capable of describing non-symmetrical distributions

−       It does not present any problems associated with the prediction of the existence of particles with zero and negative particle sizes

−       It has a particular mathematical elegance in that if the distribution by number is a Gamma distribution, then the distributions by both area and mass/volume are also distributed according to a Gamma distribution

## A.5     Moments of Distributions

Particle size distributions (which are continuous functions and not numbers) can be characterised by numbers representing some form of "average property". A generalised method of characterising distributions is the concept of moments (well summarised by Papoulis, 1965).

In its most general form, the moment of a distribution is defined as:

$$\mu_{k,r} = \int_0^{\infty} x^k \cdot f_r(x) \cdot dx$$

(A.11)

(This is sometimes referred to as the moment about the origin or the moment about zero).
However from equation A.3, with *m* set to zero, it is possible to express other distributions (eg by mass/volume) in terms of the number distribution by :

$$f_r(x) = \frac{x^r \cdot f_0(x)}{\int_0^{\infty} x^r \cdot f_0(x) \cdot dx} = \frac{x^r \cdot f_0(x)}{\mu_{r,0}}$$

(A.12)

Combining equations A.11 and A.12 gives ;

$$\mu_{k,r} = \int_0^\infty \frac{x^k \cdot x^r \cdot f_0(x) \cdot dx}{\mu_{r,0}} = \frac{1}{\mu_{r,0}} \cdot \int_0^\infty x^{k+r} \cdot f_0(x) \cdot dx \qquad \text{(A.13)}$$

And thus ;

$$\mu_{k,r} = \frac{\mu_{k+r,0}}{\mu_{r,0}} \qquad \text{(A.14)}$$

The first subscript, $k$, can be interpreted as meaning the k'th moment whilst the second subscript, $r$, refers to the type of distribution for which the moment has been calculated.

Thus $\mu_{1,0}$ is the first moment of the number distribution

and $\mu_{2,3}$ is the second moment of the mass/volume distribution

For convenience, as most of the work in this thesis is based on number distributions, the following simplification will be used;

$$\mu_k = \mu_{k,0} \qquad \text{(A.15)}$$

The zero'th moment of any distribution is unity (because of the normalisation of the PDF), i.e.

$$\mu_{0,r} = 1 \qquad \text{(A.16)}$$

The higher moments of the number distribution have particularly useful conceptual significance, which is important in the mathematical modelling of the growth processes described in Chapter 4 and Appendix B. Assuming the particles to be spheres, as a first approximation, it is possible to interpret the moments as follows :

The first moment $\mu_1$ is the average particle size. It is the sum of the lengths of all the individual particles divided by the total number of particles.

In a similar fashion, the second moment $\mu_2$, is directly related to the average particle surface area. For any given shape of particle, the surface area is proportional to the size of the particle squared. The proportionality constant is termed the area shape factor, $\alpha_s$, and for a sphere it is given by :

$$\alpha_s = \pi \qquad \text{(A.17)}$$

The average surface area of a particle is thus given by $\alpha_s \cdot \mu_2$

In the same way, the third moment $\mu_3$, is directly related to the average particle volume. For any given shape of particle, the volume is proportional to the size of the particle cubed. The proportionality constant is termed the volume shape factor, $\alpha_v$, and for a sphere it is given by :

$$\alpha_v = \frac{\pi}{6} \tag{A.18}$$

The average volume of a particle is thus given by $\alpha_v \cdot \mu_3$ The average mass of a crystal is simply the average volume multiplied by the crystal density.

The total number of crystals $N$ can thus be calculated from the third moment, the total mass of crystals $X$ and the crystal density $\rho_x$ according to the following equation :

$$N = \frac{X}{\rho_x \cdot \alpha_v \cdot \mu_3} \tag{A.19}$$

A second class of moments, the moments about the mean, are often also used. These are defined as:

$$m_{k,r} = \int_0^\infty \left( x - \mu_{1,r} \right)^k \cdot f_r(x) \cdot dx \tag{A.20}$$

where, as already defined, $\mu_{1,r}$ is the mean of the probability density function, $f_r(x)$

Again, for convenience, the following simplification will be used :

$$m_{k,0} = m_k \tag{A.21}$$

(for moments about the mean of the number distribution).

The first two moments about the mean are trivial, and are given by :

$$m_{0,r} = \int_0^\infty f_r(x) \cdot dx = 1 \tag{A.22}$$

$$m_{1,r} = \int_0^\infty x \cdot f_r(x) \cdot dx - \mu_{1,r} \cdot \int_0^\infty f_r(x) \cdot dx$$

$$= \mu_{1,r} - \mu_{1,r}$$

$$= 0 \qquad\qquad\text{(A.23)}$$

The relationship between these two types of moments, $\mu$ and $m$, is given by:

$$\mu_{j,r} = \sum_{i=0}^{j} \binom{j}{i} \cdot m_{j-i} \cdot \mu_{1,r}^{i} \qquad\qquad\text{(A.24)}$$

where $\binom{j}{i}$ is the binomial function which is defined as :

$$\binom{j}{i} = \frac{j!}{(j-i)! \cdot i!} \qquad\qquad\text{(A.25)}$$

Thus in summary, for number distributions :

$$m_0 = 1 \qquad\qquad\text{(A.26)}$$

$$m_1 = 0 \qquad\qquad\text{(A.27)}$$

Using these relationships, it is possible to determine the relationships between the two types of moments as follows :

$$\mu_1 = m_1 + m_0 \cdot \mu_1$$

$$= \mu_1 \qquad\qquad\text{(A.28)}$$

$$\mu_2 = m_2 + m_1 \cdot \mu_1 + m_0 \cdot \mu_1^2$$

$$= m_2 + \mu_1^2 \qquad\qquad\text{(A.29)}$$

$$\mu_3 = m_3 + 3 \cdot m_2 \cdot \mu_1 + 3 \cdot m_1 \cdot \mu_1^2 + m_0 \cdot \mu_1^3$$

$$= m_3 + 3 \cdot m_2 \cdot \mu_1 + \mu_1^3 \qquad\qquad\text{(A.30)}$$

Solving for $m_2$ it is possible to write :

$$m_2 = \mu_2 - \mu_1^2 \qquad\qquad (A.31)$$

And thus by substitution :

$$\mu_3 = m_3 + 3 \cdot \left(\mu_2 - \mu_1^2\right) \cdot \mu_1 + \mu_1^3$$
$$= m_3 + 3 \cdot \mu_1\mu_2 - 2 \cdot \mu_1^3 \qquad\qquad (A.32)$$

If it is assumed that a crystal size distribution is fully described by a particular two parameter distribution function, it becomes possible to fully describe a distribution by its first and second, moments only. The parameters which describe the distribution can be calculated from these moments and then any other measure of the size distribution (eg the third moment) can be calculated from the distribution function.

## A.6    Relationships Between Moments for Specific Distributions

Once it is assumed that the distribution of particle sizes is described by a particular form of two-parameter distribution function, it becomes possible to calculate the third moment of the distribution from the first two moments.

*Symmetrical Distribution :*

If it is assumed that the particle size distribution is symmetrical, then, it can be deduced from equation A.20 that :

$$m_3 = 0 \qquad\qquad (A.33)$$

(In equation A.20 the term raised to the power $k$ will have values of opposite sign for values of $x$ above and below the mean if $k$ is odd - as it is in this case of $k = 3$. Thus, a symmetrical nature of the distribution function f(x) will result in the values of the integrand above the mean cancelling out those below the mean and resulting in the integral being zero.)

and it follows from A.32 that :

$$\mu_3 = 3\mu_1\mu_2 - 2\mu_1^3 \qquad\qquad (A.34)$$

*Gamma Distribution :*

It can be shown that for the Gamma distribution described by equation A.10:

$$\int_0^\infty x \cdot f(x)dx = \alpha \cdot \beta \qquad (A.35)$$

Using this relationship and the property of the Gamma function, $\Gamma$, that :

$$\Gamma(\alpha) = (\alpha - 1) \cdot \Gamma(\alpha - 1) \qquad (A.36)$$

It is possible to show that :

$$\mu_1 = \alpha \cdot \beta \qquad (A.37)$$

$$\mu_2 = \alpha \cdot (\alpha + 1) \cdot \beta \qquad (A.38)$$

$$\mu_3 = \alpha \cdot (\alpha + 1) \cdot (\alpha + 2) \cdot \beta \qquad (A.39)$$

And further, by combining equations A.37, A.38 and A.39, to show that

$$\mu_3 = 2 \cdot \frac{\mu_2^2}{\mu_1} - \mu_2 \cdot \mu_1 \qquad (A.40)$$

## A.7    Conventional Measurements of Size Distributions

It is clearly possible to calculate a large number of moments for any given distribution in particle size, however only a limited number of these are in common usage. Furthermore, there are other commonly used parameters which can be calculated from the moments.

Mean:

The mean of a distribution, $\bar{x}$ is given by the first moment about the origin.

$$\bar{x} = \mu_1 \qquad (A.41)$$

Variance:

The variance of a distribution, Var($x$), is given by the second moment about the mean.

$$Var(x) = m_2 \qquad\qquad \textbf{(A.42)}$$

Standard Deviation:

The standard deviation, $\sigma$ , of a distribution is the square root of the variance:

$$\sigma = \sqrt{m_2} \qquad\qquad \textbf{(A.43)}$$

Coefficient of Variation:

The coefficient of variation, $CV$, of a distribution is the ratio of its standard deviation to its mean value.

$$CV = \frac{\sigma}{x}$$
$$= \frac{\sqrt{m_2}}{\mu_1} \qquad\qquad \textbf{(A.44)}$$
$$= \frac{\sqrt{\mu_2 - \mu_1^2}}{\mu_1}$$

Mean Aperture:

The measure "Mean Aperture" (or MA) as defined for the analysis of sugar is a graphical technique for estimating an "average" particle size by mass. The standard method of ICUMSA (Schneider,1979) was based on the work of Powers (1948) and is also the standard method used in the South African Sugar Industry (Anon., 1985). The technique specifies that the results of sieving tests be plotted as a cumulative distribution (ie by mass) on arithmetic probability graph paper. A "best fit" straight line is then drawn through the points by eye. The "mean aperture" is read off the graph where this line intersects the 50% probability line. This defines the size of a crystal which is smaller than 50% of the crystals by mass. (Or, equivalently, which is larger than 50% of the crystals by mass).

This specification implies that the **median** particle size is being measured but the use of a straight line on arithmetic probability paper assumes that the distribution is a Normal

distribution for which **mean, median** and **mode** are all equal. This ambiguity over whether Mean Aperture is a measure of mean or median has led to some confusion within the sugar industry, particularly as crystals sizes have been found to follow an asymmetric or skewed distribution for which mean, median and mode are not equal.

Rein and Archibald (1989) modified the standard graphical method to use logarithmic probability graph paper, thus reporting an estimate of the median crystal size. Hoekstra (1985 and 1986) in his work on continuous pan simulation assumed the term Mean Aperture to be equal to the mean size by mass, and, selecting distributions which could describe asymmetrical distributions, used computerised techniques to calculate the mean size by mass. He also derived relationships to convert between mean size by mass and mean size by number (Rein, Cox and Love, 1985) which have been used with standard Mean Aperture measurements. These relationships are :

$$\mu = \mu_m \cdot \left( \frac{\sigma_m^2}{\mu_m^2} + 1 \right)^{-3} \tag{A.45}$$

$$\sigma^2 = \sigma_m^2 \cdot \left( \frac{\sigma_m^2}{\mu_m^2} + 1 \right)^{-6} \tag{A.46}$$

$$\mu_m = \mu \cdot \left( \frac{\sigma^2}{\mu^2} + 1 \right)^{3} \tag{A.47}$$

$$\sigma_m^2 = \sigma^2 \cdot \left( \frac{\sigma^2}{\mu^2} + 1 \right)^{6} \tag{A.48}$$

Where        $\mu$        is the mean size

             $\sigma$        is the standard deviation

and the subscript $m$ is used to denote the properties of the distribution by mass as distinct from the distribution by number.

Australian researchers appear to have retained the concept of Mean Aperture as applying to the median of the distribution by mass (Miller, 1992, Miller and Beath, 2000).

Unfortunately the confusion between whether Mean Aperture should represent the mean or the median size for asymmetric distributions is perpetuated in the standard methods of ICUMSA (Anon., 1994). Four alternative methods are presented for analysing the results of sieve test results, with the choice of procedure left to the user. Three of these (the Powers method, the Rens method and the Rosin, Rammler, Sperling and Bennet method) calculate Mean Aperture as the median size by mass whilst the Butler method calculates the mean size by mass.

The particular technique used for analysing results may not be documented when MA results are reported with respect to the performance of continuous pans and the MA results must thus be treated with suitable circumspection.

Specific Grain Size :

The determination of Specific Grain Size from the results of a sieving test is described by Browne and Zerban (1948). The intention is to provide an "average" size in terms of crystal surface area. This "average" is specified so that a sample of sugar crystals, all of the Specific Grain Size would have the same total surface area as the same mass of sample of the sugar under consideration.

The standard method of SASTA (Anon., 1985) provides a set of factors for a standard set of screens to enable the Specific Grain Size to be easily calculated from a conventional screening test. The Specific Grain Size is not frequently used with respect to pan performance.

Characteristic Dimension :

The increasing use of semi-automated optical counting of individual crystals in the South African sugar industry has led to the need for a uniform method of presenting the results of this type of analysis. In particular the results are collected as length and width measurements which must be combined to give a single number to characterise the particle size. Lionnet (1998) has pioneered the use of a "characteristic dimension" in the South African industry, following the approach described by Bubnik and Kadlec (1992).

The characteristic dimension $Dc$ is defined as :

$$Dc = \left(L^2 \cdot W\right)^{1/3}$$

(A.49)

where   L       is the length of a crystal

and     W       is the width of a crystal.

Lionnet (1998) found that using this characterisation of crystal size, the volume shape factor $\alpha_v$ for white sugar crystals from his pilot crystallisation work was 0.34. This is similar to the value of 0.31 reported by Bubnik and Kadlec (1992).

If the characteristic dimensions of a representative number crystals are available, conventional statistical calculations can be used to calculate the mean, standard deviation and coefficient of variation of $Dc$. Unfortunately some of the results of earlier particle size measurements are only available as the means and standard deviations of $L$ and $W$ individually. Assuming that the $L/W$ ratio of all the crystals in the population is constant, the mean $L$ and $W$ values can be combined using equation A.45 to yield an average value of $Dc$. The procedure for calculating the standard deviation of $Dc$ is not as obvious. Following the approach used by Boas (1966) for a similar calculation of an average velocity from average time and average distance measurements, it is possible to show that :

$$s_{Dc}{}^2 = \frac{1}{9 \cdot \mu_{Dc}{}^4} \cdot \left(4 \cdot \mu_L{}^2 \cdot \mu_W{}^2 \cdot s_L{}^2 + 5 \cdot \mu_L{}^4 \cdot s_W{}^2\right)$$

(A.50)

where   $s_{Dc}$    is the standard deviation of the characteristic dimension

        $s_W$     is the standard deviation of the crystal width

        $s_L$     is the standard deviation of the crystal width

        $\mu_{Dc}$    is the average characteristic dimension

        $\mu_W$     is the average crystal width

        $\mu_L$     is the average crystal length

The derivation of this relationship also assumes that the $L/W$ ratio of the crystals in the population remains constant.

# APPENDIX B

# B. Mathematical Model of a Multi-compartment Continuous Pan

## B.1 Introduction

The multi-compartment continuous pan (of the Tongaat-Hulett Design) can be considered as a number of identical units connected in series.
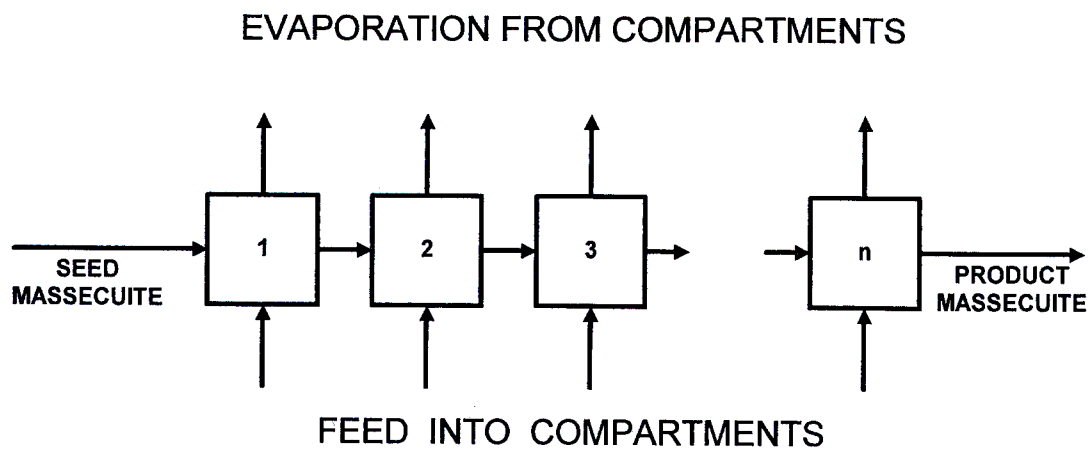
**EVAPORATION FROM COMPARTMENTS**



**FEED INTO COMPARTMENTS**

**Figure B.1** Schematic diagram of a multi-compartment continuous pan

Because of the large number of variables necessary to describe the pan, a consistent and logical nomenclature is essential for a clear description of the process. The following system uses a subscript to reference variables to a particular compartment.

## B-2    General Nomenclature and Relationships

| | | |
|---|---|---|
| $\rho_x$ | Density of crystal sucrose | $(kg \cdot m^{-3})$ |
| $\alpha_v$ | Volume shape factor of crystals | |
| $\alpha_s$ | Surface area shape factor of crystals | |
| $G$ | Crystal growth rate | $(m \cdot s^{-1})$ |
| $p$ | Size dispersion parameter | $(m)$ |
| $\mu 1$ | First moment of crystal size distribution | $(m)$ |
| $\mu 2$ | Second moment of crystal size distribution | $(m^2)$ |
| $\mu 3$ | Third moment of crystal size distribution | $(m^3)$ |

## B-3    Massecuite Stream Leaving Compartment n

(n = 0 refers to the seed massecuite entering compartment number 1)

Extensive Properties:

$ST_n$     Total flow       (kg·s$^{-1}$)

$SW_n$     Water flow       (kg·s$^{-1}$)

$SD_n$     Solids flow      (kg·s$^{-1}$)

$SS_n$     Dissolved sucrose flow  (kg·s$^{-1}$)

$SX_n$     Crystal sucrose flow      (kg·s$^{-1}$)

$SI_n$     Impurities flow  (kg·s$^{-1}$)

$SN_n$     Number of crystals flowing       (s$^{-1}$)

Intensive Properties:

$s\mu1_n$     First moment of crystal size distribution  (m)

$s\mu2_n$     Second moment of crystal size distribution       (m$^2$)

$s\mu3_n$     Third moment of crystal size distribution       (m$^3$)

$smb_n$     Massecuite dry solids content    (%)

$smp_n$     Massecuite sucrose purity        (%)

$smc_n$     Massecuite crystal content       (%)

$snb_n$     Nutsch dry solids content        (%)

$snp_n$     Nutsch sucrose purity    (%)

Relationships:

$$ST_n = SW_n + SD_n \tag{B.1}$$

$$SD_n = SS_n + SX_n + SI_n \tag{B.2}$$

$$smb_n = \frac{SD_n}{ST_n} \cdot 100 \tag{B.3}$$

$$smp_n = \frac{SS_n + SX_n}{SD_n} \cdot 100 \tag{B.4}$$

$$smc_n = \frac{SX_n}{ST_n} \cdot 100 \tag{B.5}$$

$$snb_n = \frac{SS_n + SI_n}{SS_n + SI_n + SW_n} \cdot 100 \tag{B.6}$$

$$snp_n = \frac{SS_n}{SS_n + SI_n} \cdot 100$$

(B.7)

Combining equations B.1 and B.4, it is possible to write :

$$SX_n = \left(ST_n - SW_n\right) \cdot \frac{smp_n}{100} - SS_n$$

(B.8)

Converting equation A.19 to the appropriate nomenclature for this stream yields :

$$SN_n = \frac{SX_n}{\rho_x \cdot \alpha_v \cdot s\mu3_n}$$

(B.9)

Combining equations B.8 and B.9 :

$$SN_n = \frac{\left(ST_n - SW_n\right) \cdot \dfrac{smp_n}{100} - SS_n}{\rho_x \cdot \alpha_v \cdot s\mu3_n}$$

(B.10)

## B-4    Massecuite in Compartment n

| Extensive Properties: | | | |
|---|---|---|---|
| | $CT_n$ | Total mass | (kg) |
| | $CW_n$ | Water mass | (kg) |
| | $CD_n$ | Solids mass | (kg) |
| | $CS_n$ | Dissolved sucrose mass | (kg) |
| | $CX_n$ | Crystal sucrose mass | (kg) |
| | $CI_n$ | Impurities mass | (kg) |
| | $CN_n$ | Number of crystals | (kg) |

| Intensive Properties: | | | |
|---|---|---|---|
| | $c\mu1_n$ | First moment of crystal size distribution | (m) |
| | $c\mu2_n$ | Second moment of crystal size distribution | (m$^2$) |
| | $c\mu3_n$ | Third moment of crystal size distribution | (m$^3$) |
| | $cmb_n$ | Massecuite dry solids content | (%) |
| | $cmp_n$ | Massecuite sucrose purity | (%) |
| | $cmc_n$ | Massecuite crystal content | (%) |
| | $cnb_n$ | Nutsch dry solids content | (%) |
| | $cnp_n$ | Nutsch sucrose purity | (%) |

$cniw_n$   Nutsch impurity to water ratio

$cnss_n$   Nutsch supersaturation

Relationships :

$$CT_n = CW_n + CD_n \tag{B.11}$$

$$CD_n = CS_n + CX_n + CI_n \tag{B.12}$$

$$cmb = \frac{CD_n}{CT_n} \cdot 100 \tag{B.13}$$

$$cmp_n = \frac{CS_n + CX_n}{CD_n} \cdot 100 \tag{B.14}$$

$$cmc_n = \frac{CX_n}{CT_n} \cdot 100 \tag{B.15}$$

$$cnb_n = \frac{CS_n + CI_n}{CS_n + CI_n + CW_n} \cdot 100 \tag{B.16}$$

$$cnp_n = \frac{CS_n}{CS_n + CI_n} \cdot 100 \tag{B.17}$$

$$cniw_n = \frac{CI_n}{CW_n}$$
$$= \frac{\left(CT_n - CW_n\right)}{CW_n} \cdot \left(1 - \frac{cmp_n}{100}\right) \tag{B.18}$$

By combining equations B.11 and B.14 it is possible to write :

$$CX_n = \left(CT_n - CW_n\right) \cdot \frac{cmp_n}{100} - CS_n \tag{B.19}$$

Converting equation A.19 to the appropriate nomenclature for this stream yields :

$$CN_n = \frac{CX_n}{\rho_x \cdot \alpha_v \cdot c\mu 3_n}$$ 

(B.20)

Combining equations B.19 and B.20 yields :

$$CN_n = \frac{\left(CT_n - CW_n\right) \cdot \dfrac{cmp_n}{100} - CS_n}{\rho_x \cdot \alpha_v \cdot c\mu 3_n}$$

(B.21)

## B-5    Feed Into Compartment n

Extensive Properties:      $FT_n$    Total flow      (kg·s⁻¹)

                                        $FW_n$    Water flow      (kg·s⁻¹)

                                        $FD_n$    Solids flow      (kg·s⁻¹)

                                        $FS_n$    Dissolved sucrose flow  (kg·s⁻¹)

                                        $FI_n$    Impurities flow  (kg·s⁻¹)

Intensive Properties:      $fb_n$    Feed brix      (%)

                                        $fp_n$    Feed purity      (%)

Relationships :

$$FT_n = FW_n + FD_n$$

(B.22)

$$FD_n = FS_n + FI_n$$

(B.23)

$$fp_n = \frac{FS_n}{FS_n + FI_n} \cdot 100$$

(B.24)

$$fb_n = \frac{FD_n}{FT_n} \cdot 100$$

(B.25)

## B-6    Vapour Flow Out of Compartment n

Extensive Properties:      $ET_n$    Total flow      (kg·s⁻¹)

                                        $EW_n$    Water flow      (kg·s⁻¹)

Relationships:

$$ET_n = EW_n \tag{B.26}$$

## B-7    Assumptions on Which Model is Based

The single compartment model is based on the following assumptions:

i)    The compartment behaves as a fully mixed tank or CSTR (continuously stirred tank reactor) where the properties of the massecuite leaving the compartment are equal to the uniform properties of the massecuite in the compartment. The nomenclature for the intensive properties of the massecuite in compartment n and leaving compartment n can thus be simplified as follows:

$$c\mu 1_n = s\mu 1_n = \mu 1_n \tag{B.27}$$

$$c\mu 2_n = s\mu 2_n = \mu 2_n \tag{B.28}$$

$$c\mu 3_n = s\mu 3_n = \mu 3_n \tag{B.29}$$

$$cmb_n = smb_n = mb_n \tag{B.30}$$

$$cmp_n = smp_n = mp_n \tag{B.31}$$

$$cmc_n = smc_n = mc_n \tag{B.32}$$

ii)    The mass of massecuite in the compartment remains constant.

iii)    The purity of the seed massecuite flowing into the first compartment is constant and equal to the purity of the feed syrup. The purity of massecuite in each compartment is thus equal and constant, i.e.

$$smp_0 = smp_n = cmp_n = fp_n = pur \tag{B.33}$$

## B-8    Formulation of Sucrose Solubility Equations

The solubility of sucrose in pure and impure solutions is discussed in detail in chapters 2 and 5.

Assuming that the solubility coefficient is linearly dependent on the impurity to water ratio in the compartment (as described by equations 5.1 and 5.2), it is possible to write :

$$cnsc_n = 1 - K_5 \cdot cniw_n \tag{B.34}$$

The sucrose to water ratio for a pure sucrose solution at saturation at a given temperature can be calculated from equations 2.3 (or 2.2) and 2.4. Neglecting the small changes in operating temperature between the compartments of the continuous pan that result from the sightly different levels of boiling point elevation, it is possible to assume that sucrose to water ratio of a pure sucrose solution at the massecuite temperature is a constant for the entire pan and define it , in terms of equation 2.4, as :

$$K_4 = SW_{s,p} \tag{B.35}$$

From the definition of the solubility coefficient (equation 2.5), the sucrose to water ratio at saturation of the impure solution in the compartment is given by :

$$SW_{s,i} = K_4 \cdot \left(1 - K_5 \cdot cniw_n\right) \tag{B.36}$$

Using this relationship and the definition of supersaturation (equation 2.22 ), the supersaturation in any compartment can be expressed as :

$$cnss_n = \frac{\dfrac{CS_n}{CW_n}}{K_4 \cdot \left(1 - K_5 \cdot cniw_n\right)} \tag{B.37}$$

## B-9      Formulation of Sucrose Crystal Growth Equations

The growth rate of sucrose crystals in impure solutions has been discussed in detail in Chapter 2 with the equation of Wright and White (equation 2.31) selected as the most appropriate for this investigation. Converted to the nomenclature of a pan compartment, the growth rate equation may be written as :

$$G_n = K_1 \cdot \left( cnss_n - \left( 1 + K_0 \right) \right) \cdot \exp\left( K_2 - K_3 \cdot cniw_n \right) \qquad \text{(B.38)}$$

with the constants having the following significance :

$K_0$      Offset defining level of supersaturation above which linear dependance exists

$K_1$      Proportional dependance of growth on supersaturation

$K_2$      Factor adjusting growth rate for variation of temperature from a "normal" value

$K_3$      Factor defining exponential dependance of growth rate on impurity/water ratio

## B-10    Formulation of Balance Equations

The model is formulated from a set of balances which are based on the fundamental relationship:

Flow in  -  Flow out  =  Accumulation  -  Reaction

This format can be applied to conventional mass balances of each of the components (crystal, sucrose, water etc.) and to number balances for crystals. The "reaction" term is used to describe the processes associated with sucrose crystal growth.

## B-11    Number Balance

For a number balance on the sucrose crystals, it is possible to write :

$$SN_{n-1} - SN_n = \frac{dCN_n}{dt} \qquad \text{(B.39)}$$

(since there is no breakage, agglomeration or nucleation of crystals).

## B-12    Size Distribution and Moment Balances

The balances are significantly more complex when applied to size distribution of the crystals as they pass through a compartment. The approach in this work follows that of Broadfoot (1980) and begins with the population balance of Randolph and Larson (1962), which, expressed in terms of the density function, $f$, (and, again, assuming no nucleation, agglomeration or breakage) is given by

$$\frac{\partial CN_n f}{\partial t} = SN_{n-1} f_{n-1} - SN_n f_n - \frac{CN_n \partial fG}{\partial L} \qquad \text{(B.40)}$$

Assuming size independent growth, allows the growth rate, $G$, to be taken out of the differential on the right hand side of the equation. Randolph and White (1977) included a second order differential term with a population diffusivity $Dg$, to describe the effect of size dispersion during crystal growth. Incorporating both these modifications yields :

$$\frac{\partial CN_n f}{\partial t} = SN_{n-1} f_{n-1} - SN_n f_n - CN_n \cdot G \frac{\partial f}{\partial L} + CN_n \cdot Dg \cdot \frac{\partial^2 f}{\partial L^2} \qquad \text{(B.41)}$$

This population diffusivity can be expressed in terms of a dispersion parameter, $p$, according to Wright and White (1969) as :

$$Dg = \frac{p \cdot G}{2} \qquad \text{(B.42)}$$

Equation B.41 can be simplified so that it can be expressed in terms of moments of the distribution rather than the complete distribution function. This is achieved by multiplying each term of equation B.41 by $L^j$ and then integrating over L from zero to infinity to convert the distribution functions into moments. By using values of $j$ from 1 to 3 and with considerable manipulation to simplify the resulting equations, a relatively simple equation can be derived for each of the three moments of the size distribution (Randolph and White 1977, Broadfoot 1980):

First moment, $\mu 1$       :       Equation B.43

First moment, $\mu 2$       :       Equation B.49

First moment, $\mu 3$       :       Equation B.52

Each of these equations can then be simplified and interpreted as shown below, using the simplification that the moments of the massecuite in the compartment are equal to the moments of the massecuite leaving that compartment ( equations B.27, B.28 and B.29 ).

**Crystal First Moment Balance:**

$$SN_{n-1} \cdot \mu 1_{n-1} - SN_n \cdot \mu 1_n = \frac{d(CN_n \cdot \mu 1_n)}{dt} - CN_n \cdot G_n \qquad \text{(B.43)}$$

Expanding the differential, it is possible to write:

$$\frac{d(CN_n \cdot \mu 1_n)}{dt} = CN_n \cdot \frac{d\mu 1_n}{dt} + \mu 1_n \cdot \frac{dCN_n}{dt} \qquad \text{(B.44)}$$

Substituting from the crystal number balance, B.39 :

$$\frac{d(CN_n \cdot \mu 1_n)}{dt} = CN_n \cdot \frac{d\mu 1_n}{dt} + \mu 1_n \cdot (SN_{n-1} - SN_n) \qquad \text{(B.45)}$$

Substituting equation B.45 into equation B.43 yields:

$$SN_{n-1} \cdot \mu 1_{n-1} - SN_n \cdot \mu 1_n = CN_n \cdot \frac{d\mu 1_n}{dt} + SN_{n-1} \cdot \mu 1_n - SN_n \cdot \mu 1_n - CN_n \cdot G_n \qquad \text{(B.46)}$$

Which can be simplified to :

$$\frac{d\mu 1_n}{dt} = \frac{SN_{n-1}}{CN_n} \cdot (\mu 1_{n-1} - \mu 1_n) + G_n \qquad \text{(B.47)}$$

Substituting from equation B.20 yields:

$$\frac{d\mu 1_n}{dt} = SN_{n-1} \cdot (\mu 1_{n-1} - \mu 1_n) \cdot \frac{\rho_x \cdot \alpha_v \cdot \mu 3_n}{CX_n} + G_n \qquad \text{(B.48)}$$

**Crystal Second Moment Balance:**

$$SN_{n-1} \cdot \mu 2_{n-1} - SN_n \cdot \mu 2_n = \frac{d\left(CN_n \cdot \mu 2_n\right)}{dt} - 2 \cdot CN_n \cdot G_n \cdot \mu 1_n - CN_n \cdot p \cdot G_n \qquad \text{(B.49)}$$

Following a similar procedure to that used for equation B.43 , expanding the differential and substituting from the crystal number balance B.39 yields :

$$\frac{d\left(CN_n \cdot \mu 2_n\right)}{dt} = CN_n \cdot \frac{d\mu 2_n}{dt} + \mu 2_n \cdot \left(SN_{n-1} - SN_n\right) \qquad \text{(B.50)}$$

substituting equation B.50 into equation B.49 and simplifying yields :

$$\frac{d\mu 2_n}{dt} = \frac{SN_{n-1}}{CN_n} \cdot \left(\mu 2_{n-1} - \mu 2_n\right) + 2 \cdot G_n \cdot \mu 1_n + p \cdot G_n \qquad \text{(B.51)}$$

**Crystal Third Moment Balance:**

$$SN_{n-1} \cdot \mu 3_{n-1} - SN_n \cdot \mu 3_n = \frac{d\left(CN_n \cdot \mu 3_n\right)}{dt} - 3 \cdot CN_n \cdot G_n \cdot \mu 2_n - 3 \cdot CN_n \cdot p \cdot G_n \cdot \mu 1_n \qquad \text{(B.52)}$$

Equation B.52 can be converted into a crystalline mass balance by multiplying throughout by the crystal density, $\rho_x$, and the crystal volume shape factor, $\alpha_v$. The last two terms on the right hand side of equation B.52 then express the reaction (crystal growth) aspect of a crystalline sucrose mass balance ie

$$\textit{Mass rate of crystallisation} = \; 3 \cdot \rho_x \cdot \alpha_v \cdot CN \cdot G \cdot \mu 2$$
$$+ \, 3 \cdot \rho_x \cdot \alpha_v \cdot CN \cdot p \cdot G \cdot \mu 1 \qquad \text{(B.53)}$$

## B-13    Overall Mass Balance

With a constant mass in the compartment, there is no overall accumulation of mass in the compartment.

$$ST_{n-1} + FT_n - ST_n - ET_n = 0 \qquad\qquad\text{(B.54)}$$

## B-14    Water Mass Balance

$$SW_{n-1} + FW_n - SW_n - EW_n = \frac{dCW_n}{dt} \qquad\qquad\text{(B.55)}$$

Either heuristically or using equations B.1, B.3, B.30, B.13 and B.11, it is possible to write :

$$SW_n = ST_n \cdot \frac{CW_n}{CT_n} \qquad\qquad\text{(B.56)}$$

Using equations B.56 and B.54 (the overall balance) it is possible to rewrite equation B.57 as :

$$\frac{dCW_n}{dt} = SW_{n-1} + FW_n - EW_n - \left(ST_{n-1} + FT_n - ET_n\right)\cdot\frac{CW_n}{CT_n} \qquad\qquad\text{(B.57)}$$

## B-15    Dissolved Sucrose Mass Balance

Using the description of the mass rate of crystallisation given by equation B.53

$$SS_{n-1} + FS_n - SS_n = \frac{dCS_n}{dt} + 3\cdot\rho_x \cdot \alpha_v \cdot CN_n \cdot G_n \cdot \mu2_n \\ + 3\cdot\rho_x \cdot \alpha_v \cdot CN_n \cdot p \cdot G_n \cdot \mu1_n \qquad\qquad\text{(B.58)}$$

where p is the size dispersion parameter to account for randomly different growth velocities relative to the mean growth velocity (which is assumed to be independent of crystal size). Either heuristically or using equations B.3, B.4, B.5, B.30, B.31, B.32, B.13, B.14 and B.15, it is possible to write :

$$SS_n = ST_n \cdot \frac{CS_n}{CT_n} \qquad\qquad\text{(B.59)}$$

Using equations B.59 and B.54 (the overall balance) it is possible to rewrite equation B.58 as :

$$
\frac{dCS_n}{dt} = SS_{n-1} + FS_n - \left(ST_{n-1} + FT_n - ET_n\right) \cdot \frac{CS_n}{CT_n}
$$
$$
- 3 \cdot \rho_x \cdot \alpha_v \cdot CN_n \cdot G_n \cdot \mu 2_n
$$
$$
- 3 \cdot \rho_x \cdot \alpha_v \cdot CN_n \cdot p \cdot G_n \cdot \mu 1_n
$$

(B.60)

Which can be simplified to

$$
\frac{dCS_n}{dt} = SS_{n-1} + FS_n - \left(ST_{n-1} + FT_n - ET_n\right) \cdot \frac{CS_n}{CT_n}
$$
$$
- 3 \cdot \rho_x \cdot \alpha_v \cdot CN_n \cdot G_n \cdot \left(\mu 2_n + p \cdot \mu 1_n\right)
$$

(B.61)

## B-16    Expression of Model in Standard State Space Form

The equations are formulated for compartment number $n$.

The state variables are selected as :

$$x1 = \quad CS_n$$
$$x2 = \quad CW_n$$
$$x3 = \quad C\mu 1_n$$
$$x4 = \quad C\mu 2_n$$

The input variables are selected as :

$$u1 = \quad ST_{n-1}$$
$$u2 = \quad SW_{n-1}$$
$$u3 = \quad SS_{n-1}$$
$$u4 = \quad S\mu 1_{n-1}$$
$$u5 = \quad S\mu 2_{n-1}$$
$$u6 = \quad FT_{n-1}$$
$$u7 = \quad FS_{n-1}$$
$$u8 = \quad ET_{n-1}$$

The output variables are selected as :

$$y1 = ST_n$$
$$y2 = SW_n$$
$$y3 = SS_n$$
$$y4 = S\mu1_n$$
$$y5 = S\mu2_n$$

These three sets of variables can be considered as vectors, with the elements of the vectors being the individual variables described above. The vectors are thus :

$x$      the vector of states

$u$      the vector of input variables

$y$      the vector of output variables


With these definitions, the equations describing a single compartment no longer need careful use of the subscript to differentiate between input to the compartment and outputs from the compartment. When describing a single compartment, as in some of the following equations, the subscript can be omitted without loss of clarity. The subscript can be invoked to describe the interconnection between compartments as follows :

$$u1_n = y1_{n-1}$$
$$u2_n = y2_{n-1}$$
$$u3_n = y3_{n-1}$$
$$u4_n = y4_{n-1}$$
$$u5_n = y5_{n-1}$$


To reduce the number of terms in the final expressions of the state space equations, it is useful to define some intermediate functions. This also makes it simpler to read and interpret the equations in their final form . The functions take as their inputs the vector of states in the compartment, and the vector of inputs to the compartment. The conversion of the balance equations to use these state, input and output vectors also makes use of the relationships which equate the intensive properties of the massecuite in a compartment to the intensive properties of the massecuite leaving that compartment (equations B.27 to B.31).


Function $g0$ defines the supersaturation of the mother liquor in the compartment and is determined from equations B.37 and B.18.

$$g0(x, u) = cnss_n$$

$$= \frac{\dfrac{x1}{x2}}{K_4 \cdot \left(1 - K_5 \cdot \dfrac{(CT_n - x2)}{x2} \cdot \left(1 - \dfrac{pur}{100}\right)\right)} \tag{B.62}$$

Function $g1$ defines the number flow of crystals leaving the compartment and is determined from equation B.10. The third moment of the particle size distribution $\mu3$ is expressed in terms of the first two moments, $\mu1$ and $\mu2$ according to the relationship appropriate for a Gamma distribution function defined by equation A.40.

$$g1(x, u) = SN_{n-1}$$

$$= \frac{(u1 - u2) \cdot \dfrac{pur}{100} - u3}{\rho_x \cdot \alpha_v \cdot \left(2 \cdot \dfrac{u5^2}{u4} - u5 \cdot u4\right)} \tag{B.63}$$

Function $g2$ defines the number of crystals in the compartment and is determined from equation B.21, again using the relationship between the first three moments of the particle size distribution defined by equation A.10.

$$g2(x, u) = CN_n$$

$$= \frac{(CT_n - x2) \cdot \dfrac{pur}{100} - x1}{\rho_x \cdot \alpha_v \cdot \left(2 \cdot \dfrac{x4^2}{x3} - x4 \cdot x3\right)} \tag{B.64}$$

Function $g3$ defines the linear growth rate in the compartment and is determined from equations B.38 and B.18, and using the definition of function $g0$ given by equation B.62.

$$g3(x, u) = G_n$$

$$= K_1 \cdot \left(g0(\overline{x}, \overline{u}) - (1 + K_0)\right) \cdot \exp\left(K_2 - K_3 \cdot \frac{(CT_n - x2)}{x2} \cdot \left(1 - \frac{pur}{100}\right)\right) \tag{B.65}$$

Using these intermediate functions, it is now possible to formulate the state space equations from the appropriate balance equations.

The dissolved sucrose mass balance equation (B.61) can be written as :

$$\frac{dx1}{dt} = f1(x,u)$$

$$= u3 + u7 - (u1 + u6 - u8) \cdot \frac{x1}{CT_n} - 3 \cdot \rho_s \cdot \alpha_v \cdot g2(x,u) \cdot g3(x,u) \cdot (x4 + p \cdot x3)$$

(B.66)

The water mass balance equation (B.57) can be written as :

$$\frac{dx2}{dt} = f2(x,u)$$

$$= u2 + \left( u6 - u7 \cdot \frac{100}{pur} \right) - u8 - (u1 + u6 - u8) \cdot \frac{x2}{CT_n}$$

(B.67)

The equation for the first moment of the size distribution (B.47) can be written as:

$$\frac{dx3}{dt} = f3(x,u)$$

$$= \frac{g1(x,u)}{g2(x,u)} \cdot (u4 - x3) + g3(x,u)$$

(B.68)

The equation for the second moment of the size distribution (B.51) can be written as:

$$\frac{dx4}{dt} = f4(x,u)$$

$$= \frac{g1(x,u)}{g2(x,u)} \cdot (u5 - x4) + 2 \cdot g3(x,u) \cdot x3 + p \cdot g3(x,u)$$

(B.69)

The output variables can be easily expressed in terms of the input variables and state variables without the necessity of referring back to the original nomenclature.

Since the total mass in a compartment remains constant at all times, a balance on the total flows entering and leaving the compartment can be used to calculate the total mass flow leaving the compartment. Thus :

$$y1 = u1 + u6 - u8 \tag{B.70}$$

Using this relationship, the flows of water and dissolved sucrose in the massecuite leaving the compartment can be calculated by proportioning this total flow according to the composition of the massecuite in the compartment. Thus :

$$y2 = (u1 + u6 - u8) \cdot \frac{x2}{CT_n} \tag{B.71}$$

and

$$y3 = (u1 + u6 - u8) \cdot \frac{x1}{CT_n} \tag{B.72}$$

The last two output variables, being intensive properties of the massecuite stream are equal to the corresponding properties of the massecuite in the compartment. Thus:

$$y4 = x3 \tag{B.73}$$

and

$$y5 = x4 \tag{B.74}$$

# APPENDIX C

## C.    Measuring Compartment Dynamics

### C.1    Dynamic Effects of Absolute Pressure Variations

The following pages are the print-out of a "Mathcad" worksheet to investigate the effect of variations in the absolute pressure within the body on a continuous pan on the massecuite temperature. In particular the investigation focuses on the effects of this dynamic behaviour on the use of Boiling Point Elevation (BPE) measurements as an indicator of the condition of the massecuite in the pan compartment.

This file evaluates the data collected on Compartment 1 of the A1 Continuous pan at Felixton with feed syrup controlled manually. The intention of the test was to investigate the effect of fluctuations in absolute pressure on massecuite temperature and the consequent effect on the estimation of Boiling Point Elevation (BPE) for use as a measure of mother liquor concentration.

The logged data are read into a matrix, M, from the data file "A1tste.prn" which is associated with the variable "data"

$$M := READPRN( data )$$

Vectors are created from the columns of M.
v0 is the vector of RS readings from the RF Probe
v1 is the vector of XS readings from the RF Probe
v2 is the vector of masecuite temperature readings
v3 is the vector of absolute pressure readings
v4 is the vector of digital output setting of the feed control valve

$$v0 := M^{<0>} \qquad v1 := M^{<1>} \qquad v2 := M^{<2>} \qquad v3 := M^{<3>} \qquad v4 := M^{<4>}$$

Creating a subscript variable i to reference the elements of these vectors of recorded data :
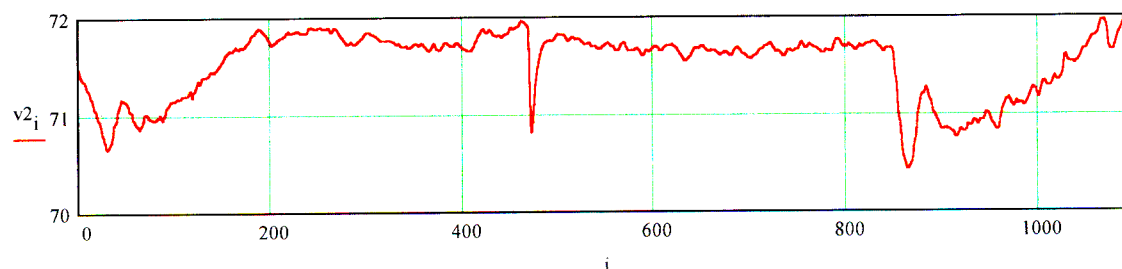
$$i := 0..1100$$

The data points are recorded every 5 seconds. The variable, delta is used to describe this time interval :
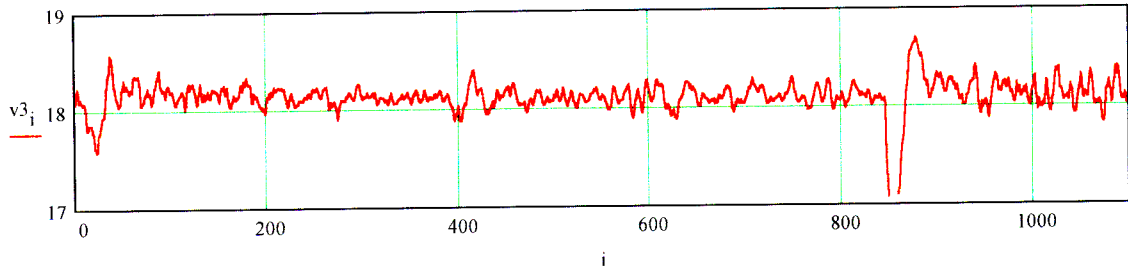
$$delta := 5$$

Plotting the recorded trends of temperature and pressure :

Massecuite Temperature (in degrees Centigrade) plotted versus Sample Number (each delta seconds appart)

Absolute Pressure (in kPa absolute) plotted versus Sample Number (each delta seconds appart)



Creating a subscript k to define the range for which the correlation functions will be calculated :
ie from +k to -k

$$k = 0..64$$

Creating another subscript s to cover the range of the auto-correlation function from + k to -k

$$s = 0..127$$

Creating a subscript p to cover the period of the test for which there is reasonably stable pressure control

pmin = 100            pmax = 800            p = pmin.. pmax

Calculating the average values of v2 and v3 over the range of p

$$n = \frac{1}{(pmax - pmin)} \cdot \sum_p v2_p \qquad n = 71.797$$

$$m = \frac{1}{(pmax - pmin)} \cdot \sum_p v3_p \qquad m = 18.148$$

Calculating the autocorrelation function of the pressure signal as follows (with the value of s=64) representing zero shift for the correlation calculation :

$$acv3_s = \sum_p \left[ (v3_p - m) \cdot (v3_{p - 64 + s} - m) \right]$$

The plot of this auto correlation function (shown below) demonstrates a clear periodic component

Auto Correlation Function
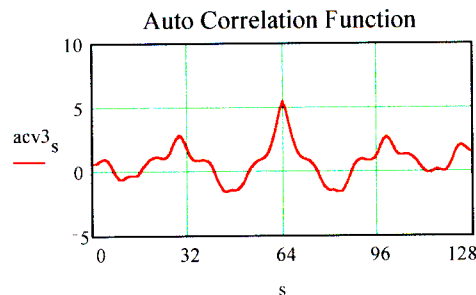


The periodicity of the signal can be investigated by appling Fourier Transform techniques. To minimise the end effects which result when applying Fourrier Transforms to finite records of data, it is necessary to apply a "windowing" function.   Defining the Blackman-Harris window function over the range of s (0 to 128) to apply to the auto and cross correlation functions prior to evaluating the Fourier Transforms:

a0 = 0.42323                    a1 = 0.49744                    a2 = 0.07922

$$w_s = a0 - a1 \cdot \cos\left(\frac{2 \cdot \pi}{128} \cdot s\right) + a2 \cdot \cos\left(\frac{2 \cdot \pi}{128} \cdot 2 \cdot s\right)$$

Weighting the auto correlation function and then applying the Fast Fourrier Transform function :

$$wacv3_s = w_s \cdot acv3_s \qquad\qquad facv3 = fft(wacv3)$$

The frequencies corresponding to the elements of the Fourrier Transformed data (facv3) are given by:

Frequency (fs) in cycles per second                    Frequency (fh) in cycles per hour

$$fs_k = \frac{k}{128} \cdot \frac{1}{delta}$$

$$fh_k = fs_k \cdot 3600$$

Period (Per) in seconds per cycle (does not apply for k = 0 hence need to temporarily redifine k )

$$k = 1..64 \qquad\qquad Per_k = \frac{1}{fs_k} \qquad\qquad k = 0..64$$

The magintudes of the sinusoidal components of the autocorrelation function of the absolute pressure signal are plotted in the graph below .
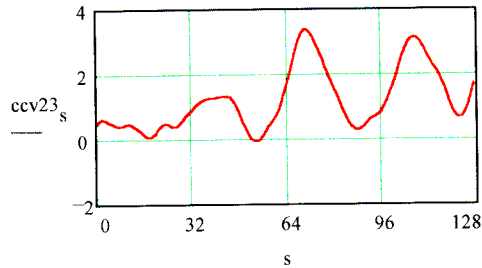
Magnitude of frequency componments of Auto Correlation Function

(magnitude plotted against frequency in cycles per hour)
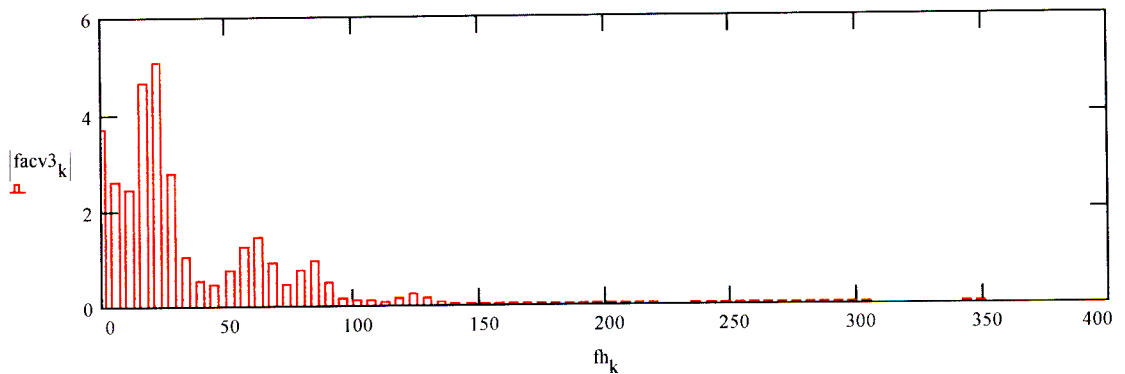


Applying a similar procedure to the calculation of the cross correlation between the absolute pressure and the massecuite temperature :

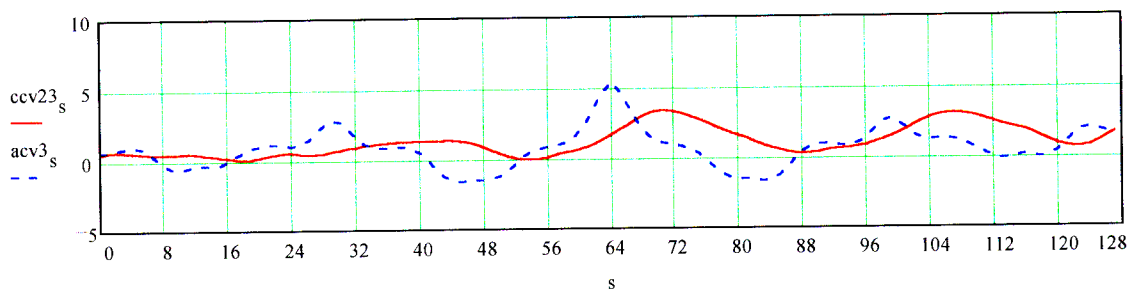$$ccv23_s = \sum_p \left[(v3_p - m) \cdot (v2_{p-64+s} - n)\right]$$

The plot of this cross correlation function (shown below) also demonstrates a clear periodic component



$$wccv23_s \ = \ w_s \cdot ccv23_s \qquad\qquad fccv23 \ = \ fft(wccv23)$$

The plot of both the autocorrelation and cross correlations on the same graph below shows evidence of a "horizontal shift" betheen the two signals of approximately 8 internals (ie 5 * 8 = 40 seconds) :



This "time shift" can be evaluated more accurately by continuing the investigation into the frequency components of the crosscorrelation function as evaluated by the Fourier Transforms as follows.

Magnitude of frequency componments of Cross Correlation Function

(magnitude plotted against frequency in cycles per hour)
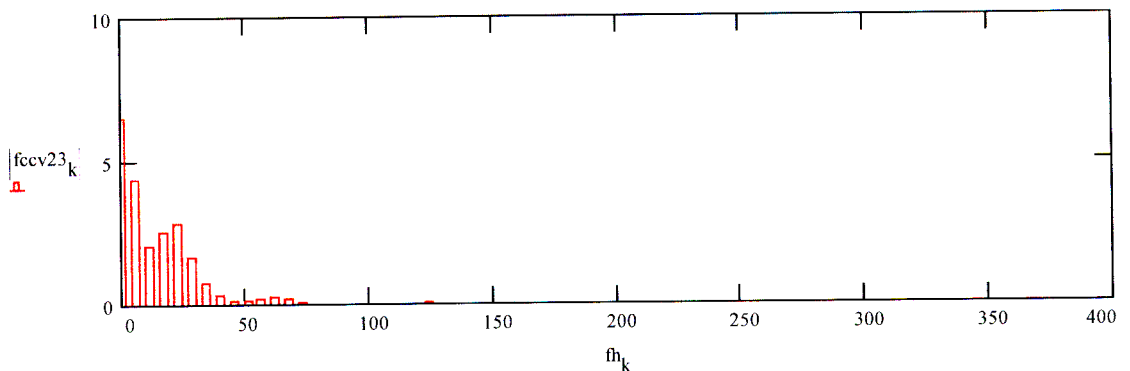


Creating a subscript q to cover the frequency components (ie 1 to 5) which have significant magnitude in both the autocorrelation and the crosscorrelation function :

$$q \ := \ 1 .. 5$$

It is possible to calculate the phase shift from autocorrelation to crosscorrelation for each of these components, expressed as a fraction of a cycle, as follows :

$$\text{Shift}_q = \frac{\arg\left(\text{facv3}_q\right) - \arg\left(\text{fccv23}_q\right)}{2 \cdot \pi}$$

The calculated phase shift can be expressed as time delay on each of these frequency components by :

$$\text{Delay}_q = \text{Shift}_q \cdot \text{Per}_q$$

| $\text{Delay}_q$ | $\text{Per}_q$ | $q$ |
|---|---|---|
| 24.994 | 640 | 1 |
| 33.808 | 320 | 2 |
| 38.879 | 213.333 | 3 |
| 36.769 | 160 | 4 |
| 32.138 | 128 | 5 |

This indicates that the variations in absolute pressure are reflected in variations in massecuite temperature delayed by between 25 and 39 seconds.

## C.2    Evaluation of PRBN Testing Technique by Simulation

This and following pages provide the print-out of a "Mathcad" worksheet which uses a simulation to investigate the suitability of using PRBN testing to measure the dynamic response of a pan compartment to changes in feed valve position.

This File is the evaluation of the PRBN test method on simulated data for a pure Integrating process

The file name is : PRBNTest.mcd

Create variables for use as subscripts :                     $i := 1..1401$              $j := 0..700$

Create a Pseudo-Random Binary Noise (PRBN) input signal, r, which begins at 50 and may change state (between its two possible values of 50 and -50) at every second time interval. The random changes can be selected so that the proportion of time that the signal is at the upper level can be defined by the variable "Prob" which can have values between 0 and 1. Setting Prob := 0.5 provides an input signal which will have an average value tending to zero over long time intervals.

Prob := 0.5

$$r_{2 \cdot j} := 50 - 100 \cdot \Phi(Prob - rnd(1))$$          $$r_{2 \cdot j + 1} := r_{2 \cdot j}$$

ra := mean(r)                    ra = 1.641

Process Input (in arbitary units) plotted versus Sample Number (each delta seconds appart)



Variation in Input with Time
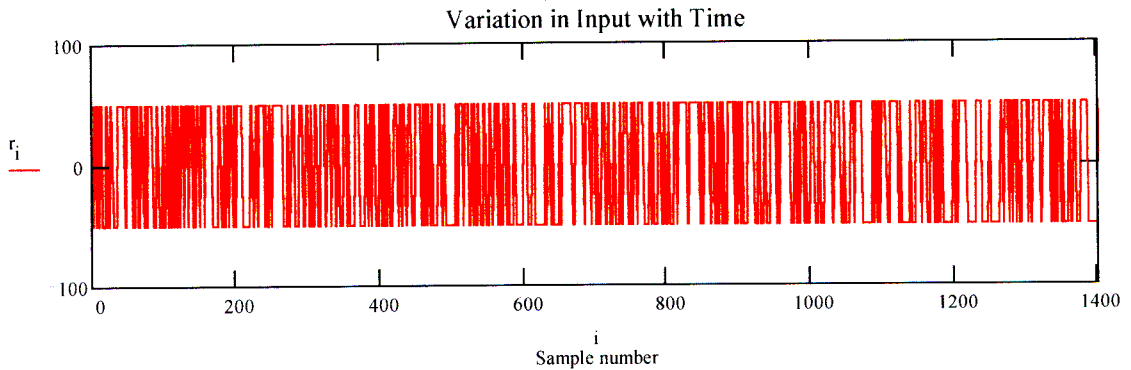
Applying a time scale, the time between each of the values in the input sequence, r, is assumed to be "delta" seconds.

delta := 5

The input signal is assumed to be applied to a pure integrating process with an effective capacity of "Cap" whose units are in seconds. Assuming an initial value for the output of the process, c, a simple calculation is sufficient to estimate the output at all other time intervals since the input remains constant over each time interval.

$$c_0 := 50$$                    Cap := 2000

$$c_i := c_{i-1} + \frac{delta}{Cap} \cdot r_i$$

Process Output (in arbitary units) plotted versus Sample Number (each delta seconds appart)

Variation in Output with Time



$i$
Sample number
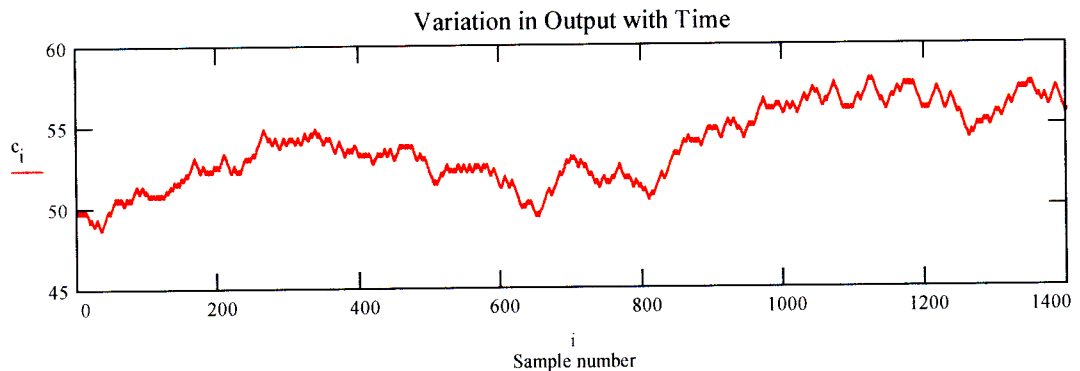
Auto-correlation and cross-correlation functions can be used to investigate the process which determines the relationship between the output and the input (in this instance of a simulation, known to be a pure integrating process). The cross-correlation of the output with the input can be shown theoretically to mimic the expected time response of the process to an input given by the auto-correlarion of the input function.

Creating some subscript variables for use in the calculation of auto and cross correlations :

$$s \quad 0..127 \qquad\qquad p \quad 64..1330 \qquad\qquad q \quad 1..63$$

The total number of readings that will be associated with the variable p is given by :

$$N \quad \sum_{p} 1 \qquad\qquad N = 1.267 \cdot 10^{3}$$

Calculating mean values for the vectors r and c

$$n \quad mean(c) \qquad\qquad m \quad mean(r)$$

$$n = 53.673 \qquad\qquad m = 1.641$$

Calculating the auto-correlation of r (the input signal) over the range of the variable p,

$$acr_s \quad \frac{1}{N} \cdot \sum_{p} \left( r_p \cdot r_{p\ 64\ \mid\ s} \right) \quad m \cdot m$$

Plotting the result to confirm that it approximates the dirac impulse function (which is expected for a PRBN signal). The peak is expected to occur for zero shift, ie at s = 64
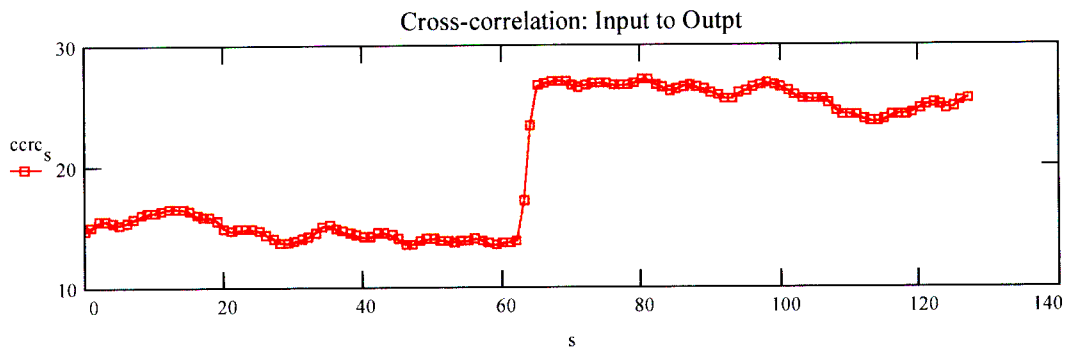
Auto-correlation of Input Signal



$s$
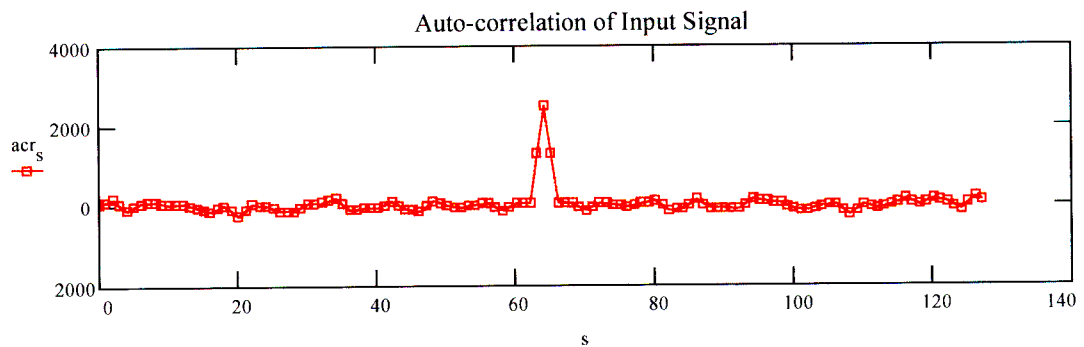
Calculating the cross-correlation between c (the output signal) and r (the input signal), over the range of variable p

$$ccrc_s = \frac{1}{N} \cdot \sum_p \left( r_p \cdot c_{p\ 64+s} \right) \quad m \cdot n$$

Plotting the result to confirm that it approximates the expected response to the impulse function :



Cross-correlation: Input to Outpt

The relationship between the correlation signals is as expected with the cross-correlation simply reflecting the time integral of the auto-correlation signal.

Plotting both signals (suitably scaled) on the same graph around the area of the impulse, it is possible to see the time relationship more clearly.
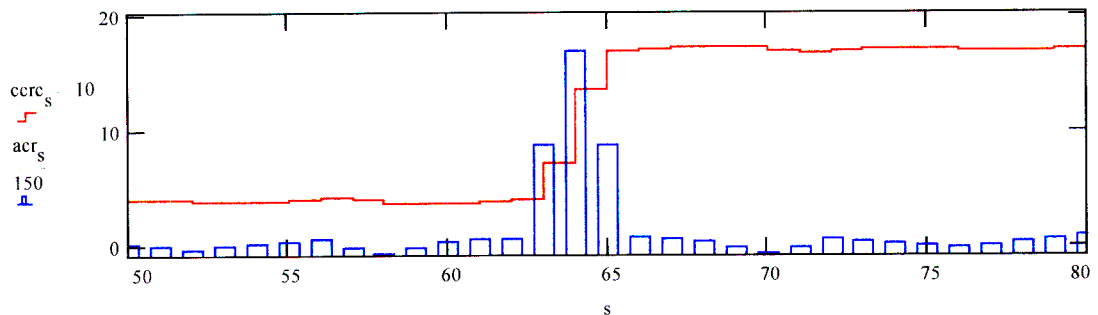


The three major steps in the cross correlation function are clearly directly associated with the three signifigantltly larger than average points on the auto-correlation function.
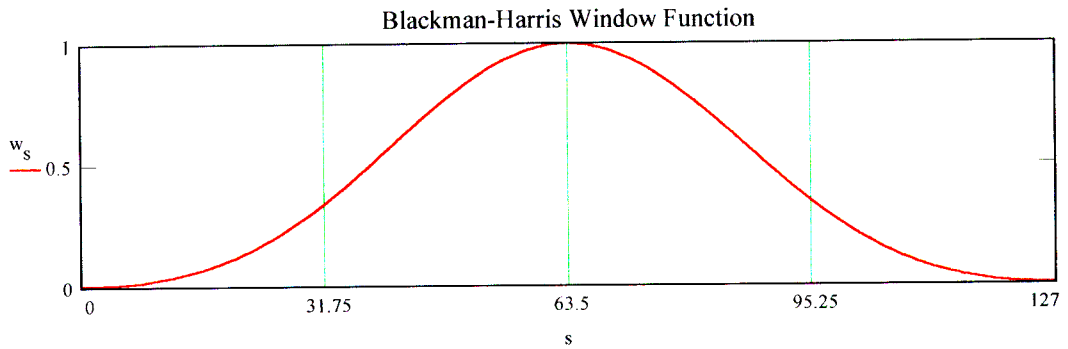
Fourier analysis of the correlation functions provides a method for determining the frequency response of the process, which can be expressed in terms of Bode plots.

To minimise the end effects which result when applying Fourrier Transforms to finite records of data, it is necessary to apply a "windowing" function.  Defining the Blackman-Harris window function over the range of s (0 to 127) to apply to the auto and cross correlation functions prior to evaluating the Fourrier Transforms:

$$a0 \quad 0.42323 \qquad\qquad a1 \quad 0.49744 \qquad\qquad a2 : 0.07922$$

$$w_s \quad a0 - a1 \cdot \cos\left(\frac{2 \cdot \pi}{127} \cdot s\right) \quad a2 \cdot \cos\left(\frac{2 \cdot \pi}{127} \cdot 2 \cdot s\right)$$

The shape of the windowing function is demonstrated in the following graph :

## Blackman-Harris Window Function



Applying the window function to both the auto and cross correlation functions :

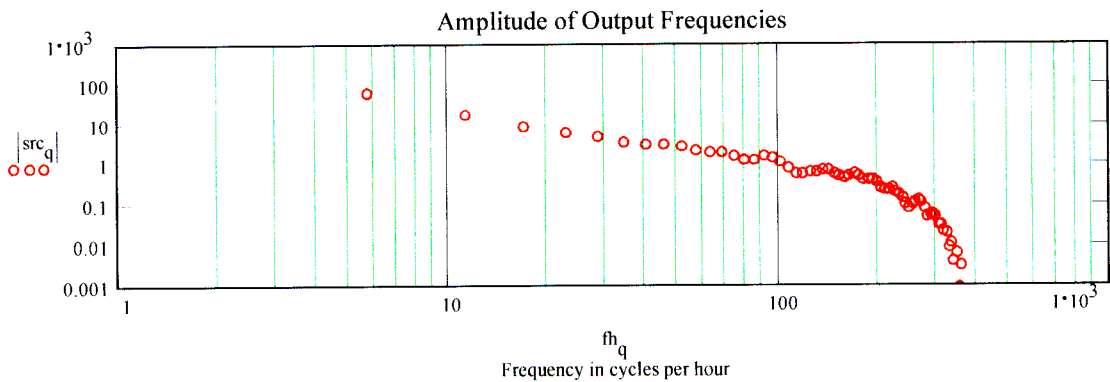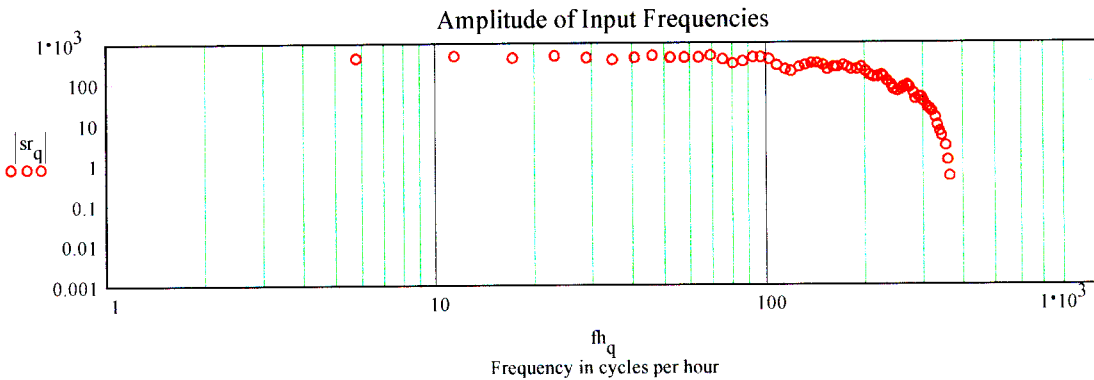$$wacr_s = acr_s \cdot w_s \qquad\qquad wccrc_s = ccrc_s \cdot w_s$$

Calculating the Fourier Transforms of the "windowed" auto and cross correlation functions :
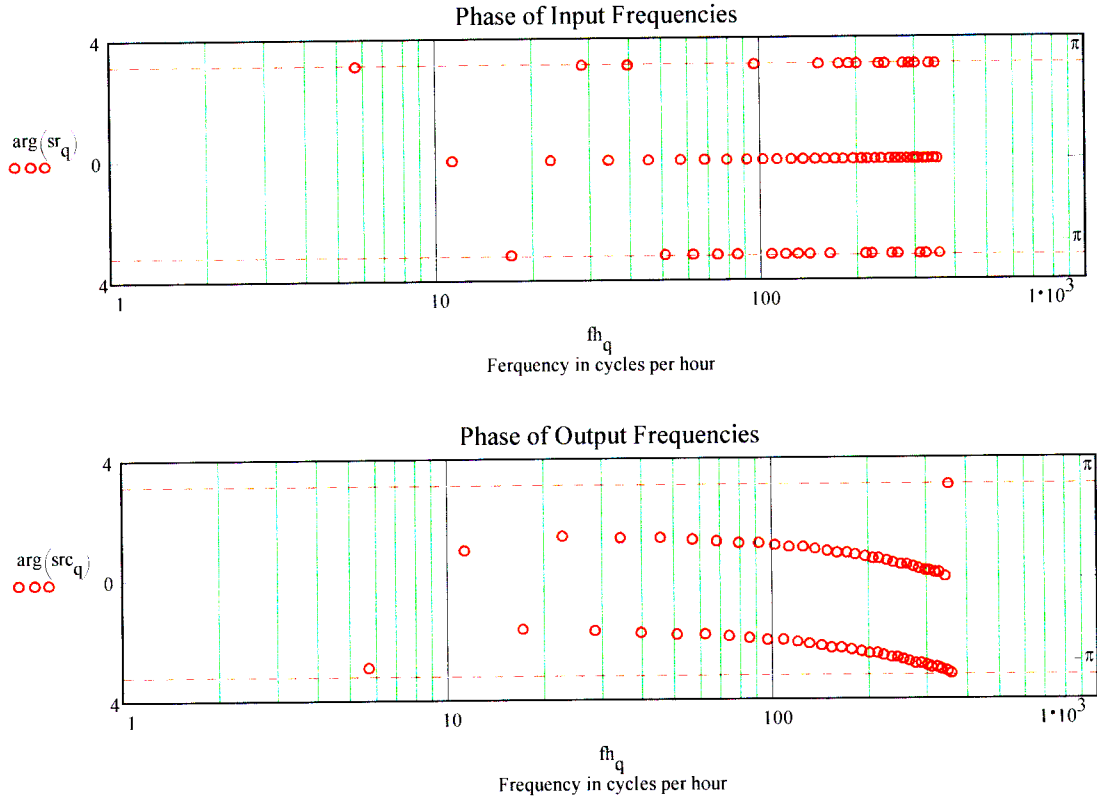
$$sr = fft(wacr) \qquad\qquad src = fft(wccrc)$$

The elements of sr and src are complex numbers which describe the sine waves which can be considered to be the components of acr and ccrc respectively. They are evaluated for only half the number of points for which the original signals are available (ie 128/2 = 64 points). The subscript of sr and src defines the frequency of the sine wave. Given that each reading is "delta" seconds apart, the frequency corresponding to each element of the Fourrier transformed variable is given by :

$$fs_q = \frac{q}{128} \cdot \frac{1}{delta} \quad \text{Frequency in cycles per second} \qquad fh_q = fs_q \cdot 3600 \quad \text{Frequency in cycles per hour}$$

Plotting the amplitude of the signals in the frequency domain :

## Amplitude of Input Frequencies



$fh_q$
Frequency in cycles per hour

## Amplitude of Output Frequencies



$fh_q$
Frequency in cycles per hour

Plotting the phase of the signals in the frequency domain :

### Phase of Input Frequencies



$$fh_q$$

Ferquency in cycles per hour

### Phase of Output Frequencies



$$fh_q$$

Frequency in cycles per hour

Using this information on the frequency content of the sr and src signals, it is possible to develop Bode plots for the process. The transfer function of the process is given by :

$$sp_q := \frac{src_q}{sr_q}$$

The Amplitude Ratio is given by :

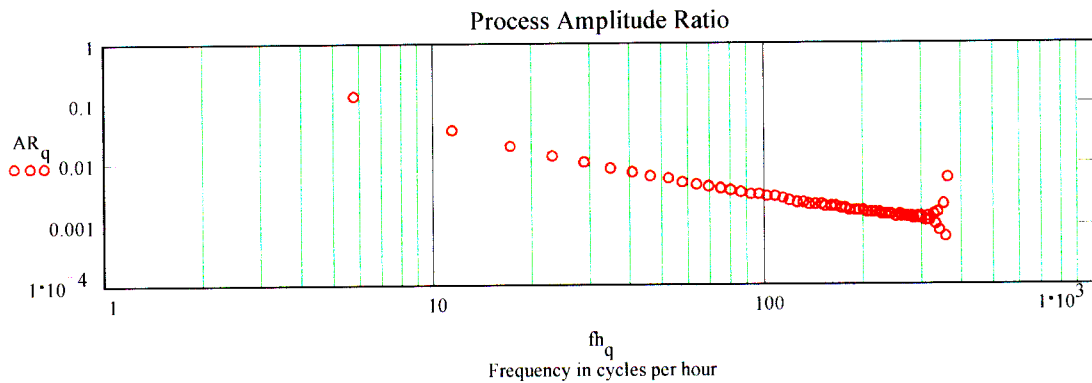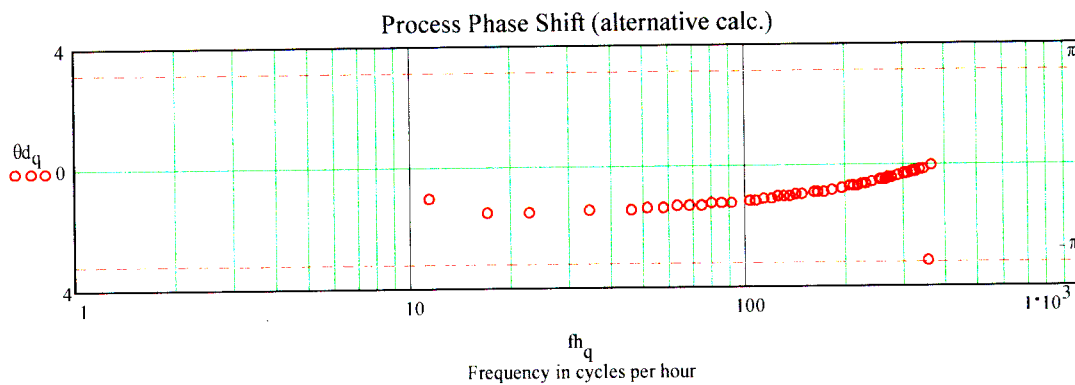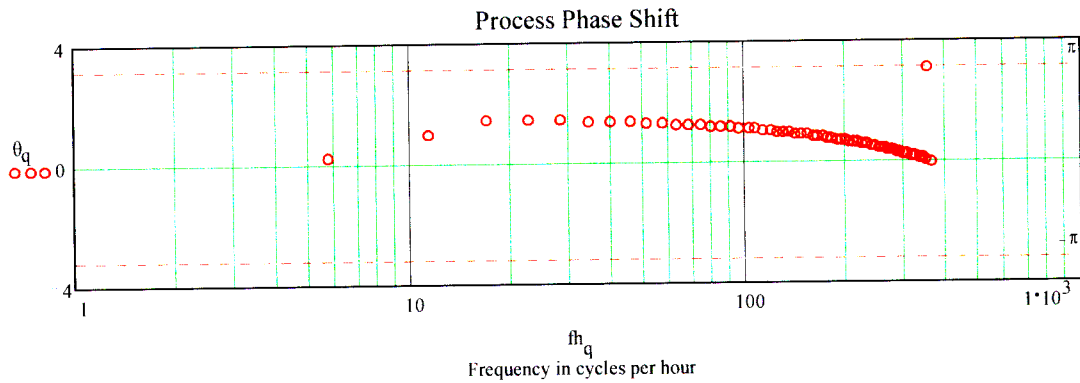$$AR_q := \left| sp_q \right|$$

The Phase Shift is given by :

$$\theta_q := \arg(sp_q)$$

Or, alternatively, Phase Shift is given by :

$$\theta d_q := (\arg(sr_q) - \arg(src_q))$$

### Process Amplitude Ratio



$$fh_q$$

Frequency in cycles per hour

## Process Phase Shift



fh$_q$
Frequency in cycles per hour

## Process Phase Shift (alternative calc.)



fh$_q$
Frequency in cycles per hour

These results can be compared with the Amplitude Ratio and Phase Shift that are predicted by theory for a pure integrating process :

A pure integrating process fed with a sinusoidal input signal of f cycles per hour, will produce a sinusoidal output signal shifted in phase by $-\pi/2$ radians and with an amplitude in the ratio Af to the amplitude of the input signal where Af is given by :
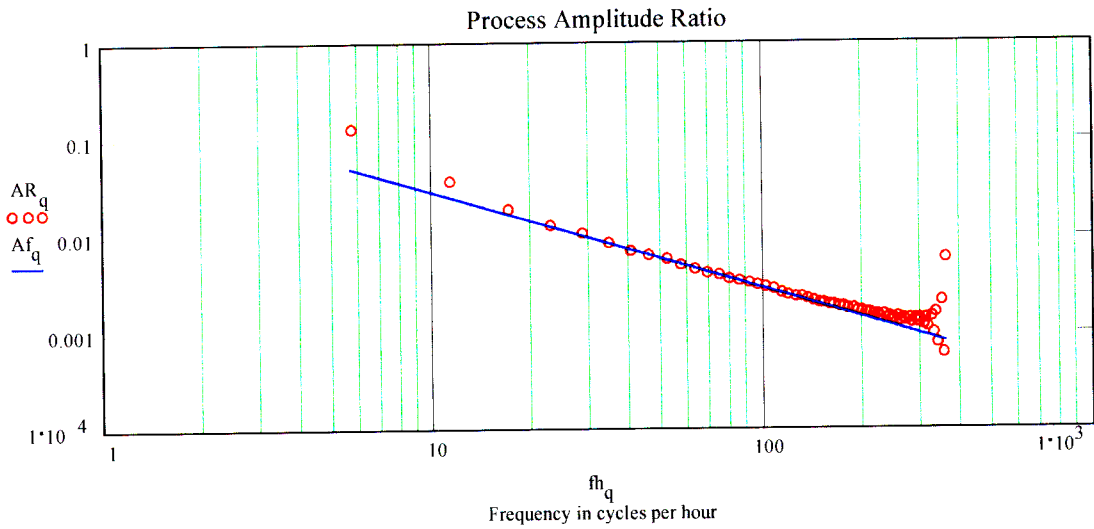
$$Af(C,f) = \frac{1}{\left(2 \cdot \pi \cdot f \cdot \frac{C}{3600}\right)}$$

Where C is the effective capacitance of the process in seconds
Thus for this simulated process the expected process amplitude ratio is given by :

$$Af_q = Af\left(Cap, fh_q\right)$$

Plotting the expected process amplitude ratio on the same graph as that determined from the simulated PRBN testing :

## Process Amplitude Ratio



$fh_q$
Frequency in cycles per hour

This graph shows reasonable agreement beween the expected amplitude ratio and that determined by simulated PRBN testing. Deviations are however evident at both the lower and, particularly, the higher end of the frequency range

The graphs for the process phase shift estimated by the simulated PRBN testing, show that the method of calculation affects the result significantly. The "alternative" calculation procedure best approaches the expected phase shift at a few low frequencies as shown in the graph below.

## Process Phase Shift (alternative calc.)



$fh_q$
Frequency in cycles per hour
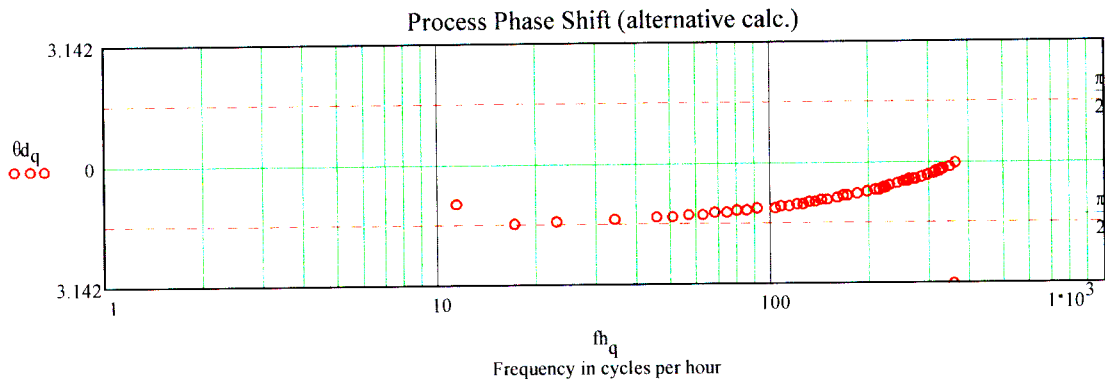
## C.3    Analysis of Plant Measurements Made Using PRBN Signals

This and the following pages are the print-out of a "Mathcad" worksheet which analyses results of PRBN testing used to measure the dynamic response of a pan compartment to changes in feed valve position.

This File is the evaluation of the test on Felixton A1 Pan, Compartment 1 Test C.
The file name is : FXA1OneTestC3.mcd

   M    READPRN(data)

   i    0..1600

Creating Vectors from the columns of the matrix :

$v0 = M^{<0>}$        $v1 = M^{<1>}$        $v2 = M^{<2>}$        $v3 = M^{<3>}$        $v4 = M^{<4>}$

Each element of a vector is a reading taken 5 seconds after/before the previous/subsequent element
v0 is the RF Probe RS Reading
v1 is the RF Probe XS Reading
v2 is the massecuite temperature in the compartment
v3 is the absolute pressure
v4 is the "digital" output to the feed control valve (0 is full closed and 1 is full open)

   $v4 = 100 \cdot v4$



RF RS Variation with Time (% of span)

Sample Number (each 5 seconds appart)



Feed Valve Position (% open)

Sample Number (each 5 seconds appart)
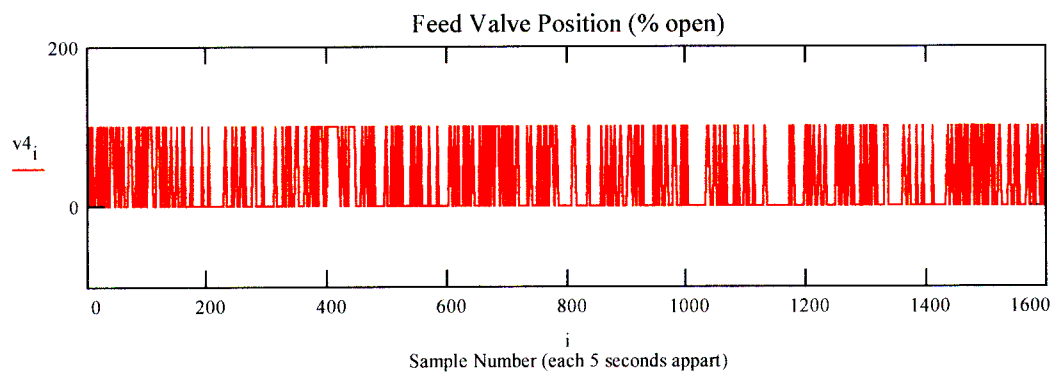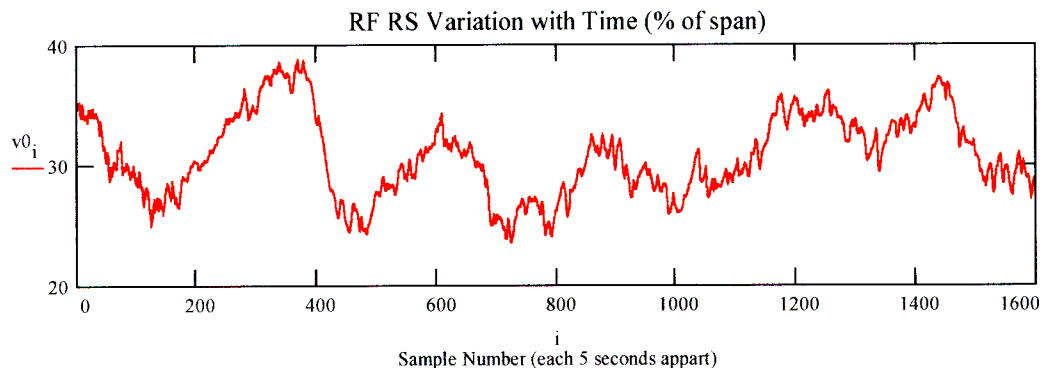
Creating subscript variables for use in the calculation of auto and cross correlations :

   s   0..127              p   64..1330                  r   1..63

C-13

The total number of readings that will be associated with the variable p is given by :

$$N \quad \sum_p 1 \qquad\qquad N = 1.267 \cdot 10^3$$

Calculating mean values for the vectors v0 and v4

$$n \quad mean(v0) \quad n = 30.742 \qquad m \quad mean(v4) \qquad m = 30.492$$

Calculating the auto-correlation of v4 (the input signal) over the range of the variable p

$$acv4_s \quad \frac{1}{N} \cdot \sum_p \left( v4_p \cdot v4_{p\ 64\ \mid\ s} \right) \quad m \cdot m$$

Plotting the result to confirm that it approximates the dirac impulse function, shifted to centre on s = 64
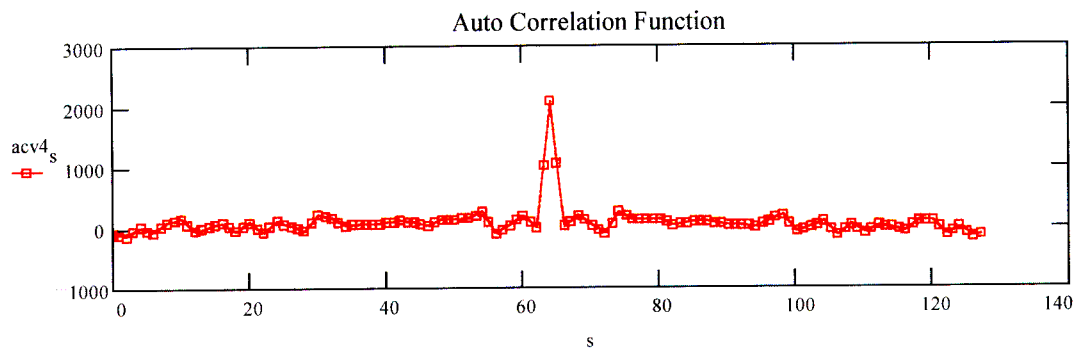


Calculating the cross-correlation between v0 (the output signal) and v4 (the input signal), over the range of variable p

$$ccv04_s \quad \frac{1}{N} \cdot \sum_p v4_p \cdot v0_{p\ 64\ \mid\ s} \quad m \cdot n$$

Plotting the result to confirm that it approximates the expected response to the impulse function :

Plotting both auto- and cross-correlation functions (suitably scaled) on the same graph for the section around the peak in the auto-correlation function :
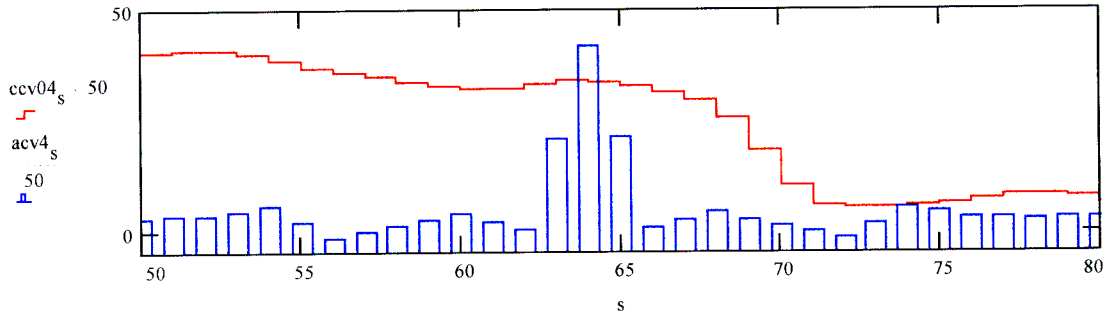


Creating another subscript variable, q, it is possible to estimate by inspection the number of sample intervals by which the cross-correlation function must be shifted for the peak in the auto-correlation function to match the step in the cross correlation 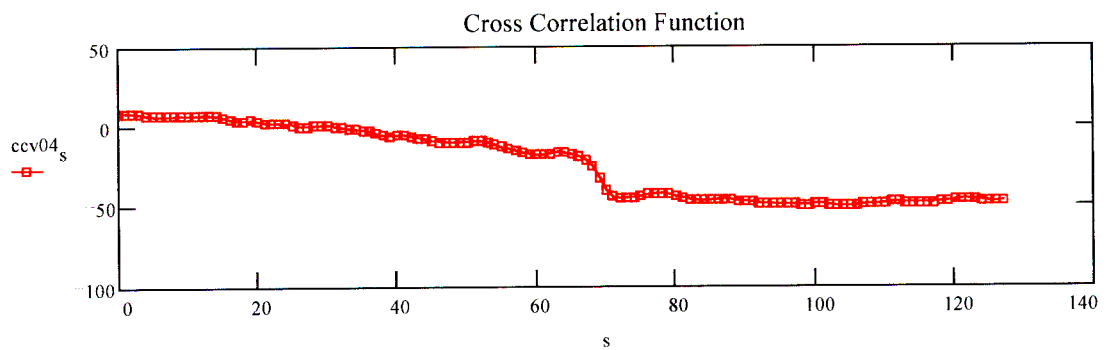function. Values of 5 intervals and 6 intervals (shown in the graph below) give the best match. This shift corresponds to a dead time of between 25 and 30 seconds.

$$q \quad 10..100 \qquad\qquad sccv04_q \quad ccv04_{q+6}$$
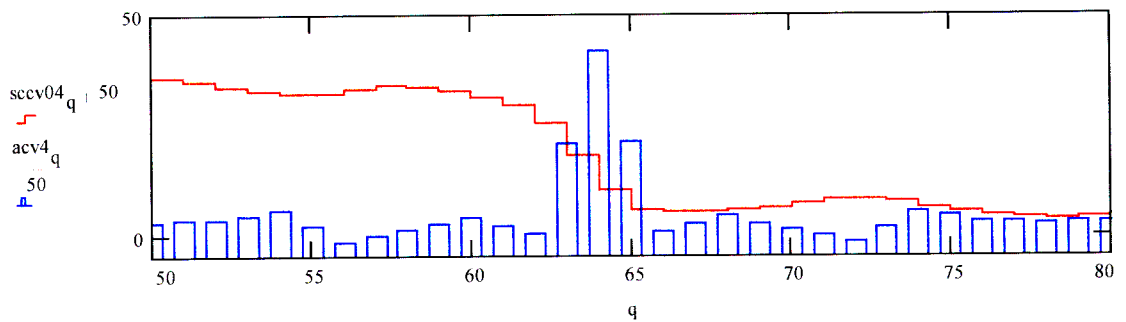


Defining the Blackman-Harris window function over the range of s (0 to 127) to apply to the auto and cross correlation functions before evaluating the Fourrier Transforms :

$$a0 \quad 0.42323 \qquad\qquad a1 \quad 0.49744 \qquad\qquad a2 \quad 0.07922$$

$$w_s \quad a0 \quad a1 \cdot \cos\left(\frac{2 \cdot \pi}{127} \cdot s\right) \quad a2 \cdot \cos\left(\frac{2 \cdot \pi}{127} \cdot 2 \cdot s\right)$$

The shape of the windowing function is demonstrated in the following graph :
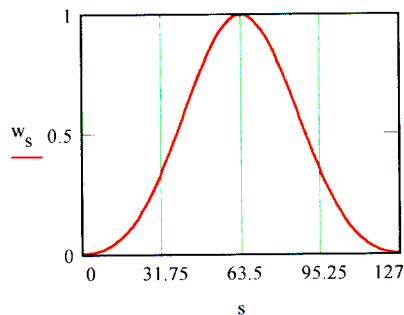
Applying the window function to both the auto and cross correlation functions :

$$wacv4_s \quad acv4_s \cdot w_s \qquad\qquad wccv04_s \quad ccv04_s \cdot w_s$$

Calculating the Fourier Transforms of the "windowed" auto and cross correlation functions :

$$s4 \quad fft(wacv4) \qquad\qquad s04 \quad fft(wccv04)$$

The elements of s4 and s04 are complex numbers which describe the sine waves which can be considered to be the components of acv4 and ccv04 respectively. They are evaluated for only half the number of points for which the original signals are available (ie 128/2 = 64 points). The subscript of s4 and s04 defines the frequency of the sine wave.

Given that each reading is 5 seconds apart, the frequency corresponding to each element of the Fourrier transformed variable is given by (see Mathcad 6.0 Manual page 275) :

$$fs_r \quad \frac{r}{128} \cdot \frac{1}{5} \qquad \text{Frequency in cycles per second}$$

$$fh_r \quad fs_r \cdot 3600 \qquad \text{Frequency in cycles per hour}$$

The range of frequencies evaluated is thus between:

$$fh_1 = 5.625 \qquad\qquad \text{and} \qquad\qquad fh_{63} = 354.375$$

Plotting the amplitude of the signals in the frequency domain :



fh$_r$
Ferquency in cycles per hour



fh$_r$
Frequency in cycles per hour
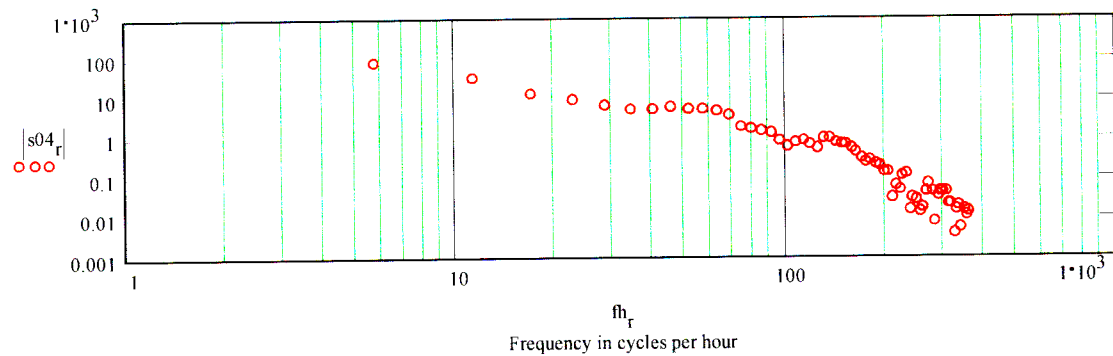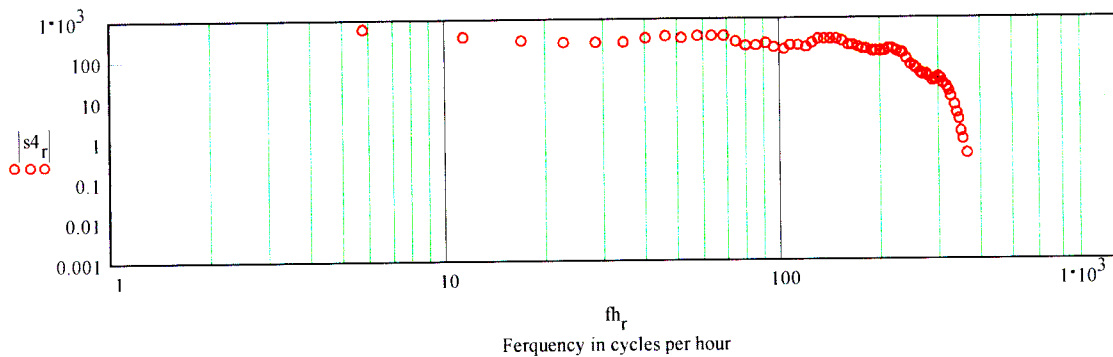
Using this information on the frequency content of the s4 and s04 signals, it is possible to develop an amplitude ratio Bode plot for the process

The Amplitude Ratio is given by :
$$AR_r \quad \frac{\left|s04_r\right|}{\left|s4_r\right|}$$

To evaluate these results in terms of the model of the pan compartment as a pure integrator, the results can be matched to the predicitions of the model for amplitude ratio :

Creating a function, Af(C,f) to describe the model prediction :
$$Af(C,f) \quad \frac{1}{\left(2 \cdot \pi \cdot f \cdot \dfrac{C}{3600}\right)}$$

Assuming a value for the capacitance of 780 seconds gives a reasonable approximation the measured amplitude response over the range of 10 to 100 cycles per hour , as shown in the graph below. Fitting to the higher frequency components is of less importance as these have the smallest magnitudes and are likely to be prone to error :

$$Af_r \quad Af(780, fh_r)$$
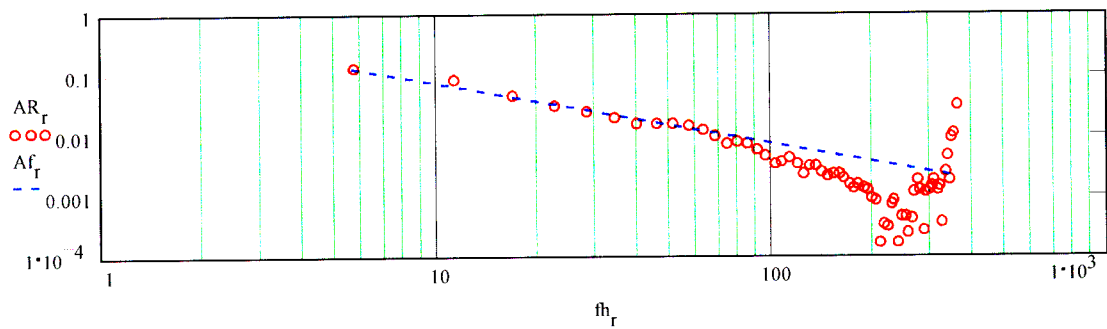
# APPENDIX D

# D.    Derivation of Control Law for Flow Stabilisation

## D.1    General

The definition of the Linear Quadratic Gaussian Control problem as applied to the problem of an optimal buffer strategy is described in detail in Chapter 11. The following two sections provide mathematical details of the symbolic solution to the single tank problem (and an check on the stability of this solution) and the extension of the technique to two tanks in series.

## D.2    Symbolic Derivation for Single Buffer Tank

Following the state space definition of the buffer control problem developed in Chapter 11 (section 11.8) it is possible to solve the Riccati equation symbolically as follows :

Writing the matrix $P$ in terms of its elements,

$$P = \begin{pmatrix} p_{11} & p_{12} \\ p_{21} & p_{22} \end{pmatrix}$$

(D.1)

the Riccati equation (11.58) can be simplified to:

$$\begin{pmatrix} \dfrac{p_{12} + p_{21}}{A_t} + p_{11}^{\,2} \cdot R^{-1} & \dfrac{p_{22}}{A_t} + p_{11} \cdot p_{12} \cdot R^{-1} \\ \dfrac{p_{22}}{A_t} + p_{11} \cdot p_{21} \cdot R^{-1} & p_{21} \cdot p_{12} \cdot R^{-1} - Q \end{pmatrix} = 0$$

(D.2)

This may be written as four simultaneous equations.

$$p_{12} + p_{21} + p_{11}^{\,2} \cdot A_t \cdot R^{-1} = 0$$

(D.3)

$$p_{22} + p_{11} \cdot p_{12} \cdot A_t \cdot R^{-1} = 0$$

(D.4)

$$p_{22} + p_{11} \cdot p_{21} \cdot A_t \cdot R^{-1} = 0 \qquad \text{(D.5)}$$

$$p_{21} \cdot p_{12} \cdot R^{-1} - Q = 0 \qquad \text{(D.6)}$$

From equations (D.4) and (D.5) it is evident that $p_{12} = p_{21}$ (i.e. the matrix $P$ is symmetric). Thus from equation (D.6):

$$p_{12}{}^2 = Q \cdot R \qquad \text{(D.7)}$$

and from equation (D.3)

$$p_{11}{}^2 = -\frac{2 \cdot p_{12} \cdot R}{A_t} \qquad \text{(D.8)}$$

Since both $R$ and $A_t$ are positive, $p_{12}$ must be negative. Thus from equation (D.7):

$$p_{12} = -\sqrt{Q \cdot R} \qquad \text{(D.9)}$$

and substituting equation (D.9) into equation (D.8) yields :

$$p_{11}{}^2 = \frac{2 \cdot \sqrt{Q \cdot R} \cdot R}{A_t} \qquad \text{(D.10)}$$

Thus

$$p_{11} = \frac{\left(4 \cdot Q \cdot R^3\right)^{\frac{1}{4}}}{\sqrt{A_t}} \qquad \text{(D.11)}$$

Substituting equations (D.11) and (D.9) into equation (D.4) yields :

$$p_{22} = \sqrt{Q \cdot R} \cdot \frac{\left(4 \cdot Q \cdot R^3\right)^{\frac{1}{4}}}{\sqrt{A_t}} \cdot \frac{A_t}{R}$$

$$= \left(4 \cdot Q \cdot R^3\right)^{\frac{1}{4}} \cdot \sqrt{A_t}$$

(D.12)

Thus the gain matrix, K, is given by:

$$K = R^{-1} \cdot B^T \cdot P$$

$$= R^{-1} \cdot \begin{pmatrix} 1 & 0 \end{pmatrix} \cdot \begin{pmatrix} \dfrac{\left(4 \cdot Q \cdot R^3\right)^{\frac{1}{4}}}{\sqrt{A_t}} & -\sqrt{Q \cdot R} \\ -\sqrt{Q \cdot R} & \left(4 \cdot Q \cdot R^3\right)^{\frac{1}{4}} \cdot \sqrt{A_t} \end{pmatrix}$$

(D.13)

$$= \begin{pmatrix} \dfrac{\left(4 \cdot \dfrac{Q}{R}\right)^{\frac{1}{4}}}{\sqrt{A_t}} & -\sqrt{\dfrac{Q}{R}} \end{pmatrix}$$

The gain matrix is thus dependent on the ratio of the weighting factors Q and R. This is what would be expected since Q and R are scalars and it is only their <u>relative</u> magnitude that is important in specifying the balance between tight level control and slow variations in outlet flow.

If we introduce the weighting factor $W = \dfrac{Q}{R}$ then the gain matrix is given by:

$$K = \begin{pmatrix} \left(\dfrac{4 \cdot W}{A_t^2}\right)^{\frac{1}{4}} & -\sqrt{W} \end{pmatrix}$$

(D.14)

The control law (equation 11.54) is :

$$u = -K \cdot x$$

(D.15)

Which can now be expressed in terms of measured variables as:

$$u = -\left(\frac{4 \cdot W}{A_t^2}\right)^{\frac{1}{4}} \cdot \left(q_o(t) - q_s\right) + \sqrt{W} \cdot \left(h(t) - h_s\right) \qquad \text{(D.16)}$$

This provides a very simple control law with a single tuning parameter, $W$. Altering the value of $W$ will allow the balance between the conflicting objectives of level control and outlet flow control to be adjusted whilst ensuring that control remains stable.

The stability of the system can be investigated by considering the closed loop system given by substituting the control law (equation 11.54) into the system equation (11.51):

$$\dot{x} = A \cdot x - B \cdot K \cdot x$$
$$\text{ie} \qquad \dot{x} = \overline{A} \cdot x \qquad\qquad\qquad \text{(D.17)}$$
$$\text{where} \quad \overline{A} = \left(A - B \cdot K\right)$$

For stability, the eigen values of the matrix $\overline{A}$ must have negative real parts. Using the notation:

$$K = \begin{pmatrix} k_1 & k_2 \end{pmatrix} \qquad\qquad \text{(D.18)}$$

It is possible to write :

$$\overline{A} = \begin{pmatrix} k_1 & k_2 \\ -A_t^{-1} & 0 \end{pmatrix} \qquad\qquad \text{(D.19)}$$

The eigen values of $\overline{A}$ are given by solving:

$$\det\left(\overline{A} - \lambda \cdot I\right) = 0 \qquad\qquad \text{(D.20)}$$

where          $\lambda$         are the eigen values

                  I          is the identity matrix

and          det          is the determinant

this gives:

$$\lambda^2 + k_1 \cdot \lambda - \frac{k_2}{A_t} = 0 \qquad\qquad \text{(D.21)}$$

and thus

$$\lambda = \frac{k_1 \pm \sqrt{k_1^2 + 4 \cdot \dfrac{k_2}{A_t}}}{2}$$

(D.22)

Substituting for $k_1$ and $k_2$ and simplifying yields:

$$\lambda = -\left(\frac{W}{4 \cdot A_t^2}\right)^{\frac{1}{4}} \pm \left(\frac{W}{4 \cdot A_t^2}\right)^{\frac{1}{4}} \cdot i$$

(D.23)

$$\text{where} \quad i = \sqrt{-1}$$

The real parts of the eigen values of $\overline{A}$ will thus always be negative, and the control is guaranteed to be stable. The damping of oscillatory behaviour is characterised by the "damping factors" of the eigen values which are given by:

$$\rho = \frac{-\operatorname{Re}(\lambda)}{|\lambda|}$$

(D.24)

Since the real and imaginary parts of the eigen values are equal:

$$\rho = 0{,}707$$

(D.25)

## D.3    Extension to Multiple Tanks in Series

As discussed conceptually in Chapter 11 (section 11.3) and demonstrated by Cheung and Luyben (1979), when conventional control algorithms are applied to a sequence of buffer tanks in series, there is an amplification of the disturbance down the train.

This problem can be avoided by formulating a multi-variable control strategy using the concept developed for a single buffer tank.. Using the notation developed in section 11.2 as a basis, it is possible to formulate differential equations to describe the behaviour of two tanks in series as

follows :

$$\frac{dh_1'(t)}{dt} = -\frac{1}{A_{1t}} \cdot q_o'(t) \tag{D.26}$$

$$\frac{dh_2'(t)}{dt} = -\frac{1}{A_{2t}} \cdot \left(-q_1'(t) + q_2'(t)\right) \tag{D.27}$$

The subscripts 1 and 2 are used to signify the first and second tanks respectively. Flows are referenced to the tank out of which they are flowing.

To express this in state space format, the state and control variables are defined as :

$$x_1(t) = q_1'(t)$$
$$x_2(t) = h_1'(t)$$
$$x_3(t) = q_2'(t)$$
$$x_4(t) = h_2'(t)$$
$$u_1(t) = \frac{dq_1'(t)}{dt} \tag{D.28}$$
$$u_2(t) = \frac{dq_2'(t)}{dt}$$
$$y_1(t) = x_2(t)$$
$$y_2(t) = x_4(t)$$

The differential equations describing the system can thus be written as :

$$\dot{x}_1(t) = u_1(t)$$
$$\dot{x}_2(t) = -\frac{1}{A_{1t}} \cdot x_1(t)$$
$$\dot{x}_3(t) = u_2(t) \tag{D.29}$$
$$\dot{x}_4(t) = \frac{1}{A_{2t}} \cdot x_1(t) - \frac{1}{A_{2t}} \cdot x_2(t)$$

Using the standard matrix format, the A, B and C matrices are defined as :

$$A = \begin{pmatrix} 0 & 0 & 0 & 0 \\ -\dfrac{1}{A_{1t}} & 0 & 0 & 0 \\ 0 & 0 & 0 & 0 \\ \dfrac{1}{A_{2t}} & 0 & -\dfrac{1}{A_{2t}} & 0 \end{pmatrix}$$

$$B = \begin{pmatrix} 1 & 0 \\ 0 & 0 \\ 0 & 1 \\ 0 & 0 \end{pmatrix} \qquad\qquad (\text{D.30})$$

$$C = \begin{pmatrix} 0 & 1 & 0 & 0 \\ 0 & 0 & 0 & 1 \end{pmatrix}$$

The control law is given by :

$$\begin{pmatrix} u_1 \\ u_2 \end{pmatrix} = \begin{pmatrix} K_{11} & K_{12} & K_{13} & K_{14} \\ K_{21} & K_{22} & K_{23} & K_{24} \end{pmatrix} \cdot \begin{pmatrix} x_1 \\ x_2 \\ x_3 \\ x_4 \end{pmatrix} \qquad\qquad (\text{D.31})$$

# APPENDIX E

## E.    Details of Computer Programs Developed

### E.1    General

The details of the computer programs provided in this appendix are intended to describe the calculation approach and the algorithms which have been used. Given the continuing changes in computing technology full printed listings of the programs which were developed and used in this research would be of questionable utility. This is particularly so when, as in this work, there is a significant use of commercial "toolboxes" of standard routines for :

- graphical display of data,
- serial communications,
- numerical analysis,
- operator interface and data input.

The development of programs for the Windows operating system using what are known as Rapid Applications Development environments (in this work the Delphi system ) also does not lend itself to providing a clear printed listing of the program.

The programming of calculations embedded in conventional spreadsheets is particularly cryptic if directly documented as lists of cell references. Fortunately the Mathcad "free-form mathematic worksheet" used in a number of application in this research (Chapter 10 and Appendix C) is to a large degree self-documenting.

Given these limitations of providing full listings of the computer programs developed in this research, the details provided in this appendix are intended merely to described the techniques employed in the programs.

The following commercial software has been used in this research :

Operating Systems

MS-DOS 3.3 by  Microsoft Corporation

MultiDos Plus by Nanosoft of Natic Massachusetts

Windows 95 by Microsoft Corporation

Spreadsheets :

Corel Quatro Pro by Corel Corporation, Ottawa, Ontario.


Programming Languages and Environments

Turbo Pascal 5.0 by Borland International Inc., Scotts Valley Calafornia.

Borland Delphi 4 by Inprise Corporation, Scotts Valley, California.

Corel Quatro Pro Spreadsheet, Corel Corporation, Ottawa, Ontario.

Mathcad by Mathsoft Inc., Cambridge, Massachusetts.

Matrix$_x$ by Integrated Systems Inc., Santa Clara, California.


ToolBoxes

Technojock's Turbo Toolkit V 5.0 by TechnoJock Software Inc. Houston Texas

Science and Engineering Tools for Turbo Pascal 4.0/5.0 by Quinn-Curtis,

Needham Massachusetts

Asynch Plus V5.0 by Blaise Computing Inc. Berkeley California

Routines from the book "Numerical Recipes in Pascal, The Art of Scientific

Computing" by Press et al. (1989)


## E.2    Control and Data Logging Program

The development of a PC control and data logging system is described in Chapter 12. The system
is based on using the features of MultiDos Plus multitasking operating system. Examples are
given below of a function and a procedure written to use the features of the multitasking
operating system by using software interrupts. The program code may then use these features in
a clear and concise way.

```
function MessAvail( n : Integer ) : boolean ;

var
  reg : registers ;

begin
  MessAvail := false ;
  reg.AX := 1280 + n ; { code for check for message in queue
```

```
                          number n }
        intr(21,reg) ;
        if reg.DX <> 0  then MessAvail := true ;
    end ;   {  OF MESSAGE AVAILABLE FUNCTION }



    procedure RecMess( high , low , n , l  : Integer  ) ;


    var
       reg : registers ;

    begin
       with reg do
         begin
            AX := 1536 + n ; ES := high ; DI := low ; CX := 1
            {n - is the message queue number                    }
            {l - is the length of the message in bytes          }
            {high - is the high address of the message destination }
            {low  - is the low  address of the message destination }
         end ;
         intr(21,reg) ;
         {Note that the task will be suspended until a message is
available }
    end ;    { OF RECEIVE MESSAGE PROCEDURE }
```

A example of how this procedure and function might be used in writing a task would be :

```
    if MessAvail(1) then RecMess(hiaddress,lowaddress,1,messlength) ;
```

This will cause the task to check for a message in queue number 1 and if it is available to receive a message from this queue of length, messlength, and place it an address specified by hiaddress and lowaddress.


## E.3    Steady State in A Continuous Pan Compartment


The determination of steady state in a continuous pan compartment is an important element of the  three programs described below ( PANSIM, PANMOD and PANOPT ). The calculation procedure follows that described in Chapter 4, using the equations derived in Appendix B. The

calculation procedure is shown as a flow chart in Figure E.1 below.
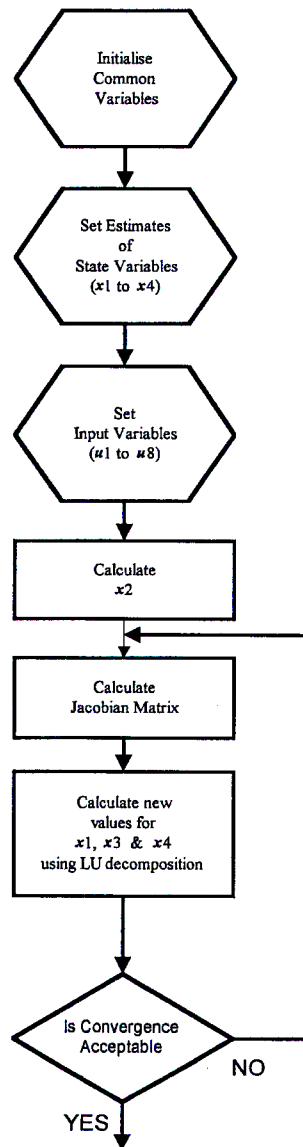


**Figure E.1** Procedure to calculate compartment steady state using Newton-Raphson method

## E.4    Simulation of Continuous Pan Performance

The ability to simulate the steady state performance of a multi-compartment continuous pan is a necessary component of both the program to estimate growth kinetics by fitting the model to experimental data (MODPAN) and the program to determine the optimum steady state performance (OPTPAN). The simulation of performance is also a useful tool in its own right as a design tool (SIMPAN). As a stand-alone simulation it is not sufficient to be able to simulate

performance for set values of the inputs, but also requires the ability to simulate automatic control which holds compartment conditions at desired set-points (eg of crystal content). Rather than attempting to simulate conventional control loops it is possible to achieve this type of model behaviour by implementing a numerical root finding technique. The Van Wijngaarden-Dekker-Brent method recommended by Press et al. (1989) has been used in this work.
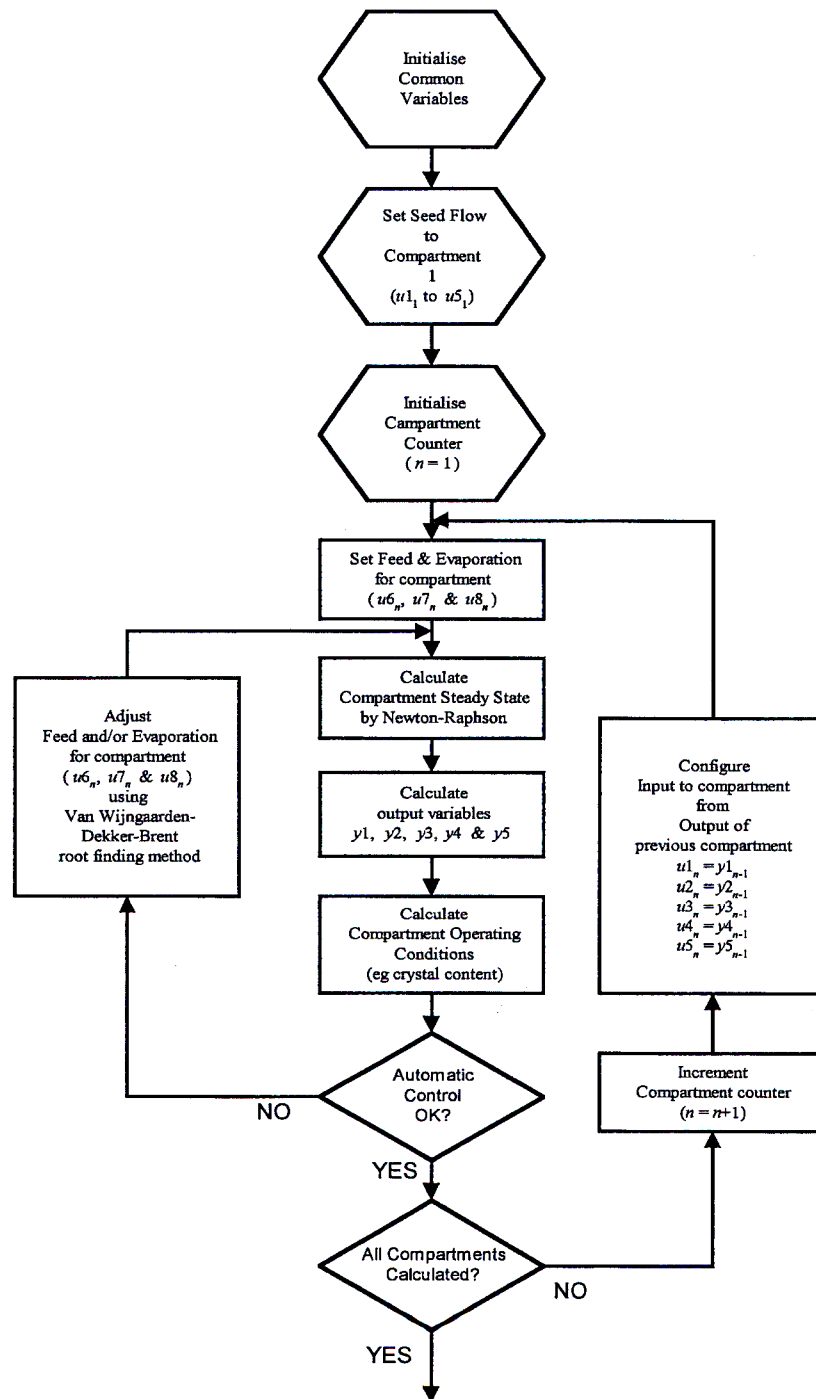


**Figure E.2** Procedure for a steady state simulation of a multi-compartment continuous pan

## E.5      Evaluation of Continuous Pan Performance

The evaluation of continuous pan performance is achieved by matching the steady state model of the continuous pan to the experimental measurements by adjusting selected model parameters. The procedure is illustrated in the schematic flow diagram of Figure E.3.
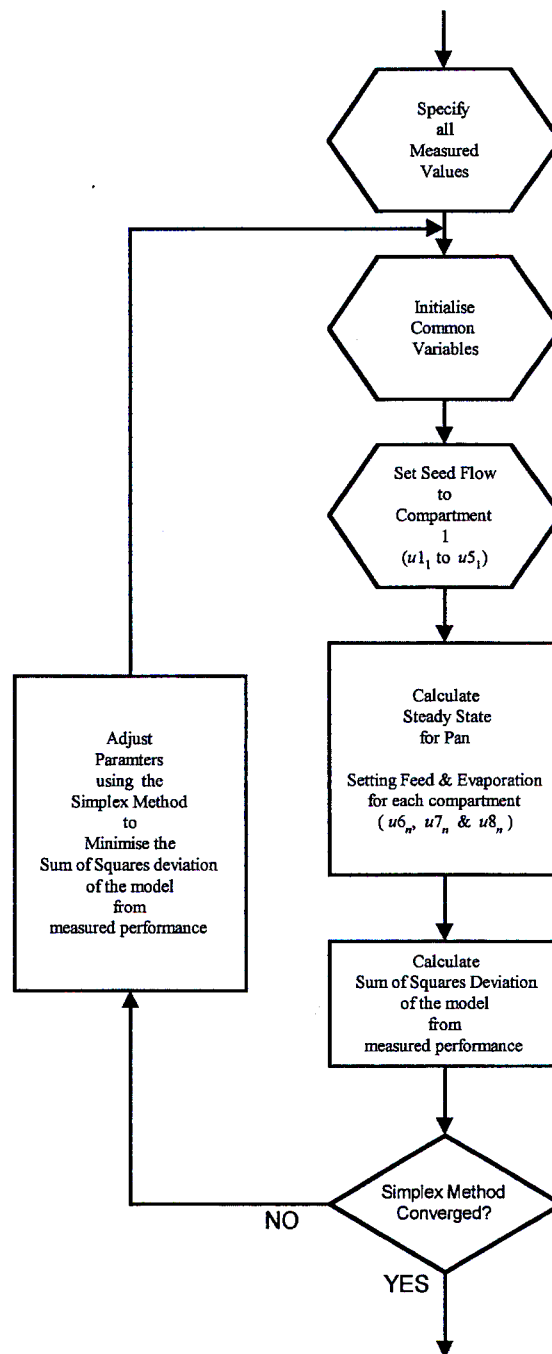


**Figure E.3** Procedure for evaluating pan performance by fitting the model to measurements

The multi-dimensional minimisation technique selected to fit the model to plant measurements is the Simplex method. The Simplex method has the particularly advantageous properties of not requiring the evaluation of derivatives and being immune to the possibility of divergence (Caceci and Cacheris, 1984). The algorithms used in this work are those of Press et al. (1989). The objective of the fitting is to minimise the weighted sum of squares differences between the model and the plant measurements, specifically;

the profiles of nutch purity, mean crystal size and variance in crystal size

and      the total evaporation, the mass flow of seed and the mass flow of massecuite.

Following the recommendations of Beckman (1982) the weighting factors are set as the inverse of the square of the standard deviation, with even approximate values of the standard deviation being reported as being adequate. Estimates of the standard deviation, $\sigma$, are calculated from estimates of the confidence interval of $\pm a$ as suggested by Kneile (1995), using:

$$\sigma = \frac{a}{1.96} \tag{E.1}$$

As discussed in Chapter 7, the program is primarily used to estimate the growth parameters,

$K_1$      the proportional dependance of growth on oversaturation

and   $p$      the size dispersion parameter.

However, because of the way the simulation works it is also necessary to adjust the seed properties ($u3$, $u4$ and $u5$) to achieve the best fit. This is because there is no reason why the measurements of the seed properties should be assumed to be any more accurate than the measurements of massecuite properties in the other compartments.

For those tests where measurements of syrup flows were not available, the syrup flows to the individual compartments were included as extra parameters to be fitted by the Simplex method. The values of the inputs $u6$ and $u7$ are calculated from the syrup flow (measured or fitted) and the syrup brix ($sybx$) and purity ($pty$) or from the measured water flow for those compartments fed with water. The evaporation rate in each compartment $u8$ is not measured but is calculated for each compartment from the measured massecuite brix, using the following relationship derived from a simple steady state mass balance over the compartment :

$$u8 = \frac{\left( u2 + u6 \cdot \dfrac{(100 - sybx)}{100} - (u1 + u6) \cdot \dfrac{(100 - mcbx)}{100} \right)}{\left( 1 - \dfrac{(100 - mcbx)}{100} \right)}$$

(E.2)

## E.6    Determination of Optimum Operating Conditions

The procedure for determining the optimum steady state operating profile for a continuous pan is described in detail in Chapter 8. The program is computationally intensive particularly if larger grid sizes around the nominal trajectory are used. There is also a large demand for the storage of intermediate variables which is addressed by the use of dynamic (pointer) variables which are available in Pascal.

A flow chart showing the major aspects of the calculation procedure is provided in Figure E.4 on the following page.

The constraints of the optimisation problem (as discussed in section 8.3.6) are handled in the section of the program where the best performance for a grid point is selected. A calculated massecuite condition that violates any of the constraints (eg allows false grain formation) is excluded at this stage of the procedure, even if the calculation indicates a better performance in terms of the criterion of minimising the mass flow of sucrose in solution. Any grid point which has no viable operating condition is noted as such for the particular compartment being considered. This grid point will not then be used when evaluating all the possible inputs to the next pan compartment in the sequence.

In this way the search for the optimum steady state profile proceeds by continually refining a viable profile whilst ensuring at each step that none of the constraints is violated.
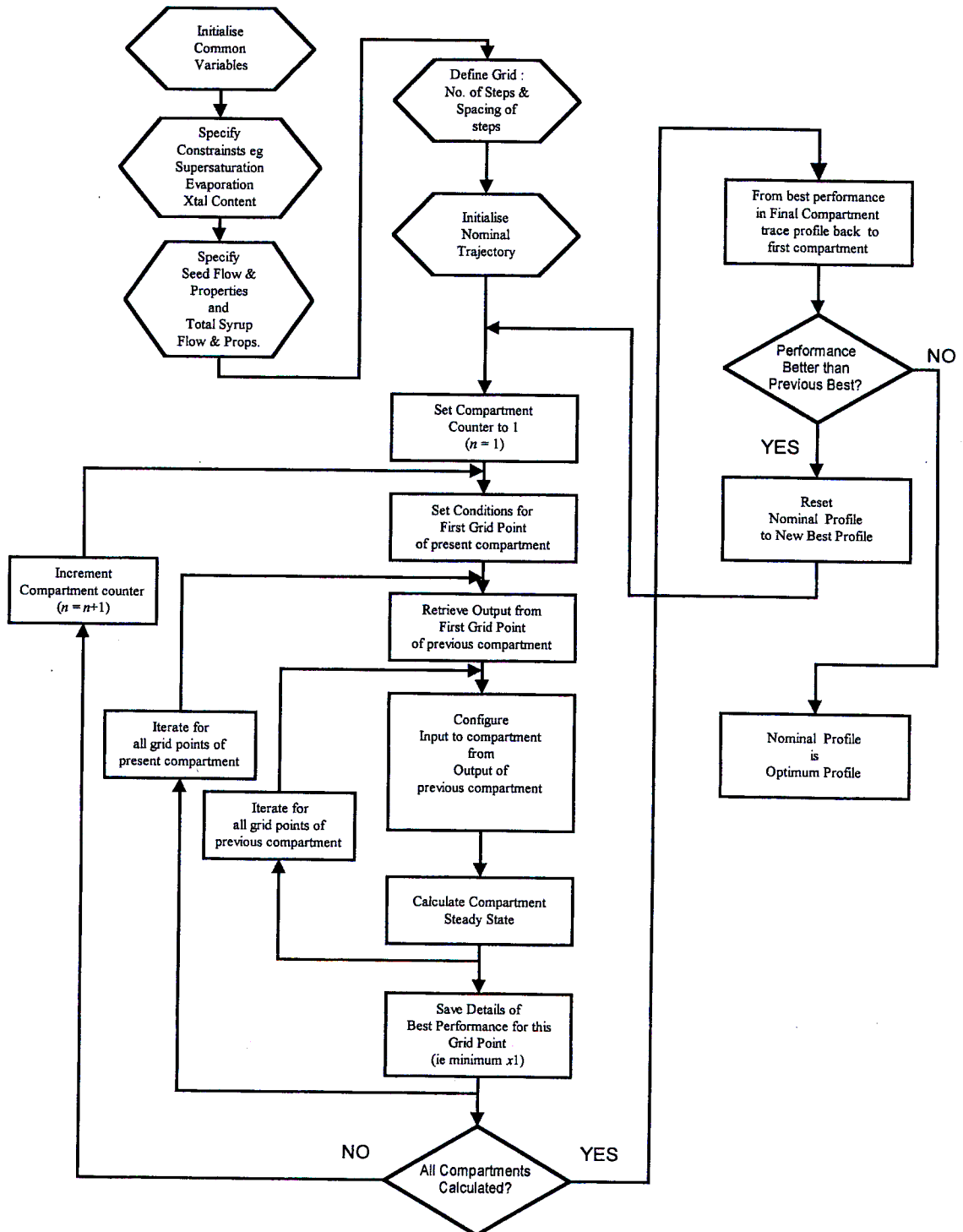
**Figure E.4** Procedure for determining optimum steady state by dynamic programming.

## E.7    Measurement of Crystal Sizes

Crystal size measurements by semi-automated counting have been available as a service from the Sugar Milling Research Institute who use a commercially available system to perform the analysis ( Kontron Videoplan as described by Lionnet, 1998 ). Samples taken during the testing of continuous pans described in Chapter 7 were analysed by this method.

Advances in computer hardware and software have enabled the functionality of the Kontron system to be emulated using cheap hardware and software developed using the Delphi programming system. Images of crystals are obtained from a monochrome video camera mounted on a microscope. These images are captured in digital format and stored (in standard formats such as .jpg or .bmp) on disk by having the video camera connected to a standard PC using the SNAPPY video interface. The images can then be subsequently analysed using the specially developed software.

The major advantage of this system, as a result of its cheap cost, was the ability to have a system dedicated for use in monitoring and analysing the results of batch pan boilings conducted in the laboratory. This removed the need for the storage of samples for later analysis, and provided the facility for capturing images directly from glass windows on the pan. The images captured directly from the pan used the body of an old microscope combined with the video camera and mounted on a bracket which allowed the unit to be positioned at an appropriate position to observe splashes of massecuite on the pan window.

Early attempts at developing software for analysing images of crystals using the Pascal language were unsuccessful because of the complexities of handling the image files. The Delphi programming system provides the necessary routines for handling the importation and display of digital images without any need to understand the complexities of the process. Combined with the ability to use a mouse to move a cursor across the screen and track its position, it becomes a simple task to calculate the size of a crystal marked out by the operator using mouse clicks.

The intention of the program is to fit rectangular boxes which approximate the crystals observed on the screen. The operator is first required to mark two adjacent corners of a crystal designated by the coordinates $(x_1, y_1)$ and $(x_2, y_2)$. The operator is then required to mark a point anywhere

along the opposite edge of the crystal from that specified by $(x_1, y_1)$ and $(x_2, y_2)$. This point is designated by $(x_t, y_t)$. The other corners of the crystal, $(x_3, y_3)$ and $(x_4, y_4)$, can be calculated by simple coordinate geometry.

The calculations are based on calculating equations of the form :

$$y = m \cdot x + c \qquad \text{(E.3)}$$

which define straight lines passing through pairs of points. The slope of a line perpendicular to a given line can be calculated from the fact that the product of the two slopes is equal to -1.

The calculation procedure first calculates the slope and intercept of the line passing through points $(x_1, y_1)$ and $(x_2, y_2)$ as :

$$m_1 = \frac{y_1 - y_2}{x_1 - x_2}$$

$$c_1 = y_1 - m_1 \cdot x_1 \qquad \text{(E.4)}$$

The equation of the line passing through the temporary point $(x_t, y_t)$ which characterises the opposite edge of the crystal, has the same slope but a different intercept given by :

$$c_2 = y_t - m_1 \cdot x_t \qquad \text{(E.5)}$$

The line perpendicular to these two lines and passing through the point $(x_2, y_2)$ has an intercept given by :

$$c_3 = y_2 + \frac{x_2}{m_1} \qquad \text{(E.6)}$$

Using these parameters it is possible to calculate the co-ordinates of the other two corners of the crystal using :

$$x_3 = \frac{\left(c_3 - c_2\right)}{\left(m_1 + 1/m_1\right)}$$

$$y_3 = m_1 \cdot \frac{\left(c_3 - c_2\right)}{\left(m_1 + 1/m_1\right)} + c_2 \qquad \text{(E.7)}$$

$$x_4 = x_1 + \left(x_3 - x_2\right)$$

$$y_4 = y_1 + \left(y_3 - y_2\right)$$

The size of the rectangle is defined by two dimensions, $d_1$ and $d_2$, the longer of which is the length and the shorter the width :

$$d_1 = \sqrt{\left((x_1 - x_2)^2 + (y_1 - y_2)^2\right)}$$
$$d_2 = \sqrt{\left((x_1 - x_4)^2 + (y_1 - y_4)^2\right)}$$

(E.8)

Some caution in the programming is necessary to ensure that precision is not lost by the use of integer variables (which are necessary to define the co-ordinates of the positions on the screen in pixel units).

The program also provides the following features :

&mdash;    the ability to save all the details of the marked crystals to disk for subsequent review or modification.

&mdash;    the ability to specify a scale factor to convert the crystal dimensions in pixel units to actual length units (eg microns).

&mdash;    the calculation of the characteristic dimension as described in Appendix A, from the length and width measurements.

&mdash;    the calculation of the mean and standard deviation of the characteristic dimension.

&mdash;    the ability to save, in a format appropriate for importation into a standard spreadsheet, the dimensions of all the crystals counted.

# APPENDIX F

# F.   Data from Tests on Continuous Pan Performance

## F.1   Details of Measurement and Control Techniques

Logging and Control System

The PC based data logging and control system was installed to be able to log all on-line process measurements. By implementing the feed controls for all the compartments on this system, it was also possible to record the outputs to the feed control valves. The system also implemented a time proportional on/off control strategy for which the flow to a compartment would be directly proportional to the percent opening signal. With full control over the compartment feed valves, it was also possible to take over manual control of these valves and investigate the feed flow to individual compartments with the feed valve full open.

Syrup Flow

The syrup flow is measured by a magnetic flow meter, sized with sufficient turndown to be able to measure the syrup flow to individual compartments.

The correlation between percent valve opening and syrup flow was investigated for a number of compartments by operating the feed valves on manual as shown in the graph below.
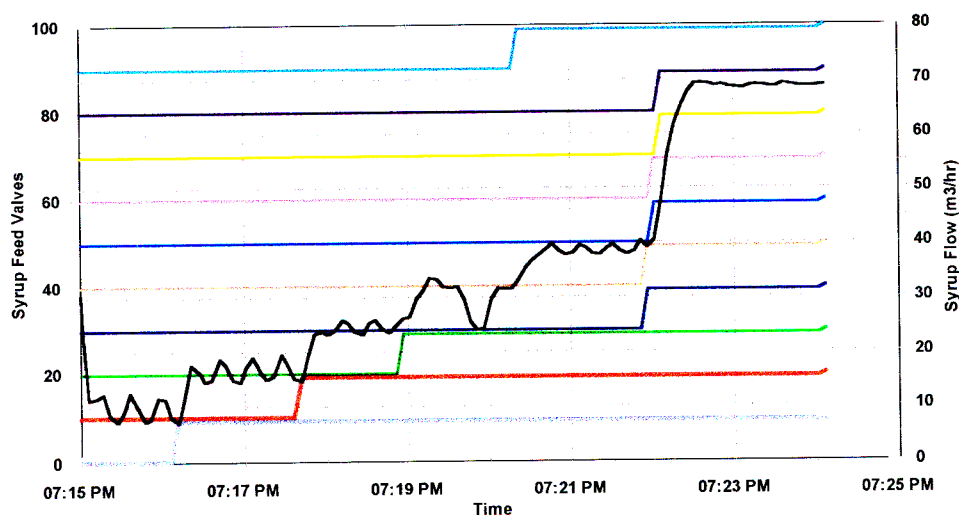


**Figure F.1** Syrup flow as a function of feed valve position

The horizontal lines, with steps, are arranged to indicate the positions of the feed valves for the first ten compartments which feed syrup into the pan. At the start of the test, all ten valves are closed and then, sequentially valves 1, 2, 3, 10 and then all the rest of the valves are fully opened. With all the valves closed there is a leakage of 10 m³/hr (subsequently confirmed as leakage and not a flow measurement off-set by closing all manual valves). For each of the individual compartments tested, the flow increases by approximately 7 m³/hr , indicating a full open flow of 8 m³/hr for each feed valve (assuming that the leakage is evenly distributed as 1m³/hr per feed valve). The total flow with all ten feed valves open of approximately 70m³/hr is less than the 80m³/hr indicated by the tests on individual compartments but can be explained in part by the higher pressure drop across the syrup flow meter at this maximum rate.

For individual tests, it is possible to fit an average flow for an open feed valve which ensures that the sum of all the individual feed flows calculated from the valve positions is equal to the total measured syrup flow.

## Water Flow

No measurement of total water flow was available. Only two of the compartments (11 and 12 ) were fed with water. These two compartments were fitted with small mechanical water meters - of the integrating type used for metering domestic water supplies. For some of the tests, water supply to each compartment was from an individual 200 litre drum, allowing the  flow to be checked by measuring level changes in the drums.

## Condensate Flow

The evaporation rate in the pan was estimated as being equal to the condensate flow which was measured by a magnetic flow meter  (Selected for its ability to operate on low conductivity fluids  and  positioned in a u-leg ahead of the steam trap.)

## Seed Flow by Seed Receiver Ullage Measurements

The seed massecuite for the two continuous A pans is created in batch A pans. The massecuite is discharged in batches of 85 m³ into a seed receiver. From here it is pumped into the continuous pans via positive displacement gear pumps with variable speed

drives. If only one continuous A pan is operating, the seed flow rate can be estimated by ullage measurements on the seed receiver. The seed receiver is a long horizontal rectangular tank with a base which is a half cylinder. The vessel is agitated, to prevent crystal settling, by paddles on a shaft running the length of the vessel. The dimensions of the seed receiver are shown in the diagram below in an end elevation:
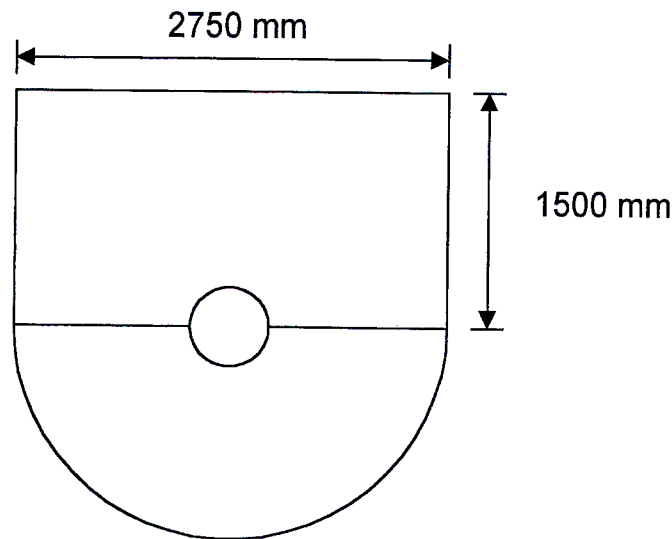


**Figure F.2** Dimensions of seed receiver

The central shaft has a diameter of 500 mm

The length of the seed receiver is 26 400 mm

The radius of the "half-cylinder" which forms the base of the vessel is thus 1 375 mm

Level measurements were taken manually with a tape measure at intervals throughout the duration of the test. An output from an ultrasonic level measuring device was also available from the computer logging system. This reading was calibrated against the manual measurements, allowing a continuous measurement of flow to be estimated from the rate of change of level. Significant filtering was necessary to eliminate the effect of noise spikes on the level measurement.

Seed Flow by Test Tank Ullage Measurements

To obtain estimates of seed flow to the test continuous A pan when both continuous A pans were running, a small test tank was installed . The arrangement of the tank was as shown in the diagram below.
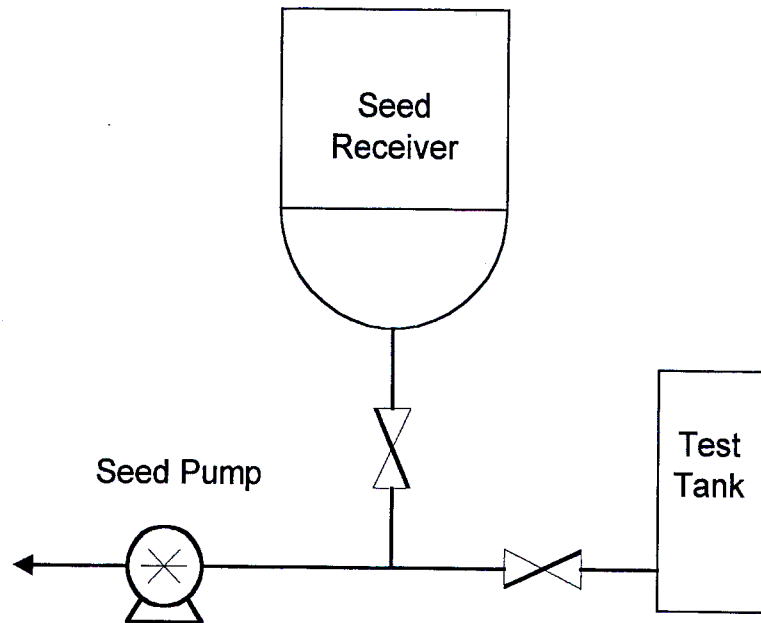
**Figure F.3** Configuration of test tank for seed flow measurement

By suitable switching of the valves during normal operation, the test tank can be allowed to fill and then the rate of drop in this tank monitored whilst the pump draws exclusively from this vessel. The test tank was a cylindrical vessel with an internal diameter of 1002mm (giving a cross-sectional area of 0,788 m²) and a height of approximately 1.5m.

Seed Flow from Pump Specification.

The seed pumps are positive displacement gear pumps (Broquet Model BB40) with a rated capacity of 20 m³/hr at 40rpm. Without wear or slippage, the pump can be expected to vary linearly in capacity with rotational speed giving a capacity of 0.5m³/hr/rpm. The pump is driven by a variable speed electric motor through a gear box with a reduction ratio of 30.99:1. The controlled and logged speeds are the motor speeds.

Massecuite Flow

Massecuite flow rates are particularly difficult to measure because of their high viscosities, low velocities and the conventional use of gravity flow (which limits pressure losses in measurement devices). For these tests, some of the cooling crystalliser vessels which are conventionally used in continuous mode, were converted to operating in a semi-batch fashion. Crystallisers were partially emptied before the test by increasing the

rate at which massecuite was processed in the centrifugals. The massecuite flow out of these crystallisers was then stopped and the massecuite leaving the ccontiuous pan under test diverted into them. The massecuite flow could then be estimated by ullage measurements.

The crystallisers used for these ullage measurements were pairs of vertical cylindrical crystallisers with inside diameters of 4000mm and stirrer shafts of 750mm in diameter. The cross-sectional area of massecuite per vessel to be used for ullage measurements is thus 12.12 m$^2$ .

## Vessel Pressure (Absolute Pressure)

Experience with absolute pressure measurement on pans in a factory environment has shown that these measurements were often in error. Examples of the sources of these problems are

- differential pressure transmitters used to measure the vacuum relative to atmospheric pressure and the output scaled to represent absolute pressure by assuming a constant atmospheric pressure.
- absolute pressure transmitters calibrated relative to an assumed atmospheric pressure of 100kPa abs using a standard manometer
- absolute pressure transmitters ranged from 0 to 100 kPa abs, giving them poor precision when operating at their set point of between 10 and 20 kPa abs.

For this test work, a dedicated absolute pressure transmitter ranged 0 to 30 kPa abs was installed and connected to the data logging system. The calibration was checked on-line using either a closed end manometer or a conventional manometer and a mercury barometer.

## Calandria Pressure

The calandria pressure was simply recorded as a gauge pressure

## Massecuite Sampling

During the preliminary test work on the continuous pans, the sampling system was modified to enable samples to be taken with a "syringe type" of sampling device. The device could be inserted into the centre of the circulating massecuite stream to enable a

representative sample to be taken.

Massecuite Analysis

Full understanding requires analysis of both the heterogenous massecuite and its mother liquor. The conventional method of obtaining a mother liquor sample is via pressure filtration in a device known as a "Nutch Bomb" . The mother liquor sample obtained in this way is known as "nutch molasses". For these tests the separation was done using specially designed centrifuge tubes. The tubes are manufactured from aluminium and consist of two parts which are screwed together. At the point where the two halves join, a centrifugal screen (with a supporting backing screen) is secured.

The tubes are sized to fit into the mechanism of a laboratory centrifuge. Centrifuging at 2000 rpm for between 5 and 10 minutes is sufficient to separate the mother-liquor sample whilst also leaving a sugar sample devoid of most of the molasses (unlike pressure filtration). A further advantage of this technique is the ability to determine an approximate crystal content by recording the weight of sugar separated as a fraction of the mass of massecuite centrifuged.

As discusssed in Chapter 3, the samples of massecuite and molasses were analysed for pol and brix. The sugar samples were analysed for particle size distribution by the semi-automatic microscopic counting method (Kontron analyser) used by the Sugar Milling Research Institute.

## F.2    Test A on 6 November 1991

An example of a full set of results from a test (Test 2-A) on the A1 continuous pan, and their analysis is summarised in this section.

The period of the test was between 12:30 and 2:30 pm. Summaries of the logged data for the individual compartments over this period are plotted below. These show average values plotted as crosses with error bars to indicate plus and minus 2 standard deviations.
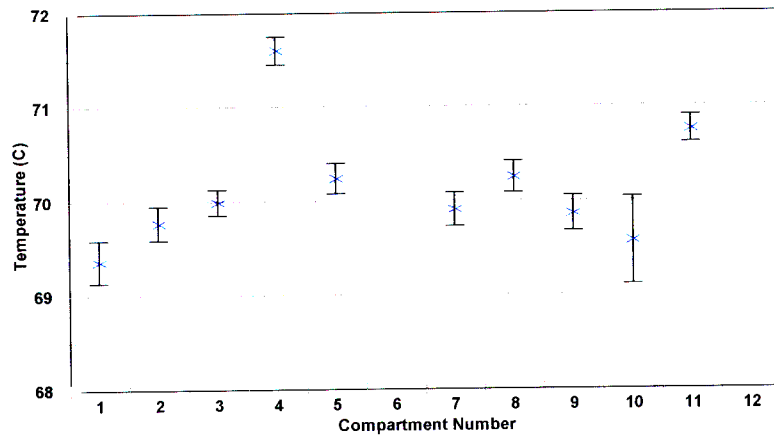
**Figure F.4** Average compartment temperature
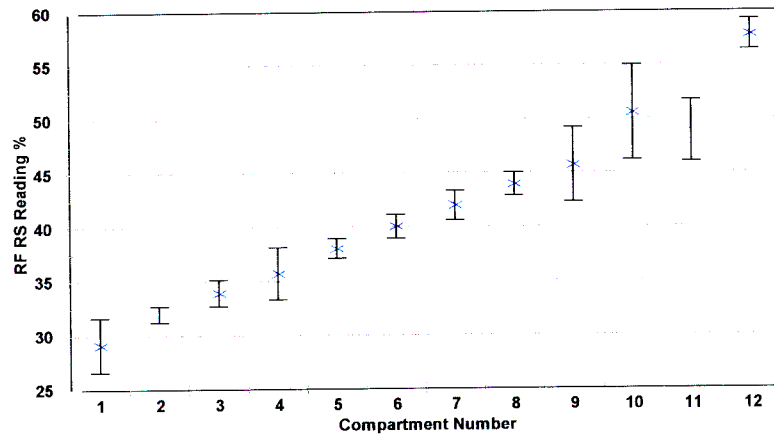


**Figure F.5** Average compartment RF probe reading
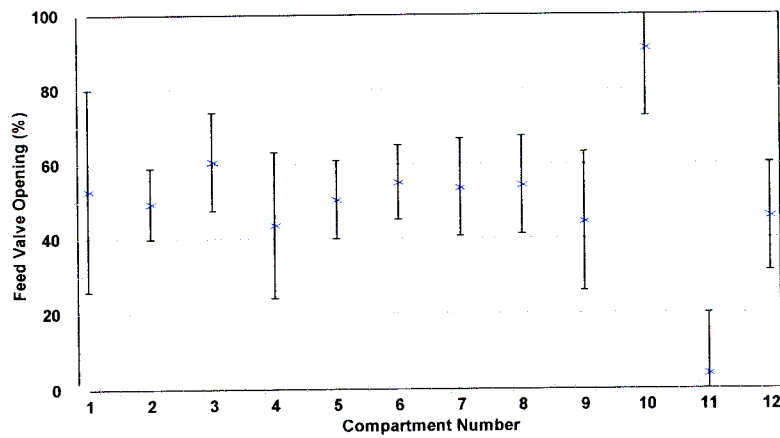


**Figure F.6** Average compartment feed valve position
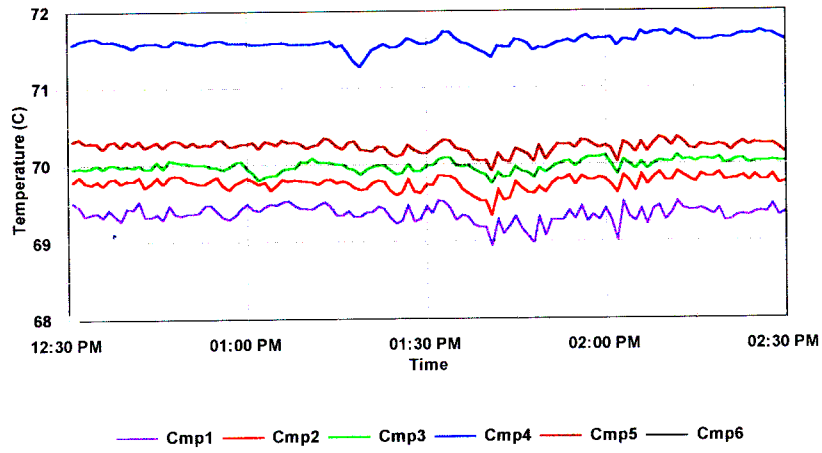
**Figure F.7** Trends of compartment temperatures for compartments 1 to 6
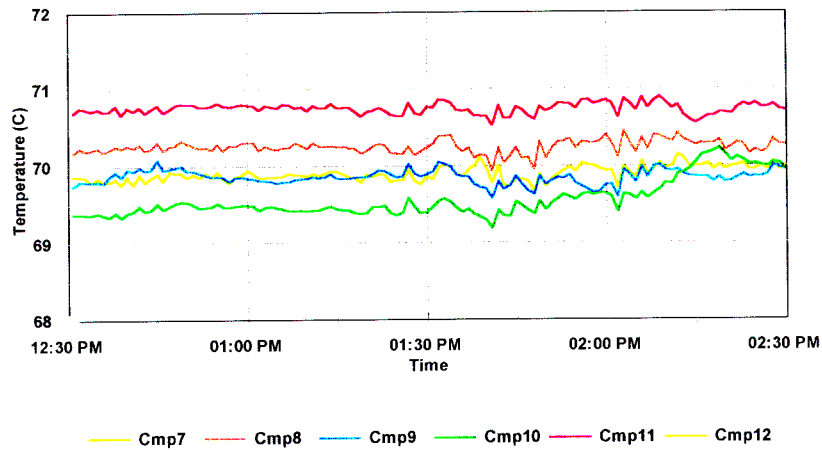


**Figure F.8** Trends of compartment temperatures for compartments 7 to 12
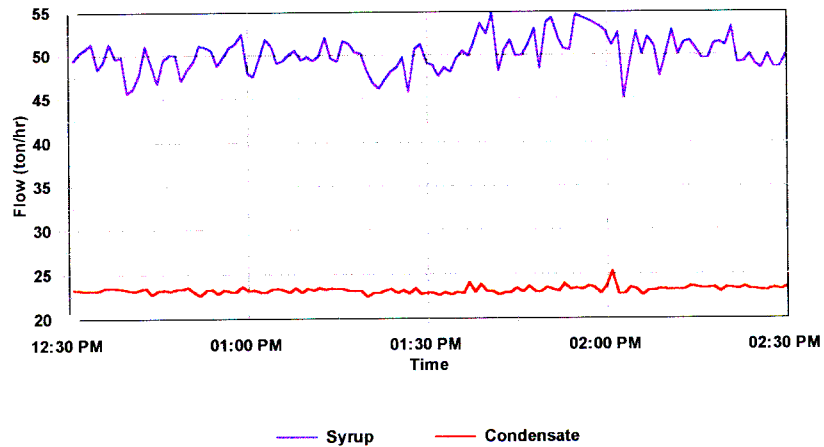


**Figure F.9** Trends of syrup and condensate flow
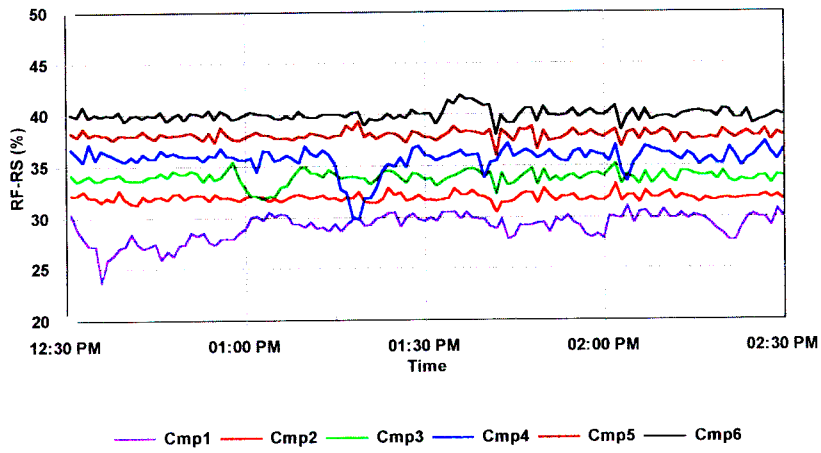
**Figure F.10** Trends of RF probe readings for compartments 1 to 6
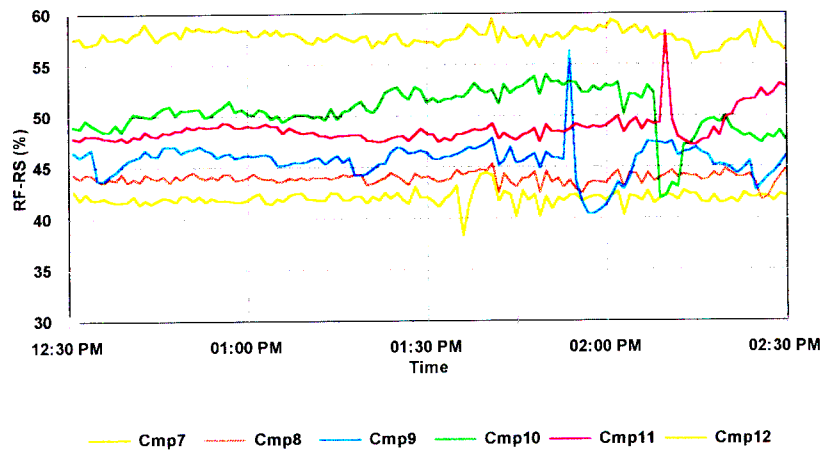


**Figure F.11** Trends of RF probe readings for compartments 7 to 12
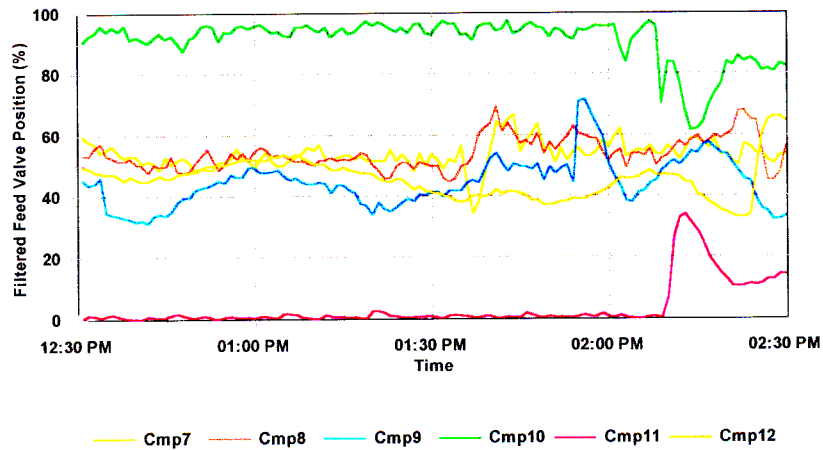


**Figure F.12** Trends of (filtered) feed valve positions for comps. 1 to 6
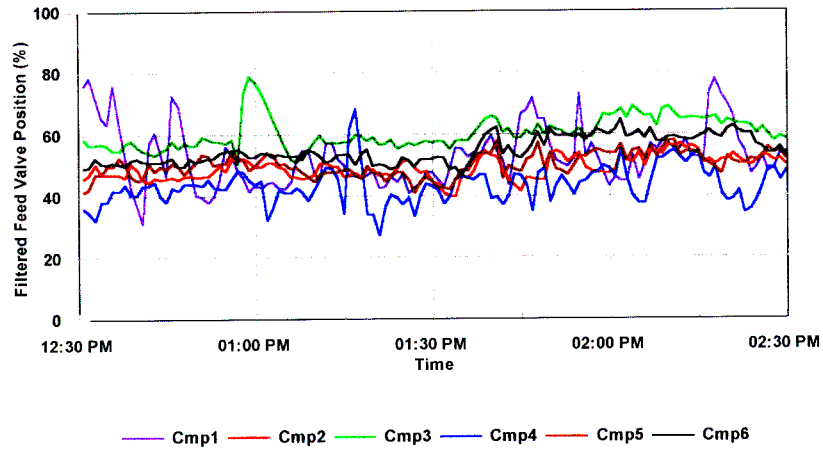
**Figure F.13** Trends of (filtered) feed valve positions for comps. 7 to 12
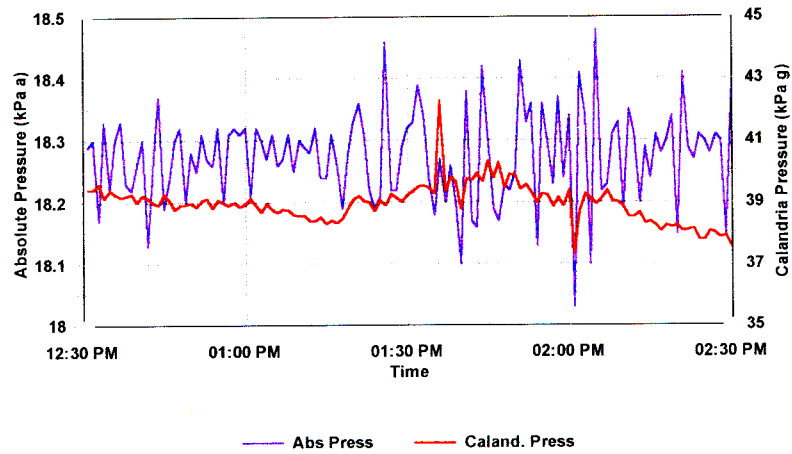


**Figure F.14** Trends of pan absolute pressure and calandria pressure
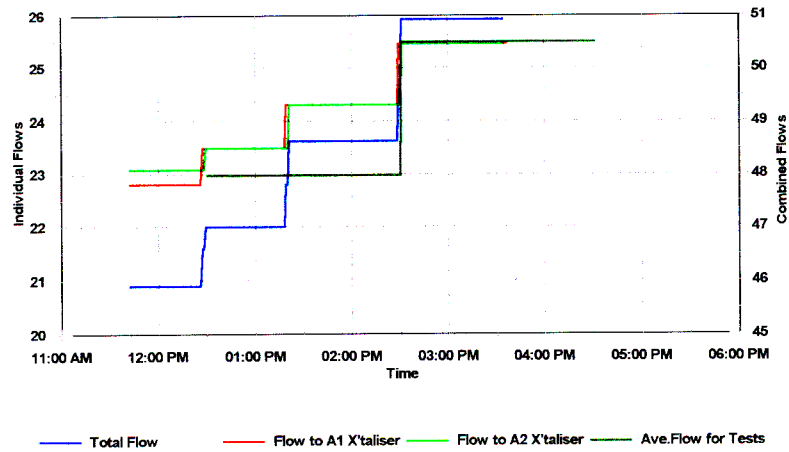


**Figure F.15** Trends in final massecuite flow estimated from levels
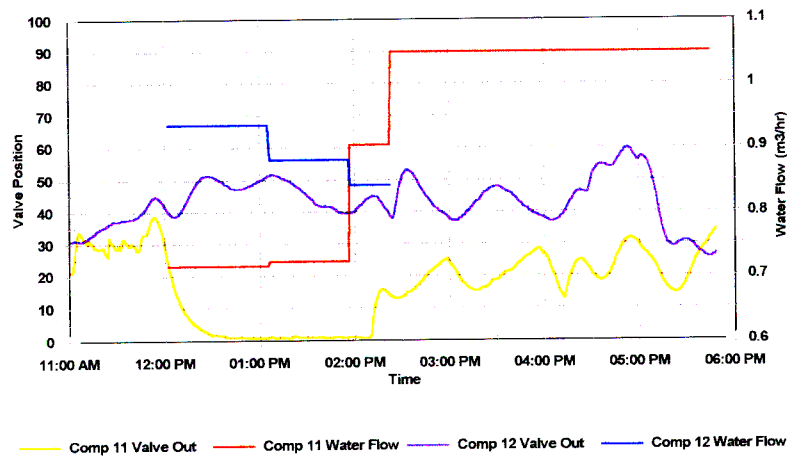
**Figure F.16** Trends of compartment water flows and valve positions
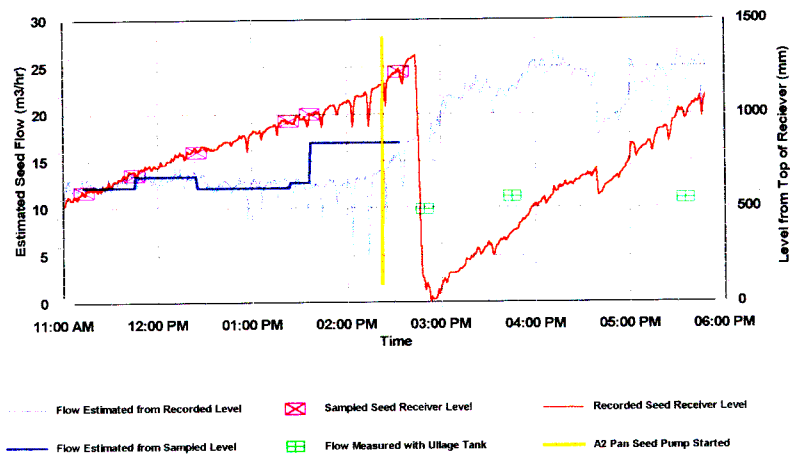


**Figure F.17** Trends in seed flows and levels

The water flow data can be interpreted by plotting average valve outputs against readings from the flow meters to determine linear correlations which express water flow as a function of valve position for each of the two compartments fed with water.. The average water flow for the test can be obtained by applying this correlation to the average valve output for the period of the test.

The seed flow estimated from the pump speed and its specification as a positive displacement pump gives a flow of 12 m³ /hr. This agrees well with the measurements taken from variations in the level of the seed receiver with time and the tests using the small "ullage tank".

The average flow of product massecuite estimated over the period of the test from the changes in the levels of the vertical crystallisers was 47.98 m³ /hr.

**Table F.1** Average values of variables logged during Test 2-A

Felixton A1 test on 6 November 1991   Test A : 12:30 pm to 2:30 pm

| | COMP 1 TEMP °C | COMP 2 TEMP °C | COMP 3 TEMP °C | COMP 4 TEMP °C | COMP 5 TEMP °C | COMP 6 TEMP °C | COMP 7 TEMP °C | COMP 8 TEMP °C | COMP 9 TEMP °C | COMP 10 TEMP °C | COMP 11 TEMP °C | COMP 12 TEMP °C | AVE TEMP °C |
|---|---|---|---|---|---|---|---|---|---|---|---|---|---|
| Comp. No. | | | | | | | | | | | | | |
| Ave. | 69.36 | 69.77 | 69.99 | 71.60 | 70.24 | —— | 69.91 | 70.25 | 69.86 | 69.57 | 70.75 | —— | 70.13017 |
| Std Dev | 0.11 | 0.09 | 0.07 | 0.07 | 0.08 | —— | 0.09 | 0.08 | 0.09 | 0.23 | 0.07 | —— | |

| | COMP 1 RF (%) | COMP 2 RF (%) | COMP 3 RF (%) | COMP 4 RF (%) | COMP 5 RF (%) | COMP 6 RF (%) | COMP 7 RF (%) | COMP 8 RF (%) | COMP 9 RF (%) | COMP 10 RF (%) | COMP 11 RF (%) | COMP 12 RF (%) |
|---|---|---|---|---|---|---|---|---|---|---|---|---|
| Comp. No. | | | | | | | | | | | | |
| Ave. | 29.13 | 32.00 | 33.95 | 35.74 | 38.05 | 40.05 | 42.02 | 43.96 | 45.73 | 50.57 | 48.85 | 57.79 |
| Std Dev | 1.27 | 0.38 | 0.63 | 1.20 | 0.45 | 0.56 | 0.69 | 0.55 | 1.74 | 2.21 | 1.43 | 0.71 |

| | COMP 1 VO | COMP 2 VO | COMP 3 VO | COMP 4 VO | COMP 5 VO | COMP 6 VO | COMP 7 VO | COMP 8 VO | COMP 9 VO | COMP 10 VO | COMP 11 VO | COMP 12 VO |
|---|---|---|---|---|---|---|---|---|---|---|---|---|
| Comp. No. | | | | | | | | | | | | |
| Ave. | 52.89 | 49.39 | 60.67 | 43.69 | 50.45 | 55.12 | 53.75 | 54.30 | 44.56 | 91.10 | 4.02 | 45.81 |
| Std Dev | 13.53 | 4.76 | 6.53 | 9.74 | 5.24 | 5.01 | 6.53 | 6.60 | 9.33 | 9.12 | 7.96 | 7.24 |

| | ABS PRESS (kPa abs) | SEED PUMP (rpm) | CALND PRESS (kPa g) | SYRUP FLOW (m³/hr) | COND FLOW (ton/hr) |
|---|---|---|---|---|---|
| Ave. | 18.27 | 902.37 | 38.98 | 50.21 | 23.26 |
| Std Dev | 0.07 | 1.92 | 0.62 | 1.96 | 0.34 |

**Table F.2** Analyses of samples collected during Test 2-A

F-13

Felixton A1 Pan test on 6 November 1991        Test A

Analysis of Massecuite samples

| Value of R calculated for Felixton Molasses - week ending 10 Nov '91 | |
|---|---|
| Suc = | 30.8 |
| Pol = | 29.5 |
| Dry Sol = | 78.38 |
| R = | 0.026596 |

| Mass Of Centrifuge Tubes | | |
|---|---|---|
| Tube Number | 1 | 2 |
| Total mass | 341.47 | 341.17 |
| Top mass | 191.14 | 192.26 |
| Bottom mass | 150.33 | 148.91 |

| Compartment Number | Seed | 1 | 2 | 3 | 4 | 5 | 6 | 7 | 8 | 9 | 10 | 11 | 12 | Final | Average |
|---|---|---|---|---|---|---|---|---|---|---|---|---|---|---|---|
| Time (adjusted to computer time) | 12:39 PM | 12:39 PM | 12:54 PM | 12:57 PM | 01:15 PM | 01:17 PM | 01:34 PM | 01:36 PM | 01:52 PM | 01:54 PM | 02:08 PM | 02:10 PM | 02:25 PM | 02:25 PM | |
| Sample Name | A Seed | A1 | A2 | A3 | A4 | A5 | A6 | A7 | A8 | A9 | A10 | A11 | A12 | MCTEA | |
| Chemical Analysis | | | | | | | | | | | | | | | |
| Massecuite Brix | 90.55 | 90.25 | 90.15 | 90.2 | 91.05 | 90.85 | 90.45 | 90.4 | 91 | 90.9 | 90.55 | 90.55 | 91.8 | 92.45 | 90.80 |
| Massecuite Pol | 78.3 | 78.55 | 78.55 | 78.3 | 79.5 | 79 | 78.45 | 78.2 | 78.9 | 78.65 | 78.55 | 77.95 | 79.35 | 80.45 | 78.76 |
| Massecuite Apparent Purity | 86.47 | 87.04 | 87.13 | 86.81 | 87.31 | 86.96 | 86.73 | 86.50 | 86.70 | 86.52 | 86.75 | 86.09 | 86.44 | 87.02 | 86.75 |
| Nutch Brix | 80.7 | 82.45 | 82.35 | 82.7 | 82.9 | 83.2 | 82.6 | 82.8 | 83.05 | 83.35 | 82.75 | 83.4 | 83.55 | 83.5 | 82.81 |
| Nutch Pol | 55.9 | 60.35 | 60.8 | 61.3 | 60.45 | 60.7 | 60.6 | 60.8 | 60.35 | 60.7 | 60.8 | 60.6 | 59.25 | 58.65 | 60.09 |
| Nutch Apparent Purity | 69.27 | 73.20 | 73.83 | 74.12 | 72.92 | 72.96 | 73.37 | 73.43 | 72.67 | 72.83 | 73.47 | 72.66 | 70.92 | 70.24 | 72.56 |
| Crystal Content (apparent) from Analysis | 50.69 | 46.60 | 45.82 | 44.21 | 48.40 | 47.03 | 45.40 | 44.48 | 46.73 | 45.82 | 45.31 | 44.46 | 48.99 | 52.13 | 46.86 |
| Exhaustion (apparent) | | | | | | | | | | | | | 61.74 | 64.80 | |
| Est.Massecuite Dry Solids | 89.88 | 89.62 | 89.52 | 89.56 | 90.42 | 90.20 | 89.80 | 89.74 | 90.34 | 90.23 | 89.90 | 89.87 | 91.11 | 91.78 | 90.14 |
| Est. Massecuite Sucrose | 78.61 | 78.84 | 78.84 | 78.60 | 79.79 | 79.30 | 78.75 | 78.51 | 79.20 | 78.96 | 78.85 | 78.27 | 79.66 | 80.75 | 79.07 |
| Est. Massecuite True Purity | 87.45 | 87.98 | 88.07 | 87.77 | 88.25 | 87.91 | 87.70 | 87.48 | 87.67 | 87.51 | 87.71 | 87.09 | 87.43 | 87.98 | 87.71 |
| Est. Nutch Dry Solids | 79.50 | 81.36 | 81.29 | 81.64 | 81.78 | 82.08 | 81.51 | 81.71 | 81.92 | 82.22 | 81.66 | 82.26 | 82.33 | 82.26 | 81.68 |
| Est. Nutch Sucrose | 56.53 | 60.91 | 61.34 | 61.84 | 61.02 | 61.27 | 61.16 | 61.36 | 60.92 | 61.27 | 61.35 | 61.18 | 59.86 | 59.28 | 60.66 |
| Est. Nutch True Purity | 71.10 | 74.87 | 75.47 | 75.75 | 74.61 | 74.65 | 75.03 | 75.09 | 74.37 | 74.52 | 75.13 | 74.37 | 72.71 | 72.07 | 74.27 |
| Est. Crystal Content (true) from Analysis | 50.86 | 46.76 | 45.98 | 44.37 | 48.56 | 47.19 | 45.56 | 44.65 | 46.89 | 45.98 | 45.47 | 44.61 | 49.15 | 52.29 | 47.02 |
| Est. Exhaustion (true) | | | | | | | | | | | | | 61.70 | 64.75 | |
| Size Analysis (Kontron) dimensions in microns and microns[2] | | | | | | | | | | | | | | | |
| Width - mean | 468 | 440 | 497 | 520 | 558 | 522 | 572 | 594 | 561 | 559 | 602 | 564 | 589 | 629 | |
| Width - standard dev | 175 | 165 | 183 | 198 | 214 | 182 | 224 | 213 | 235 | 225 | 235 | 241 | 255 | 249 | |
| Length - mean | 732 | 681 | 818 | 842 | 921 | 866 | 963 | 981 | 942 | 948 | 971 | 967 | 1011 | 1047 | |
| Length - standard dev | 259 | 246 | 282 | 293 | 285 | 325 | 339 | 324 | 370 | 337 | 348 | 371 | 372 | 386 | |
| L/W Ratio | 1.56 | 1.55 | 1.65 | 1.62 | 1.65 | 1.66 | 1.68 | 1.65 | 1.68 | 1.70 | 1.61 | 1.71 | 1.72 | 1.66 | |
| Mean Characteristic Dimension, Dc | 631 | 589 | 693 | 717 | 779 | 732 | 809 | 830 | 793 | 795 | 828 | 808 | 844 | 883 | |
| Variance of Characteristic Dimension, | 53017 | 47180 | 61508 | 69083 | 75475 | 69639 | 91920 | 82596 | 104301 | 92373 | 97170 | 108919 | 117145 | 115098 | |
| Std Dev. of Characteristic Dimension | 230 | 217 | 248 | 263 | 275 | 264 | 303 | 287 | 323 | 304 | 312 | 330 | 342 | 339 | |
| CV of characteristic dimension | 37 | 37 | 36 | 37 | 35 | 36 | 37 | 35 | 41 | 38 | 38 | 41 | 41 | 38 | |
| Second Moment of Char. Dimension | 450677 | 393782 | 541509 | 583228 | 682821 | 604783 | 747209 | 771380 | 732422 | 724327 | 782695 | 761681 | 830127 | 895579 | |
| Quick Centrifuge" Analysis | | | | | | | | | | | | | | | |
| Tube No | 1 | 2 | 1 | 2 | 1 | 2 | 1 | 2 | 1 | 2 | 1 | 2 | 1 | 2 | |
| Mass - Tube & Mc | 512.56 | 510.6 | 506.93 | 503.94 | 514.55 | 515.51 | 517.78 | 494.45 | 510.76 | 499.92 | 510.07 | 503.39 | 513.63 | 515.19 | |
| Mass - Top & Xtal | 285.15 | 273.78 | 271.34 | 270.1 | 278.68 | 279.54 | 278.56 | 267.38 | 277.22 | 273.36 | 274.43 | 275.12 | 282.65 | 290.46 | |
| Mass - Bottom & Nutch | 226.52 | 235.76 | 234.72 | 233.02 | 234.83 | 235.22 | 238.46 | 226.31 | 232.73 | 226.11 | 234.9 | 227.44 | 230.3 | 223.86 | |
| Loss (%) | 0.52 | 0.63 | 0.53 | 0.50 | 0.60 | 0.43 | 0.43 | 0.50 | 0.48 | 0.28 | 0.44 | 0.51 | 0.39 | 0.50 | |
| Estimated Crystal Content (%) | 54.95 | 48.11 | 48.47 | 47.82 | 50.58 | 50.06 | 49.58 | 49.01 | 50.85 | 51.09 | 49.40 | 51.08 | 53.15 | 56.43 | |
| Assumed sugar Brix | 99.9 | 99.9 | 99.9 | 99.9 | 99.9 | 99.9 | 99.9 | 99.9 | 99.9 | 99.9 | 99.9 | 99.9 | 99.9 | 99.9 | |
| Assumed sugar Purity | 98.7 | 98.7 | 98.6 | 98.6 | 98.6 | 98.5 | 98.5 | 98.4 | 98.4 | 98.3 | 98.3 | 98.2 | 98.2 | 98.1 | |
| Corrected Crystal content | 52.07 | 45.29 | 45.33 | 44.70 | 47.43 | 46.73 | 46.21 | 45.45 | 47.27 | 47.26 | 45.58 | 47.05 | 49.22 | 52.12 | |

| Analysis of Syrup Samples | | | | |
|---|---|---|---|---|
| Time (adjusted to computer time) | 12:46 PM | 01:48 PM | 02:41 PM | Average |
| Sample Name | 1A | 2A | 3A | |
| Chemical Analysis | | | | |
| Syrup Brix | 66.28 | 66.88 | 66.72 | 66.63 |
| Syrup Pol | 58.12 | 58.72 | 58.4 | 58.41 |
| Syrup Purity | 87.69 | 87.80 | 87.53 | 87.67 |
| Est. Syrup Dry Solids | 65.92 | 66.52 | 66.35 | 66.27 |
| Est. Syrup Sucrose | 57.91 | 58.51 | 58.19 | 58.20 |
| Est. Syrup True Purity | 87.85 | 87.96 | 87.69 | 87.84 |

| Combined Average Purity for Test (syrup and massecuitre) | |
|---|---|
| Apparent Purity | 86.9 |
| Estimated True Purity | 87.7 |

**Table F.3** Reconciliation of process flows of Test 2-A

Felixton A1 Pan test on 6 November 1991          Test A : 12:30 pm to 2:30 pm

| Description | units | Meas Value | 95% Conf. Intv. (+ - a) | Std Dev | Weighting Factor | Fitted Value | Fract'al Adj'stmt | Weighted Squared Adj'stmt | Fitting Factor |
|---|---|---|---|---|---|---|---|---|---|
| Seed Flow | m³/hr | 12 | 1 | 0.51 | 3.84 | 12.79 | -0.07 | 2.387259 | 1.065692 |
| Massecuite Flow | m³/hr | -48 | 2 | 1.02 | 0.96 | -44.84 | 0.07 | 9.577759 | 0.934209 |
| Water flow to Comp 11 | m³/hr | 0.77 | 0.1 | 0.05 | 384.16 | 0.78 | -0.01 | 0.024245 | 1.010317 |
| Water flow to Comp 12 | m³/hr | 0.9 | 0.1 | 0.05 | 384.16 | 0.91 | -0.01 | 0.024223 | 1.008823 |
| Evaporation Rate | ton/hr | -23.3 | 2 | 1.02 | 0.96 | -20.12 | 0.14 | 9.6927 | 0.863655 |
| Syrup Flow | m³/hr | 50.2 | 1 | 0.51 | 3.84 | 50.98 | -0.02 | 2.333518 | 1.015526 |
| Seed Dry Solids | % | 89.9 | 0.4 | 0.20 | 24.01 | 89.89 | 0.00 | 0.00171 | 0.999906 |
| Massecuite Dry Solids | % | 91.5 | 0.4 | 0.20 | 24.01 | 91.53 | -0.00 | 0.020499 | 1.000319 |
| Syrup Dry Solids | % | 66.3 | 0.4 | 0.20 | 24.01 | 66.27 | 0.00 | 0.020608 | 0.999558 |
| | | | | | | | | 24.08252 | |

| Description | Volumetric Flow m³/hr | Density kg/m³ | Dry Soilds % | Mass Flow (kg/s) | Solids Flow (kg/s) | | | |
|---|---|---|---|---|---|---|---|---|
| Seed | 12.79 | 1454 | 89.89 | 5.17 | 4.64 | | | |
| Massecuite | -44.84 | 1463 | 91.53 | -18.22 | -16.68 | Sum of | | |
| Water to Comp 11 | 0.78 | 1000 | 0.00 | 0.22 | 0.00 | Weighted | | |
| Water to Comp 12 | 0.91 | 1000 | 0.00 | 0.25 | 0.00 | Squared | | |
| Evaporation | ----- | ----- | 0.00 | -5.59 | 0.00 | Imbalance | | |
| Syrup | 50.98 | 1283 | 66.27 | 18.17 | 12.04 | | | |
| | | Imbalance | | -0.01097 | 0.0038523 | 0.1352116 | | |
| Mass balance weighting factor | 1000 | | | | | | | |

Total imbalance to be minimised    24.21773

| | Seed Massecuite | Final Massecuite |
|---|---|---|
| Crystal content | 50.8 | 52.3 |
| Nutch Dry Solids | 79.5 | 82.3 |
| Temperature | 60 | 70 |
| Massecuite Density | 1454 | 1463 |

| | Syrup |
|---|---|
| Dry Sol. | 66.3 |
| Temp. | 60 |
| Density | 1283 |

| Estimation of CDR | Seed Xtal Con (%) | Massecuite Xtal Con (%) | Pan Volume (m³) | Pan CDR (kg/m³/hr) |
|---|---|---|---|---|
| | 50.86 | 52.29 | 120 | 207.06 |

## F.3 Summaries of Reconciled Test Results

| Test Number : | 1-A |
|---|---|

### Flows and Properties for Compartments

| Compartment Number | Syrup Flow kg/s | Water Flow kg/s | Massecuite Dry Solids % | Nutch Dry Solids % | First Moment m | Second Moment m² |
|---|---|---|---|---|---|---|
| Seed | | | 89.85 | 79.99 | 5.07e-04 | 2.82e-07 |
| 1 | | 0.00 | 89.96 | 81.59 | 5.54e-04 | 3.42e-07 |
| 2 | | 0.00 | 89.92 | 81.39 | 5.75e-04 | 3.74e-07 |
| 3 | | 0.00 | 89.75 | 81.69 | 5.79e-04 | 3.75e-07 |
| 4 | | 0.00 | 91.10 | 81.96 | 5.71e-04 | 3.70e-07 |
| 5 | | 0.00 | 90.34 | 81.99 | 6.41e-04 | 4.75e-07 |
| 6 | | 0.00 | 90.04 | 81.24 | 6.01e-04 | 4.17e-07 |
| 7 | | 0.00 | 90.32 | 81.72 | 6.35e-04 | 4.62e-07 |
| 8 | | 0.00 | 89.91 | 81.17 | 6.47e-04 | 4.79e-07 |
| 9 | | 0.00 | 90.46 | 82.23 | 6.08e-04 | 4.23e-07 |
| 10 | | 0.00 | 90.65 | 81.85 | 7.17e-04 | 6.04e-07 |
| 11 | | 0.45 | 91.09 | 82.17 | 7.03e-04 | 5.61e-07 |
| 12 | | 0.05 | 91.64 | 82.21 | 7.49e-04 | 6.88e-07 |

### Flow Rates of Major Streams

| | | |
|---|---|---|
| Total Syrup | 19.59 | kg/s |
| Total Evaporation | 6.77 | kg/s |
| Seed Massecuite flow | 3.98 | kg/s |
| Product Massecuite flow | 17.31 | kg/s |

### Overall Properties

| | | |
|---|---|---|
| Massecuite and Syrup purity | 87.90 | % |
| Syrup Dry Solids | 63.35 | % |
| Volume Shape Factor | 0.34 | |
| Average Massecuite Temperature | 69.78 | °C |
| Dry Solids of Saturated Pure Solution * | 76.40 | % |
| Activation Energy for Growth * | 54.58 | kJ/mol |
| Growth Parameter  K2 | 0.562 | |
| Solubility Parameter  K4 | 3.24 | |
| Solubility Parameter  K5 | 0.08 | |

### Seed Properties Expressed in Terms of Model Parameters

| | | |
|---|---|---|
| Total Flow                      - u1 | 3.984 | kg/s |
| Flow of water                   - u2 | 0.405 | kg/s |
| Flow of dissolved sucrose  - u3 | 1.100 | kg/s |
| 1st Moment of xtal size      - u4 | 5.07e-04 | m |
| 2nd Moment of xtal size    - u5 | 2.82e-07 | m² |

Table F.4 Reconciled results for Test 1-A

Test Number :          1-B

### Flows and Properties for Compartments

| Compartment Number | Syrup Flow kg/s | Water Flow kg/s | Massecuite Dry Solids % | Nutch Dry Solids % | First Moment m | Second Moment m² |
|---|---|---|---|---|---|---|
| Seed |  |  | 90.39 | 79.68 | 4.94e-04 | 2.70e-07 |
| 1 |  | 0.00 | 90.04 | 81.45 | 5.12e-04 | 2.92e-07 |
| 2 |  | 0.00 | 89.92 | 81.18 | 5.50e-04 | 3.45e-07 |
| 3 |  | 0.00 | 90.21 | 81.58 | 5.78e-04 | 3.74e-07 |
| 4 |  | 0.00 | 90.34 | 81.39 | 6.17e-04 | 4.36e-07 |
| 5 |  | 0.00 | 90.12 | 81.86 | 6.26e-04 | 4.46e-07 |
| 6 |  | 0.00 | 90.31 | 81.60 | 6.70e-04 | 5.09e-07 |
| 7 |  | 0.00 | 89.80 | 81.80 | 7.37e-04 | 6.29e-07 |
| 8 |  | 0.00 | 90.01 | 81.49 | 7.30e-04 | 6.16e-07 |
| 9 |  | 0.00 | 90.39 | 82.00 | 7.57e-04 | 6.57e-07 |
| 10 |  | 0.00 | 90.53 | 82.07 | 7.16e-04 | 5.98e-07 |
| 11 |  | 0.45 | 91.22 | 82.53 | 7.25e-04 | 6.17e-07 |
| 12 |  | 0.03 | 91.94 | 82.52 | 7.16e-04 | 6.08e-07 |

### Flow Rates of Major Streams

| | | |
|---|---|---|
| Total Syrup | 19.91 | kg/s |
| Total Evaporation | 6.79 | kg/s |
| Seed Massecuite flow | 3.94 | kg/s |
| Product Massecuite flow | 17.54 | kg/s |

### Overall Properties

| | | |
|---|---|---|
| Massecuite and Syrup purity | 87.92 | % |
| Syrup Dry Solids | 63.67 | % |
| Volume Shape Factor | 0.34 | |
| Average Massecuite Temperature | 69.92 | °C |
| Dry Solids of Saturated Pure Solution * | 76.43 | % |
| Activation Energy for Growth * | 54.47 | kJ/mol |
| Growth Parameter K2 | 0.569 | |
| Solubility Parameter K4 | 3.240 | |
| Solubility Parameter K5 | 0.08 | |

### Seed Properties Expressed in Terms of Model Parameters

| | | | |
|---|---|---|---|
| Total Flow | - u1 | 3.935 | kg/s |
| Flow of water | - u2 | 0.405 | kg/s |
| Flow of dissolved sucrose | - u3 | 1.100 | kg/s |
| 1st Moment of xtal size | - u4 | 4.94e-04 | m |
| 2nd Moment of xtal size | - u5 | 2.70e-07 | m² |

**Table F.5** Reconciled results for Test 1-B

| Test Number : | 2-A |
|---|---|

### Flows and Properties for Compartments

| Compartment Number | Syrup Flow kg/s | Water Flow kg/s | Massecuite Dry Solids % | Nutch Dry Solids % | First Moment m | Second Moment $m^2$ |
|---|---|---|---|---|---|---|
| Seed | | | 89.88 | 79.50 | 6.31e-04 | 4.51e-07 |
| 1 | 1.75 | 0.00 | 89.62 | 81.36 | 5.89e-04 | 3.94e-07 |
| 2 | 1.65 | 0.00 | 89.52 | 81.29 | 6.93e-04 | 5.42e-07 |
| 3 | 1.95 | 0.00 | 89.56 | 81.64 | 7.17e-04 | 5.83e-07 |
| 4 | 1.50 | 0.00 | 90.42 | 81.78 | 7.79e-04 | 6.83e-07 |
| 5 | 1.68 | 0.00 | 90.20 | 82.08 | 7.32e-04 | 6.05e-07 |
| 6 | 1.80 | 0.00 | 89.80 | 81.51 | 8.10e-04 | 7.47e-07 |
| 7 | 1.77 | 0.00 | 89.74 | 81.71 | 8.30e-04 | 7.71e-07 |
| 8 | 1.78 | 0.00 | 90.34 | 81.92 | 7.93e-04 | 7.32e-07 |
| 9 | 1.53 | 0.00 | 90.23 | 82.22 | 7.95e-04 | 7.24e-07 |
| 10 | 2.75 | 0.00 | 89.90 | 81.66 | 8.28e-04 | 7.83e-07 |
| 11 | 0.00 | 0.22 | 89.87 | 82.26 | 8.08e-04 | 7.62e-07 |
| 12 | 0.00 | 0.25 | 91.11 | 82.33 | 8.44e-04 | 8.30e-07 |

### Flow Rates of Major Streams

| | | |
|---|---|---|
| Total Syrup | 18.17 | kg/s |
| Total Evaporation | 5.59 | kg/s |
| Seed Massecuite flow | 5.17 | kg/s |
| Product Massecuite flow | 18.22 | kg/s |

### Overall Properties

| | | |
|---|---|---|
| Massecuite and Syrup purity | 87.74 | % |
| Syrup Dry Solids | 66.27 | % |
| Volume Shape Factor | 0.34 | |
| Average Massecuite Temperature | 70.13 | °C |
| Dry Solids of Saturated Pure Solution * | 76.48 | % |
| Activation Energy for Growth * | 54.29 | kJ/mol |
| Growth Parameter K2 | 0.58 | |
| Solubility Parameter K4 | 3.25 | |
| Solubility Parameter K5 | 0.08 | |

### Seed Properties Expressed in Terms of Model Parameters

| | | |
|---|---|---|
| Total Flow        - u1 | 5.166 | kg/s |
| Flow of water       - u2 | 0.523 | kg/s |
| Flow of dissolved sucrose  - u3 | 1.447 | kg/s |
| 1st Moment of xtal size  - u4 | 6.31e-04 | m |
| 2nd Moment of xtal size  - u5 | 4.51e-07 | $m^2$ |

**Table F.6** Reconciled results for Test 2-A

Test Number :          2-B

**Flows and Properties for Compartments**

| Compartment Number | Syrup Flow kg/s | Water Flow kg/s | Massecuite Dry Solids % | Nutch Dry Solids % | First Moment m | Second Moment m² |
|---|---|---|---|---|---|---|
| Seed |  |  | 90.06 | 79.40 | 6.37e-04 | 4.57e-07 |
| 1 | 1.91 | 0.00 | 89.72 | 81.04 | 6.41e-04 | 4.64e-07 |
| 2 | 1.67 | 0.00 | 89.56 | 81.21 | 7.06e-04 | 5.62e-07 |
| 3 | 1.93 | 0.00 | 89.66 | 81.36 | 7.12e-04 | 5.85e-07 |
| 4 | 1.53 | 0.00 | 89.99 | 81.66 | 7.70e-04 | 6.79e-07 |
| 5 | 1.66 | 0.00 | 89.73 | 81.99 | 7.42e-04 | 6.41e-07 |
| 6 | 1.79 | 0.00 | 89.53 | 81.51 | 7.82e-04 | 6.93e-07 |
| 7 | 1.67 | 0.00 | 90.33 | 81.93 | 7.57e-04 | 6.66e-07 |
| 8 | 1.90 | 0.00 | 89.98 | 82.06 | 7.93e-04 | 7.29e-07 |
| 9 | 1.50 | 0.00 | 89.96 | 82.25 | 7.98e-04 | 7.38e-07 |
| 10 | 2.38 | 0.00 | 90.39 | 81.95 | 8.56e-04 | 8.77e-07 |
| 11 | 0.00 | 0.29 | 90.18 | 82.51 | 7.87e-04 | 7.42e-07 |
| 12 | 0.00 | 0.24 | 90.99 | 82.40 | 8.46e-04 | 8.27e-07 |

**Flow Rates of Major Streams**

| | | |
|---|---|---|
| Total Syrup | 18.94 | kg/s |
| Total Evaporation | 5.46 | kg/s |
| Seed Massecuite flow | 5.39 | kg/s |
| Product Massecuite flow | 18.42 | kg/s |

**Overall Properties**

| | | |
|---|---|---|
| Massecuite and Syrup purity | 87.45 | % |
| Syrup Dry Solids | 65.54 | % |
| Volume Shape Factor | 0.34 | |
| Average Massecuite Temperature | 70.23 | °C |
| Dry Solids of Saturated Pure Solution * | 76.50 | % |
| Activation Energy for Growth * | 54.21 | kJ/mol |
| Growth Parameter  K2 | 0.583 | |
| Solubility Parameter  K4 | 3.260 | |
| Solubility Parameter  K5 | 0.08 | |

**Seed Properties Expressed in Terms of Model Parameters**

| | | |
|---|---|---|
| Total Flow                   - u1 | 5.390 | kg/s |
| Flow of water                - u2 | 0.536 | kg/s |
| Flow of dissolved sucrose  - u3 | 1.414 | kg/s |
| 1st Moment of xtal size    - u4 | 6.37e-04 | m |
| 2nd Moment of xtal size   - u5 | 4.57e-07 | m² |

**Table F.7** Reconciled results for Test 2-B

# APPENDIX G

## G.  Interpretation of Published Crystallisation Rate Data

### G.1  Pilot Plant and Industrial Scale Data of Lionnet on Refined Sugar Boilings

Lionnet (1999) measured growth rates in a laboratory/pilot scale batch pan as part of an investigation into colour transfer in refined sugar boilings. The growth rate measurements were based on size measurements by number determined by the Kontron particle analyser (see Appendix A). His data showed two periods of approximately linear growth rates - a fast initial growth period followed by a significantly slower second period. For comparison, he measured growth rates in industrial refinery (batch) pans and found a similar two stage growth curve, but at higher growth rates, particularly in the second stage. The data from these tests (Lionnet, private communication) are summarised in the table below :

| | | Crystallisation Velocity | | | |
|---|---|---|---|---|---|
| | | µm/s | µm/min | µm/hr | m/s |
| Laboratory Pan | 1st Period run 1 | 0.160 | 9.600 | 576 | 1.60e-07 |
| | run 2 | 0.120 | 7.200 | 432 | 1.20e-07 |
| | run 3 | 0.200 | 12.000 | 720 | 2.00e-07 |
| | run 4 | 0.320 | 19.200 | 1152 | 3.20e-07 |
| | run 5 | 0.180 | 10.800 | 648 | 1.80e-07 |
| | Average | 0.196 | 11.760 | 706 | 1.96e-07 |
| | 2nd Period run 1 | 0.006 | 0.378 | 22.68 | 6.30e-09 |
| | run 2 | 0.007 | 0.444 | 26.64 | 7.40e-09 |
| | run 3 | 0.013 | 0.780 | 46.80 | 1.30e-08 |
| | run 4 | 0.009 | 0.528 | 31.68 | 8.80e-09 |
| | run 5 | 0.008 | 0.450 | 27.00 | 7.50e-09 |
| | Average | 0.009 | 0.516 | 30.96 | 8.60e-09 |
| Industrial Pans | 1st Period Run HR1 | 0.300 | 18.000 | 1080 | 3.00e-07 |
| | Run HR2 | 0.300 | 18.000 | 1080 | 3.00e-07 |
| | Run HR3 | 0.250 | 15.000 | 900 | 2.50e-07 |
| | Run HR5 | 0.210 | 12.600 | 756 | 2.10e-07 |
| | Run HR6 | 0.240 | 14.400 | 864 | 2.40e-07 |
| | Run GH1 | 0.180 | 10.800 | 648 | 1.80e-07 |
| | Average | 0.247 | 14.800 | 888 | 2.50e-07 |
| | 2nd Period Run HR1 | 0.040 | 2.400 | 144 | 4.00e-08 |
| | Run HR2 | 0.030 | 1.800 | 108 | 3.00e-08 |
| | Run HR3 | 0.030 | 1.800 | 108 | 3.00e-08 |
| | Run HR5 | 0.050 | 3.000 | 180 | 5.00e-08 |
| | Run HR6 | 0.020 | 1.200 | 72 | 2.00e-08 |
| | Run GH1 | 0.010 | 0.600 | 36 | 1.00e-08 |
| | Average | 0.030 | 1.800 | 108 | 3.00e-08 |

Table G.1 Growth rates in refined sugar batch boilings - laboratory and industrial scale

The two stage growth process can probably be explained by the fact that, for high purity refined sugar boiling, the crystallisation in the early stages is super-saturation limited (the need to avoid false grain formation) whilst in the latter stages, it is evaporation rate limited. This fact is a well known aspect of refinery boilings and Wright (1983) provides an equation for estimating evaporation limited growth. Unfortunately insufficient information is available for these tests to confirm the evaporation rate limited growth quantitatively.

## G.2     Tongaat-Hulett Sugar Data on High Grade Continuous Pans

During the development of the Tongaat-Hulett continuous pans, tracer tests were conducted to measure crystal residence times (Rein,. Cox and Love, 1985). The data from these tests can be combined with crystal size data reported in the same paper to determine crystal growth rates and the dispersion parameter $p$, as shown in the table below.

| Factory | Units | AK | MS | MS | FX |
|---|---|---|---|---|---|
| Duty (massecuite) | | A | A | A | A |
| Year | | 1981 | 1983 | 1983 | 1984 |
| Tanks in Series (equivalent) | | 5 | 17 | 17 | 12 |
| Residence Time | hr | 1.6 | 5.1 | 5.1 | 5.2 |
| Seed Massecuite Crystal Sizes | | | | | |
| By mass | | | | | |
|   Mean Aperture | mm | 0.48 | 0.43 | 0.43 | 0.39 |
|   CV | % | 40.6 | 39.9 | 33.1 | 39 |
|   Variance (sigma2) | mm2 | 0.038 | 0.029 | 0.020 | 0.023 |
| By number | | | | | |
|   Mean | mm | 0.304 | 0.276 | 0.315 | 0.255 |
|   Variance (sigma2) | mm2 | 0.015 | 0.012 | 0.011 | 0.010 |
| Product Massecuite Crystal Sizes | | | | | |
| By mass | | | | | |
|   Mean Aperture | mm | 0.6 | 0.61 | 0.61 | 0.61 |
|   CV | % | 33.7 | 33.4 | 26.5 | 36 |
|   Variance (sigma2) | mm2 | 0.041 | 0.042 | 0.026 | 0.048 |
| By number | | | | | |
|   Mean | mm | 0.435 | 0.444 | 0.498 | 0.423 |
|   Variance (sigma2) | mm2 | 0.021 | 0.022 | 0.017 | 0.023 |
| Growth Rate (v) | | | | | |
| By mass | mm/hr | 0.075 | 0.035 | 0.035 | 0.042 |
| | microns/hr | 75.0 | 35.3 | 35.3 | 42.3 |
| By number | mm/hr | 0.082 | 0.033 | 0.036 | 0.032 |
| | microns/hr | 81.8 | 33.0 | 35.9 | 32.3 |
| Dispersion Parameter (p) | mm | 0.0215 | 0.0489 | 0.0250 | 0.0652 |

**Table G.2** Growth rates in South African high grade continuous pans

The table includes conversions of the size data from those for a distribution by mass (as measured by the sieving process to get the conventional MA and CV values) to average size on a number basis, as discussed in Appendix A. The dispersion parameter, $p$, is calculated from the change in the variance ( from $\sigma_i^2$ to $\sigma_f^2$ ) of the size distributions by number, the growth rate ($v$), the average retention time ( $\tau$ ), and the equivalent number of tanks in series ( $n$ ), according to the equation given by Rein, Cox and Love (1985).

$$\sigma_f^2 = \sigma_i^2 + \frac{v^2 \cdot \tau^2}{n} + p \cdot v \cdot \tau \tag{G.1}$$

The published data do not provide information on operating temperatures or purity levels in the mother liquor. Based on other data (eg Hoekstra 1985 and Appendix F) it is reasonable to assume temperatures in the range 60 to 70°C and purities in the range 65 to 75.

Hoekstra (1985) presented a computer fit to results of measurements of a continuous A-Pan at Maidstone. The fitted growth rates for each compartment vary between 12 and 22 microns per hour with an average of 19 microns per hour. These measurements are reported to be at the reasonably low temperature, for A-massecuites, of 62°C. The purity of the mother-liquor varies between 67 and 74.

## G.3    Australian Data on High Grade Batch Pans

Miller and Broadfoot (1997) measured crystal growth rates in industrial scale batch pans boiling high grade massecuites in the Australian cane sugar industry. Large samples of massecuite were taken at stages during batch cycles, the crystals separated and their size distribution measured by sieve analysis. The crystal growth rates were calculated from the change in mean aperture (MA) with time and are thus based on mass distributions rather than number distributions. Insufficient information is provided in the paper to estimate growth rates based on distributions by number, but the data presented in section G.2 indicate that for typical high grade pan operations theses on not very different.

To estimate the range of the mother liquor purity during the growth process, it was necessary to assume a massecuite exhaustion (of 65%) at the end of the batch cycle. The maximum mother liquor purity was taken at the extreme case of the massecuite purity ie at an infinitely small crystal content.

Miller and Broadfoot (1997) report data on average growth rates for complete batch cycles at four different factories, which are analysed in the table below. The different pans are operated at different temperatures and to facilitate comparison, the data are all corrected to a nominal boiling temperature of 65°C assuming an Arrhenius type of temperature dependance (ie exponential) with an activation energy of 58.6kJ/mol. The mother liquor purity at the initial stage of the batch cycle has been estimated by assuming that the magma footing is of the same purity as the massecuite and has been washed to a crystal content of 15% ( Broadfoot, Miller & Bartholomew, 1996)

| Factory | Test | Temp. (°C) | Massecuite Purity | Molasses Purity | Initial Mother Liquor Purity | Meas. Growth Rate ($\mu$m/hr) | Growth Rate Corr. To 65°C ($\mu$m/hr) |
|---|---|---|---|---|---|---|---|
| A | 1 lo Temp | 74 | 89 | 74 | 87 | 113 | 66 |
| A | 1 hi Temp | 78 | 87 | 70 | 84 | 113 | 52 |
| A | 2 | 80 | 83 | 63 | 79 | 138 | 57 |
| B | 1 | 65 | 88 | 72 | 85 | 105 | 105 |
| C | 1 | 75 | 87 | 70 | 84 | 100 | 55 |
| D | 1 | 64 | 87 | 70 | 84 | 98 | 104 |
| D | 2 | 63 | 87 | 70 | 84 | 107 | 121 |
| D | 3 | 65 | 80 | 58 | 76 | 53 | 53 |

**Table G.3**  Growth rates in Australian high grade batch pans

## G.4    Interpretation of Pan Time Index used for Estimating Batch Pan Requirements

Prior to the development of continuous pans, the installed capacity of batch pans in a factory would be defined by the factory throughput and the average crystal growth rates which can be achieved on each grade of massecuite. Archibald and Smith (1975) defined the concept of a Pan Time Index, $t_n$ which is defined as :

$$t_n = \frac{\text{m}^3 \text{ pan capacity employed on nth massecuite}}{\text{m}^3 \text{ of nth massecuite per hour}} \tag{G.2}$$

The standard values of pan time index (PTI) which they quoted, viz.

For A-massecuite      $t_A$ =   4.5     hours

For B-massecuite      $t_B$ =   6.0     hours

For C-massecuite      $t_C$ =   9.0     hours

have proved to be a suitable basis over many years within the Tongaat-Hulett Sugar company for estimating pan requirements for expansions and modifications of sugar factories in Southern Africa. Whilst these pan time indices are representative of average growth rates they need further information on crystal sizes and actual pan cycles before they can be expressed as linear growth rates. To provide this extra information necessary to interpret crystal growth rates from the overall performance of batch pans, data were collected from the Amatikulu factory during the 1990/2000 crushing season. Data from Amatikulu is particularly appropriate as this factory has no continuous pans and all the batch pans are of a relatively modern design which give good performance.

A typical set of pan cycles (as conventionally recorded in a pan log book) were analysed for each grade of massecuite to provide estimates of the actual crystal residence times, whilst also providing a check of the pan time index values against those of Archibald and Smith (1975). The summarised details are presented below. The diagrams are "conceptual" summaries to follow the histories of the crystals. The actual cycles are more complex as they involve transfers to seed tanks, idle times and "balancing cycles" (when no crystallisation takes place) to match the production requirements to pan availability.

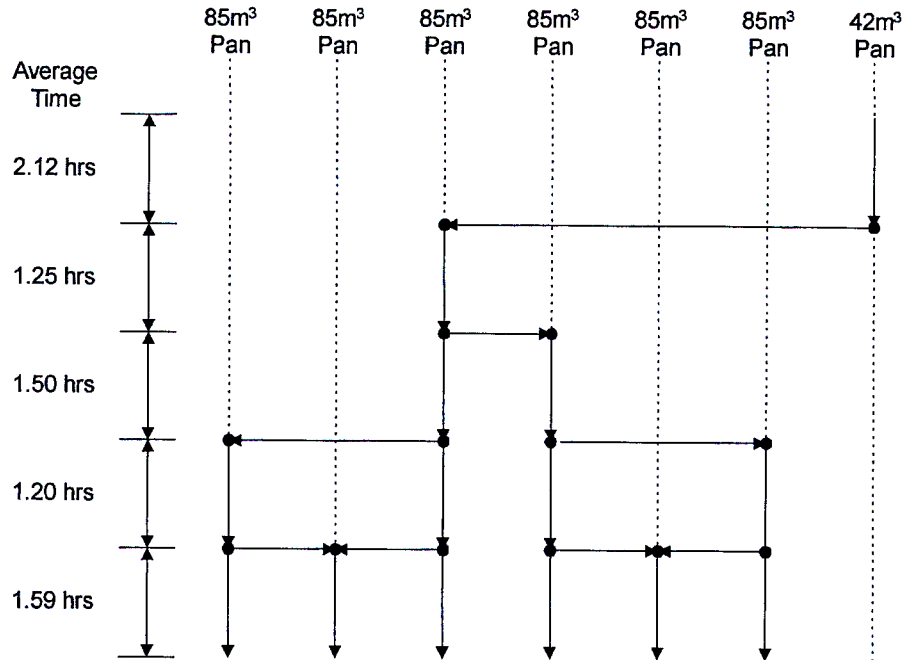The data for the A-massecuite pan cycles is summarised in the diagram below :

**Figure G.1** Pan cycles for A-massecuite

The average crystal residence time $\tau_A$ is given by summing the time in each stage of the complete pan cycle and allowing 15 minutes at the transitions between stages (cut-over time). The cut-over time is not included in the crystal residence time as growth will be drastically reduced (or stop) during these periods. Thus :

$$\tau_A = 2.12 + 1.25 + 1.50 + 1.20 + 1.59 - (4 \cdot 0.25)$$
$$= 6.66 \quad hrs \tag{G.3}$$

The pan time index can be estimated from the total production of 6 by 85m³ batch strikes and the total pan utilisation to achieve this, in terms of m³ hrs, as follows :

$$t_A = \frac{2.12 \times 42 + 1.25 \times 85 + 1.5 \times 2 \times 85 + 1.2 \times 4 \times 85 + 1.59 \times 6 \times 85}{6 \times 85} \tag{G.4}$$
$$= 3.27 \quad hrs$$

This figure does not account for the time lost due to transfers, idle times and "balancing cycles" mentioned above. An analysis of the three 85m³ batch pans used for A-massecuite showed that over a 24 hour period, 13.5 hrs were consumed by these activities, indicating an effective time utilisation of 81.2%. Applying this necessary correction gives a pan time index of :

$$t_A = 3.27 \div 0.8125$$
$$= 4.02 \; hrs$$

<div align="right">(G.5)</div>

In a similar analysis, the pan cycles for B-massecuite production are given by :



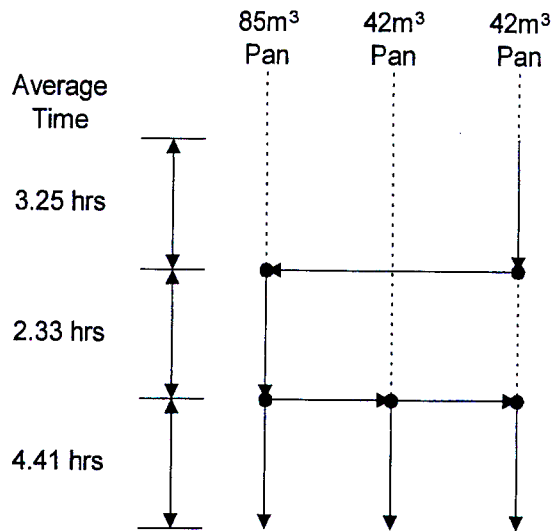**Figure G.2** B-massecuite pan cycles

Following the same procedure, it is possible to estimate the average crystal residence time $\tau_B$ as :

$$\tau_B = 3.25 + 2.33 + 4.41 - (2 \cdot 0.25)$$
$$= 9.49 \;\; hrs$$

<div align="right">(G.6)</div>

The pan time index can be estimated from the total production of 1 by 85m$^3$ and 2 by 42m$^3$ batch strikes and the total pan utilisation to achieve this, in terms of m$^3$ hrs, as follows :

$$t_B = \frac{3.25 \times 42 + 2.33 \times 85 + 4.41 \times 85 + 4.41 \times 2 \times 42}{1 \times 85 + 2 \times 42}$$
$$= 6.39 \;\; hrs$$

<div align="right">(G.7)</div>

This is slightly greater than the standard value of 6.0 hours.

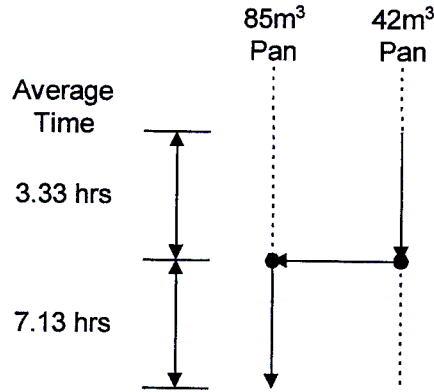In a similar analysis, the pan cycles for C-massecuite production are given by :

**Figure G.3** C-massecuite pan cycles

From this information, it is possible to estimate the average crystal residence time $\tau_C$ as :

$$\tau_C = 3.33 + 7.13 - (1 \times 0.25)$$
$$= 10.21 \quad hrs$$

(G.8)

The pan time index can be estimated from the total production of 1 by 85m³ batch strike and the total pan utilisation to achieve this, in terms of m³ hrs, as follows :

$$t_B = \frac{3.33 \times 42 + 7.13 \times 85}{1 \times 85}$$
$$= 8.77 \quad hrs$$

(G.9)

It is difficult to individually adjust the pan time index figures for B and C massecuite to compensate for un-utilised pan time (as done for the A-massecuite boiling) because it is not possible to allocate the un-utilised time to each duty. Considering the 5 pans which are used for both B and C-massecuite as a group, a total of 20.25 hours of un-utilised pan time occurred in a 24 hour period. This is equivalent to a percentage utilisation of 83.1%. Adjusting the B and C pan time indices by this figure gives :

$$t_B \quad = \quad 7.69 \quad hrs$$
$$t_C \quad = \quad 10.55 \quad hrs$$

These crystallisation times and pan time index values can be summarised as follows :

| Grade of Massecuite | Standard PTI (hrs) | Amatikulu Pan Performance | | |
|---|---|---|---|---|
| | | Utilised PTI (hrs) | Installed PTI (hrs) | Crystallisation Time (hrs) |
| A | 4.5 | 3.27 | 4.02 | 6.66 |
| B | 6.0 | 6.39 | 7.69 | 9.49 |
| C | 9.0 | 8.77 | 10.55 | 10.21 |

**Table G.4** Estimates of Pan Time Index for different grades of massecuite

The standard value for PTI should fall between the utilised and installed values. It should be equal to the installed value if the un-utilised time is essential to co-ordinating cycles - as is more likely with the complex and short A-massecuite boiling cycles. However, it should be equal to the utilised value if it is possible to productively use the un-utilised time to accommodate increasing throughput -as is likely with the simpler and longer B and C massecuite boiling cycles. Given these arguments, there is reasonable agreement between the Amatikulu values for PTI and the standard values. This agreement on pan time index values indicates that the measured crystallisation times for the Amatikulu mill should be reasonably representative of the local industry.

To convert the crystallisation times into average crystal growth rates requires the crystal sizes at the beginning and end of each cycle. Estimates have been made from the following sources :

A-massecuite

     initial size   -   The seed crystals are B sugar crystals. This stream is not routinely measured but some representative size data is reported by Rein and Archibald (1989)

     final size   -   the final crystal size is estimated as equal to the product crystal size. Data is available on raw sugar which was sent to the South African Sugar Terminal for export during the 1999/2000 season.

B- massecuite

     Initial size   -   the initial crystal size is that of the slurry which is used as a seed. Based on values reported in the literature (Jensen, 1967, Lionnet, 1998), this is assumed to have a size of 4 microns.

|  |  |  |
|---|---|---|
| final size | - | Rein and Archibald (1989) also provided some data on crystal size in B-massecuite. |

C- massecuite

|  |  |  |
|---|---|---|
| Initial size | - | the initial crystal size is that of the slurry which is used as a seed. As for B-massecuite, this is also assumed to have a size of 4 microns. |
| final size | - | data are available on from monthly surveys of crystal size in C-massecuite undertaken for the South African Sugar Industry by the Sugar Milling Research Instute (SMRI). |

Where appropriate, these size data have been converted from a mass to a number basis according to the relationships given by Rein, Cox and Love (1985) ie using equation A.45. The results are summarised in the table below:

| Product | Stage of boiling | Mass based Crystal Size | | | Number based Ave. Xtal Size (mm) |
|---|---|---|---|---|---|
|  |  | MA (mm) | CV (%) | Std. Dev. (mm) |  |
| A Massecuite | Start | 0.30 | 50 | 0.15 | 0.154 |
|  | End | 0.69 | 31 | 0.214 | 0.524 |
| B Massecuite | Start | --- | --- | --- | 0.004 |
|  | End | --- | --- | --- | 0.210 |
| C Massecuite | Start | --- | --- | --- | 0.004 |
|  | End | --- | --- | --- | 0.187 |

**Table G.5**   Changes in crystal size over boiling for different grades of massecuite

Combining these numbers on the increase in crystal size with the estimations of crystallisation time, it is possible to estimate the following crystal growth rates :

|  |  |  |  |
|---|---|---|---|
| A- Massecuite | : | 56 | microns/hr |
| B- Massecuite | : | 22 | microns/hr |
| C- Massecuite | : | 18 | microns/hr |

These data are average rates over the whole pan cycle and thus reflect the effect of the range of mother liquor purities encountered over the cycle. The range of purities can be estimated from the standard production data for the Amatikulu factory over the 1999/2000 season as follows :

A-massecuite

| | |
|---|---|
| Massecuite purity | 86 |
| Maximuum purity is mother liquor purity of footing* | 83 |
| Minimum purity is molasses purity | 67 |

B-massecuite

| | |
|---|---|
| maximum purity is A-molasses purity (graining on A-molasses) | 67 |
| minimum purity is B-Molasses purity | 47 |

C-massecuite

| | |
|---|---|
| maximum purity is A-molasses purity (graining on A-Molasses) | 67 |
| minimum purity is C-massecuite purity - purity drop over boiling | 38 |

* The footing for the A-massecuite boiling is assumed to be created by partial dissolution of B-magma of the same purity as the A-massecuite purity. The extent of the dissolution is assumed to be defined by achieving a crystal content of 15% in the footing (based on the work of Broadfoot, Miller and Bartholomew, 1996).

# APPENDIX H

## H.  Simulating Compartment Dynamics

### H.1  Simulation of Dynamics of Feed Fluctuations

The following pages are the print-out of a "Mathcad" worksheet to simulate the effect of variations in the feed flow to a single compartment of a continuous pan, using the dynamic process model developed in Chapter 4 and Appendix B.

$ORIGIN \equiv 1$          Defines all vectors and matrices to begin at 1 rather than the default of 0

For this evaluation of the dynamic behaviour of a single compartment of a continuous pan, the behaviour is evaluated at points in time spaced "delta" seconds apart.

$delta := 5$     (sample spacing in seconds)

$N := 1024$     (total number of sample points to be evaluated - selected as a power of 2 to facilitate frequency analysis by Fast Fourier Transforms)

$MaxTime := delta \cdot N$

$MaxTime = 5.12 \cdot 10^3$     (MaxTime is the length of time over which the behaviour is evaluated)

The dynamic behaviour is evaluated by making steps in the inputs to the compartment

The equations are structured to provide the option of stepping twice, at times "ts1" and "ts2"

$ts1 := 1000$     First step at time "ts1" (seconds)

$ts2 := 1010$     Second step at time "ts2" (seconds)

The simulation is based around the first compartment of a Felixton Continuous A-pan and uses the results of test 2-A as done in section 8.7.
Common Proporties for this simulation are thus:

$CT := 14500$     Total mass in a compartment (kg)

$\rho x := 1588$     Density of crystal sucrose $(kg/m^3)$

$\alpha v := 0.34$     Volume shape factor for crystals

$sybx := 66.27$     Syrup Brix (%)

$pur := 87.74$     Common Purity of syryp and massecuite (%)

K0 := 0.0046

K1 := 0.00000087

K2 := 0.578

K3 := 1.75

K4 := 3.254

K5 := 0.08

p := 0.000199

Parameters K0 to K5 and p are used to describe the sucrose solubility and growth kinetics. The definifinition of these variables is described in Chapter 2 and their incorporation in the compartment model is described in Chapter 4. The values used in this simulation are based on the experimental results described in Chapter 7.

k := 1 .. 10000        k is a subscript variable for use in plotting graphs

Input Variables u1 to u5 describe the seed masecuite flowing into the compartment

u1 := 5.17                               Total Mass flow (kg/s)

u2 := 0.523                              Mass flow of water (kg/s)

u3 := 1.446                              Mass flow of disolved sucrose (kg/s)

u4 := 0.000631                           First moment of crystal size (m)

u5 := 0.000000451                        Second moment of crystal size (m$^2$)

Input Variables u6 and u7 describe the water or syrup feed into the compartment
They use the Heaviside step function $\Phi(t)$ (which is zero for negative values and unity for positive values and zero) to create steps in the input.

$u6(t) := 1.5 + \Phi(t - ts1) \cdot 5 - \Phi(t - ts2) \cdot 5$        Total Mass flow (kg/s)

$u7(t) := (u6(t)) \cdot \dfrac{sybx}{100} \cdot \dfrac{pur}{100}$        Mass flow of disolved sucrose (kg/s)

Input Variable u8 defines the evaporation from the compartment

u8 := 0.46                               Total Mass flow (kg/s)

The syrup feed flow has uses equal up and down steps, to create a pulse increase between times ts1 and ts2.

$$x := \begin{bmatrix} 4245 \\ 1328 \\ 0.0006667 \\ 0.0000005058 \end{bmatrix}$$

The vector x describes the conditions in the compartment with:
x1 - the mass of disolved sucrose (kg)
x2 - the mass of water (kg)
x3 - the first moment of crystal size (m)
x4 - the second moment of crystal size (m$^2$)

Following the model formulation described in Chapter 4, the intermediate functions g0 to g3 are defined.

$$g0(x,t) := \frac{\dfrac{x_1}{x_2}}{\left[ K4 \cdot \left[ 1 - K5 \cdot \left( \dfrac{CT - x_2}{x_2} \right) \cdot \left( 1 - \dfrac{pur}{100} \right) \right] \right]}$$

$$g1(x,t) := \frac{(u1 - u2) \cdot \dfrac{pur}{100} - u3}{\rho x \cdot \alpha v \cdot \left[ 2 \cdot \dfrac{(u5)^2}{u4} - u5 \cdot u4 \right]}$$

$$g2(x,t) := \frac{\left( CT - x_2 \right) \cdot \dfrac{pur}{100} - x_1}{\rho x \cdot \alpha v \cdot \left[ 2 \cdot \dfrac{\left( x_4 \right)^2}{x_3} - x_4 \cdot x_3 \right]}$$

$$g3(x,t) := K1 \cdot (g0(x,t) - (1 + K0)) \cdot \exp \left[ K2 - K3 \cdot \frac{CT - x_2}{x_2} \cdot \left( 1 - \frac{pur}{100} \right) \right]$$

Using these intermediate functions it is possible to program the equations describing the dynamic behaviour of the states of the compartment ($x_1$ to $x_4$) in the matrix format require by Mathcad. This format is necessary to perform a Runge-Kutta solution of the set of simultaneous differential equations - ie equations 4.7 to 4.10 of Chapter 4.

$$D(t,x) := \begin{bmatrix} u3 + u7(t) - (u1 + u6(t) - u8) \cdot \dfrac{x_1}{CT} - 3 \cdot \rho x \cdot \alpha v \cdot g2(x,t) \cdot g3(x,t) \cdot \left( x_4 + p \cdot x_3 \right) \\[2mm] u2 + \left( u6(t) - u7(t) \cdot \dfrac{100}{pur} \right) - u8 - (u1 + u6(t) - u8) \cdot \dfrac{x_2}{CT} \\[2mm] \dfrac{g1(x,t)}{g2(x,t)} \cdot \left( u4 - x_3 \right) + g3(x,t) \\[2mm] \dfrac{g1(x,t)}{g2(x,t)} \cdot \left( u5 - x_4 \right) + 2 \cdot g3(x,t) \cdot x_3 + p \cdot g3(x,t) \end{bmatrix}$$

Executing the rkfixed function creates a matrix whose columns to represent time and the values of the four states, $x_1$, $x_2$, $x_3$ and x4. The rows provide the values at consecuitive time intervals.

$$i := 1 .. N \qquad\qquad\qquad Z := rkfixed(x, 0, MaxTime, N, D)$$

The values of the states at the end of the time interval under consideration are thus :

$$Z_{N,1} = 5.115 \cdot 10^3$$        $Z_{N,1}$ is the time in seconds of the last data point

$$Z_{N,2} = 4.251 \cdot 10^3$$        $Z_{N,2}$ is the mass of dissolved sucrose in the compartment

$$Z_{N,3} = 1.331 \cdot 10^3$$        $Z_{N,3}$ is the mass of water in the compartment

$$Z_{N,4} = 6.666 \cdot 10^{-4}$$        $Z_{N,4}$ is the first moment of the xtal size distribution

$$Z_{N,5} = 5.056 \cdot 10^7$$        $Z_{N,5}$ is the second moment of the xtal size distribution

To demonstrate the compatment behaviour in terms of more commonly understood properties, the following variables are calculated :
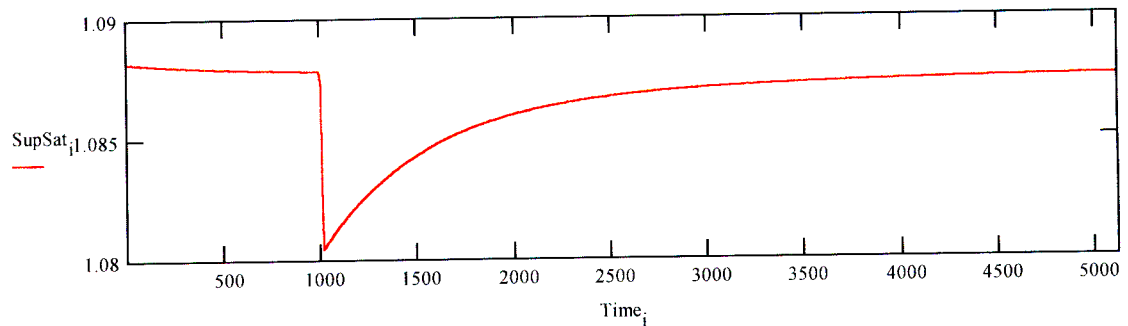
$$Time_i = Z_{i,1}$$

$$McBrix_i = CT - Z_{i,3} \cdot \frac{100}{CT}$$        Massecuite brix in %

$$XtalCont_i = \left( CT - Z_{i,3} \cdot \frac{pur}{100} - Z_{i,2} \right) \cdot \frac{100}{CT}$$        Mean crystal size in microns
Crystal content in %

$$XtalSize_i = Z_{i,4} \cdot 1000000$$        Mean crystal size in microns

$$SupSat_i = \frac{\dfrac{Z_{i,2}}{Z_{i,3}}}{\left[ K4 \cdot 1 - K5 \cdot \left( \dfrac{CT - Z_{i,3}}{Z_{i,3}} \cdot 1 - \dfrac{pur}{100} \right) \right]}$$        Mother liquor supersaturation
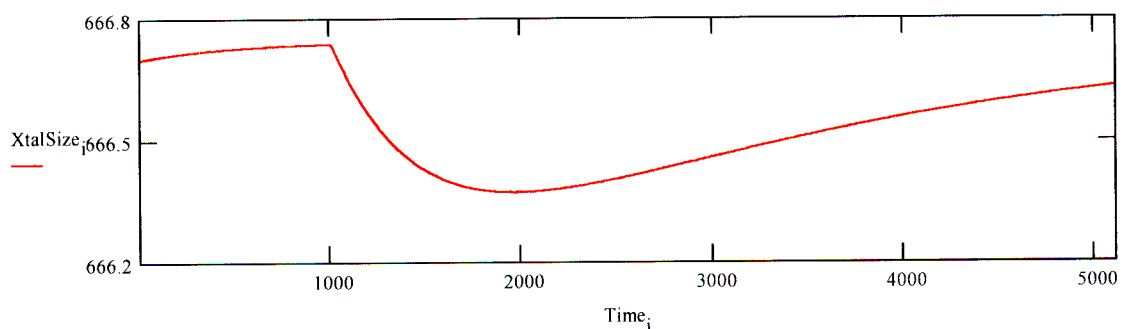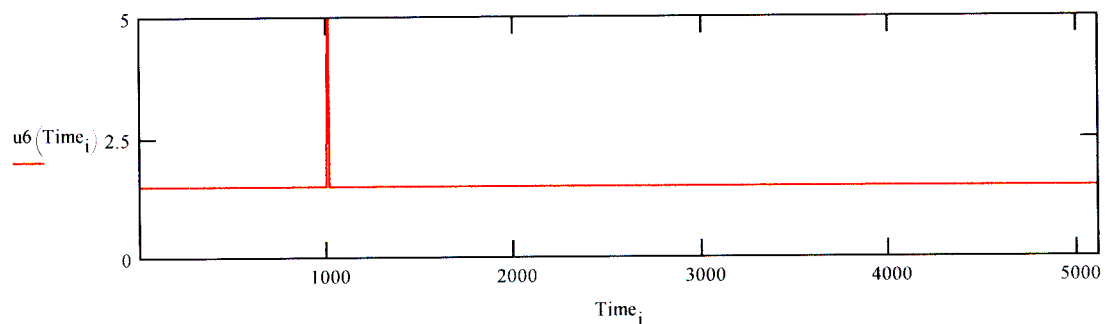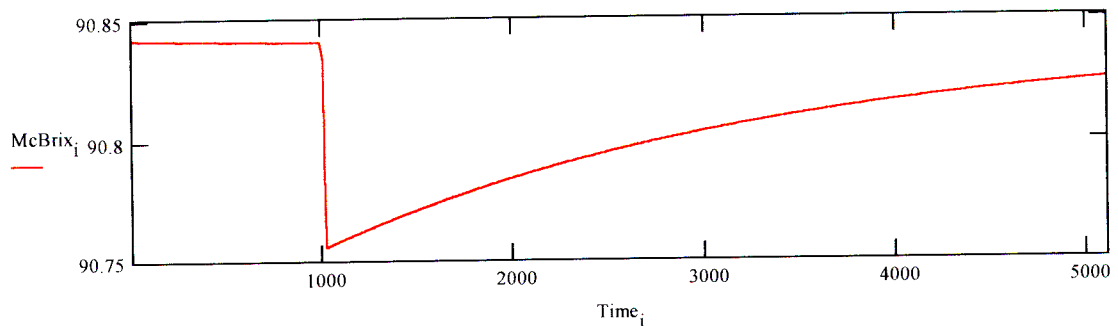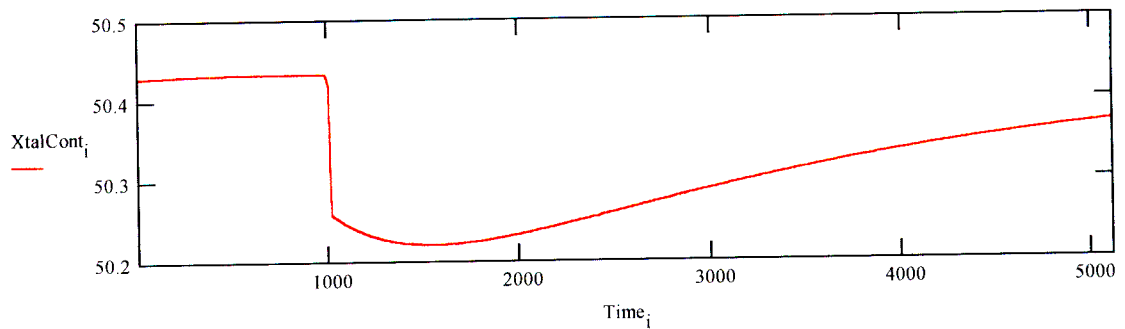
Fourier analysis of the correlation functions provides a method for determining the frequency response of the process, which can be expressed in terms of Bode plots.

To minimise the end effects which result when applying Fourrier Transforms to finite records of data, it is necessary to apply a "windowing" function.   Defining the Blackman-Harris window function over the range of i (1 to 1024) to apply to the auto and cross correlation functions prior to evaluating the Fourrier Transforms:

$$a0 := 0.42323 \qquad a1 := 0.49744 \qquad a2 := 0.07922$$

$$w_i := a0 - a1 \cdot \cos\left(\frac{2 \cdot \pi}{N} \cdot i\right) + a2 \cdot \cos\left(\frac{2 \cdot \pi}{N} \cdot 2 \cdot i\right)$$

Applying the window function to both the process input and process output :

$$wu6_i := u6(Time_i) \cdot w_i \qquad\qquad wXtalCont_i := XtalCont_i \cdot w_i$$

Calculating the Fourier Transforms of the "windowed" inputs and outputs :

$$su6 := fft(wu6) \qquad\qquad sXtalCont := fft(wXtalCont)$$

The elements of su6 and sXtalCont are complex numbers which describe the sine waves which can be considered to be the components of u6 and XtalCont respectively. They are evaluated for only half the number of points for which the original signals are available (ie N/2 points). The subscript of su6 and sXtalCont defines the frequency of the sine wave.  Given that each reading is "delta" seconds apart, the frequency corresponding to each element of the Fourrier transformed variable is given by :

Create a new subscript variable to refer to the frequency components :  $\qquad q := 1 .. \dfrac{N}{2}$

$$fs_q := \frac{q}{\left(\dfrac{N}{2}\right)} \cdot \frac{1}{delta} \qquad \text{Frequency in cycles per second}$$

$$fh_q := fs_q \cdot 3600 \qquad \text{Frequency in cycles per hour}$$

Plotting the amplitude of the signals in the frequency domain :
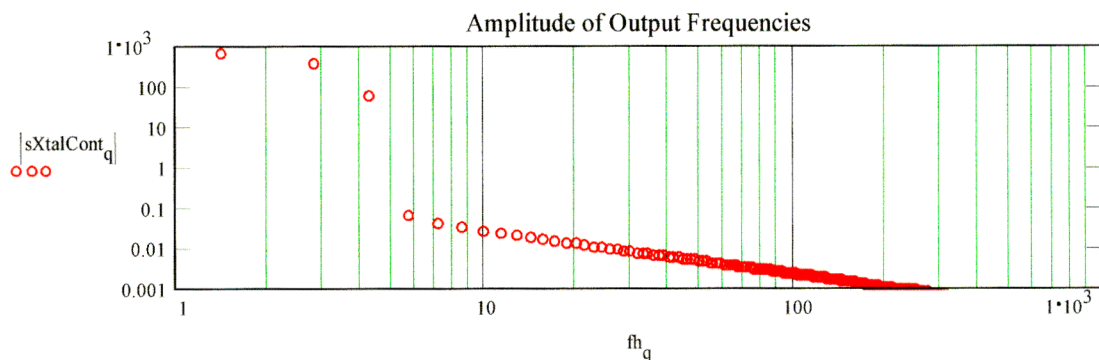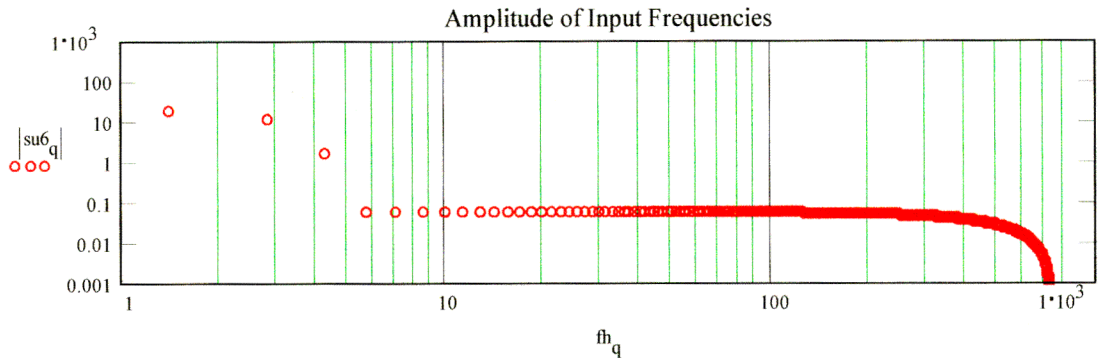




Using this information on the frequency content of the sr and src signals, it is possible to develop  Bode plots for the process. The transfer function of the process is given by :

$$sp_q := \frac{sXtalCont_q}{su6_q}$$

The Amplitude Ratio is given by :                 $AR_q \quad |sp_q|$

The Phase Shift is given by :                     $\theta_q \quad arg(sp_q)$

Or, alternatively, Phase Shift is given by :      $\theta d_q \quad arg(su6_q) \quad arg(sXtalCont_q)$



Process Amplitude Ratio



Process Phase Shift